Experimental Studies of a Direct Injection Diesel Engine Fuelled with Light Fraction Pyrolysis Oil-Diesel Blend

Kapura Tudu

Department of Mechanical Engineering
National Institute of Technology Rourkela

Experimental Studies of a Direct Injection Diesel Engine Fuelled with Light Fraction Pyrolysis Oil-Diesel Blend

Dissertation submitted in partial fulfillment
of the requirements of the degree of

Doctor of Philosophy
in
Mechanical Engineering
by

Kapura Tudu

(Roll Number: 511ME118)

based on research carried out
under the supervision of

Prof. Saroj Kumar Patel

and

Prof. S. Murugan

January, 2017

Department of Mechanical Engineering
National Institute of Technology Rourkela

Department of Mechanical Engineering
National Institute of Technology Rourkela

January 07, 2017

Certificate of Examination

Roll Number: 511ME118
Name: Kapura Tudu
Title of Dissertation: Experimental Studies of a Direct Injection Diesel Engine fuelled with Light Fraction Pyrolysis Oil-Diesel Blend

We the below signed, after checking the dissertation mentioned above and the official record book (s) of the student, hereby state our approval of the dissertation submitted in partial fulfillment of the requirement of the degree of Doctor of Philosophy in Mechanical Engineering at National Institute of Technology, Rourkela. We are satisfied with the volume, quality, correctness, and originality of the work.

S. Murugan Co-supervisor	**Saroj Kumar Patel** Principal Supervisor
Alok Satapathy Member (DSC)	**Mithilesh Kumar** Member (DSC)
Raghubansh Kumar Singh Member (DSC)	**N. V. Mahalakshmi** External Examiner
Ashok Kumar Satapathy Chairman (DSC)	**Siba Sankar Mahapatra** Head of the Department

Department of Mechanical Engineering
National Institute of Technology Rourkela

Saroj Kumar Patel
Principal Supervisor
S. Murugan
Co-supervisor

January 07, 2017

Supervisors' Certificate

This is to certify that the work presented in this dissertation entitled *"Experimental Studies of a Direct Injection Diesel Engine Fuelled with Light Fraction Pyrolysis Oil-Diesel Blend"* by *"Kapura Tudu"*, Roll Number: 511ME118, is a record of original research carried out by him under our supervision and guidance in partial fulfillment of the requirements of the degree of *Doctor of Philosophy* in *Mechanical Engineering*. Neither this dissertation nor any part of it has been submitted for any degree or diploma to any institute or university in India or abroad.

S. Murugan	**Saroj Kumar Patel**
Co-supervisor	Principal Supervisor

Declaration of Originality

I, Kapura Tudu, Roll Number: 511ME118, hereby declare that this dissertation entitled *"Experimental Studies of a Direct Injection Diesel Engine Fuelled with Light Fraction Pyrolysis Oil-Diesel Blend"* represents my original work carried out as a doctoral student of NIT Rourkela and, to the best of my knowledge, it contains no material previously published or written by another person, nor any material presented for the award of any degree or diploma of NIT Rourkela or any other institution. Any contribution made to this research by others, with whom I have worked at NIT Rourkela or elsewhere, is explicitly acknowledged in the dissertation. Works of other authors cited in this dissertation have been duly acknowledged under the section "References". I have also submitted my original research records to the scrutiny committee for evaluation of my dissertation.

I am fully aware that in case of my non-compliance detected in the future, the Senate of NIT Rourkela may withdraw the degree awarded to me on the basis of the present dissertation.

January 07, 2017

NIT Rourkela

Kapura Tudu

ACKNOWLEDGEMENT

I would like to express my heartfelt and sincere thanks to my supervisor **Prof. Saroj Kumar Patel**, for giving me an opportunity to work in this interesting research work. I am also thankful for his valuable guidance, inspiration, constant encouragement, heartfelt good wishes and support through all the phases of my research work.

I also thank my co-supervisor **Prof. S. Murugan** for his unflagging encouragement and supportive guidance throughout my research career. He constantly encourages me to remain focused on achieving my goal. His observations and research ideas helped me to establish the overall direction of the research and to move forward for innovative investigation. I thank him for providing me an the opportunity to work with him in the IC Engines Laboratory. I would not have completed my research task without his constant support.

I am ever grateful to **Prof. Sunil Kumar Sarangi**, Director who has motivated me to carry out this research work and given me a constant support all time during this study. I also sincerely thank **Prof. Siba Sankar Mahapatra**, Head, Department of Mechanical Engineering for extending all departmental facilities needed for my Ph. D. work.

I take this opportunity to express my deep sense of gratitude to the members of my Doctoral Scrutiny Committee members **Prof. Ashok Kumar Satapathy** and **Prof. Alok Satapathy**, Mechanical Engineering Department; **Prof. Mithilesh Kumar**, Metallurgical and Materials Engineering Department; and **Prof. Raghubansh Kumar Singh**, Chemical Engineering Department for their valuable suggestions, while carrying out this research work.

I sincerely thank **Mr. Narayan Prasad Barik, Mr. Naren Kumar Bisoi, Mr. Ramkrishna Mandal, Mr. Laxman Kumar Mahanta** and other staff who have been kind enough to help in their respective roles that I needed.

I would like to express my gratitude to my research colleagues **Mr. R. Prakash, Mr. Arun Kumar Wamankar, Mr. Debabrata Barik, Mrs. Dulari Hansdah, Mr. Abhishek Sharma** and **Mr. Hari Sankar Bendu** for their assistance in my research

work. I am also thankful to my other research colleagues for their support and good wishes.

I would like to thank my parents, brothers, sisters, parents-in-law, my husband **Mr. Antu Hansdah**, and my son **Debabrat Hansdah** (Prince) for their great support, patience and unconditional love during my good and bad times. Above all, I owe it all to Almighty God for granting me the wisdom, health and strength to undertake this research task and enabling me to its completion.

.

(Kapura Tudu)

ABSTRACT

One of the important problems currently faced by the humanity is disposal of different wastes that originate everywhere. Different wastes are present in houses, villages, municipalities, agricultural lands and industries, and they are found in the form of solid, liquid and gas. It is impossible to completely avoid disposal of wastes. But, it can be minimized by adopting effective waste management practices. Generally, wastes can be categorized into two types viz., (i) non reusable, and (ii) recyclable and reuse. A few examples of non-reusable wastes are broken glass, broken concrete and some of the liquid effluents. Most of the organic wastes can be considered as recyclable or reusable. Few examples include food waste, textile waste, wood waste and agricultural waste. Waste to energy (W2E) is one of the methods adopted in recycling of organic wastes.

Among all the wastes available for waste to energy process, automobile tyres and waste plastics are beleived to have adequate potential of energy source, as they are disposed in a large quantity throughout the world. Pyrolysis is one of the methods for converting waste automobile tyres into energy and value added products. In pyrolysis process, the waste tyres are heated in a closed vessel by external heating with the presence of little oxygen. The evolving volatiles in the pyrolysis reactor are condensed in a condenser to obtain the value added energy or chemicals. Generally, the temperature required for pyrolysis of tyres is in the range of 400-600^{o}C. The process offers three principal products namely, (a) pyrolysis oil, (b) pyrogas and (c) carbon black.

In recent years, the recycling of waste tyres by pyrolysis process has been found to be more attractive and technically feasible. There have been several tyre recycling pilot level and demonstrative plants installed, and commissioned in the world. In such a pyrolysis plant that follows vacuum pyrolysis process, four products are obtained such as, (i) light and heavy fraction oils, (ii) pyro gas, (iii) carbon black and (iv) steel wire. The light and heavy fraction oils are obtained in different condensers, based on the method of condensing the volatiles that are evolved from the pyrolysis reactor. In the present research study, the light fraction pyrolysis oil (LFPO) was examined for its suitability as a partial substitute to diesel fuel for compression ignition (CI) engines. Eight different modules of experimental investigations have been proposed and performed in a single cylinder, four stroke, air cooled, direct injection (DI) diesel engine with a power of 4.4 kW

at a constant speed of 1500 rpm. Few fuel and engine modifications were carried out to examine the engine behaviour in terms of combustion, performance and emissions when the engine was run on LFPO mode.

Before examining the utilization of LFPO in a CI engine, identification of group compounds of LFPO was done using Fourier Infra-Red Spectrometer and Gas Chromatograph. Also, LFPO was tested for its physio-chemical properties in a standard fuel testing laboratory. The physio-chemical properties were compared with that of diesel fuel, and tyre pyrolysis oil in crude form (TPO) which was obtained in a laboratory level reactor.

In the first module of experimental work, LFPO at different proportions (i.e., 20%, 40%, 60% and 80%) was blended with respective proportions of diesel fuel. The LFPO-diesel blends were denoted as 20LFPO, 40LFPO, 60LFPO and 80LPFO where the numeric value indicates the percentage of LFPO in the LFPO-diesel blend. All these four blends were tested in the test engine at no load, 25%, 50%, 75% and 100% load. The combustion, performance and emission parameters of the engine run on different blends were evaluated, analysed and compared with those of diesel fuel operation. Based on the results, 40LFPO comprising 40% LFPO and 60% diesel fuel was chosen as an optimum fuel blend.

In the second module, the 40LFPO blend was tested in the same engine by varying the fuel injection timing of the engine. Two advancements i.e., 26 and 24.5^{o}CAbTDC (crank angle before top dead centre) and two retardations (i.e., 21 and 20^{o}CAbTDC) of injection timings were considered to optimize the fuel injection timing for the 40LFPO operation. The combustion, performance and emission parameters of the engine run on 40LFPO at varied injection timings were evaluated, analysed and compared with those of diesel fuel operation. Based on the experimental results, 26^{o}CAbTDC was observed to be the optimum fuel injection timing.

The main problem with the 40LFPO is its lower cetane number compared to diesel fuel. Therefore, an attempt was made to add small quantities of an ignition improver with the 40LFPO in the third module. Diethyl ether (DEE), whose cetane number is greater than that of diesel was added to the 40LFPO. The percentage of DEE was varied from 1% to 4% in steps of 1% on a volume basis. The results of the combustion, performance and emission parameters of the engine run on the 40LFPO-DEE blend were evaluated and

compared with those of the diesel operation of the same engine. The addition of 4% DEE gave better performance and some exhaust emissions lower than those of 40LFPO at full load. However, they were marginally higher than those of diesel operation at full load.

Therefore, in the fourth module, another attempt was made in which an oxygenate additive was tried for improving the performance of the engine. Dimethyl carbonate (DMC) was used as an oxygenate additive for the investigation, and it was added in small quantities with the 40LFPO blend. The test fuels were designated as 40LFPO2DMC, 40LFPO4DMC, 40LFPO6DMC, 40LFPO8DMC, 40LFPO10DMC and 40LFPO12DMC where the numeric values like 2, 4, 6, 8, 10 and 12 indicate the percentage of DMC in the blend keeping LFPO constant at 40%. The combustion, performance and emission parameters of the engine were evaluated and compared with those of diesel fuel operation. The engine operated with 40LFPO10DMC exhibited better performance and lower emissions than that operated with other 40LFPODMC blends.

From the previous experimental results, it was understood that even with the oxygenated additive, the 40LFPO blend exhibited inferior performance and higher smoke emission than those of diesel operation at full load in the same engine. Hence, as a fifth module, turbulence was created in the combustion chamber by providing an internal jet in the piston for the engine run with 40LFPO10DMC. The investigation results in terms of combustion, performance and emissions were compared with those of the engine run with the conventional diesel fuel, and 40LFPO10DMC with and without turbulence inducement.

The engine run on 40LFPO10DMC produced higher quantities of NO and CO_2 in the engine exhaust. Hence, an attempt was made to reduce NO emission from the LFPO based operation. Exhaust gas was cooled and recirculated at four different percentage viz., 10%, 20%, 30% and 40%. The engine behavior in terms of the combustion, performance and emission were evaluated for the exhaust gas recirculation (EGR) operation, when the engine was run on 40LFPO10DMC. The results indicated that 20% EGR gave better performance and lower emission than the other EGR flow rates.

The CO_2 was found to be higher by about 47% in operating the engine with internal jet piston modification and 20% EGR fuelled with a blend consisting of 40% LFPO, 10% DMC and 50% diesel (i.e. in short, 40LFPO10DMC+IJP+20EGR operation) compared to that of diesel operation at full load. Hence, a carbon capture method was used to reduce

the CO_2 emitted from the engine exhaust. A metal chamber was fabricated and fitted in the engine exhaust. Zeolite pellets of size 3 mm were filled in the chamber. The combustion and emission were evaluated for 40LFPO10DMC+IJP+20EGR with and without zeolite and compared with those of diesel operation. The results revealed that by introducing carbon capture in the engine exhaust, CO_2 was reduced by about 48% with zeolite pellets compared to that of 40LFPO10DMC+IJP+20EGR operation respectively at full load.

As a final step, a short term durability test was carried out to assess various engine components and contamination in lubricating oil, when the engine was run on 40LFPO10DMC+IJP+20EGR.

After running 100 hours the engine was opened and engine components were dismantled for observation. The lubricating oil was analysed using atomic absorption spectroscopy. It was found that the results of the visual inspection of carbon deposits on different engine components showed the traces of carbon deposits in the cylinder head, piston crown and injector nozzle tip of the engine fuelled with 40LFPO10DMC+IJP+20EGR operation. The marginal wear of the engine components was noticed in the case of fuel injection pump. The lubricating oil properties were found to be deteriorated with the 40LFPO10DMC+IJP+20EGR operation. This may be the lower lubricity offered by LFPO with the 20EGR operation of the engine.

Based on the present research study, it is finally concluded that 40LFPO10DMC blend can be recommended to substitute pure diesel fuel for running a CI engine having two modifications i.e., internal jet piston and 20% EGR. Further, zeolite pellets are also recommended for use in the engine exhaust chamber to reduce CO_2 emission.

Keywords**: **Combustion; diesel engine; diethyl ether (DEE); dimethyl carbonate (DMC); durability; emission; exhaust gas recirculation (EGR); performance; pyrolysis oil; scarp tyre; zeolite.

Contents

List of Figures

List of Tables

NOMENCLATURE

AAS	Atomic absorption spectroscopy
ADC	Analog to digital converter
ASTM	American society for testing and materials
BET	Brunauer–emmett–teller
BP	Brake power
BSEC	Brake specific energy consumption
BSFC	Brake specific fuel consumption
BTE	Brake thermal efficiency
CA	Crank angle
CCS	Carbon capture and storage
C&D	Construction and demolition
CFR	Co-operative fuel research
CI	Compression ignition
CO	Carbon monoxide
CO_2	Carbon dioxide
CR	Compression ratio
CSB	Conical spouted bed
DEC	Diethyl carbonate
DEA	Diethyl adipate
DEE	Diethyl ether
DES	Diethyl succinate
DF	Diesel fuel
DI	Direct injection
DLF	Diesel like fuel
DMC	Dimethyl carbonate
DME	Dimethyl ether
DMM	Dimethoxymethane
DTG	Derivative thermo gravimetric
DTPO	Distilled tyre pyrolysis oil
ECU	Electronic control unit

EGR	Exhaust gas recirculation
EGT	Exhaust gas temperature
EPA	Environmental protection agency
FAME	Fatty acid methyl ester
FBR	Fixed bed reactors
FT-IR	Fourier transforms-infrared spectroscopy
GC-MS	Gas chromatography-mass spectrometry
GHG	Greenhouse gas
GWP	Global warming potential
HC	Hydrocarbon
HDPE	High density polyethylene
HDS	Hydrodesulphurization
HFPO	Heavy fraction pyrolysis oil
HHV	Higher heating value
HRR	Heat release rate
IC	Internal combustion
ICFB	Internally circulating fluidized bed
IP	Injection pressure
IT	Injection timing
JME	Jatropha methyl ester
LDPE	Low density polyethylene
LFPO	Light fraction pyrolysis oil
MSW	Municipal solid waste
NDIR	Non dispersive infrared
NO	Nitric oxide
NO_x	Oxides of nitrogen
NZ	Natural zeolite
PAH	Polycyclic aromatic hydrocarbon
PC	Personal computer
PGL	Pyrolysis, gasification and liquefaction
PJO	Preheated jatropha oil
PM	Particulate matter
PODE3-4	Polyoxymethylene dimethyl ethers

PS	Pyrolysis of polystyrene
RDF	Refuse-derived fuel
RFG	Recycled flue gas
SFB	Swirling fluidized bed
SI	Spark ignition
SOI	Start of fuel injection
STPO	Scrap tyre pyrolysis oil
TCD	Thermal conductivity detector
TDC	Top dead centre
TDF	Tyre derived fuel
TGA	Thermo gravimetric analyser
THC	Total hydrocarbon
TPL	Tyre pyrolysis liquid
TPO	Tyre pyrolysis oil
UHC	Unburnt hydrocarbon emissions
VOC	Volatile organic carbons
W2E	Waste to energy
WPO	Wood pyrolysis oil
WTPO	Waste tyre pyrolysis oil
ZDDP	Zinc di-alkyl-di-thio-phosphate

Chapter 1

INTRODUCTION

1.1 General

One of the major problems associated with the human life today is disposal of different kinds of waste. Generally, waste in any form originates from individual houses, streets and roads, municipal areas, agriculture sites, industries, etc. Disposal of waste cannot be fully eliminated, but it can be minimized by adopting different waste management practices. While developed countries have much better waste management practices, developing and underdeveloped countries are still struggling to plan and implement waste management practices. Among different wastes available, waste tyres and plastics are potentially converted into value added products in the form of energy or fuels and chemicals. This chapter presents problems of waste disposal, different types of organic waste, waste management practices that are followed in the world. This chapter also presents different waste tyre management options that are carried out today in various parts of the world. Further, this chapter also provides the importance of tyre recycling and their updated information of tyre recycling industry in some of the developed countries including India. Finally, the chapter also briefs the organization of the thesis.

1.2 EPA's Policy

The United Nations' Environmental division indicated that the increasing volume and complexity of waste associated with the modern economy is a growing problem to ecosystems and human health. It is reported that about 11.2 billion tons of solid waste are collected worldwide every year, and decay of the organic proportion of solid waste is contributing about 5 per cent of global greenhouse gas (GHG) emissions. Therefore, developing a cleaner environment is one of the foremost tasks of any country. According to the Environmental Protection Agency's (EPA's) clean and green policy, six objectives are focused today which include: (i) protect human health and the environment by taking necessary steps, (ii) utilization of waste land, (iii) maintain and improve water

resources and quality, (iv) reduce air emissions and greenhouse gas (GHG) production, (v) minimize material use and waste production, and (vi) conserve natural resources and energy. Some of the methods adopted by many countries to meet these objectives are: (i) utilization of renewable energy resources to a maximum extent possible, (ii) introducing clean diesel technologies, (iii) water conservation and efficiency approaches, (iv) sustainable site design, (v) reuse and recycling of different materials with in regulatory requirements that are available in municipal, industrial and other sites (vi) environmentally preferable purchasing, and (vii) introducing GHG emission reduction technologies [1].

In this context, conversion of waste to energy (W2E) process is considered as an important approach to meet some of the objectives. In recent years, many research works have been funded by several government agencies to convert different organic substances originated from agriculture, municipal and industrial wastes into energy [2].

1.3 Organic Wastes

Waste is generated universally and is a direct consequence of all human activities. Waste substances in the form of solid, liquid and gas are generated everywhere in the world. The quantity of waste disposed in all these three categories cannot be estimated as it is a continuous process.

Wastes in the form of solid, liquid and gas are found in the following types:

a) Household waste
b) Municipal waste (MSW) and agriculture waste
c) Commercial and non-hazardous industrial wastes
d) Hazardous (toxic) industrial wastes
e) Construction and demolition (C&D) waste
f) Health care wastes (e.g. hospitals, medical research facilities)
g) Human and animal wastes, and incinerator waste
h) Biomass waste

1.3.1 Solid organic wastes

Solid wastes are mainly disposed in the open land or a landfill, because it is the simplest, cheapest and most cost-effective method of disposing waste. In many of the developing countries and underdeveloped countries, the generated wastes are disposed in landfills, while in developing countries the fraction of disposal is comparatively less. Although the

proportion of waste to landfill may decrease in future, the total volumes of municipal, industrial and agriculture wastes will increase. Solid waste composition, its rate of generation, and methods of treatment and disposal vary considerably throughout the world and largely determine the potential of waste to impair ground water quality [3]. The solid organic wastes can be segregated from other wastes and easily transported to the process units for different applications, such as composting, secondary products by reuse or recycling.

1.3.2 Liquid wastes

Liquid wastes are commonly discharged into sewers or rivers or sea. Many countries impose different rules and regulations for pretreatment before discharging them into appropriate places. In many countries, the rules and regulations are either not sufficiently implemented, or partially discharged into water bodies or allowed to infiltrate into the ground. Indiscriminate disposal of liquid wastes causes a major threat to both surface and groundwater. General examples of liquid wastes include effluent from leather industries, and wastes from process industries, such as textiles, food industry and sugar industry. The different solid and liquid organic wastes are potentially available in the form of agricultural, industrial and municipal areas. Table 1.1 lists some of the commonly available organic wastes that can be used for deriving energy and fuels.

1.3.3 Gaseous wastes

Gaseous waste is normally vented to the atmosphere, either with or without pretreatment depending on composition and the specific regulations of the country involved. The examples of gaseous waste include gas exhausted from the chemical industry, sugar industry, fertilizer industry, etc. Almost all the waste gases are vented to the atmosphere after necessary pretreatment.

1.4 Waste Management Practices

Figure 1.1 shows the inverted pyramid that represents different methods that are adopted in waste management. In waste management, there are mainly four options considered which are (a) refuse (b) reuse (c) recycle, and (d) reduce. Many of the combustible components of municipal solid waste are also biodegradable, and thus can serve as substrates for biological conversion to a fuel gas that is immediately converted into energy (i.e., direct conversion into heat energy), or that can be stored or transported for later

conversion (i.e., indirect conversion). The energy possessed by different wastes and the methods by which the energy is derived from them are not the same.

Table 1.1: Different organic wastes available for waste to energy options [4]

Sector	Solid wastes	Remark
Industrial	Paper, cardboard, plastics, wood, food wastes, glass, metals, hazardous wastes, rubber, plastics, leather, tyre, electronic wastes, chemicals, metals, construction material wastes, bagasse, oil cakes, wood waste, nuclear waste.	Non-recyclable materials are dumped in open sites. Nuclear waste is disposed of in safe dump yards.
Commercial	Paper, cardboard, plastics, wood, food wastes, glass, metals, hazardous wastes, construction material wastes, bagasse, oil cakes, wood waste.	Non-recyclable materials are not dumped properly.
Municipal	Street sweepings, landscape and tree trimmings, general wastes from parks, beaches, and other recreational areas, construction material wastes.	Recyclable and Non-recyclable materials are segregated in some municipalities and most of the corporations.
Institutional	Paper, cardboard, plastics, wood, food wastes, glass, metals, hazardous waste, construction material wastes.	Non-recyclable materials are not dumped properly.
Hospital	Rubber and plastics, blood, small metals like syringe needles, glass bottles, cotton waste, hazardous chemicals	Non-recyclable materials are not dumped properly. Recyclable materials are not properly reused or recycled.
Residential	Food wastes, paper, cardboard, plastics, rubber, leather, textiles, cotton, glass, metals, ashes, special wastes (bulky items, consumer electronics, batteries, oil, tyre), household hazardous wastes	Non-recyclable materials are not dumped properly. Recyclable materials are not properly recycled.
Agricultural	Plant and crop residues, animal and poultry wastes, vegetable seeds, bagasse, primary and secondary wood	Reusable and recyclable materials are not properly reused or recycled.

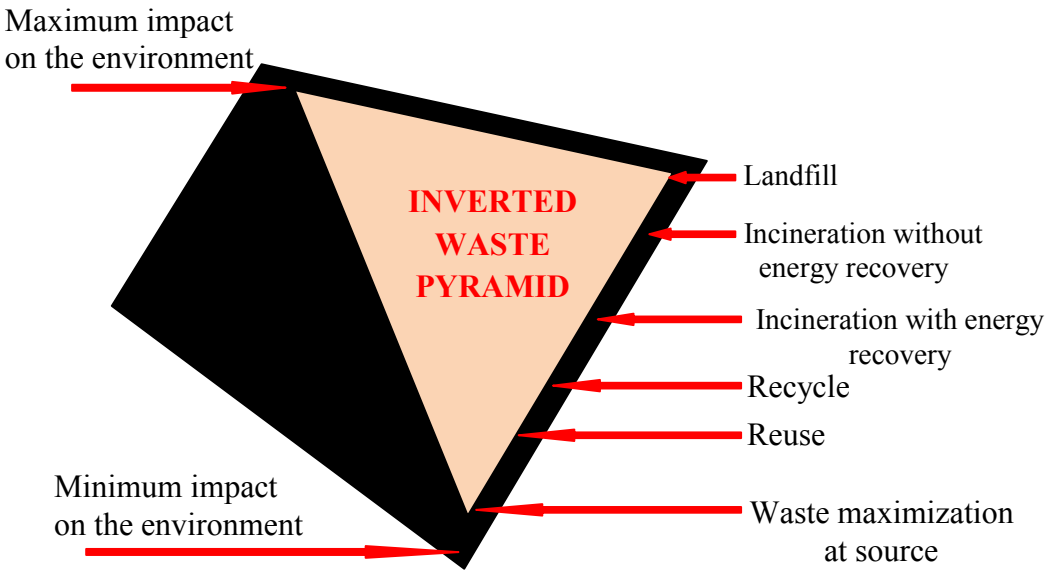

Figure 1.1: Inverted pyramid representing waste management options [5]

Figure 1.2 shows the various methods of energy recovery, and the types of fuel and forms of energy that can be produced from municipal wastes. It can be observed from the figure that energy recovery can be accomplished with or without mechanical, manual, or mechanical/manual processing of the wastes prior to their conversion (i.e., pre-processing). Energy recovery through pre-processing may be accomplished by one or more of the methods. In pre-processing of a waste, recovery of the organic or combustible fraction is segregated from the remainder of the waste.

1.4.1 Incineration

The incineration of raw (unprocessed) wastes is practiced throughout the world, particularly in European countries where it has been in use for many decades. The simplest method of incineration is open burning. With the continuous changes that have taken place in technology and environmental concerns, the incineration process has gradually improved. Initially, the main objective of the process was to reduce the volume of the material requiring disposal. Later, the products of combustion (hot gases) were used to generate steam. Incineration reduces the volume of the original waste by 95-96%. Two main advantages of incineration are (i) waste volumes are reduced by an estimated of 80-95% and (ii) the need for land and landfill space is greatly reduced. For urban areas, this is important, as urban land bear comparatively higher price. The main disadvantages of incineration are (i) it is expensive to build, operate, and maintain, (ii) it requires skilled staff to run and maintain them; and (iii) it emits carcinogenic emissions.

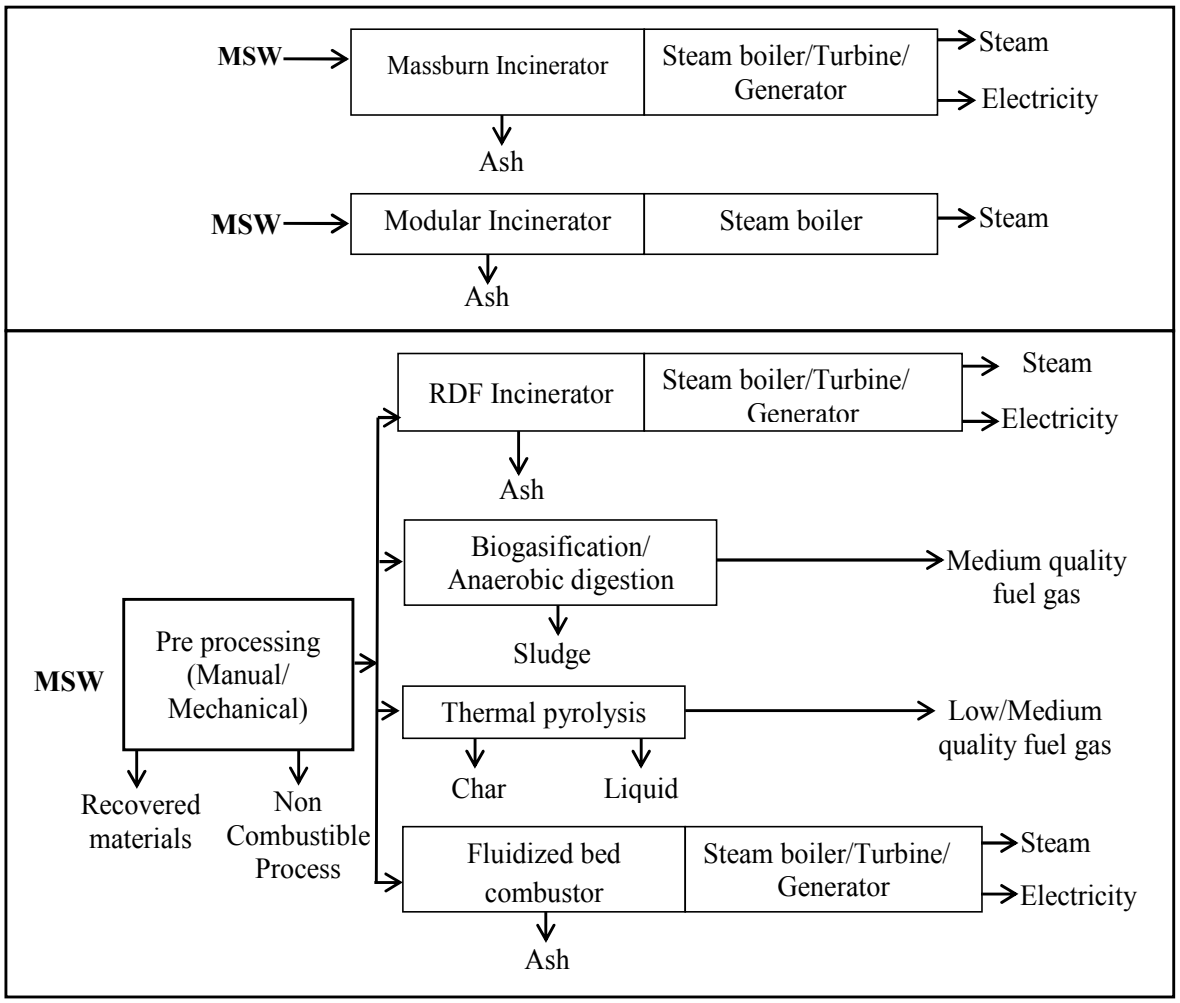

Figure 1.2: Different methods of solid wastes to energy options

1.4.2 Refuse derived fuel

The production of refuse-derived fuel (RDF) typically involves the use of a number of operations which include size reduction, screening and magnetic separation. Manual operations (e.g., sorting of materials) are also used, especially if material recovery and RDF recovery are integrated into one processing facility. Manual processes of separation are especially appropriate in many cases in developing countries, singularly or in combination with mechanical processing operations. For recovery of RDF, separation of the combustibles from the non-combustibles in the waste is important. RDF can serve as a feedstock in incineration systems combined with energy recovery equipment.

1.4.3 Thermal gasification

Thermal gasification is one of the solid waste techniques used in the solid waste management from which energy or fuels and chemicals are obtained. Indeed, with certain

processes the fraction in the form of a combustible gas may be much less than that in a solid or a liquid form, or in both. Gasification can be complex and expensive.
Pyrolysis is the fractional distillation of the organic matter in a waste in absence of oxygen or little presence of oxygen. The end products are gases, liquids (oils and tars), and solids (char).

1.5 Disposal of Tyres

It is reported that about one billion waste vehicle tyres are disposed every year across the world. Vehicle tyres contain long-chain polymers (butadiene, isoprene and styrene-butadiene) which are cross-linked with sulphur. They do not have excessive resistance to degradation and hence ultimately cause severe environmental problems [6]. There are different methods for the waste management of disposed tyres, which are described below.

1.5.1 Landfill

At present, about 50% of the waste automobile tyres are used for landfill. Some tyres are also used for engineering purposes in landfill sites. If disposed off in large volumes, tyres in landfill sites can lead to fire which is difficult to control. It also causes instability by rising to the surface. This affects long-term settlement, and may cause problems for future use and land reclamation. Tyres buried in landfill sites create a fire hazardous, and polluting surroundings. Such fires are difficult to control. This condition can result in uncontrolled pyrolysis of the tyres, which will produce a complex mixture of chemicals. Many countries insist to reduce the quantity of waste tyres used for land fill.

1.5.2 Crumbing

Another method of disposal is crumbing. This method involves cutting of tyres at several stages until rubber attains crumb form. This product can then be used in several applications such as:

a) Rubber blocks for children's play areas
b) Low quality rubber products
c) Production of asphalt.

There are several possible outlets for tyre crumbing. But, the current use is only around 25% of the total waste. It potentially offers the most effective solution for recycling and does not directly cause the additional pollution problem.

1.5.3 Remould

Remould of waste tyres requires a lot of work on the part of the manufacturers, as many designs of tyres are not suitable for remould. About 20% of total waste automobile tyres are removable, and in turn this will increase by 5% more in future.

1.5.4 Incineration

An alternative method for disposal of waste automobile tyres is incineration. By incineration of waste automobile tyres, electricity can be generated. However, high investment cost and high pollution are the two major problems associated with incineration of waste automobile tyres.

1.5.5 Tyre derived fuel

Tyre has a high energy value, and it can be utilised for the generation of heat and electrical power. The substance obtained from tyre for such purposes is called Tyre Derived Fuel (TDF). It is composed of shredded waste tyres approximately 1-5 mm in size. The application of TDF is to substitute coal as the energy source, because waste tyre has a higher heating value than coal. Instead of coal, TDF is burnt in cement kilns for heating purpose. However, because of chemicals in the tyres, the manufacturing ability of cement kiln decreases. There is also a potential problem of atmospheric pollution. Any process that utilizes TDF as a fuel is required to meet statutory air quality requirements for emissions.

1.5.6 Pyrolysis and gasification

The current disposal method of waste tyres by land filling causes a loss of valuable resources. Pyrolysis is a better method of disposing waste automobile tyres [6, 7]. In this process, waste organic substances are converted into value added products such as fuels or chemicals in the form of solid, liquid or gas. It is a thermo-chemical conversion process in which an irreversible chemical change is caused by the action of heat in the absence of oxygen [8]. In the process of pyrolysis, the feedstock is fed into an oxygen free or less oxygen present reactor, and heated. As the temperature rises, the organic matter breaks down into simpler substances and condensed into volume added products. The end products of the reaction depend on the conditions employed. At a lower temperature around 500^{o}C organic liquid predominates while at a temperature nearer 1000^{o}C a combustible mixture of gases results. The chemical process in pyrolysis is similar to

distillation of coal to produce synthetic gases, tars, oils and coke. The reaction of water on heated coals with reduced air supply is:

$H_2O+C = H_2 +CO$ (1.1)

$C+O_2 = CO_2$ (1.2)

$CO_2+C = 2CO$ (1.3)

The input material needs to be graded to remove the non-combustible materials (e.g., soil, metal). It is dried if necessary, chopped or shredded and then stored for use. The pyrolysis units are most easily operated below 600^{o}C. In principle, the waste automobile tyres are thermally decomposed in the absence of oxygen or little presence of oxygen in a closed chamber by the application of heat. The main advantages of pyrolysis include compactness, simple equipment, low pressure operation, negligible waste product and high energy conversion efficiency of the order of 83% [9]. In the last three decades, many researchers have documented their research works by adopting different methods of pyrolysis such as vacuum pyrolysis **[**10-12], flash pyrolysis [13], fluidized bed pyrolysis [14-15], steam pyrolysis [16] and catalytic pyrolysis [17-18].

The percentages of these products vary depending on the nature of the feedstock, heating rate, heat input, method of pyrolysis and nature of condensation. The tyre pyrolysis oil (TPO) percentage is the highest among the products obtained, and the oil is composed of lighter and heavier fractions of hydrocarbons containing carbon percentage varying from 5 to 20 in it. This indicated that TPO has gasoline, diesel, kerosene fractions and small fractions of benzene in it. The TPO has a lower cetane number, higher aromatic content, higher density and lower heating value than those of diesel fuel. Other physical and chemical properties are similar to those of diesel fuel. Figure 1.3 illustrates the pyrolysis process of waste tyres, products and different applications of the pyrolysis products. In the last decade, countries such as India, China, Canada and France made attempts in running batch type, pilot level tyre pyrolysis plants with capacities of 5 and 10 tons per batch for recycling tyres. In this kind of plants, light and heavy fractions were obtained separately. The complete description is given in Chapter 3.

It is to be noted that pyrolysis, incineration, combustion, TDF, liquefaction and gasification can recover energy and/or valuable chemicals from the treatment of waste tyres. Incineration and TDF generate the emission of hazardous pollutants extremely harmful to human health and natural environment. The fumes emitted from sites are packed with many toxic chemicals like volatile organic compounds (e.g., benzene), metals

(e.g., lead), polycyclic aromatic hydrocarbons (e.g., benzo, pyrene), and synthetic rubber components (e.g., butadiene and styrene). The chlorine content in tyres also leads to the creation of dioxins and furans, which are extremely toxic chemicals when tyres are burned.

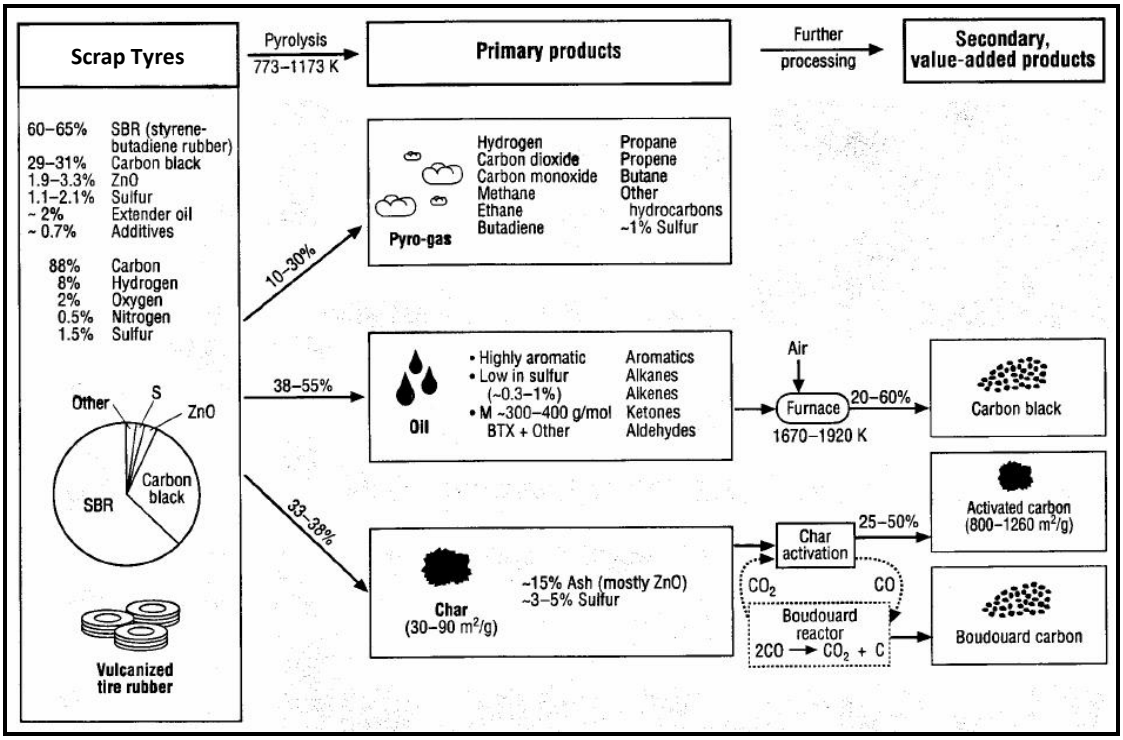

Figure 1.3: Pyrolysis process, products and applications of products

The incineration and co-combustion of whole tyre in cement kilns has been banned in many countries concerning the emissions generated. Moreover, the sulphur composition of waste tyre is normally larger than 1 wt%. Pyrolysis, gasification and liquefaction (PGL) may be considered to be better ways for the treatment of waste tyres. These technologies may become more important as the supplies of fossil fuels become depleted.

In recent years, the commercialization of pyrolysis oil obtained by recycling of waste automobile tyres for heat and power applications have been found to be more attractive and technically feasible. There have been several tyre recycling pilot level and demonstrative plants installed, and commissioned in the world. In such a pyrolysis plant that follows vacuum pyrolysis process, there are four products obtained which are (i) light fraction pyrolysis oil (LFPO) and heavy fraction oil (HFPO), (ii) pyro-gas, (iii) carbon black and (iv) steel slag in solid form. The LFPO and HFPO are obtained in two different condensers, based on the method of condensing volatiles that are evolved from the pyrolysis reactor.

1.6 Organisation of Thesis

This research study is aimed to examine the possibilities of using LFPO as an alternative fuel for direct injection compression ignition engines. The complete objectives are given at the end of Chapter 2. The remainder of the thesis comprises the following chapters:

Chapter 2 presents the literature survey on different types of pyrolysis process, and feedstock used in pyrolysis. It also provides a brief review of compression ignition (CI) engine fuel properties, phenomenon of CI engine combustion, emissions from CI engines, suitability of pyrolysis oil for CI engines, review on methods to use alternative fuels in CI engines and pyrolysis oil in CI engines. The chapter finally provides summary and research gaps.

Chapter 3 discusses the characterization of the LFPO. It also includes the FTIR and GC-MS analyses of LFPO. The chapter also provides proximate and ultimate analyses of LFPO. Furthermore, the physio-chemical properties of LFPO are compared with those of diesel and crude tyre pyrolysis oil.

Chapter 4 details the experimental methodology adopted in this study. The chapter initially provides information on different instruments that were used for experimentation. Furthermore, different techniques adopted in this study to use LFPO as an alternative fuel in a CI engine are described completely.

Chapter 5 discusses the experimental results that are obtained for the combustion, performance and emission parameters of the LFPO fuelled engine at different operating conditions in comparison with the diesel operation of the same engine.

Chapter 6 summarizes the conclusions drawn from the above studies and produces the scope for future work.

Chapter 2

LITERATURE REVIEW

2.1 General

In recent years, the term “Waste to Energy” is gaining popularity because of two reasons i.e., (i) it can reduce the environmental problem, and (ii) it can contribute to energy sustainability to some extent. Among different methods available for waste to energy conversion, a thermo-chemical conversion method called pyrolysis has been largely adopted by many researchers, because it is not climate or seasonal dependent; it is faster process to produce the products, and any organic substances can be converted into value added energy or fuels and chemicals. As the researcher has developed interest to work in the area of alternative fuels for internal combustion (IC) engines, and anticipated that there would be a better research scope in utilizing pyrolysis oil for compression ignition (CI) engines, literature available in the area of production of pyrolysis oils, and their utilization in CI engines have been reviewed in this chapter. It also provides a review of literature related to different methods of pyrolysis process, different reactors and different feedstocks used in pyrolysis process. Further, the different research works that have been carried out on utilization of tyre pyrolysis oil in CI engines with and without engine modifications are also discussed.

2.2. Types of Pyrolysis

There are different types of pyrolysis depending on the operating conditions, such as the heating rate, the volatiles residence time and the temperature. Based on the nature of process, it can be classified into two groups i.e., (i) slow and (ii) fast. It can also be classified on the basis of the environment used, such as vacuum pyrolysis, oxidative pyrolysis, hydro-pyrolysis, steam-pyrolysis, catalytic-pyrolysis and fluidised bed pyrolysis. Depending on the heater system, it can be classified as (a) microwave pyrolysis and (b) plasma pyrolysis. Conventionally, fluidized and entrained beds reactors are associated with fast pyrolysis, while fixed bed reactors (FBR) are associated with slow

pyrolysis (a batch or semi-batch process). It is possible to perform fast pyrolysis in FBR adjusting the heating rate and the volatiles residence time for research purposes. Other types of reactors, such as the ablative reactor and the rotating cone reacting (i.e., usually used for liquid production since the heating rate is high and the vapour residence time is relative short), may also be categorized for carrying out fast pyrolysis.

2.2.1 Slow pyrolysis

This type of pyrolysis is considered as a low pyrolytic decomposition at low temperatures. The process is characterized by low heating rates, relatively long solid and vapour residence times (in the order of minutes to hours) and sometimes by low temperature. Longer residence times result in a secondary conversion of primary products, yielding more coke, tar, and thermally stable products [19]. Unlike in fast pyrolysis, more char is produced, in the slow pyrolysis although tar and gases are also obtained.

2.2.2 Fast pyrolysis

The process implies a rapid thermal decomposition which is categorized by higher heating rates. It usually requires small particle sizes and devices with a special design to remove the vapours released quickly. High heating rates with short hot zone residence times and rapid quenching of the volatile products favour the condensation of the volatiles released in the pyrolysis process into liquid pyrolysis oil [20]. Thus, a liquid fuel with a higher calorific value is obtained. In fact, fast pyrolysis is recognized as an effective conversion route for the production of liquid fuels, chemicals and derived products with higher yield (usually around 50-60 wt% for rubber feedstock). Fast pyrolysis is usually performed in fluidized beds, entrained, ablative and free-fall reactors where the reaction time is of the order of milliseconds to seconds. It is generally accepted that the volatiles residence time must be lower than 2s [21]. Longer residence times result in significant reduction in organic yield resulting in the occurrence of secondary reactions as thermal cracking. Ultra-pyrolysis or ultra-rapid pyrolysis refers to thermal cracking under conditions of high temperature (in excess of 700^{o}C), very short reaction time (much less than 500 ms), higher heating rate (greater than 1000 ^{o}C/s) and rapid product quenching [22].

2.2.3 Catalytic pyrolysis

Normally, catalytic pyrolysis is the name given to any pyrolytic process that comprises a catalytic material in the same process in order to favour or upgrade some yield or some

properties of the products. For example, catalytic pyrolysis of waste tyres was carried out for the production of single ring aromatic compounds in the liquid fraction, such as benzene, toluene and the m-, p- and o-xylenes using zeolite catalysts (Y-type and ZSM-5) [23]. Kar [24] found an enhancement of the liquid fraction yield and its fuel properties using an expanded perlite as catalyst. A catalyst to tyre ratio of 0.1l leads to an increase of 8.48 wt% of the liquid fraction compared to that of the non-catalytic pyrolysis. Zhang et al **[**25**]** reported that the NaOH addition favoured lower pyrolysis temperatures. They were able to achieve 49.7 wt% of liquid yield at 480^{o}C as well as a remarkably increase of H_2 in the gas fraction. Similarly, a considerable increase of the gas yield at expense of the liquid yield was also reported by Dung et al [26] using Ru/MCM-41 as a catalyst. In addition to this, higher yield to light olefins (4 times higher than non-catalytic pyrolysis) was also obtained. Elbaba et al [27] observed a high increase in H_2 and CO concentrations as well as a reduction in CH_4 and C_2-C_4 concentrations, when waste tyre was subjected to a two-stage pyrolysis-gasification process at 500 and 800^{o}C respectively, in presence of a Ni-Mg-Al (1:1:1) catalyst.

2.3 Feed Stocks in Pyrolysis

Many researchers carried out basic research in pyrolysis to determine the process yields, the effects of the heating rate, heating time, etc. Most of the researchers stated that the important variables that affect the maximum yield and the quality of the product are: (i) the nature of feed stock (density, percentage of volatile matter, etc.), (ii) heating rate, (iii) vapor residence time, (iv) effectiveness of condensation, and (v) reactor design and nature of process. Depending upon the feedstock used, the liquid obtained in the process can be referred to as simply (i) bio-oil and (ii) pyrolysis oil. The most important feed stocks used in research work for possible commercialization are (i) biomass, (ii) waste tyres, and (iii) waste plastics. The following subsections provide a review about pyrolysis of these substances, operating conditions, yield of products etc.

2.3.1 Biomass pyrolysis

The pyrolysis oil obtained from biomass sources has great attraction, but it has not been used in proper way. Many attempts have been made in the recent past, to extract fuel through pyrolysis of various biomass sources like (i) wood and agriculture residue, (ii) edible oil cakes, (iii) edible oil seeds and (iv) non-edible oil seeds.

Generally, the liquid obtained from biomass sources is referred in the literature by various terms, such as bio oil, bio-crude oil, bio-fuel oil, wood liquid, wood pyrolysis oil (WPO), liquid smoke, wood distillates, pyroligneous tar and pyroligneous acid. The oil derived from other than biomass sources is called pyrolysis oil. Some researchers name the pyrolysis oil following the feedstock name. For example, pyrolysis oil derived from waste rubber is referred as rubber pyrolysis oil.

Prakash et al [28] produced wood pyrolysis oil (WPO) from waste wood that was obtained from timber industries. They used a fixed bed reactor and pyrolysis was carried out under vacuum conditions. The process was carried out between 200-400^{o}C and the heating rate was 10^{o}C. The reactor was externally heated with the help of an electrical heating coil. The percentage of WPO obtained in the process was about 30-40%.

They indicated that WPO obtained from the pyrolysis of wood, is a free flowing dark-brown organic liquid accompanied by a strong acid smell. It comprised of different sized molecules, which were derived from the depolymerization and fragmentation reaction of three biomass building blocks namely, cellulose, hemicellulose and lignin. The WPO had a high oxygen and moisture contents, but poor volatility, high viscosity, corrosiveness and cold flow properties. Which limit its use as a transportation fuel by itself without the addition of suitable additives. After analysing the physiochemical properties of WPO, they recommended that the WPO cannot be blended directly with diesel due to poor miscibility, different surface tension and hydroscopic characteristics [29]. Water content is commonly seen in the bio-oil obtained from any biomass feedstock. The mass fraction of water content in the bio-oil is in the range of 10-35% in most of the cases. They indicated that this value would depend on the original moisture content of biomass and also on the pyrolysis conditions. The bio-oil becomes unstable, if more than a certain amount of water is added to it. Further the microstructure of the bio oil will be destroyed, and it will separate into water soluble and oily phases. Bridgewater et al [30] suggested that the bio-oil can be used as a fuel in boilers, diesel engines or gas turbines for heat and electricity generation.

Nasir and Jamil [31] studied the prospects of rubber pyrolysis oil as a fuel in diesel engines. The properties of this oil were determined to check its suitability as fuel in diesel engine. The authors reported that this had properties similar to that of diesel fuel, and based on the results they suggested that the oil could be used as a substitute to diesel.

There are considerable number of research works documented in the area of pyrolysis of different feed stocks that originate from agriculture, municipal and industrial sectors.

Table 2.1 summarizes the names of feedstocks used, nature of pyrolysis, pyrolysis conditions, bio-oil yield, etc. when pyrolysis is carried out with wood and agriculture residues. Research results indicated that the presence of ash in the feed stock can affect the pyrolysis products and the process. Polymerization occurs in the passages between the reactor and condenser which needs more attention in practical situations. Heat loss in the reactor due to conduction and radiation is inevitable in practice. Optimization of condensation will help to increase pyrolysis oil yield, and reduce the pyrogas and char/carbon black.

Sarkar and Chowdhury [32] examined the possibility of using mustard seed cake as a feedstock in a pyrolysis process with and without a catalyst. The reactor used in the process was a semi-batch type which had dimensions of 50 mm diameter and 640 mm long and the reactor was operated in the temperature range of 400 to 700^{o}C in a nitrogen atmosphere. The mustard press cake (MPC) was impregnated with NaCl (Merck purity > 99%) by quenching of MPC with the NaCl solution, and by the subsequent evaporation of the moisture in the hot air oven. The catalytic pyrolysis of MPC was carried out at temperatures of 400, 500 and 600^{o}C with the addition of 5 and 15% NaCl (w/w). The catalytic effects of NaCl on the pyrolysis of MPC were also investigated at three different temperatures viz., 200, 300 and 400^{o}C, and when catalyst loading was varied from 5-15% (w/w MPC).

Table 2.1 Pyrolysis of biomass and agricultural residues [4]

Feed stock	**Reactor type**	**Size of feed stock**	**Working conditions**	**Catalyst used**	**Product yield, (%)**
Subabul wood	Packed bed reactor, N_2 inert	~10-25g powder	500°C	Nil	22.6
Eucalyptus	Slow pyrolysis, sample size, Vacuum	< 1 mm, 1–2 mm 2–5 mm & 5–10 mm	350 to 600°C, 20°C/min	Mordenite, kaolin, silica–alumina, and fly ash	60.5
Bagasse	Packed bed reactor, N_2	~10-25g powder	500°C	Nil	NR
Rice Husk	Packed bed reactor, N_2	~10-25g powder	500°C	Nil	41.2
Millet Husk	Packed bed reactor, N_2	~10-25g powder	500°C	Nil	NR
Rice Straw	Packed bed reactor, N_2	~10-25g powder	500°C	Nil	47
Wheat Straw	Packed bed reactor, N_2	~10-25g powder	500°C	Nil	
Coconut shell	Packed bed reactor,	~10-25g powder	500°C	Nil	NR
Coconut shell powder	Slow pyrolysis fixed bed, Vacuum	NR	400 and 60°C/min, 600°C	Nil	Char-22-31, Liquid- 38-44 and Gas 30-33
Coconut shell powder	Slow-semi batch reactor, Vacuum	NR	NR	Nil	49.5
Cashew nut	Packed bed reactor, N_2	~10-25g powder	500°C	Nil	NR
Ground nut	Packed bed reactor, N_2	~10-25g powder	500°C	Nil	40.5
Coir Pith	Packed bed reactor, N_2	~10-25g powder	500°C	Nil	29.5
Corn Stalks	Packed bed reactor, N_2	~10-25g powder	500°C	Nil	NR

NR: Not Reported

The research results obtained from pyrolysis of edible oil seed cakes and seeds are tabulated in Table 2.2. Although a significant research works were carried out using different edible oil seed cakes and seeds, only few researchers have explored the possibilities of using edible oil seeds as feedstock for pyrolysis. The effect of temperature on the yield of product was examined and the results are given in Table 2.2.

Table 2.2: Pyrolysis of edible oil seed cakes and seeds

Feed stock	Reactor type	Size of feed stock	Working condition	Catalyst used	Product yield (%)
Mustard seed press cake	Fixed bed	NR	673K, 500°C and 873K	Nil	41.17
Mustard seed press cake	Fixed bed	NR	673K, 500°C and 873K	5 % Nacl 5-15%	35.1
Deoiled ground nut cake	Slow pyrolysis, semi- batch	30 g	200-500^{o}C, 20 ^{o}C/min	Nil	50
Seasame seed	Slow pyrolysis, semi- batch	30 g	25 ^{o}C/min	Nil	58.97
Ground nut	Slow pyrolysis, semi- batch		25 ^{o}C/min	Nil	70.95

Similarly, Table 2.3 provides information on the pyrolysis of non-edible oil seed cakes and seeds.

Table 2.3: Pyrolysis of non-edible oil seed cakes and seeds.

Feed Stock	Reactor type	Working temperature	Heating rate	Vacuum /inert	Catalyst used	Optimum conditions	Product yield (%)
Jatropha curcas	Fixed bed slow pyrolysis	*	4 and 8 ^{0}C/min	Vaccum		550 ^{0}C/min	
Jatropha curcas	Flash pyrolysis-fludised bed reactor	350-550 ^{0}C	*	N_2	Nil	500 N2-1.75m> ^{3}/h, 0.7-1.0mm	64.25
Jatropha curcas	Fixed bed slow pyrolysis Electric heated	350-550 ^{0}C	*	Vaccum	*	*	*
Jatropha curcas	Flash pyrolysis-fluidised bed reactor, Electric heated	*	*	Vacuum	*	*	*
Jatropha curcas	Fixed bed	*	*	N_2 at 50 to 200 ml/min	*	550 ^{0}C, 150 ml/min N2	18.42
Pungam/ pongamia	Flash pyrolysis-fluidised bed reactor	400-550 ^{0}C		1.25-2.4 m^3h	*	0.3-0.6 mm, nitrogen flow rate of 1.75 m^3h and at 550 ^{0}C	46
Polanga	Slow pyrolysis-semi batch reactor	400-600 ^{0}C	*	Vacuum	Nil	550 ^{0}C	40

* Not reported

2.3.2 Municipal and industrial wastes

Municipal and industrial sectors dispose a large quantity of organic and inorganic wastes in the form of solid, liquid and gaseous form, and different kind of debris. For example, metal, junk, paper waste, wood waste, broken glass, plastic waste, cotton waste, leather waste, oil waste, etc. Among these, many of them are reusable, recyclable while some of them are disposed in land, sea or river, and air

Table 2.4: Industrial and municipal wastes (except waste tyres and plastics)

Feed stock	Reactor type	Size of feed stock	Working conditions	Product Yield (%)
Pine wood from packing box	Packed bed reactor, vacuum	5-10 mm	10 ^{o}C/min 400-600^{o}C	45-50
LDPE	Fixed bed, slow Pyrolysis, vacuum	160 mesh, 10 g + 0.5 g of the catalyst powder	30-550 °C. 10^{o}C/min	85.3
Cotton based varieties	Fixed bed, slow Pyrolysis, N_2	NR	573K to 1173K, 10^{o}C/min	58
Double chrome tanned waste	Double pyrolysis process (primary reactor for feedstock, secondary reactor for residual carbon)		900^{o}C	33.32
Spent engine oil	Quartz reactor, N_2	NR	573K to 873K; 10, 20, 30, 40, 50, 60 min	69
Glossy paper cup	Batch type pyrolyser, semi-batch reactor, slow pyrolysis, N_2	60 g	100 ^{o}C/min	11.25
Paper cup waste	Vacuum	15 g	325-425◦C, 20^{o}C/min	52

Limited studies are available on energy recovery through pyrolysis of dairy waste, leather waste and spent engine oil. Less density materials, such as waste wood and dairy waste require heating of maximum 500^{o}C, while municipal waste requires higher temperatures. Table 2.4 summarizes the experimental results of pyrolysis of some of the municipal and industrial wastes that were used as feedstock by different researchers.

2.3.3 Waste tyres

Passenger car tyres and truck tyres have a high calorific value of 35-40 MJ/kg, even greater than the most of conventional coal used in power plants by around 25-50%. Motor cycle tyre has a lower calorific value because it contains lower volatile fraction (58 wt%) and higher ash content (20 wt%) [33]. Generally, the ash content varies in the range between 2.5 and 20.1 wt%, the volatile matter varies between 57.50 and 73.7 wt%, and the fixed carbon ranges from 19.45 to 32.3 wt%. Although tyres and coal are materials with different nature, the substantial difference lies in the moisture and ash contents; which are usually greater for coal. Several research works have been carried out in the area of pyrolysis of waste automobile tyres. Some examples are discussed below and the important summary of the research results are tabulated in Table 2.5.

Chaala and Roy [34] carried out research studies on vacuum pyrolysis of used tyres. It was reported that the heavy fraction (b.p. > 350 ^{o}C) of the oil obtained during vacuum pyrolysis of used tyres was mainly composed of aromatic hydrocarbons. The possibility to use this fraction as a raw material in the coke industry was also investigated. The heating temperature rate maintained in the process was l0 ^{o}C/min. It was also reported that pyrolytic oil obtained from scrap tyres might represent an alternate feedstock for the coke industry.

Chang [7] studied on the degradation rate and product yields of waste tyre during pyrolysis without a catalyst. The weight loss of waste tyre during pyrolysis was measured using thermos-gravimetric analyser (TGA). Yields of gas, liquid and char products were measured, and the composition of liquid and the gas was analysed by a gas chromatograph (GC). It was reported that pyrolysis of waste tyre was found to be a fast reaction and the degradation rate was correlated in terms of pyrolysis conversion and temperature. It was stated that the rate increased with the temperature of pyrolysis. It was further reported that, the effect on the degradation rate of pyrolysis at temperature below 400°C is more sensitive than that above this temperature.

Cunliffe and Williams [20] studied the composition of oils derived from the batch pyrolysis of tyres in a nitrogen purged static bed batch reactor which was used to pyrolyse three kg in a batch of shredded scrap tyres at temperatures between 450°C and 600°C. It was stated that pyrolysis of scrap tyres produced oil similar to light fuel oil with respect to properties like calorific value, sulphur and nitrogen contents. The oils contained significant concentrations of polycyclic aromatic hydrocarbons some of which have been shown to be either carcinogenic or mutagenic. The concentration of poly aromatic hydrocarbon (PAH) increased from 1.5 to 3.4 wt. % of oil as the pyrolysis temperature increased from 450°C to 600°C.

Roy et al [11] studied about the carbon black produced from vacuum pyrolysis of used tyres. The potential applications of the different products were also analysed. It was mentioned that vacuum pyrolysis of used tyres has several advantages over other alternative tyre recycling methods. The main difference between atmospheric pyrolysis and vacuum pyrolysis is that at low temperatures (approximately 500°C), the residence time of the hydrocarbons formed from the cracked rubber is considerably shorter in the vacuum process than atmospheric pyrolysis so that undesirable reactions such as the formation of carbonaceous deposits on the pyrolytic carbon black and the secondary decomposition reactions of valuable compounds such as D-limonene are limited. It was concluded that the total pyrolytic oil may be directly used as a fuel or after distillation.

Rodriguez et al [35] studied the behavior and chemical analysis of tyre pyrolysis oil. The percentage of aromatics, aliphatics, nitrogenated compounds, benzothiazol were determined in tyre pyrolysis oil at various operating temperatures of the pyrolysis process. It was reported that tyre pyrolysis oil is a complex mixture of organic compounds of 5-20 carbons and a higher proportion of aromatics. Aromatics were found to be about 34.7% to 75.6% when the operating temperature was varied between 300^{o}C and 700^{o}C, while aliphatics were about 19.8% to 59.2%. In the same work, an automatic distillation test was also carried out at 500^{o}C to analyse the potential use of tyre pyrolysis oil as a petroleum fuel. It was also observed that more than 30% of the tyre pyrolysis oil was easily distillable with boiling points between 70^{o}C and 210^{o}C, which is the boiling point range specified for commercial petrol. On the other hand, 75% of the pyrolytic oil had a boiling point under 370^{o}C, which is the upper limit specified for 95% of distilled products of diesel oil. It was mentioned that distillation carried out between 150^{o}C and 370^{o}C exhibited a higher

proportion of lighter and heavier products, and a lower proportion of the middle range products than commercial diesel oil.

Zabaniotou and Stavropoulos [36] carried out pyrolysis of used automobile tyres and residual char utilization. In this study, the rubber portion of used car tyres was transformed by atmospheric pyrolysis into oil, gas and char in a captive sample reactor at atmospheric pressure, under helium atmosphere. The effect of temperature on the product yield was investigated. The alternative uses of pyrolysis char, such as combustion, gasification and active carbon preparation were examined, in order to produce fuels and value added materials. Initially, the pyrolysis char was burned and its reactivity was measured with respect to pyrolysis temperature. Then the char was gasified with steam and CO_2 to produce fuel gases, in a tubular stainless steel reactor. It was also further activated to produce high added value materials. The results revealed that tyre chars present higher reactivity with steam than with CO_2, and also active carbons produced from tyre chars possessed surface areas, comparable with those of commercially available active carbons.

Ucar et al [37] investigated on the evaluation of two different scrap tyres as hydrocarbon source by pyrolysis. The effect of the polymer in scrap tyres on the pyrolysis products was also investigated. Two different types of scrap tyres from passenger car tyre and truck tyre were pyrolysed in a fixed bed reactor at temperatures 550^{o}C, 650^{o}C and 800^{o}C under N_2 atmosphere. Pyrolysis products (gas, oil and carbon black) obtained from these two types of tyres was investigated and compared. It was reported that the physical properties of pyrolytic oils from them were similar at the same temperature. However, the composition of aromatic and sulphur content from the pyrolysis of passenger car tyre was higher than that of truck tyre.

Ayanoglua and Yumrutas [38] used waste tyre as a feed stock in a rotary kiln reactor to obtain more gas, light liquid, heavy liquid, wax products; and less carbon black. Then, the heavy and light oils were reacted with additives, such as natural zeolite (NZ) and lime (CaO) at different mass ratios of 2, 6, and 10 wt% respectively, in the batch reactor to produce liquids similar to standard petroleum fuels. The heavy and light liquids with 10 wt% of CaO were as good as diesel like fuel (DLF). The chemical and physical features of the waste tyre, light oil, heavy oil and DLF were analyzed by TG (thermogravimetric) /dTG (derivative thermo gravimetric), proximate, ultimate, higher heating value (HHV), fourier transform infrared spectroscopy (FTIR), Brunauer–Emmett–Teller (BET), sulphur, density, viscosity, gas chromatography–mass spectroscopy (GC-MS), flash point, moisture and

distillation tests. The test results were found to be very close to the standard petroleum fuel.

Kwona et al [39] examined the possibilities of recovering energy and chemical products from pyrolysis of waste tyres. The experiments were conducted using a laboratory-scale batch-type reactor. In order to examine the influence of CO_2 in pyrolysis of a tyre, the pyrolytic products including C1-5-hydrocarbons (HCs), volatile organic carbons (VOCs), and polycyclic aromatic hydrocarbons (PAHs) were evaluated qualitatively by gas chromatography (GC) with mass spectroscopy (MS) as well as with a thermal conductivity detector (TCD). It was inferred from the results that the amount of gaseous pyrolytic products increased when using CO_2 as a pyrolysis medium, while substantially altering the production of pyrolytic oil in absolute content (7.3-17.2%) and in relative composition (including PAHs and VOCs). Thus, the co-feeding of CO_2 in the pyrolysis process could be considered as an environmentally benign and energy efficient process.

Hita et al [40] made an attempt to remove undesired sulphur, nitrogen and unsaturated compounds from the upgrading of Scrap tyre Pyrolysis Oil (STPO) for improving the properties of its different fractions (naphtha, diesel and gasoil) for using at as a potential blend in the refinery. The hydro treating method for STPO using tailored NiMo catalysts yielded high quality fuels and these catalysts allowed removing 92% sulphur, yielding 27% naphtha and 57% diesel. The hydro-treating trial runs were carried out in a fixed bed reactor at 275-375^{o}C and 65 bar. The studied catalysts were NiMo supported on 5 porous materials viz., C-Al_2O_3, SiO_2-Al_2O_3, SBA-15, MCM-41 and an equilibrated FCC catalyst. The catalysts were characterized by ICP-AES, N_2 adsorption desorption isotherms, H_2 chemisorption, XRD, XPS, TPR and terc-butylamine adsorption-desorption (TPD).

Hita et al [41] also investigated the effect of using a bifunctional Pt-Pd catalyst, which was tested in the hydrocracking of hydro-treated tyre pyrolysis oil. The product had a following composition: 48-78 wt% naphtha and 19-42 wt% diesel fractions, with moderate amounts of aromatics (b40 wt%) and sulphur (250 ppm). The Pt-Pd/ACP bifunctional catalyst was capable of removing 97.3% of the original sulphur and up to 97 wt% of the heavy gasoil molecules in the pretreated tyre oil.

Table 2.5: Pyrolysis of automobile, and cycle tube and tyres

Feed stock	Reactor type	Size of feed stock	Working conditions	Catalyst used	Product yield
Waste automobile truck tyres	Slow pyrolysis-Fixed bed reactor	10kg/batch	600^{o}C	Nil	50-55
Waste automobile truck tyres	Slow pyrolysis-Fixed bed reactor	10kg/batch	600^{o}C	Nil	50-55
Cycle tubes and tyres	Slow pyrolysis-Fixed bed reactor	NR	450-800 ^{o}C	Nil	49.65
Cycle tubes and tyres	Slow pyrolysis-Fixed bed reactor SiO_2/Al_2O_3, Kaolin, CaO, and MgO	NR	450-800 ^{o}C		49.60
Shredded waste tyres	Fluidized bed reactor-Flash pyrolysis	0.3 mm and 1.18 mm, 2 kg	350 ^{o}C to 600 ^{o}C, 10 g/min to 25 g/min	Nil	44.95

Jantaraksa et al [42] investigated the sulphur content, in the from waste tyre pyrolysis oil (WTPO) and use of this oil for alternative energy source. Generally the large amount of sulphur compound (1.15 weight %) was present in the WTPO, which were not appropriate for use in combustion of the engines. Therefore, they improved the waste tyre pyrolysis oil via hydrodesulhurization (HDS) catalyzed by molybdenum, nickel- molybdenum (NiMo) or cobalt-molybdenum supported on alumina (C-Al_2O_3). The maximum percentage of sulphur removal was achieved 87.8%, when the reaction was performed at 250^{o}C for 30 min using a 2 wt% NiMo/c-Al_2O_3 catalyst loading based on the WTPO content and 20 bar initial hydrogen pressure. The heating value of the HDS-WTPO (i.e, 44 MJ/kg) was similar to those for commercial diesel (i, e., 45 MJ/kg).

2.4 Pyrolysis of Waste Plastics

A large quantity of different plastics are disposed in the world every year. Some of them are recyclable while rest are non-recyclable. Since plastics originate from polymers and they contain hydrocarbon "waste to energy" is a possible option. Plastics are mainly classified into two types i.e., (i) thermosetting and (ii) thermo-plastic.

It is reported that in comparison with polyethylene and polypropylene, polystyrene can be thermally depolymerised to obtain the monomer styrene with a high selectivity. Many research works on pyrolysis of waste plastics were carried out using fluidized bed and bubble fluidized bed reactors. A major drawback found with all these reactors is stickiness of sand particles coated with melted plastics which results in defluidisation and agglomeration. Different reactors such as conical spouted bed reactor (CSB), internally circulating fluidized bed reactor (ICFB), swirling fluidized bed reactor (SFB) were also proposed to overcome this issue in which a uniform temperature inside the reactor should be maintained. The CSB reactor enables vigorous gas-solid contact. Therefore, the reactor can reduce the segregation of particulates observed in the fluidized bed. However, this reactor suffers from the plastic particles after melting, which clogs and blocks particle circulation [43].

Babu [44] investigated the effect of the catalyst amount, reaction temperature, plastic type High density polyethylene (HDPE) and weight ratio of waste plastic to catalyst, with a semi-batch reactor, based on the results of the yields and yield distributions of liquid products as a function of lapsed time. They studied the product yields and their distribution with different types of catalysts (Silica-Alumina, Activated Carbon, Mordenite) with respect to time and temperature. They also studied the effects of the particle size and structure of the catalyst on product distribution and yield. They performed a quantitative analysis of gaseous, liquid and solid products from thermal and catalytic degradation of HDPE.

Panda et al [45-47] optimized the production of liquid fuel by the catalytic pyrolysis of different plastic wastes, such as polypropylene, low density polyethylene and polystyrene, using kaolin and acid treated kaolin as the catalysts, in a laboratory batch pyrolysis reactor. The effect of silica alumina, which was extensively studied, by different investigators for the pyrolysis of different plastics was also studied and compared with that of the catalytic performance of kaolin. From the experimental results, they concluded

that kaolin was found to be suitable as a catalyst for the degradation of plastic waste to liquid fuel and valuable chemicals. However, silica alumina showed a superior performance in comparison with kaolin, in terms of yield and reaction time. It was reported that the rate of reaction, oil yield and quality of oil obtained from the catalytic pyrolysis were significantly improved compared to thermal pyrolysis. The catalytic activity of kaolin was further enhanced by treating it with sulphuric acid of different concentrations. Acid treatment increased the surface area and acidity, and also altered the pore volume distribution of kaolin, which supported the cracking reaction.

Raja and Murali [48] used a mixture of zeolite, clay, alumina and silicates in different proportions for obtaining fuel oil from waste plastics in a catalytic pyrolysis reactor. An improved apparatus was used for the pyrolysis process, which was heated by electrical heating coils or other forms of energy. The catalyst for the process was prepared by using the ingredients in the proportion viz., Faujasite zeolite: 0.5 - 35 wt%; Pseudo boehmite alumina: 10-40 wt%; Poly ammonium silicate:01- 10 wt%; Kaolin clay: 15 - 60 wt%; Liquid Distillate > 110% - 115%; Coke > 09% - 10%; Gas > 21% - 22%; LPG > 14% - 16%; Hydrogen > 01% -02%. They milled the ingredients and made it into slurry using demineralized water, spray drying the slurry to micro-spheres, and calcining them at 500°C for one hour. It was reported that the finished oil consisted of gasoline (60%) and diesel oil (40%).

Kumar and Singh [49-52] and Kumar et al [53] carried out experimental investigations to recover a liquid fuel through the pyrolysis process from high density polyethylene waste. A simple pyrolysis reactor system was used to pyrolyse waste HDPE with the objective of optimizing the liquid product yield at a temperature range of 400ºC to 550ºC with a heating rate of 20^{o}C/min. The effects of the process parameters on pyrolysis were studied. Further, they characterized the pyrolysis oil obtained from the pyrolysis process by FTIR and GC-MS for determining the functional group compounds present in the hydrocarbon fuel. They reported that the pyrolysis oil had a mixture of gasoline, diesel and kerosene, and a carbon chain varying in the range C_{10}-C_{20}.

Cleetus et al [54] carried out an investigation on the catalytic pyrolysis of polythene bags for producing liquid fuel. The catalysts used for the study included silica, alumina, Y zeolite, barium carbonate, zeolite, and their combinations. The pyrolysis reaction was carried out at polymer to catalyst ratio of 10:1. The reaction temperature ranged between 400^{o}C and 550^{o}C. The inert atmosphere for the pyrolysis was provided by using nitrogen

as a carrier gas at a flow rate of 10 mL/min. It was noted that the liquid yield was available only at temperatures above 350°C for all the catalysts. With the increase in temperature, the liquid yield decreased after a particular temperature (which was different for different catalysts). They indicated that no liquid yield was obtained for any catalyst, thereby making it clear that, the liquid yield was obtained between 400 and 550°C. They also further indicated that they observed a gel portion with impurities, which was filtered and removed.

Guntur et al [55] made an attempt to convert mixed plastic wastes into liquid fuel by pyrolysis. Plastic waste was treated in a cylindrical reactor at a temperature of 300-350ºC. The plastic waste was gently cracked by adding the catalyst, and the gases were condensed in a series of condensers to give a low sulphur content distillate. They reported that when 1000 kg of waste plastic was used as a feed stock in pyrolysis, the pyrolysis oil yield was in the range between 65% and 90%. The carbon black was obtained in between 5-10%, while the non-condensable gases will be in the range of 5-7%.

Parasuram et al [56] used polystyrene in a catalytic pyrolysis process. Catalytic cracking reactions were performed in a reactor at 380 to 420°C in the presence of bentonite as a catalyst, at atmospheric pressure. The mixture of the catalyst and olystyrene was added into the reactor, and heated. Products, like liquid and gas coming out from the reactor, were separated in a condenser and accumulated. They obtained three different products, viz., pyrolysis oil (55 wt%), pyro gas (10 wt%) and char (34 wt%). They also analysed the effect of varying temperature on the product yields. They reported that the conversion at lower temperature in the presence of a catalyst of waste plastic into liquid would be a feasible process. They also indicated that an important difference was that the liquid obtained from the catalytic pyrolysis would be relatively of a greater volume and low boiling range, in comparison with pyrolysis in the absence of a catalyst.

Liu et al [57] developed a specially designed laboratory fluidized-bed reactor for the pyrolysis of polystyrene waste in the range 450-700°C with nitrogen as the carrier gas and 20-40 mesh quartz sand as the fluidization medium, operating isothermally at atmospheric pressure. The yield of styrene monomer reached a maximum of 78.7 wt.% at a pyrolysis temperature of 600°C. Some mono-aromatics with boiling point lower than 200°C was also obtained as high-octane gasoline fraction. Styrene monomer with 99.6 wt.% purity was obtained after vacuum distillation of the liquid products, which could be used as the raw material to produce high-quality polystyrene circulation.

Lee et al [58] used a swirling fluidized-bed reactor to recover the styrene monomer and valuable chemicals effectively from the polystyrene waste, since it can control the residence time of the feed materials and enhance the uniformity of the temperature distribution. In order to increase the selectivity and yield of styrene monomer in the product, catalysts such as Fe_2O_3, BaO or HZSM-5 (Si/Al=30) were used. Effects of temperature, volume flow rate of gas, pyrolysis time and the ratio of swirling gas to the amount of primary fluidizing gas on the yields of oil product as well as styrene monomer were determined. It was found that the reaction time and temperature can be reduced profoundly by adding the solid catalyst. The swirling fluidization mode exhibited the temperature fluctuations more periodic and persistent, which increased the uniformity of temperature distribution by reducing the temperature gradient in the reactor.

Polystyrene wastes were degraded in a free-fall reactor under vacuum to regain the monomer at temperatures between 700°C and 875°C, and determined its effects on the phase yields, the benzene, styrene, toluene, and naphthalene distribution of the liquid output and C_1-C_4 content of the gaseous output. The liquid yield maximized at around 750 °C and the styrene yield at 825 °C. In general, operating at higher temperatures decreased the solid residue, and increased the gaseous yield and total conversion. Employing waste particles in four different size ranges, it was observed that, the finer the waste particles fed, the higher the gaseous yield and total conversion took place [59].

Catalysts, such as metal oxides, metal complexes, and alkali metal carbonates or alkaline metal carbonates have appeared to be used mainly for enhancement of monomer recovery. Degradation of polyethylene on solid bases (ZnO, MgO, TiO_2) may yield more oils than on solid acids, though the time required to complete the degradation on solid bases was much longer than on solid acids. The composition of oil on solid bases was reported to be rich in 1-olefins, and was poor in aromatics and branched isomers. So, the oils mainly consisting of olefins were not expected for fuel oils, because of their polymerization during preservation and/or transportation. Moreover, a low octane number is expected for the oils produced on solid bases, since the oils mainly consisted of straight chain hydrocarbons, n-paraffins and 1-olefins.

Table 2.6 summarises some of the research works that have been carried out by different researchers and the table provides information on type of feed stock, reactor used, size of feed stock, operating conditions and the product yields.

Table 2.6: Pyrolysis of waste plastics

Feed stock	Reactor type/process	Size of feed stock	Working conditions	Catalyst used	Product yield
Polypropylene	Small reactor, Vacuum	20 g	400-550 ^{o} C	Kaoline	89.5
Polypropylene	Small reactor	Catalyst:poly propylene = 1:2, 1:3, 1:4, 1:6, 1:10, 1:20, or 1:40	400-550 ºC catalyst ratio 3:1, 500 ºC	Si-Cl	90
Polystyrene	Thermal pyrolysis	20g	400ºC to 550ºC	Nil	28
Polystyrene	Catalytic cracking	1.5 kg loading Catalyst ratio, 4 : 1	350 ºC and 450 ºC	Silica, alumina, zeolite, barium carbonate, zeolite and their combinations	NR
Polystyrene	Thermo-catalytic cracking	4 to 67 mm	380 to 420°C	2SM-5 catalyst	55 wt %

2.4.1 Co-pyrolysis

Martínez et al [59] carried out co-pyrolysis of forestry wastes and waste tyres using a fixed bed reactor and a continuous auger reactor. It was reported that when acidity, density and oxygen content decreased, pH and calorific value increased with respect to the biomass pyrolysis liquid, leading to upgraded bio-oil. In addition, it was observed that, the addition of waste tyres to the feedstock blend was significantly decreasing the amount of aldehydes and phenolic compounds, which would be beneficial for improving the stability of the new bio-oils.

Duan et al [60] examined the co-pyrolysis of micro-algae and waste rubber tyre (WRT) in supercritical ethanol. The effects of reaction temperature (290-370^{o}C), time (10-120 min), WRT to microalgae (M) mass ratio (R/M, 5/0-0:5), and ethanol: feedstock ratio 5:5-30:5 were assessed. The interaction between WRT and microalgae favored the deoxygenation, denitrogenation and desulphurization of the resulting oil, producing a bio-oil with an energy density close to that of petroleum diesels. Generally, the bio-oils contain N, O and

S. So, additional treatments of these bio-oils were required when they were proposed as alternative fuels.

Rober and Prakash [61] studied the characteristics of sawdust oil and tyre pyrolysis oil (TPO) as fuels for diesel engine. In this work, pyrolysis oil was derived from sawdust and waste tyre in a fixed bed reactor. They reported that the viscosity of sawdust oil was 2 times higher than that of diesel, whereas that of TPO was 1.2 times higher. Densities of sawdust oil and TPO were greater than that of diesel by 14% and 8% respectively. Calorific values of sawdust oil and TPO were 28.7 MJ/kg and 39.7 MJ/kg respectively. They concluded that the sawdust oil and TPO could be used as fuel in the burners, boilers and wick stoves.

2.5 CI Engine Fuel Properties

CI engines are preferable to SI engines due to higher thermal efficiency and durability. Owing to increasing energy consumption and environmental regulations, there is a need for alternative fuels which can be derived from renewable energy sources. The two important types of process that can be used for deriving liquid alternative fuels from agriculture, municipal and industrial wastes are (i) biochemical and (ii) thermos-chemical conversions. When such liquid alternative fuels are obtained from these processes, they must be characterized before they are used as alternative fuels in CI engines. The following paragraphs discuss some of the important fuel properties that are desirable for CI engine applications.

Cetane number, viscosity, density, heating value, sulphur content, aromatic and distillation range, low temperature properties and stability are some of the important properties considered for selection of an alternative fuel for CI engines. Fuel with a higher cetane number ignites more readily, providing shorter ignition delay period. A minimum cetane number of 40 is recommended for diesel fuels in the United States and 50 in Europe, as well as in most other parts of the world. The cetane number of the fuel decreases with increase in aromatic content. Fuel structure affects the fuel properties that influence combustion. The viscosity of diesel fuel is an important property that affects fuel spray formation and subsequently affects air fuel mixture formation [62]. As per ASTM standards, kinematic viscosity of a CI engine fuel is in the range 2-4 cSt. If fuel viscosity is too high, it may cause higher pump resistance, filter damage, and adversely affect fuel spray patterns. Some injection pumps can experience excessive wear and power loss due

to injector or pump leakage, if viscosity is too low. Low viscous fuels exhibit poor lubrication properties. Fuel density can affect fuel consumption, power, wear and exhaust smoke.

Viscosity also affects the combustion behavior of CI engines as there is difficulty in atomizing the fuel and spray formation. The heating value or heat of combustion of diesel fuel is the measured amount of energy possessed by a fuel. Diesel fuels with higher heating values result in higher power and less fuel consumption. Two factors that affect the heating value of a fuel are: (a) increase in the aromatic content, and (b) the distillation profile by raising the initial boiling point and/or the end point. However, these factors are also influenced by other fuel properties. Aromatic content is also influenced by the distillation temperature. Distillation temperatures, such as T10, T50 and T90 are determined for an alternative fuel before examining its suitability for CI engines. For diesel, T90 lies between 280 ºC and 338 ºC. The flash point is the lowest temperature at which the volatile vapor of a fuel sample will momentarily produce spark under the prescribed test conditions. The flash point of the fuel is affected by the boiling point of the fuel [63]. But, it is not related directly to engine performance. The flash point is controlled to meet safety requirements for fuel handling and storage. As per ASTM D975, the flash point should be minimum of 52 ºC for No. 2 diesel fuel. Pour point is the lowest temperature at which the fuel will flow and is used to predict the lowest temperature at which the fuel can be pumped.

The volatility of diesel fuel is expressed in terms of the temperature at which successive portions of the fuel are distilled from a sample of fuel under controlled heating in a standardised apparatus. Ideal fuel volatility requirements will vary based on engine size and design, speed and load conditions, and atmospheric conditions.

Distillation temperature can give an idea of boiling point of a fuel [64]. Changing the boiling range may affect more than one fuel property. When the boiling range is raised to higher temperature, heavy compounds can be included in their final condition, thereby increasing their yield of diesel fuel. However, the heavier compounds in this fuel may produce higher soot and cause injection nozzle choking. Diesel fuel consists of a mixture of hydrocarbons with different molecular weights and boiling points. Fuels with this character tend to exhibit somewhat higher HC emissions than others in diesel engines.

Akasaka and Sakurai [65] studied on the exhaust emissions from a commercial DI diesel engine for petroleum fuels with a wide range of fuel properties. Three series of samples of

varying aromatic content, distillation temperature and cetane numbers were taken for the study. The total aromatic content was changed in the diesel fuel base stock from 1.4% to 52.8% for aromatic series. Cetane number was varied from 59 to 64. A 90% distillation temperature was changed from 248 to 338ºC. The cetane number, aromatic content, type and distillation temperature were adjusted to be independent from each other. From the results they concluded that aromatic content in a fuel affects NO_x formation and particulates in CI engines. Increase in particulate with increase in aromatic content is mainly due to the SOF emission. It has been concluded that the chemical properties of fuel are the controlling factor for NO_x and particulates, and not the physical properties.

Many researchers have characterized the pyrolysis oil or bio-oil obtained from pyrolysis of different feedstock which includes biomass, agriculture, municipal and industrial wastes. For instance, Prakash et al [28, 29] examined the fuel properties of bio-oil obtained from waste wood originated from wood industries. They reported that the bio-oil from waste wood contained water content which might be useful to reduce the oxides of nitrogen (NO_x). They also determined the physio-chemical properties of different bio-oil biodiesel emulsions. Important properties of pyrolysis oil/bio-oil obtained from different feedstocks are tabulated in Tables 2.7-2.8. The values of these fuel properties of pyrolysis oils obtained from tyre and plastics by various researchers are shown in Tables 2.9 and 2.10 respectively.

Table 2.7: Important fuel properties of pyrolysis oil obtained from different biomass feed stocks

Property	Cashew nut	Cashewnut deoiled	Coconut shell	Coconut shell	Mustard seed	Ground nut	Seasame	Karanja	Linseed	Cotton	Sal	Mahua	Jatropha
Density (kg/m^3)	993 @ 28°C	987@ 28°C	1090	1053@15 °C	NR	961	936.8	938.4	939.1	943.1	921.1	9.12	1029.1
Viscoity (cSt@ 40°C)				1.47	NR	4.71	48.9	27	1.97	62.05	1.32	NR	8
Lower heating value (MJ/kg)	33	40	38.6	19.75	NR	24-25	32-33	32-34	30-31	25-26	~20-21	NR	33.9
Flash point (°C)	180	164	80	44	NR	46	48	40	24	42	53	NR	NR

Table 2.8: Important physical properties of pyrolysis oil originated from industrial and municipal wastes [4]

Property	Wood	Dairy waste	Municipal waste
Waste	Pine wood	LDPE	Paper cup waste
Density (g/cm^3)	-	NR	1.0136
Viscosity(cSt @ 40^{o}C)	25.3	1.47	0.8
Net calorific value (MJ/kg)	20.58	36	19
Flash point (^{o}C)	98	45	64
Fire point (^{o}C)	108	NR	NR
Sulphur content (%)	0.05	0.001	Nil

NR: Not Reported

Table 2.9: Important physical properties of tyre pyrolysis oil

Property	Murugan et al [66]		Pradhan and Singh [67]	Pradhan and Singh[67]	Raj et al [68]		Sharma and Murugan [69]	Bhatt and Patel [70]
	Crude	Distilled	Waste tyres	Waste tubes	Raw	Distilled	TPO	TPO
Density (g/cm^3)	0.935	0.871	0.917	0.9184	0.950	0.900	0.92	0.88
Viscosity (cSt @ 40^{o}C)	3.2	1.7	5.31	2.94	11.69	3.2	5.4	6.3
Net calorific value (MJ/kg)	~42	~38	~30	~30	36-39	37	~34	38.3
Flash point (^{o}C)	43	36	-9	-10	NR	60	43	32
Fire point (^{o}C)	50	48	-4	-6	NR	65	50	NR
Sulphur content (%)	0.95	0.26	1.38	1.01	0.54-1.12	0.06	NR	NR

Table 2.10: Physical properties of plastic pyrolysis oil [4]

	Feed stock		
Property	LDPE	HDPE	Waste plastic oil
Density (g/cm^3)	0.7787	0.790	0.8355
Viscosity(cSt @ 40^{o}C)	1.89	2.1	2.52
Net calorific value, (MJ/kg)	~38-39	40.17	40-40.5
Flash point (^{o}C)	-23	-2	42
Fire point(^{o}C)	-20	5	45
Sulphur content (%)	NR	0.12	0.03

NR: Not Reported

2.6 Phenomenon of CI engine combustion

Combustion in a CI engine is predominantly influenced by complicated physical and chemical process, starting with compression of air, fuel injection into the combustion chamber and exhausting the combustible gases. The nature of combustion depends on many parameters, such as fuel air mixing, injection timing, spray characteristics, air motion, etc [71]. Fuel vaporization is also a parameter that affects combustion. Fuel content and self-ignition of fuel vapour are also related to the chemical process in the cylinder [72]. The fuel and air admission, ignition delay, and pre- and post-combustion are represented in the piston and cylinder assembly of a CI engine.

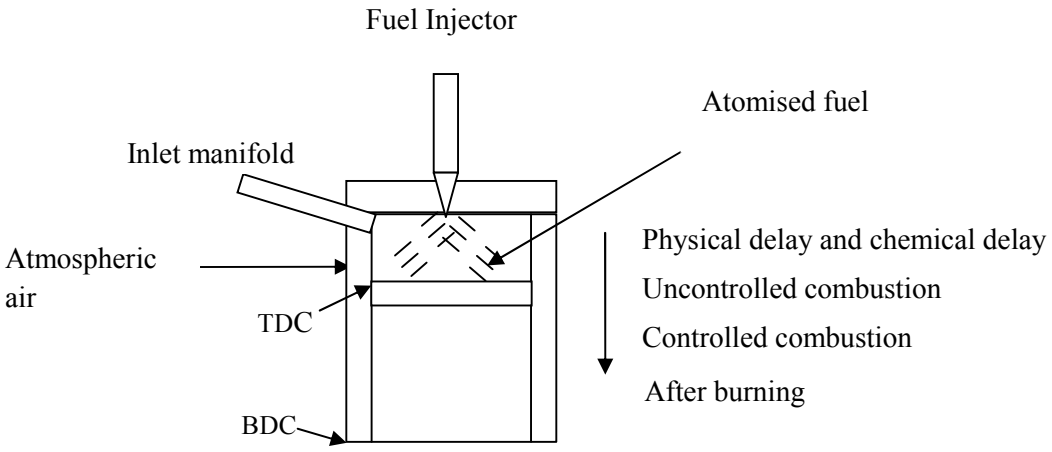

Figure 2.1: Combustion stages in piston and cylinder assembly

The followings are the four stages of combustion, after fuel is injected into the air stream of the CI engine:

(i) Delay period

(ii) Uncontrolled combustion or premixed combustion

(iii) Controlled combustion or diffusion combustion

(iv) Late combustion

All these four stages are represented with respect to heat release rate as shown in Figure 2.2.

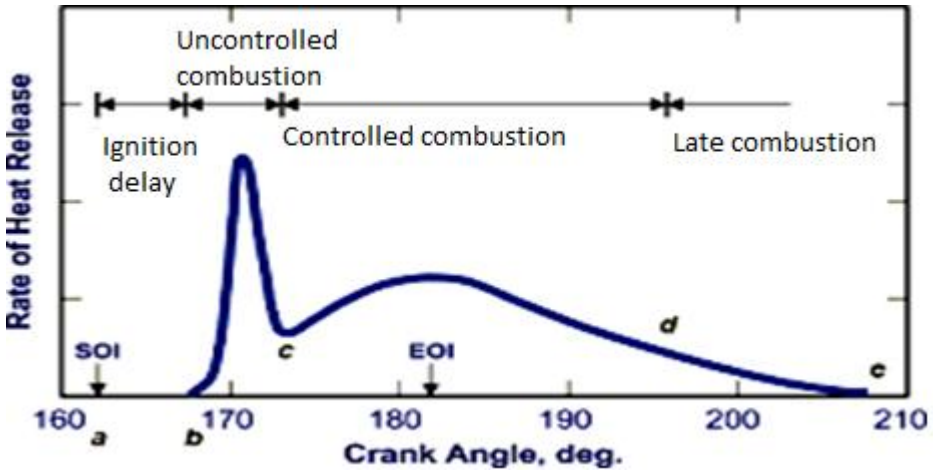

Figure 2.2: Heat release pattern of a CI engine

The delay period is divided into two parts, i.e., (i) physical delay and (ii) chemical delay. During physical delay, the injected fuel disintegrates into tiny droplets into the air stream present in the combustion chamber. The fine fuel droplets mix with the air forming a liquid-vapour phase. The heat available with the hot compressed air in the combustion chamber is utilized by fuel droplets for evaporation. The fuel vapour is then mixed with the air and resulting in formation of fuel air mixture in the combustion chamber. During chemical delay, preflame oxidation of fuel occurs inside the combustion chamber and subsequently local ignition begins which is known as start of ignition.

Once fuel is ignited, the fuel undergoes *uncontrolled combustion* (which is also known as premixed combustion) phase. The magnitude of heat release in uncontrolled combustion depends upon the amount of fuel injected during delay period, air fuel mixing rate and time available for combustion. During this period, amount of heat release is enormous. The peak heat release is generally attained at about 2-3^{o}CAbTDC (Crank angle before top dead centre) and the maximum pressure reached in the cylinder is exerted on the piston. Hence the piston moves from top dead centre (TDC) to bottom dead centre (BDC). Further, fuel injection continues simultaneously, but the remaining fuel is injected. This results in *controlled combustion* during which a second peak heat release can be observed which will be useful to push the piston further down towards the BDC. As the piston is approaching the BDC, the amount of heat evolves inside the combustion chamber would be less and ineffective. However, very less quantity of fuel is burned and this duration is called *late combustion.*

2.7 Emission in CI Engines

The engine emissions in IC engines are mainly due to improper combustion in the combustion chamber [73-75]. Main pollutants from CI engines are $NO_{x,}$ hydrocarbon emission, carbon monoxide emission, particulate matter, soot and other minor emissions like aldehydes, sulphur dioxides, lead and phosphorous. NO_x formation is mainly due to the combustion temperature and availability of oxygen. Higher cetane fuels exhibit lower NO_x and higher smoke due to shorter premixed combustion and longer diffusion combustion. Low cetane fuels produce higher NO_x due to higher heat release in the premixed combustion. At the same time aromatic content, oxygen content, injection timing, and combustion duration also influence the NO_x emission in CI engines.

Unburnt hydrocarbon (HC) emissions mainly result from the incomplete combustion of hydrocarbons. Diesel fuel contains on an average higher molecular weight compared than in a gasoline blend and results in higher boiling and condensing temperatures. Therefore, soot formation is more in CI engines. Some HC particles condense into the surface of the solid carbon soot that is generated during combustion. Because of higher molecular weight compounds present in the fuel, pyrolysis of fuel occurs in some places during combustion. This results in unburnt or partially burnt hydrocarbons. Most of the heavier unburnt hydrocarbons are absorbed on the soot particles in the form of soluble organic fractions. Generally, emissions from CI engines are low as they are operated with an overall lean fuel air equivalence ratio. The causes for higher HC emissions are (i) viscosity, (ii) poor fuel air mixing, (iii) combustion temperature and (iv) injection timing/delivery. Viscosity affects the atomization and vaporization of fuel, while volatility ensures even mixing of fuel with air. Poor air mixing is due to the deflection of spray patterns away from the optimum for that particular combustion system.

The formation of carbon monoxide (CO) emission depends on the available oxygen concentration, the temperature of the gases and the time left for the reactions to take place. In rich mixture, the CO concentrations increase steadily with fuel/air ratio and lack of oxygen causes incomplete combustion. In a lean mixture, the CO concentrations are low and vary only marginally with air fuel ratio. CI engines generally produce lower emissions of CO as they are supplied with excess air compared to spark ignition (SI) engines, which operate nearer to the stoichiometric mixture. Smoke is nothing but solid carbon soot particles suspended in the exhaust gas [76]. Soot emissions from CI engines are formed

from three processes occurring from the fuel and air, primarily in the first combustion phase, and from the burnt gases in the second combustion phase. The soot formation is due to pyrolysis of fuel droplets at low as well as at high temperatures. By reducing the fuel density, the nitrogen oxide (NO_x) and particulate matter (PM) emissions can be significantly reduced. The amount of sulphur content of a diesel fuel depends upon the quality of the crude oil from which it is refined, and the components used in the final blend. Sulphur in diesel fuel improves lubricity to certain extent. Therefore, engine wear and deposits can vary according to fuel used. As per ASTMD975 standards, the maximum sulphur content permissible for No. 2 diesel fuel is 500 ppm.

2.8 Suitability of Pyrolysis Oil for CI Engines

As mentioned in Section 2.5 any alternative fuel must have properties closer to those of diesel fuel, when it is proposed as an alternative fuel for CI engines. But, it is not possible to get an alternative fuel of such kind. The alternative fuel should also be under any one hydrocarbon family. Some of the important properties to check suitability of a fuel for CI engines are: (i) density or viscosity, (ii) heating value, (iii) flash point and fire point, (iv) sulphur content, (v) acidity, (vi) cetane number and (vii) distillation temperature. If these properties are closer to those of diesel fuel, it can be considered for using it as an alternative fuel for CI engines.

2.9 Methods to Use Alternative Fuels in CI Engines

Bio-oil and pyrolysis oil require fuel modification or engine modification if their fuel properties are not similar to those of diesel fuel. Hence, they can be used in CI engines by adopting any one or more of the techniques modification which are described below.

2.9.1 Fuel modification techniques

2.9.1.1 Fuel blending

It is the simplest method of using an alternative fuel in a CI engine. It is reported that some alternative fuels can be used even upto 90% with conventional diesel fuel, or properties similar to that of diesel fuel. Some fuels may even be solely used without blending it with diesel fuel. But, literature indicates that no pyrolysis oil was solely used as an alternative fuel in a CI engine. For instance, Huang et al [77] studied the combustion characteristics and heat release of a CI engine operating on a diesel methanol blend at different fuel

injection timings. Methanol was blended with diesel using some solvents. It was reported that the increase in methanol fraction resulted in increase in heat release in the premixed burning phase and shorter combustion duration in the diffusive burning phase. The results also indicated that,the ignition delay increased with increase in methanol fraction. The maximum cylinder pressure and rate of pressure rise were higher since methanol has oxygen in it inspite of higher heat of evaporation of diesel methanol blend. The authors pointed out that the major advantage of fuel blending is the absence of engine modification and direct use of fuel in diesel engines.

2.9.1.2 Emulsification

Emulsion is prepared and used in CI engines when two fuels have different surface tension and densities, and they are not miscible. Many research works have been carried to emulsifiy water with diesel to simultaneously reduce the NO_x and smoke emissions of a diesel fuelled diesel engine. For example, Lou et al [78] conducted an experimental study to compare the effects of water–diesel emulsion and water injection into the intake manifold on performance, combustion and emission characteristics of a DI diesel engine under similar operating conditions. The water to diesel ratio for the emulsion was maintained at 0.4:1 by mass. The same water-diesel ratio was maintained for water injection method in order to assess both potential benefits. All tests were done at a constant speed of 1500 rpm at different outputs. The static injection timing of 23°CAbTDC was kept as constant for all experimental tests. In this investigation, two phases of experiments were conducted. In the first phase, they carried out the experiments to assess the performance, combustion and emission parameters of the engine using the water-diesel emulsion. The emulsion was prepared using the surfactant of hydrophilic-lipophilic balance (HLB):7. The emulsion was injected using the conventional injection system during the compression stroke. In the second phase of the experiment, water was injected into the intake manifold of the engine using an auxiliary injector during the suction stroke. An electronic control unit (ECU) was developed to control the injector operation, such as start of injection and water injection duration with respect to the desired crank angle. The experimental results indicated that both the methods (emulsion and injection) could reduce NO emission drastically in diesel engines. Smoke emission was lower with the emulsion than with water injection compared to that of diesel. However, CO and HC levels were higher with emulsion than with water injection.

2.9.1.3 Preheating

As mentioned earlier, high viscosity fuels tend to produce poor spray formation causing more incomplete combustion. Preheating is one of the techniques to reduce the viscosity of a fuel. By preheating the fuel before admitting into the engine combustion chamber, the viscosity is brought closer to that of diesel fuel. Many experimental research works were carried out to study the effect of fuel preheating on the combustion, performance, and emission parameters of CI engines. For example, Pradhan et al [79] conducted an experimental investigation to study the effect of preheating Jatropha Curcas oil on the combustion and performance of a DI diesel engine. The oil was preheated with the help of exhaust gas heat, which was obtained from the same engine. The results also indicated that BSFC (brake specific fuel consumption) and EGT (exhaust gas temperature) increased, while BTE (brake thermal efficiency) decreased with preheated Jatropha Oil (PJO) in comparison with diesel in the entire engine operation. The reductions in CO_2 (carbon dioxide), HC (hydrocarbon) and NO_x (nitrous oxide) emissions were observed for PJO along with increased CO (carbon monoxide) emission in comparison with diesel operation.

2.9.1.4 Thermal cracking

Thermal cracking is used to break high molecular and complex hydrocarbon to simplify the structure by the application of heat. For instance, Parvizsedghy et al [80] carried out a study to thermally crack transesterified vegetable oil. They conducted the experiments in a continuous cracking reactor system using castor methyl ester as a feedstock. It was reported that pre-transesterification improved thermal cracking of vegetable oil by increasing the yield of the desirable liquid cracking product (up to 94%) and decreasing the water content to a negligible amount. The diesel fraction separated from primary liquid crackate, as the main product of this study, contained very low high-molecular-weight fatty acid methyl esters (FAMEs) compared to original feedstock, which contained nearly 100% FAME. Thus, the diesel fraction produced by this method showed a similar distillation curve to typical petrol, diesel, unlike biodiesel feedstock. Properties of the diesel product, including heating value, kinematic viscosity, cetane index, cloud point, and pour point were comparable to those of standard diesel No. 2. It was also reported that, thermal cracking would be an attractive process to produce bio-based diesel. Moreover, thermal cracking could be used to upgrade biodiesel by improving the heating value, viscosity, and cold properties.

2.9.1.5 Ignition improver

A fuel with a higher cetane number reduces the ignition delay period and causes stable running of the engine at a given speed [81]. However, if the cetane number is excessively higher than the normal value, the ignition delay will be too low. As a result, the engine performance will be affected and the smoke value will increase [82]. Ignition improvers can reduce the ignition delay of the fuel and reduces the NO_x emission in a diesel engine. The effect of cetane improver blended with a low cetane fuel on emissions was investigated in a co-operative fuel research (CFR) diesel engine by Ladommatos et al [83]. In this investigation, a base fuel having a cetane number of 40.2 was splitted into eight batches. Different quantities of ignition improver were added to eight batches resulting in cetane numbers from 48 to 62. The basic chemical structure and physical properties of the fuel were almost unaltered. The exhaust emissions of NO_x, unburnt hydrocarbons (UHC) and smoke were measured from the engine. The results showed that the NO_x emission progressively decreased with increasing cetane number, due to the reduction in ignition delay and the amount of premixed fuel burnt.

2.9.2 Engine modification

CI engines are generally designed to operate with diesel fuel only; which can be No.1 diesel fuel or No.2 diesel fuel. As the alternative fuels do not have densities as equal as diesel fuel, the diesel engine may give adverse or negative effect in terms of combustion, performance and emissions, when the alternative fuel is used in it. Therefore, fuel injection timing may be advanced or retarded to obtain the engine behavior similar to those of diesel operation.

2.9.2.1 Increasing fuel nozzle opening pressure and compression ratio

Increasing the fuel injection pressure of a high viscous fuel (vegetable oil) decreases the particle diameter and produces the fuel spray quickly. However, beyond certain injection pressures, the liquid injected into the combustion chamber cannot penetrate deeply. So, a higher injection pressure causes faster combustion initially, which slows down due to slow flame propagation [84]. Increasing the injection pressure causes lower CO and smoke emissions, but increases NO_x emission [85]. Increasing compression ratio (CR) will also help to achieve better performance of the engine.

2.9.2.2 Dual fuel mode/Fumigation

Dual fuel mode is used when a low cetane fuel or low quality fuel is used as an alternative fuel in a CI engine. A high cetane fuel, generally diesel, is injected into the combustion chamber that is used to initiate combustion. The injected fuel is referred as a pilot fuel. Once warm condition is achieved in the combustion chamber, the low quality fuel is introduced along with the air in suction. This enables the engine to run with the low quality fuel which can replace certain quantity of primary fuel.

2.10 Pyrolysis Oil in CI Engines

As mentioned in Chapter 1, considerable number of researchers has carried out their research on utilization of pyrolysis oil as an alternative fuel for CI engines. The following subsections discuss the research works related to study of the combustion, performance and emission behavior of CI engines that were run on different pyrolysis oils.

2.10.1 Bio-oil and wood pyrolysis oil in CI engines

Solantausta et al [86] studied the flash wood pyrolysis oil as an alternative fuel for diesel power plants. In this research study, engine tests were carried out on a single cylinder, four stroke, diesel engine for three cases: (i) only with wood pyrolysis oil, (ii) ignition improver enhanced pyrolysis oil and ethanol and (iii) poor quality reference fuel. Engine test was also conducted on a multi cylinder high speed diesel engine with pilot injection. It was reported that NO_x were higher by about 28% and smoke was less by about 23% for wood pyrolysis oil compared to diesel. It was also reported that both NO_x and smoke have reduced by about 80% when ignition improver was added to pyrolysis oil. The ignition delay was found to be 6^oCA (crank angle) for diesel fuel, and with poor ignition quality reference fuel it was 8°CA. They also reported that the ignition improver was not as effective with pyrolysis oil as with ethanol. The minimum concentration of additive used was 3% and the ignition delay was 15°CA, and the engine operation was unstable. A marginal difference was noticed in ignition delay when improver concentration was increased from 5 to 9% in pyrolysis oil, and ignition delay was still longer than that of poor quality reference fuel. Combustion started late with ethanol, pyrolysis oil containing 3% additive, and poor-quality reference fuel (10% heat released at 5-16°CAbTDC). Pyrolysis oil with 5% and 9% improver and conventional diesel were considerably faster (10% heat release at 3°CAbTDC). Combustion duration for 50% heat release was roughly

the same for pyrolysis oil (5 and 9% additive) and diesel. The time needed for 90% heat release was the shortest with pyrolysis oil, approximately 15 °CA for pyrolysis oil when compared to that of 25 °CA for diesel operation. The time needed between 10% and 90% heat release was roughly 22°CA for diesel and 13-17°CA for pyrolysis oil.

Frigo et al [87] investigated the feasibility of using flash wood pyrolysis oil in diesel engines. It was reported that wood pyrolysis oil contained high oxygen content of about 42% to 50% by mass than diesel fuel, and the heating value was much lower than that of diesel. The viscosity of wood pyrolysis oil was in between heavy fuel oil and light diesel fuel. Wood oil contained tar and polymer in the form of gummy like materials. In this study, three types of wood oil with the addition of different proportions of ethyl alcohol were considered. It was observed that the wood pyrolysis oil did not produce self ignition in conventional engine and also resulted in poor spray characteristics. The major drawbacks noticed when WPO was used in diesel engines were excessive carbonaceous deposit, injection system failure, incompatibility with engine lubricants and high acid aggressiveness. It was also estimated that the ignition delay of Canada oil with 12% alcohol and that of modified oil were 7^{o}CA and 6^{o}CA respectively, and the cetane numbers were 30 and 35 respectively. It was suggested that, improvement would be required for the use of wood pyrolysis oil in large size, low speed engines.

Bertoli et al [88] studied the performance, emission and combustion characteristics of a light duty DI diesel engine with wood pyrolysis oil (WPO). During this study, long run tests were also performed on a single cylinder with blends of WPO with different percentage of oxygenated compound, micro emulsions of WPO in diesel fuel and the results were compared with diesel fuel. It was reported that a reliable operation was achieved with 44.1% of WPO in diethylene glycol dimethyl ether. Similar results were obtained with two different emulsions with 30% of WPO in diesel fuel. No trace of corrosion was detected. From the emission point of view, WPO diglyme blends produced lower hydrocarbon (HC) and NO_x than diesel fuel with comparable carbon monoxide (CO). Micro-emulsion of WPO did not deviate much except NO_x. It was also reported that no major trouble on the important components of the engine was noticed.

Prakash [89] made an attempt to study the effects of using bio oil as an extender to biodiesel on engine combustion, performance, emission and durability issues. He used WPO in low percentages (i.e., 5%, 10% and 15%). Waste wood from the packing container boxes was used as a feedstock for the production of WPO, while the Jatropha

Methyl Ester (JME) was collected from a commercial pilot plant in India. The JME-WPO emulsions were obtained using six different surfactant combinations viz., 2% and 4% of Span 20 (Sorbitan monolaurate), 2% and 4% of mixture of Span 80 (Sorbitan monooleate), and 2 and 4% of (Span 80 + Tween 80 (Polysorbate 80). Three different percentages of emulsions containing 5, 10 and 15% of WPO were prepared using six different surfactants and tested as fuels in a single cylinder, four stroke, air cooled, direct injection diesel engine developing a power of 4.4 kW at a constant speed of 1500 rpm. After assessing the combustion, performance and emission parameters of the engine fueled with different emulsions, an optimum emulsion (Z2JOE15) was chosen, which contained 15% WPO, 81% JME and 4% of a mixed surfactant (i. e., Span 80-Tween 80). It was reported that highest thermal efficiency was noticed with the Z2JOE15 emulsion compared to all other emulsions tested in this study. The thermal efficiency for the Z2JOE15 was found to be higher by 11.3% compared to that of diesel at full load. Lower HC, CO and smoke emissions were noticed with the Z2JOE15 emulsion compared to that of diesel operation at full load. The NO emissions for all the emulsions were found to be lower than that of JME operation, but higher than that of diesel operation at full load. A maximum reduction in the NO emission of 16.8% was observed with the Z2JOE15 emulsion compared to that of JME operation.

After performing preliminary tests with bio oil diesel, bio-oil biodiesel emulsions, the Z2JOE15 emulsion was upgraded for its quality by an acid treatment process. The acid treated emulsion (ATJOE15) was tested in the same engine to evaluate the engine behavior in terms of the combustion, performance and emission, and compared with that of diesel operation. It was reported that the brake thermal efficiency of ATJOE15 emulsion was found to be higher by about 8.2% and 8.5% than those of diesel and JME at full load. The HC emissions were found to be lower by about 73% for the ATJOE15 emulsion at full load compared to that of diesel. The CO emissions of ATJOE15 emulsion were found to be higher by about 46% than that of diesel at full load. An increase of about 2% in the NO emission was noticed with the ATJOE15 emulsion at full load compared to that of diesel.

Further, the engine was run with the ATJOE15 emulsion to evaluate the combined effects of different compression ratio (CR), injection timing (IT) and injection pressure (IP) on the combustion, performance and emission parameters of the engine. Engine experiments were conducted with the ATJOE15 emulsion only at three different compression ratios

(16.5, 17.5 and 18.5). For each compression ratio, three injection pressures (200, 220, and 240 bar) and three injection timings (21.5, 23 and 24.5^{o}CAbTDC) were selected, and conducted as per the full factorial design (3^3 = 27). With the ATJOE15 emulsion, about 25.81% higher brake thermal efficiency was obtained at 18.5 compression ratio with the standard injection timing and injection pressure compared to that of diesel. The HC and smoke emissions were found to be lower by 45% and 9.6% respectively at full load with the same operating condition. The CO and NO emissions were found to be higher by about 10% and 4.88% in comparison with diesel at full load. The NO emissions were found to be lower with a lower compression ratio (16.5) and retarded injection timing (21.5^{o}CAbTDC) conditions.

2.10.2 Waste plastic oil as alternative fuel

Mani et al [90-92] assessed the combustion, performance and emission behavior of a single cylinder, four stroke, air cooled DI diesel engine run on four different waste plastic oil-diesel blends. The engine rated power was 4.4 kW at a constant speed of 1500 rpm. The percentage of waste plastic oil was varied from 10% to 70% at a regular interval of 20% on volume basis. 100% waste plastic oil was also tested in the same engine. They used the waste plastic oil which was obtained from the catalytic pyrolysis process. It was reported that the engine could operate with 100% waste plastic oil and can be used as fuel in diesel engines. They have also reported that oxides of nitrogen (NO_x) was higher by about 25% and carbon monoxide increased by 5% for the waste plastic oil operation compared to that of diesel fuel (DF) operation. Hydrocarbon was higher by about 15%. Smoke increased by 40% at full load with waste plastic oil compared to that of DF. The engine fueled with waste plastic oil exhibited higher thermal efficiency upto 80% of the full load and the exhaust gas temperature was higher at all loads compared to that of DF operation. They have further studied the effect of varying the injection timing of the same engine which was run on 100% WPO. Four fuel injection timings 23^{o}, 20^{o},17^{o} and 14^{o} bTDC were considered for the study. It was reported that when compared to the standard injection timing of 23^{o}bTDC the retarded injection timing of 14^{o}bTDC resulted in lower NO, CO and HC emissions, while the brake thermal efficiency, CO_2 and smoke increased under all the test conditions.

Mani et al [93] have further studied the effect of exhaust gas recirculation (EGR) in the same engine which was run with the waste plastic oil. Two different flow rates viz., 10% and 20% EGR was applied to the engine. They compared the results of the combustion,

performance, and emission parameters of the waste plastic oil fuelled engine run without and with EGR. They obtained higher oxides of nitrogen emissions, when fueled with waste plastic oil without EGR. NO_x emissions were reduced when the engine was operated with cooled EGR. The EGR level was optimized as 20% based on significant reduction in NO_x emissions, minimum possible smoke, CO, HC emissions, and comparable brake thermal efficiency. Smoke emissions from the engine run on waste plastic oil were higher at all loads. Combustion parameters were found to be comparable with and without EGR.

2.10.3 TPO as an alternative fuel

Murugan et al [94] have carried out tests to evaluate the performance and emission characteristics of a single cylinder, four stroke, air cooled, direct injection, diesel engine fueled with 10, 30 and 50% blends of tyre pyrolysis oil (TPO) with diesel. TPO was derived from waste automobile tyres through vacuum pyrolysis in one kg batch pyrolysis unit. They indicated that the brake thermal efficiency of the engine fuelled by TPO-diesel blends increased with increase in blend concentration and it is higher than diesel at full load. The HC, CO and smoke emissions were found to be higher at higher loads due to high aromatic content and longer ignition delay at original injection timing. The cylinder peak pressure increased from 71.4 to 73.8 bar. The ignition delays were longer than that of diesel at all loads.

Murugan et al [66] have taken 80% and 90% of distilled tyre pyrolysis oil (DTPO) blended with 20% and 10% diesel respectively, and conducted investigations in a four stroke, single cylinder, air cooled, diesel engine without any engine modification. The performance, emission and combustion characteristics of a single cylinder, four stroke, air cooled, DI diesel engine running with the DTPO-diesel blends at higher concentrations were studied. About 3% reduction in the brake thermal efficiency was noticed. The NO emissions were found to be lower by about 18% and smoke emissions were found to be higher by about 38% compared to that of diesel at full load.

Murugan et al [95] have further carried out an experimental investigation to study the effect of increasing fuel nozzle opening pressure when the engine was operated with TPO30. The fuel nozzle opening pressure was increased from 200 bar to 240 bar, and the combustion, performance and emissions of the engine were evaluated. It was reported that

the engine run on TPO30 with the fuel nozzle opening pressure and 220 bar exhibited better performance and lower emissions than that with TPO at 200 bar.

Hariharan et al [96] have conducted experiments on a single cylinder, four stroke, DI diesel engine using TPO as a main fuel. Results indicated that the engine performs better with lower emissions when diethyl ether (DEE) was admitted at the rate of 170 g/h with TPO and NO emission in TPO-DEE operation reduced by 5% compared to that of diesel fuel operation. The HC, CO and smoke emissions were higher for the TPO-DEE operation by 2%, 4.5% and 38% than diesel mode.

Dogan et al [97] have examined the effect of tyre derived fuel (TDF) on the engine performance and exhaust emissions in a diesel engine. The TDF and diesel blends, such as were TDF10, TDF30, TDF50, TDF70, TDF90 were prepared to test in a diesel engine, where TDF10 blend indicated that 10% TDF and 90% was the diesel fuel in volume basis. These six test fuels were tested in a single cylinder, four stroke, unmodified, and naturally aspirated DI high speed diesel engine at full load with four engine speeds (1400 rpm, 2000 rpm, 2600 rpm and 3200 rpm) respectively. The engine was able to run up to the TDF90 blend. The smoke opacity, HC, and CO emissions reduced while nitrogen oxides emissions increased with the increasing TDF content in the fuel blends.

Koc and Abdullah [98] have investigated the 4-cylinder diesel engine running by the tyre oil-biodiesel-diesel blend, where the blend contained 5% and 10% tyre oil. The performance and emissions parameters were evaluated for a constant speed engine at full load. The blend containing 10% tyre oil with 10% biodiesel and 80% diesel fuel shown the highest torque and power outputs, and reduced the brake specific fuel consumption significantly. The NO_x and CO emissions from the tyre oil (10%) containing a ternary fuel blend were significantly lower than the binary fuel consisting of diesel in the ratio of 10:90. It was concluded that tyre oil can be used as an alternative fuel for diesel engines, if the tyre oil has been properly filtered and desulphurized.

Sharma and Murugan [69] have investigated on the use of the blend of TPO and JME and used this blend as an alternative in a diesel engine. A single cylinder, four stroke, air cooled, DI diesel engine developing 4.4 kW engine was used for the experimental investigation. The cetane number of JME is higher than that of diesel, and five different blends of TPO varying from 10% to 50% at steps of 10% on a volume basis, were considered for the investigation. The combustion and emission behavior of the engine

deviated after 20% TPO in the blend. There was a reduction in the efficiency with 30%, 40% and 50% TPO in the blend at full load.

Frigo et al [99] have investigated the thermos-mechanical cracking process using the liquid tyre pyrolysis oil at temperatures in the range of 300-500^{o}C. The physical properties of TPO were analysed and compared with the diesel fuel. TPO has the lower cetane number and sulphur content. The engine investigation was carried out on a 440 cm^3 single cylinder diesel engine using two TPO-diesel blends i.e., TPO20 (containing 20% TPO and 80% of DF in volume basis) and TPO40. The cytotoxicity and genotoxiticy of the particulate from the engine exhaust emissions were evaluated. The performance of the engine with TPO20 did not show much difference, compared to that of diesel fuel, but with TPO40 the engine showed worsened combustion characteristics. Lubricant oil analysis showed a certain level of contamination.

Martínez et al [100] have blended 5% the tyre pyrolysis liquid (TPL) fuel produced in a continuous auger reactor on pilot scale and with commercial diesel fuel (100D) to produce 5TPO blend and tested it in a 4-cylinder, 4-stroke, turbocharged, intercooled, 2.0 L Nissan diesel automotive engine (model M1D) with a common-rail injection system. The performance and exhaust emissions were analysised and compared with the diesel operation. The performance parameters like brake specific fuel consumption and brake thermal efficiency seemed to be deteriorated by the addition of 5TPL in the blend fuel. Combustion duration was marginally longer for 5TPL than 100D. In case of the emissions parameters, total hydrocarbon (THC), NO_x and smoke emission also increased with addition of TPL in the blend fuel.

Martínez et al [101] have investigated on the use of tyre pyrolysis liquid (TPL) as an alternative fuel in a diesel engine by using simulated New European Driving Cycle (NEDC). TPL was blended in 5 vol.% with commercial diesel fuel (5TPL) and tested in a light-duty diesel Euro 4 engine. The engine test was characterized as the exhaust gas recirculation (EGR), relative fuel/air ratio, and regulated (THC, NO_x, CO) and unregulated gaseous emissions (CH_4, C_2H_4, C_3H_6 and SO_2), smoke opacity and particulate matter (PM) emissions were monitored for both fuels (5TPL and diesel fuels) during the tests. The performance in EGR was found to be marginally higher, for 5TPL than that of diesel fuel, but it influenced the gaseous emissions. It was concluded that the 5TPL blend could be used in the diesel engine without constructive modifications, although some properties of TPL should be improved if the blending percent is intended to be increased.

Wang et al [102] have examined the TPO derived from various pyrolysis temperatures and mixed with regular diesel at different proportions, and tested in a DI diesel engine. The engine performance, such as fuel consumption, cylinder pressure, engine power, and SO_2 emission were examined and discussed. The results indicated that by increasing the TPO fraction in diesel the engine performance worsened. But, it could be recovered using TPOs produced from higher pyrolysis temperatures. Increasing the pyrolysis temperature produced a high calorific value TPO and therefore enhanced the engine brake horse power.

2.10.4 Other pyrolysis oils

Sarkar et al [103] studied the effect of pyrolysis temperature on the products of pyrolysis of spent engine oil in a 30 mm diameter and 195 mm long quartz load cell placed in a tubular furnace from 300^{o}C to 500^{o}C in a nitrogen atmosphere. The spent engine oil sample was also pyrolysed in a thermos-gravimetric analyzer (TGA) under the same experimental conditions. The TGA analysis has been performed at constant heating rate of 10^{o}C/min. The maximum pyrolysis oil was obtained at 500^{o}C. They reported that the pyrolysis reactions proceeded considerably in the temperature range of 26 to 700^{o}C.

2.10.5 Studies on effect of acidity on engine components

So far no body has carried out research using the pretreated pyrolysis oil in diesel engines. However, some researchers have investigated the effect on acidity of bio oil on engine components. A s brief review of them are given below;

Frigo et al [87] tested the corrosion properties of wood pyrolysis was produced using flash pyrolysis. They immersed steel plates with high surface to volume ratio in pyrolysis liquid (PL) baths at different temperatures and durations. The resulting metal losses after 2 h 34% and 43.5% at 50 ^{o}C and 90 ^{o}C respectively and 90 % was lost after 24h at 90 ^{o}C.

Corrosion tests were also carried out by Qiang et al [104] using both crude and up graded pyrolysis with fossil diesel. The crude pyrolysis was centrifuged to eliminate large solid particles and, using an ultrasonic emulsifier; two emulsions were prepared with 88.5% and 68.5% PL (wt). The emulsions were stable for up to 10 days.the samples were tested with four different metals: aluminum, mild steel, brass and austenite stainless steel. The results showed that aluminum and mild steel have poor resistance to crude pyrolysis oil and its emulsions; brass is also affected by them. Stainless steel however, was corrosion resistant

against both crude pyrolysis oil and its emulsions, because a Cr_2O_3 film formed on its surface prevented the underlying iron from being corroded.

Corrosion tests of pyrolysis oil with standard injector components were also conducted at VTT, Finland. Jay et al [105] measured the and observed the dimensional changes of injector components after soaking in wood pyrolysis for 7 weeks. They observed severe corrosion [105]. Later, VTT and Watrsila jointly worked on the material development of the injector components and recommended the stainless steel alloys and polymers. It was suggested to use the metals/alloys for engine components, when pyrolysis oil would be used in diesel engines, as mentioned appendix I[106].

2.11 Summary and Research Gaps

After reviewing the research articles, the following important points and research gaps were noted:

(i) All the pyrolysis oils possess alkene/alkane which contain hydrocarbons in them. Pyrolysis oil obtained from waste automobile tyres and plastics contains aliphatic and aromatic compounds.

(ii) Presence of alcohols and phenols is identified with most of the pyrolysis oils.

(iii) Pyrolysis oils contain small percentage of moisture, which depends upon the type of feedstock used. Moisture in bio-oil cannot be separated.

(iv) Pyrolysis oils are acidic in nature which requires further treatment to avoid corrosion in combustion devices, vessels or storage tanks.

(v) Pyrolysis oils possess alkali metals, char which may deteriorate engine components. Most of the researchers reported that pyrolysis/bio oils have poor miscibility. Most of the pyrolysis oils exhibit poor odor, particularly pyrolysis oil from tyres and plastics produce pungent smell.

(vi) Most of the pyrolysis oils have the density and viscosity which are higher than diesel.

(vii) Pyrolysis oil from waste automobile tyres and plastics has higher sulphur content.

Most of the researchers focused their research on utilization of bio-oil, tyre pyrolysis oil and waste plastic oil as alternative fuels for CI engines. In the case of utilization of pyrolysis oil obtained from waste tyres, all of them have used the oil which was obtained in the crude form. Nobody has used the pyrolysis oil derived from demonstrated or pilot plant of tyre recycling plant. One of the recently demonstrated plants in India produces

two different categories of tyre pyrolysis oil based on condensation namely, (i) Light fraction pyrolysis oil (LFPO) and (ii) Heavy fraction pyrolysis oil (HFPO). In this study, it was decided to examine the possibilities of using LFPO as an alternative fuel for a small power generation offered by a diesel engine.

2.12 Objectives of the Present Research

The present investigation is aimed to study the following:

i. Characterization of the light fraction of pyrolysis oil (LFPO) and LFPO-diesel blends.
ii. Investigation on the engine behavior in terms of combustion, performance and emission parameters of the engine run on different LFPO-diesel blends.
iii. Investigation on the engine behavior in terms of combustion, performance and emission parameters of the engine run on an optimum LFPO-diesel blend with an ignition improver.
iv. Investigation on the engine behavior in terms of combustion, performance and emission parameters of the engine run on an optimum LFPO-diesel blend with an oxygenated additive
v. Investigation on the engine behavior in terms of combustion, performance and emission parameters of the engine run on an optimum LFPO-diesel blend with internal jet piston geometry.
vi. Investigation on the engine behavior in terms of combustion, performance and emission parameters of the engine run on an optimum LFPO-diesel blend with internal jet piston geometry and exhaust gas recirculation (EGR) to reduce nitric oxide (NO) emission.
vii. Investigation of CO_2 capture by zeolites from the engine run on an optimum LFPO-diesel blend with internal jet piston geometry and exhaust gas recirculation.
viii. Engine durability test with optimum LFPO blend.

Chapter 3

FUEL PRODUCTION AND CHARACTERIZATION

3.1 General

When an alternative fuel is proposed for internal combustion (IC) engines, it is very much necessary to first understand the method of fuel production and its physiochemical properties. Although a few researchers have carried out research works related to production of crude tyre pyrolysis oil (TPO) in laboratory level pyrolysis reactors and utilization of it in both SI and CI engines, no one has made attempts to use the pyrolysis oil obtained from a pilot plant in an IC engine. The method of pyrolysis of waste automobile tyres in a demonstration plant and its principal products are described in this chapter. Furthermore, the characterization of pyrolysis liquid obtained in the plant is also presented in this chapter.

3.2 Fuel Production

Pyrolysis is one of the methods to recycle waste rubber, waste tyre and industrial plastic wastes [11]. In this investigation, an attempt was made to use pyrolysis oil obtained from a commercial type recycling plant that uses vacuum pyrolysis. The plant is situated in the outskirts of Rourkela town, Odisha state, India.

Figure 3.1:Photograph of the tyre pyrolysis plant

The photograph of the tyre pyrolysis plant situated in Rourkela, India is shown in Figure 3.1. It uses automobile shredded tyres as feed stock. Figure 3.2 illustrates the schematic layout of the pilot tyre pyrolysis plant. The light fraction of pyrolysis oil (LFPO) obtained after the first distillation in a batch type pyrolysis unit from this plant was collected for the present work.

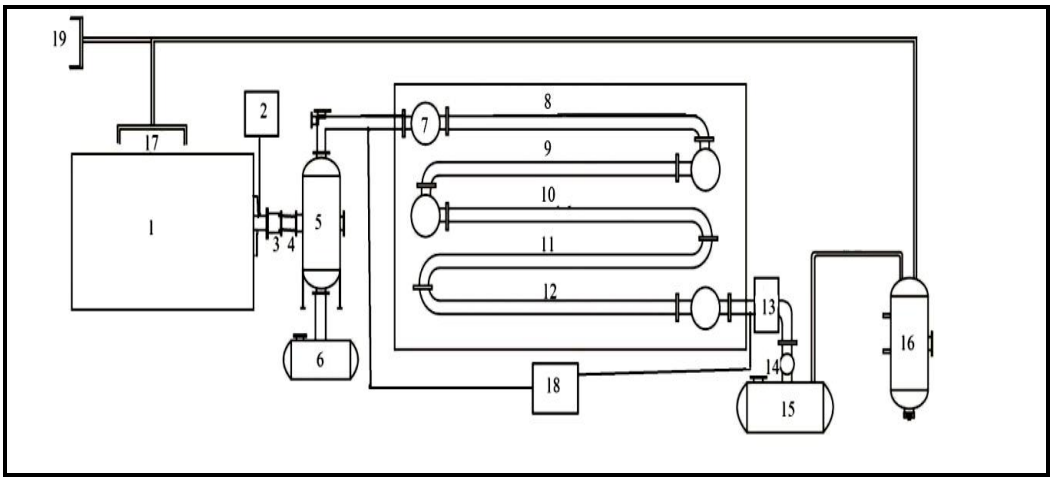

Figure 3.2: Pilot plant for pyrolysis of waste tyres

1. Reactor 2. Electric motor 3. Sealing elements 4. Flexible connection 5. Oil separator 6. Heavy oil tank 7. Damper 8-12. Condenser tubes 13. Cooling tower 14. Smooth inspection mirror 15. Light oil tank 16. Water sealing and gas recycling system 17. Gas burner 18. Pump 19. Control panel

The plant has a cylindrical rotary type pyrolysis reactor (1). The plant has a batch process with a capacity of 10T. The length of the reactor is approximately 6.6 m, and the diameter is 2.8 m. The reactor is rotated with the help of an electric motor (2) and a pulley arrangement. The pyrolysis reactor is initially heated up by waste wood. The wood consumption per batch is about 2T. In the pilot plant, the shredded tyres are fed into the pyrolysis reactor. The front end of the reactor has a door with fasteners. The door can be opened or closed by unlocking or locking the fasteners. The other end of the reactor is connected to sealing elements (3) and a flexible connection (4). An oil separator (5) is connected to the reactor by the sealing element and the flexible connection. The volatile vapor evolves during pyrolysis, passes through the oil separator, where heavy oil is separated by gravity and collected in a heavy oil tank (6). A damper (7) is provided at the outlet of the oil separator that connects a bunch of water cooled condenser tubes (8-12). Further, the volatile gases enter the bunch of water cooled condenser tubes, where the light oil fractions are converted into liquid. A cooling tower (13) is used to bring down the

temperature of the coolant close to atmospheric temperature, which is used in the water cooled condenser. A smooth inspection mirror (14) is used to know whether the gas is converted into liquid or not. The light fraction oil is collected in a tank (15).A certain quantity of gases, which is not condensed in the heavy oil tank passes through a water sealing (16) and enters the gas recycling system. The non-condensable gas is cleaned in the gas recycling system, and then given to a gas burner (17), which is located in the reactor for heating. A pump (18) is used to recirculate the coolant leaving the cooling tower to the condenser. The pyrolysis reactor and the accessories are operated by motors and pumps with the help of a control panel. The initial temperature at which volatile vapors evolve in the reactor is around 160^{o}C at about four hours of plant operation. During the process, carbon black and steel are also generated. The yields of products obtained from a pilot plant are given below:

(a) Fuel oil (40 to 45%)
(b) Carbon black (30 to 35%)
(c) Steel wire (3 to 5%)
(d) Non-condensable gases (8 to 10%)
(e) Moisture (3 to 5%)

The moisture is removed from TPO at 100^{o}C by heating. Therefore, the heating value is higher for the LFPO than for TPO. Since the waste tyres used in the plant is of mixed natures (tyres produced by different manufacturers), the composition of waste tyres, elementary composition and proximate analysis are given in Tables 3.1-3.3.

Table 3.1: Composition of waste tyres used in the plant [107]

Sl. No.	Composition	Content (%)
1	Rubber	38
2	Fillers (Carbon black, silica, carbon chalk)	30
3	Reinforcing material (steel, rayon, nylon)	16
4	Plasticizers (oils and resins)	10
5	Vulcanisation agents (Sulphur, zinc oxide, various chemicals)	4
6	Antioxidants to counter ozone effect and material fatigue	1
7	Miscellaneous	1

Table 3.2: Elementary composition of waste tyre [107]

Sl. No.	Elementary Composition	Content (%)
1	Carbon	86
2	Hydrogen	8
3	Nitrogen	1
4	Sulphur	2
5	Oxygen	3

Table 3.3: Proximate analysis of waste tyre [107]

Sl. No.	Proximate Analysis	Content (%)
1	Volatiles	62
2	Fixed carbon	30
3	Ash	7
4	Moisture	1

Table 3.4 indicates the tyre pyrolysis carried out by the early researchers and compared with the LFPO. In this table NA1-NA3, and EU1-EU7 refer to a macroscopic description of the Automobile Shredder Residue (ASR) taken from North American (NA) and European (EU) shredding plants [11]. This table, shows that LFPO is subjected to a higher vacuum reactor pressure of 19 kPa and reactor capacity than the other products.

Table 3.4: Experimental conditions for the samples studied* [11]

Product	NA1	NA2	NA3	EU1	EU2	EU3	EU4	EU5	EU6	EU7	LFPO
Reactor type	A	A	A	B	C	C	C	C	C	C	C
Capacity of reactor (kg)	25	25	25	1	504	686	175	86	86	130	8000-10,000
Average pressure (kPa)	4	4	4	0.9	-	3.4	1.2	2.8	1.6	4.7	1.9
Maximum bed temperature (°C)	530	530	530	536	-	520	513	496	424	520	375-440
Number of consecutive runs	1	1	1	1	3	5	2	2	1	1	1

*A=Multiple hearth furnace; B=Laboratory batch reactor; C=Horizontal pilot reactor

3.3 Fourier Transform Infrared Spectrometer

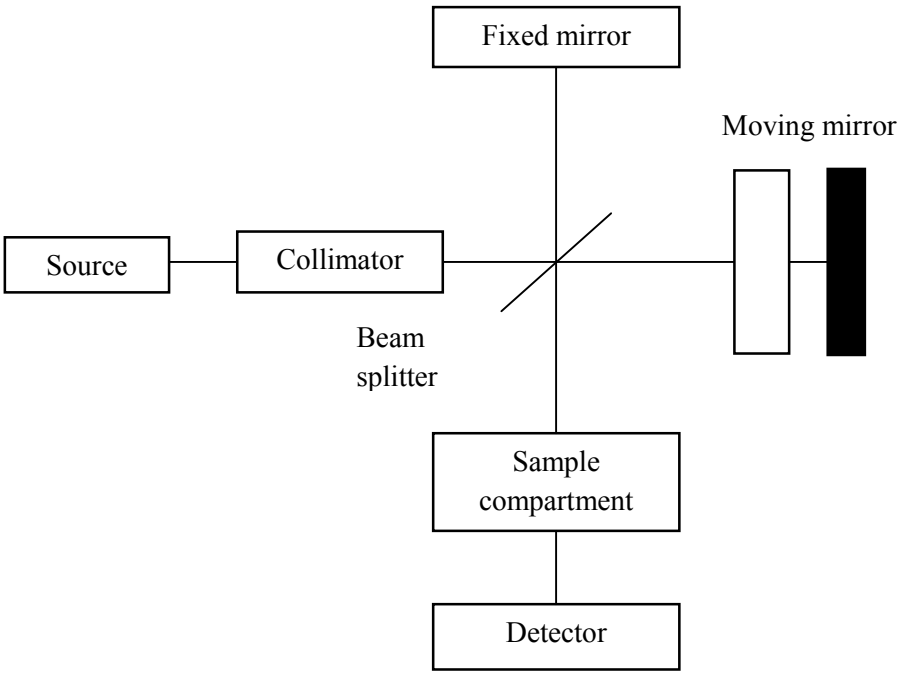

Figure 3.3: Block diagram of an FTIR spectrometer

The LFPO obtained in the pyrolysis plant was initially checked by a Fourier Transformer Infrared (FTIR) Spectrometer to ensure the organic compounds present in the LFPO. Figure 3.3 illustrates the working principle of a FTIR spectrometer. A common FTIR spectrometer consists of a source, collimator, Beam splitter, sample compartment, detector, fixed and moving mirror. It also contains amplifier A/D convertor, and a computer. The source generates radiation, which passes the sample through the interferometer and reaches the detector. Then, the signal is amplified and converted to a digital signal by the amplifier and analog-to-digital converter respectively [108]. On the interaction of an infrared light with oil, a chemical bond will stretch, contract and absorb infrared radiation in a specific wavelength range, regardless of the structure of the rest of the molecule. The photograph of the FTIR spectrometer of Perkin Elmer Rx1, which was used for this investigation, is shown in Figure 3.4.

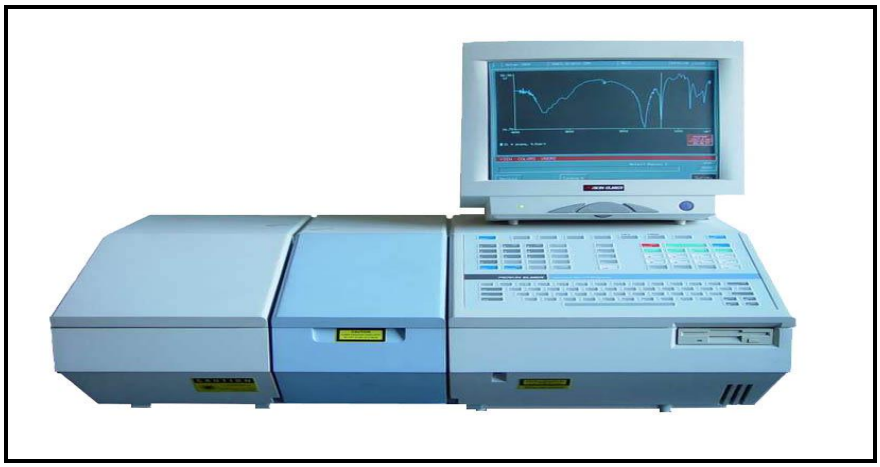

Figure 3.4: Photographic view of spectrophotometer (make: Perkin Elmer Rx1)

Based on this principle, the functional groups present in the diesel and LFPO were identified by using the FTIR spectrometer of make Perkin Elmer Rx1. The FTIR spectra were collected in the range of 400-4000 cm^{-1} region with 8 cm^{-1} resolution. The results of the FTIR analysis are in the form of a graph plotted between the wave number and the percentage transmittance, which will give the information about the position of various bond vibrations distinguished by several modes, such as stretching, distorting, bending etc. The graphical results obtained for diesel and LFPO are shown in Figure 3.5. Table 3.5 gives the FTIR analysis of LFPO and diesel. The compounds of LFPO are alkanes, alkenes, aromatic compounds, but in case of diesel compounds are alkanes, alkenes, amides, alcohol, nitrate, chloride and bromide.

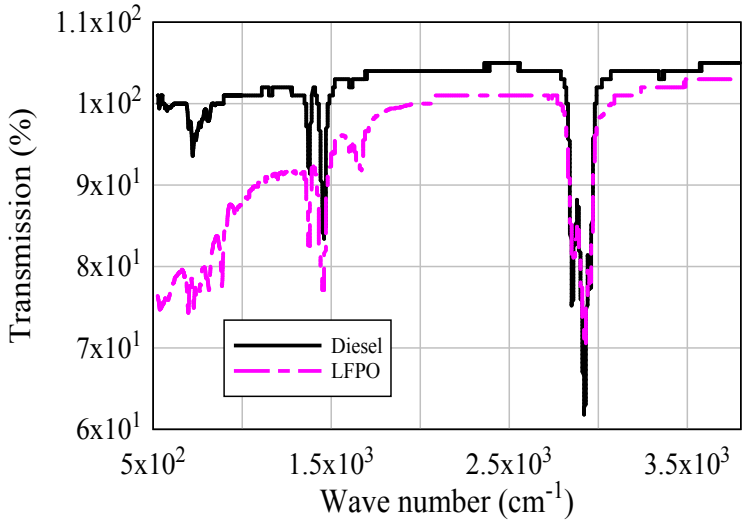

Figure 3.5: FTIR analysis of diesel and LFPO

Table 3.5: FTIR Analysis of diesel and LFPO

Diesel			**LFPO**		
Frequency ($cm^{-1)}$	Bonds	Class of compounds	Frequency range (cm^{-1})	Bonds	Class of compounds
2921.33	C-H, Stretch	Alkanes	3095-3005	C=C stretching	Alkenes
2812.72	C-H, Stretch	Alkanes	3000-2800	C-H stretching	Alkanes
1605.47	C=C, C=N, Stretch	Alkenes, Amide	1680-1620	C=C stretching	Alkenes
1461.19	O-H, Bending	Alcohol	1600-1525	Carbon-carbon stretching	Aromatic compounds
1376.55	Nitrate	Nitrate	1520-1220	C-H bending	Alkanes
722.05	C-Cl	Chloride	1035-830	C=C stretching	Alkenes
468.67	C-Br	Bromide	825-650	C-H out of plane bending	Aromatic compounds

3.4 GC-MS Analysis of LFPO

The gas chromatography (GC) and mass spectrometry (MS) make an effective combination for the chemical analysis. The gas chromatography- mass spectrometry (GC-MS) analysis is used both for the qualitative identification and quantitative measurement of the volatile and semi-volatile organic compounds in complex mixtures. This analysis can be done on solids, liquids and gases [109]. By using a GC-MS-QP2010 [SHIMADZU] analyser determines the chemical compounds present in the oil. It is a method that combines the features of gas-liquid chromatography and the mass spectrometry, to identify different substances present within a test sample. The working principle of the GC-MS instrument is illustrated in Figure 3.6.

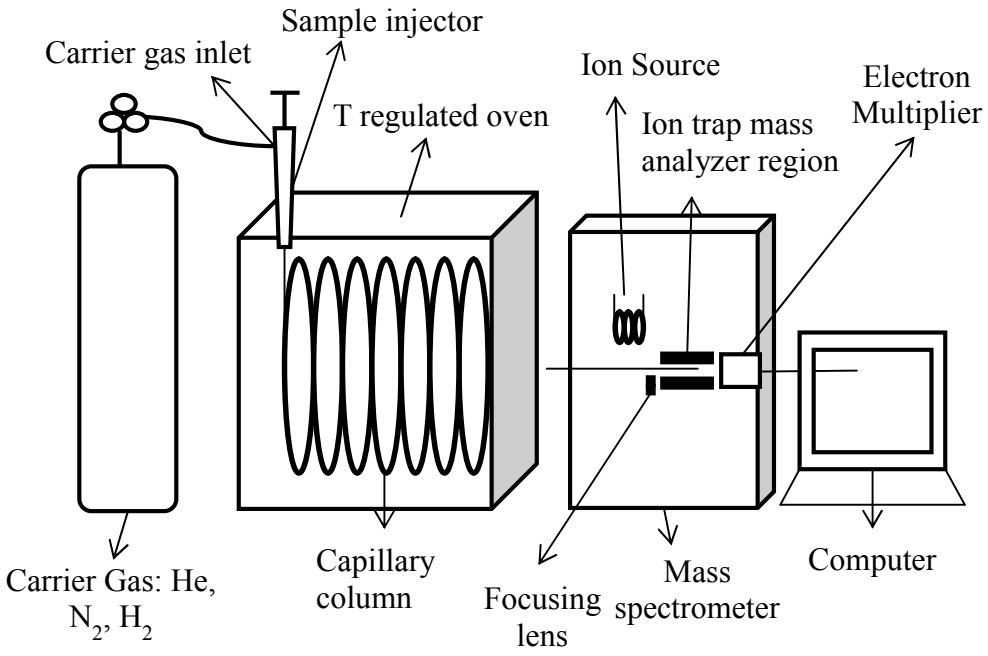

Figure 3.6: Working principle of GC-MS instrument.

A capillary column coated with a 0.25 µm film of DB-5 with a length of 30 m and diameter 0.25 mm is used. The GC is equipped with a split injector at 200^{o}C with a split ratio of 1:10. The helium gas of 99.99% purity is used as the carrier gas at a flow rate of 1.51 ml/min. The oven's initial temperature is set at 70^{o}C for 2 min, and then increased to 300^{o}C at a rate of 10^{o}C/min and maintained for 7 min. All the compounds were identified by means of the software developed by the National Institute of Standards and Technology (NIST), USA library. The mass spectrometer is operated at an interface temperature of 240^{o}C, with an ion source temperature of 200^{o}C in the range of 40-1000 m/z. The LFPO obtained was characterized by using GC/MS-QP 2010 SHIMADZU, equipped with flame ionization and mass spectrometry detection (GC-FID-MS). Table 3.6 gives the comparison of results obtained from the GC-MS analysis for LFPO and diesel.

Table 3.6: GC-MS Analysis of major compounds present in LFPO compared with diesel fuel

GC-MS Analysis of LFPO				**GC-MS Analysis of Diesel**			
Retention Time (s)	Area (%)	Name of Compound	Molecular Formula	Retention Time (s)	Area (%)	Name of Compound	Molecular Formula
3.29	4.85	p-Xylene Benzene, 1, 3-dimethyl	C_8H_{10} or $C_6H_4(CH_3)_2$, $C_{10}H_{14}$	3.06	0.98	1-Ethyl-Metylcycl hexane	C_9H_{18}
4.85	6.24	Benzene,	C_9H_{12}	3.35	1.06	Propyl cyclohexane	$C_6H_{11}CH_2$ CH_2CH_3
5.23	2.17	Benzonitrile	C_6H_5CN	3.78	1.04	M-Ethyl methyl benzene	C_9H_{12}
5.96	15.24	Benzene,1,2,3, 4-tetramethyl, o-Cymene	$C_{20}H_{26}O$, $CH_3C_6H_4CH$ $(CH_3)_2$	4.27	3.51	Decane	$C_{10}H_{22}$
6.03	5.19	D-Limonene	C10H16	5.82	2.14	n-Undecane	$C_{11}H_{24}$
10.45	2.19	1H-Indene, 2, 3-dihydro-1,1,5-trimethyl-	C_9H_8	7.35	2.71	Dodecane	$CH_3(CH_2)_{10}$ CH_3
12.20	3.77	Naphthalene, 2, 7-dimethyl	$C_{10}H_8$, $C_{10}H_6(CH_3)_2$	15.99	3.38	n-Hexadecane	CH_3 $(CH_2)_{14}$ CH_3
12.41	4.58	Quinoline, 4, 8-dimethyl	C_9H_7N, $C_{11}H_{18}$	17.85	2.57	Octadecane	$CH_3(CH_2)_{16}$ CH_3
13.58	4.65	Naphthalene, 2,3, 6-trimethyl	$C_{10}H_8$, $C_9H_{12}O$	19.64	1.61	Octacosane	$C_{28}H_{58}$
19.58	2.68	Heptadecane nitrile, Octadecanenitrile, Hexadecanenitrile	$C_{17}H_{33}N$. $C_{18}H_{35}N$, $C_{16}H_{31}N$	20.47	1.35	Tetracosane	$H(CH_2)_{24}H$

The amount of time that a compound is retained in the GC column is known as the retention time. The LFPO is composed of hydrocarbons, which are in the range of C_6 to C_{20} (benzene to octacosane). The LFPO has mixed hydrocarbons in it, which reflect that it may be used as fuel either SI or CI engine.

3.5 Chemical Composition of LFPO

The chemical composition of LFPO was tested with a CHN analyser available in NIT Rourkela. The chemical composition of LFPO in comparison with diesel and the crude TPO (obtained in a laboratory reactor) are listed in Table 3.7.

Table 3.7: Chemical composition of diesel, TPO and LFPO

	% Composition			
Sl. No.	Element (%)	Diesel	TPO	LFPO
1	C	87	63.10	42.00
2	H	13	6.62	3.87
3	S	0.29	2.58	0.70
4	O	0	27.07	52.31

3.6 Physicochemical Properties

3.6.1 Measurement of density

Density, specific gravity and API gravity can all be determined by using either ASTM D 287 or D 1298, standard where a hydrometer, which is a weighted and graduated float, is placed in the liquid to give a direct reading as the scale crosses the liquid surface. Hydrometers are available with scales that have been calibrated to indicate either density, specific gravity or API gravity. Correction of the reading may be necessary, if the fuel sample temperature is not at or near the reference temperature of 15^{o}C [110].

3.6.2 Measurement of viscosity

The viscosity of a fluid indicates its resistance to flow. The higher the viscosity, the greater the resistance to flow. It may be expressed as absolute viscosity or kinematic viscosity. The unit of absolute viscosity is poise (P), which is the force in dyne required to move an area of 1 cm^2 at a speed of 1 cm/s past a parallel surface 1 cm away and separated from it by the fluid. The kinematic viscosity unit is stoke (St), measured in cm^2/s. For numerical convenience, viscosity values are often reported in centipoise (cP) or centistoke (cSt). The term centistoke is often replaced by its corresponding SI unit i.e., mm^2/s. The two viscosities are related by the following equation:

$$cP = cSt \times \text{oil density} \quad (3.1)$$

A widely used laboratory method for determining the kinematic viscosity of diesel fuel is ASTM D445 [111], which measures the time taken for a fixed volume of the fuel to flow under gravity through a capillary tube viscometer immersed in a thermostatically controlled bath. As viscosity varies inversely with temperature, the relevant temperature at which the viscosity is determined must always be quoted; and for diesel fuel, it is usually either 20^{o}C or 40^{o}C [110].

3.6.3 Measurement of cetane number

The readiness of a fuel to ignite when injected into a diesel engine is indicated by its cetane number. The higher the number, the easier it is to ignite. The most ideally accepted measure of ignition quality is determined by a test engine using the Cooperative Fuel Research (CFR) Cetane Engine method, as per ASTM D613 standard [112]. The cetane number of a fuel is determined by comparing its ignition quality under standard operating conditions with two reference fuel blends of known cetane number. The reference fuels are prepared by blending normal cetane (n-hexadecane) having a value of 100, with α-methyl naphthalene, a highly branched paraffin with an assigned value of 15.

When a fuel has the same ignition quality as a mixture of the two reference fuels, its cetane number is derived from the equation:

Cetane number = % n-cetane + 0.15% (heptamethyl nonane) (3.2)

In practice, the compression ratio of the engine is varied to give the same ignition delay period for the test fuel and two references blends of higher and lower quality than the test fuel, which differ by less than five cetane numbers. The cetane number of the unknown test fuel is calculated by interpolation between the lowest and highest compression ratios [110].

The important physical properties of LFPO obtained in the plant was tested in a standard test laboratory in Chennai, India. Because of non-availability of instrumentation for measuring the cetane number, the cetane number was calculated by using an empirical relation. The cetane numbers were calculated as a function of ignition delay (ID) of the fuel with the following empirical relations [113]:

CN0 % = 0.1136 ID2 - 8.9208 ID +160.13 (3.3)

CN25% = 0.0626 ID2 - 6.9835 ID + 140.14 (3.4)

CN50% = 0.0409 ID2 - 7.0376ID +141.93 (3.5)

CN75% = 0.0609 ID2 -7.5772 ID +143.38 (3.6)

CN100% = 0.0773 ID2 - 8.1886 ID + 147.46 (3.7)

The average cetane number (C_{AN})

= (CN0% + CN25% + CN50% + CN75% + CN100%)/5 (3.8)

The results on cetane numbers of different LFPO and its diesel blends are discussed in Chapter 5.

The properties of diesel, crude TPO and LFPO are given in Table 3.6. From this table, it can be inferred that, density of LFPO is less than that of TPO but higher than that of diesel. Viscosity is also marginally higher than that of diesel fuel. The calorific value is higher than that of TPO, but lower than that of diesel fuel.

Table 3.8: Properties of diesel, crude TPO* and LFPO

Properties	ASTM Method	Diesel	TPO*	LFPO
Density (kg/m^3 @20 ^{o}C)	D1298	830	920	910
Kinematic viscosity (cSt@40 ^{o}C)	D445	2.70	5.4	3.06
Calorific value (MJ/kg)	D4809	43.8	38	39.2
Cetane number	D613	50	20-30	32
Flash point (^{o}C)	D93	50	43	30
Fire point (^{o}C)	D92	56	50	50
Sulphur Content (% wt)	D2622	0.29	0.72	0.70
PH	D6423	7	4-7	5-7

*Properties of TPO obtained as crude from a laboratory level pyrolysis reactor [114].

Chapter 4

EXPERIMENTAL METHODOLOGY

4.1 General

CI engines are designed to run on diesel fuel only. Also, the fuel property values of the alternative fuels are not as equal as diesel fuel properties. From the fuel characterization, it is understood that the light fraction of pyrolysis oil (LFPO) can be used as a source of energy and substituted for diesel fuel. Therefore, before introducing LFPO for commercial use in CI engines, a necessary fuel or engine modification is essential. This chapter presents the details of the experimental test setup used for examining the applicability of LFPO for CI engines. A complete description of the instrumentation and the step by step methodology followed for the experimental investigation are also provided in this chapter.

4.2 Engine Experimental Setup

For the entire investigation, a single cylinder, four stroke, air cooled, direct injection, diesel engine, with a developing power of 4.4 kW at 1500 rpm was used. The reasons for using a single cylinder instead of a multicylinder advanced diesel engine for the investigation are given below:

(i) It is easy to dismantle and assemble the engine components, while carrying out a study with engine modification.

(ii) Fuel consumption of a single cylinder engine will be less than that of a multi cylinder engine.

(iii) It is easy to forecast its applicability for a long term use.

A schematic diagram of the experimental setup is shown in Figure 4.1. The technical details of the engine are listed in Appendix II.

A fuel sensor measured the lower and upper menisci of the fuel flow in the fuel burette and gave it to a data acquisition system. With this data, the total fuel consumption (TFC) was determined for every load. An electrical dynamometer coupled with the shaft of the

engine provided the loading to the engine. An air flow sensor connected after an air box measured the intake air flow rate to the engine. A temperature sensor mounted near the exhaust manifold measures the exhaust gas temperature. A quartz piezo-electric pressure transducer (Make: KISTLER, Model: 5395A) which was mounted on the engine cylinder head, and connected to a charge amplifier was used to measure the pressure inside the cylinder at each crank angle (CA). The cylinder pressure obtained for each crank angle was collected and stored in a computer. For every load, the combustion parameters such as ignition delay, heat release rate, combustion duration, etc. were calculated in an excel sheet using different formulae. An AVL DiGas444 exhaust gas analyzer measured the exhaust emissions such as unburnt hydrocarbon (HC), carbon monoxide (CO), carbon dioxide (CO_2) and nitric oxide (NO). The HC, CO and CO_2 emissions are measured by the NDIR (non-dispersive infrared) principle. The NO emission was measured by an electrochemical sensor. The complete description of each and every instrument used in the experimental setup and the method of measurement in the investigation are given in the subsequent sections.

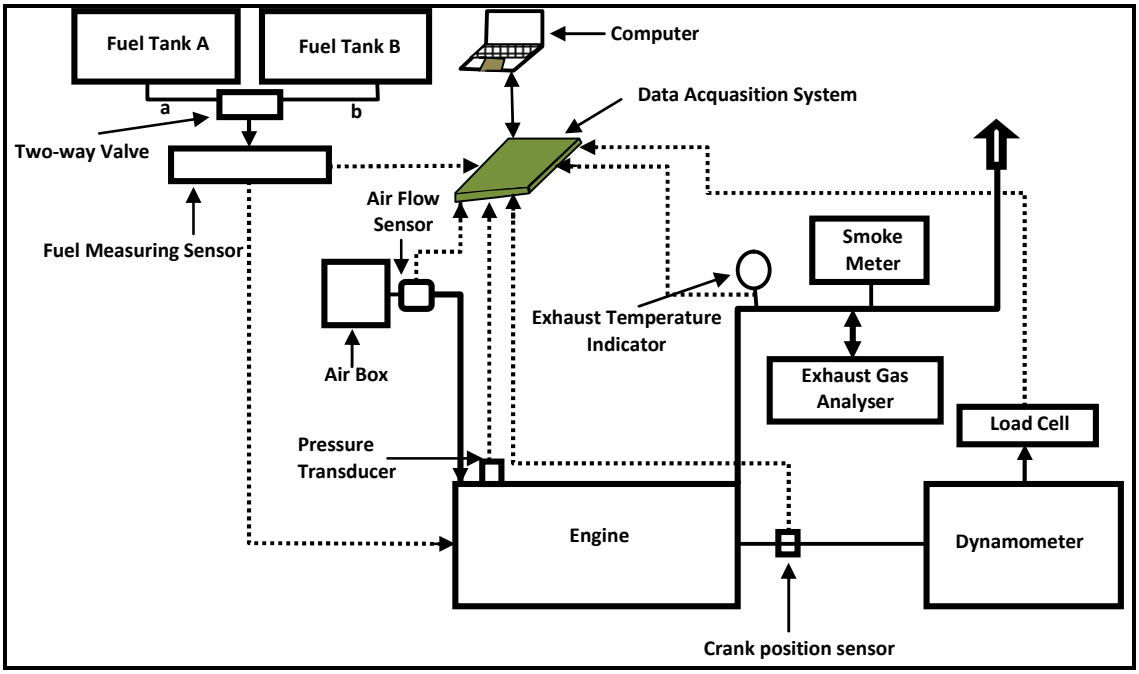

Figure 4.1: Engine experimental setup

4.3 Engine Loading

A resistive load bank assisted electrical dynamometer is used in this study to measure the load. A photograph of the load bank is shown in Figure 4.2. The load bank was able to provide electrical resistance to the dynamometer in multiples of 500A and the maximum current given was 16-18.7 A. By varying the resistance, the load to the engine was varied. The calculation for determining the correct amperage for a particular engine loading is obtained from the expression given below:

Load in watt = VI cosθ (4.1)

where V = Voltage in volt

I = Current in ampere

cosθ = Power factor

Although the engine can withstand up to 110%, only 100% load was applied.

Figure 4.2: Photograph of load bank

4.4 Fuel Consumption Measurement

4.4.1 Fuel flow measurement

The photographic view of the fuel measuring device is shown in Figure 4.3. A burette is located between the two fuel tanks provided for diesel fuel (Tank A) and alternative fuel (Tank B), and the fuel line as shown in Figure 4.1. A two way valve (v) is fitted at the entry of the burette. By turning the valve to position "a", fuel from the diesel tank (i.e., Tank A) will enter into the burette whereas by turning to position "b", fuel from LFPO tank B (Tank B) will enter.

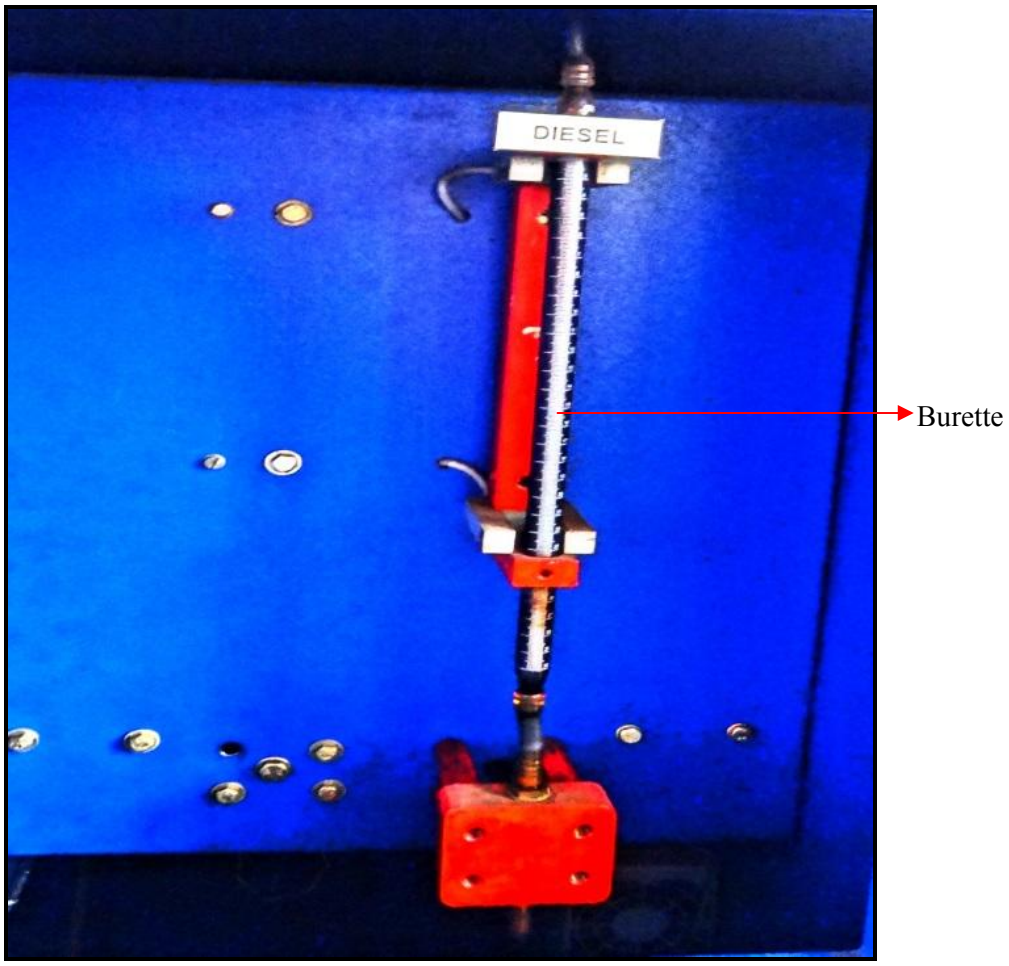

Figure 4.3: Photographic view of fuel measuring device.

In the experimental setup, a fuel flow sensor is located between the outlet of the fuel burette and the fuel injection pump. A three way valve is fitted at the bottom of the burette. The photographic view of the three way valve is shown in Figure 4.4.

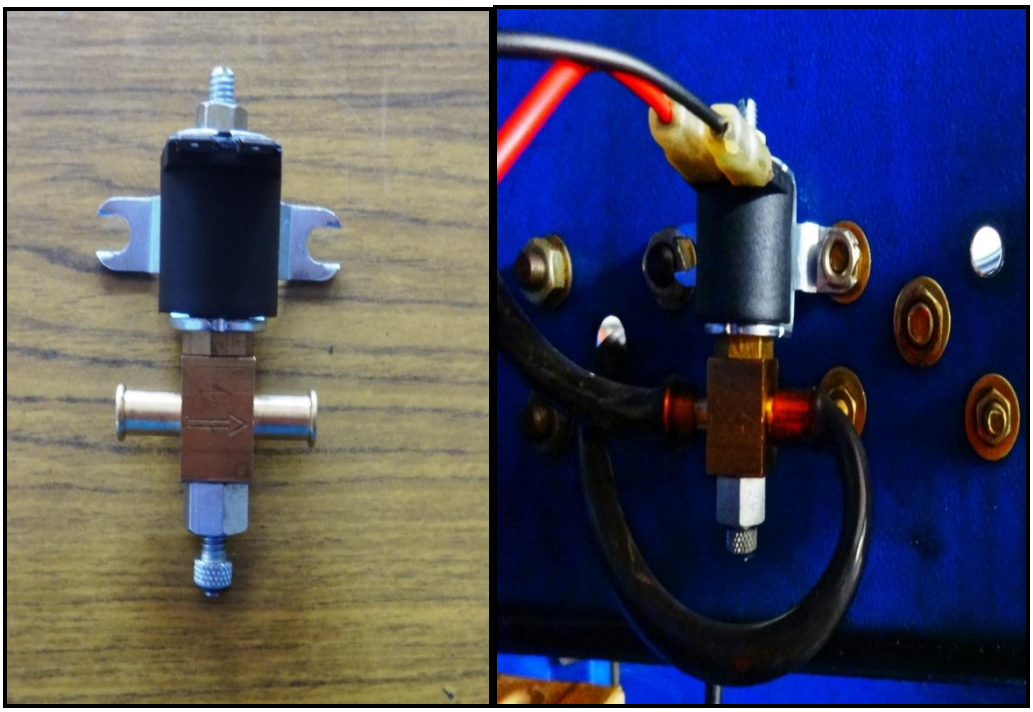

Figure 4.4: Three way valve

Three small diameter hose pipes are fixed to the three way valve. One pipe is connected to the fuel pump, the second pipe to the fuel tank outlet valve and the third valve to the burette. By turning the three way valve in a proper position, the fuel from the fuel tank flows to the engine via the burette. Two sensors located in front of the burettes are used to measure the level of the fuel flow. When the fuel is consumed by the engine, the fuel flow in the burette drops. The sensor senses the fuel levels (initial and final) and gives the input to a data acquisition system. For the corresponding engine load, the fuel consumption is calculated by the following formula, which is provided in an Excel sheet, a part of data acquisition system.

4.4.2 Fuel and energy consumption

The brake specific energy consumption (BSEC) is a reliable parameter, when two fuels with different densities and heating values are blended together, and used in an engine. It is directly proportional to the brake specific fuel consumption (BSFC). BSEC is found out by the following formula:

$$BSEC = BSFC \times CV \tag{4.2}$$

where CV is the calorific value of the fuel and BSFC is found by the formula:

$$BSFC = FC / BP \tag{4.3}$$

where FC is fuel consumption per unit time and BP is the brake power of the engine. BSEC is inversely proportional to the thermal efficiency of the engine.

4.5 Air Consumption Measurement

The air consumed by the engine in this investigation was measured, using the air box method. The photograph of the air box used for the air consumption measurement is given in Figure 4.5.

Figure 4.5: Photograph of the Air Box

The air consumption in kg/h is measured by the following formula

$$M_a = Q\rho_a 3600 \tag{4.4}$$

where M_a= Mass flow rate of air in kg/ h, Q = Volume flow rate of air in m^3/h,

ρ_a = Density of air in kg/m^3

$$Q = AV_a \tag{4.5}$$

where A = Area of orifice $= \frac{\pi d^2}{4}$, V_a = Velocity of air in m/s

d = diameter of orifice in m

Velocity of air is expressed as

$$V_a = C_d\sqrt{2gh_a} \tag{4.6}$$

where C_d = Coefficient of discharge

g = Acceleration due to gravity in m/s^2

h_a = Head of air in m

$$h_a = \frac{h_w \ \rho_w}{\rho_a}$$

h_w = Head of water, m = h_1-h_2 (4.7)

ρ_w = Density of water in kg / m^3

ρ_a = Density of air in $kg / \ m^3$

The brake thermal efficiency (BTE) is found out by the formula:

$$BTE = \frac{BP}{FC} \times CV \quad (4.8)$$

where BP is the brake power of the engine, FC is the fuel consumption per unit time and CV is the calorific value of the fuel.

4.5.1 Thermal energy balance

Thermal energy is the amount of heat supplied and heat utilised, in various ways in the system. The necessary information concerning the performance of the engine can be obtained from the heat balance sheet. The various ways in which heat is utilised are: (a) useful work, (b) heat carried away by the exhaust gases and (c) unaccounted heat losses (coolant, friction, radiation, lubrication oil, etc.). The thermal energy balance can be calculated using the following equations:

(i) The heat supplied by the fuel Q in kJ/h is given as:

$Q = CV \times m_f$ (4.9)

where CV = Calorific value in kJ/kg and m_f = Mass rate of fuel consumption in kg/h.

(ii) Heat converted to useful work or brake work L_1 in kJ/h is given as:

$L_1 = B\ P \times 3600$ (4.10)

where BP = Brake power in kW

(iii) Percentage of useful work $= \frac{L_1}{Q} \times 100$

(iv) Heat loss through the exhaust L_2 in kJ/ h is given as:

$$L_2 = \left(m_a + m_f\right) \times C_{pg} \times \left(T_g - T_a\right) \ \left(kJ / h\right) \quad (4.11)$$

where m_a= Mass rate of air consumption in kg/h,

m_f = Mass rate of fuel consumption in kg/h

C_{pg} = Specific heat of gas at constant pressure in kJ/kg ^oC

T_g = Exhaust gas temperature ^oC and T_a =Atmospheric temperature = 32^oC

(v) Heat carried away by the lubricating oil (L_3) is neglected, because the heat loss is very less.

(vi) Unaccounted heat loss L_4 in kJ/h is given as:

$$L_4 = Q-(L_1+L_2+L_3) \quad (4.12)$$

4.6 Exhaust Gas Emission Measurement

The exhaust gas of the diesel engine consists of different pollutants such as unburnt hydrocarbon (UHC), carbon monoxide (CO), carbon dioxide (CO_2), oxides of nitrogen (NO_x), particulate matter (PM), oxides of sulphur (SO_x) etc. [115]. The important gas emissions, namely, hydrocarbon (HC), carbon monoxide (CO), oxides of nitrogen (NO_x), and smoke opacity can be measured using different instruments. As mentioned in the general description of the experimental setup, HC, CO and CO_2 were measured using the non-dispersive infrared (NDIR) principle which is described in the following subsection.

4.6.1 NDIR Principle

The working principle of an NDIR analyzer is shown schematically in Figure 4.6. The NDIR analyzers employ the Beer-Lambert's Law. It defines the extent of absorption of radiations when they pass through a gas column as given below,

$$I = I_o (1 - e^{-k.c.d}) \quad (4.13)$$

where

I = Radiation energy absorbed

I_o = Incident radiation energy

k = Characteristic absorption constant for the gas, m^2/g-mole

c = Concentration of the gas, g-mole/m^3

d = Length of the gas column, m

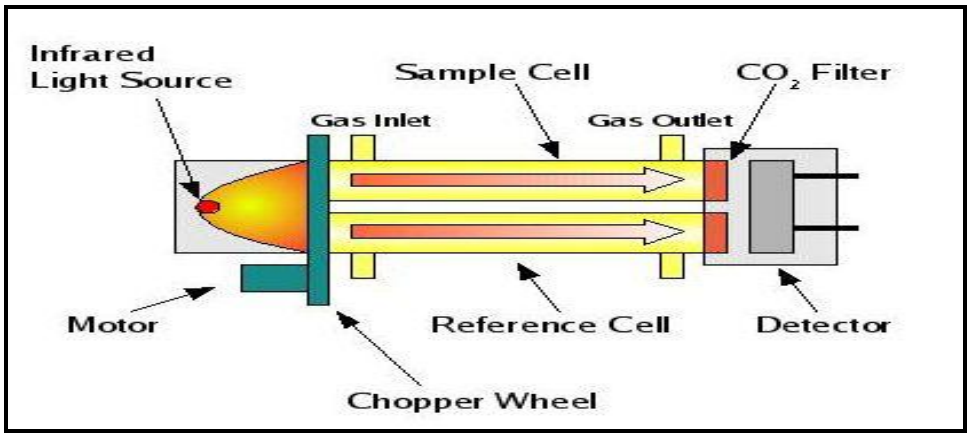

Figure 4.6: NDIR Principle

According to this, the analyzer operates on the principle of the different absorption of energy from two columns of gas: (i) the gas to be analyzed in the sample cell and (ii) a gas of invariant composition contained in the reference cell. The gas in the reference cell is free of the interest and relatively non-absorbing in the infrared region. Infrared radiation sources of the same intensity are positioned at one end of each cell and a differential detector at the other end. The infrared radiations from a single source are usually split into two beams of the same intensity, one each for the sample and reference cells. The detector is filled with the gas of interest, so that the energy transmitted to the detector is fully absorbed. The flexible diaphragm of the detector senses the differential pressure between the two halves of the detector caused by the difference in the amount of energy absorbed. The deflection in the diaphragm is used to generate an electrical signal that determines the concentration of the gaseous species of interest [116].

Carbon monoxide exhibits a strong absorbance in the wave length band 4.5-5 μm. Interference caused by CO_2 and water vapor is overcome by using optical filters or an interference cell filled with CO_2 saturated with water vapor. The NDIR analyzer is used for accurate measurements of CO and CO_2 in the exhaust gases.

4.6.2 Electrochemical sensor principle

The specific detection of nitric oxide (NO) by the electrochemical sensors is based on a general principle used in electro chemistry. In brief, the NO diffuses across a gas-permeable membrane, and a thin film of electrolyte covering the probe. The NO species are oxidized on the sensor which consists of a working and Ag/AgCl reference electrode pair. A potential (approx 900 mV) is applied to the working/measuring electrode, relative to a reference electrode, and the resulting small redox current due to the oxidation of NO

according to the following reaction, is measured by an amplifier system and recorder [117].

$$NO + 4OH^- \rightarrow NO_3^- + 2H_2O + 3e^- \quad (4.14)$$

4.6.3 Exhaust gas analyzer

The exhaust gas sample was analyzed by a Gas analyzer (Make: AVL India, Model: 444) fitted with a DiGas sampler. The gas analyzer sampling was certified by the Automotive Research Association of India (ARAI), which is the authority to assign test certificate to all IC engine based automotive vehicles in India. The principle of measuring the CO, HC, CO_2 emissions was the NDIR, and for the NO and O_2, it was electrochemical. The CO, CO_2, O_2 emissions were measured in volume percentage, while the total unburnt hydrocarbon was measured in ppm (vol.) of n-hexane equivalent, and the NO emission was measured in ppm (vol.) during each run of the engine operation. The photographic view of the AVL Digas 444 analyzer is shown in Figure 4.7. The complete technical specification of the AVL Digas 444 analyzer are given in Appendix III.

Figure 4.7: Photographic view of the AVL Digas 444 analyzer

The analyzer recorded the emissions over a span of 120 s in consecutive intervals of 20 s, which was greater than the instrument response time of 15 s, for each case of the engine operation. The exhaust gases were tapped from a T joint between the exhaust gas outlet and the smokemeter tapping point. A fine filter to remove the advected particulates and a condensate trap were incorporated, after the main exhaust gas cooler so that the exhaust inlet temperature to the analyzer was maintained less than 40^{o}C as per the instruction manual. Stray condensates, if any, were tackled by the condensate separator inbuilt in the

analyzer, which was flushed before every case of data recording. Leak check, HC residue test, zero adjustment and condensate purging of the analyzer, were carried out before each observation. The CO, CO_2 and HC emission were measured by the Non-Dispersive-Infrared (NDIR) detection principle, while the O_2 and NO emissions were measured by the pre-calibrated electrochemical sensors in the analyzer. The analyzer was periodically calibrated with the recommended calibration gas mixture, before experimentation.

The detector in the gas analyzer was made up of a Selenium photocell with a diameter of 45 mm. Its maximum sensitivity in light was within the frequency range of 550-570 nm. Below 430 nm and above 680 nm, the sensitivity of the instrument was less than 4% related to the maximum sensitivity. Emission tests were carried out by inserting a probe into the engine's exhaust tube by opening the ball valve. Before taking the emission test, a leak check was conducted in the digital gas analyzer, to discharge the residual gases by closing the probe's nozzle manually.

4.6.3.1 Brake specific emission calculation

It is a general practice to express the emission data on a brake specific basis, except for the smoke opacity. The brake specific emissions are the mass flow rates of the individual pollutant divided by the engine power. The formulae used to convert the emissions of HC, CO and NO from ppm, and % vol into g/kWh are given below:

$$\text{HC (in g/kWh)} = \{(m_f+m_a)/(29\times1000)\} \times \text{HC (in ppm)} \times 13/\text{BP} \quad (4.15)$$

$$\text{CO (in g/kWh)} = \{(m_f+m_a)/29)\times10\} \times \text{CO (in \% vol)} \times 28/\text{BP} \quad (4.16)$$

$$\text{NO (in g/kWh)} = \{(m_f+m_a)/(29\times1000)\} \times \text{NO (in ppm)} \times 32.4/\text{BP} \quad (4.17)$$

where m_f = mass of fuel consumption, m_a = mass of air consumption, BP = brake power

4.6.4 Gas analyzer calibration procedure

4.6.4.1 Pre-test calibration

The gas analyzer was calibrated prior to the emission test with calibration gases certified to ± 2% accuracy as per the Environmental Protection Agency (EPA) 40 CFR part 60 and ISO 3930, 1976 test methods. Three calibration gases (zero, mid and high) for CO, NO, and NO_2 were used. The purified ambient air was used as the zero gas. The mid-level gas concentration was 40% to 60% of the high range calibration gas. A high level gas concentration of the high range calibration gas was higher than 125% of the expected

concentration and less than 90% of the expected concentration. The high level gas was equal to the calibration span. The analyzer calibration error was no more than ±5% of the calibration span value for the mid and high range calibration gases, or 5 ppm, whichever was less restrictive [117].

The calibration error was calculated as follows:

% Difference = {(Analyzer Response – Gas Concentration)/(Calibration Span)} x 100 (4.18)

For zero gas, the calibration error shall be no more than10 ppm.

Difference in ppm = Analyser response – Zero gas concentration (4.19)

The steps involved in calibration are given in Figure 4.8.

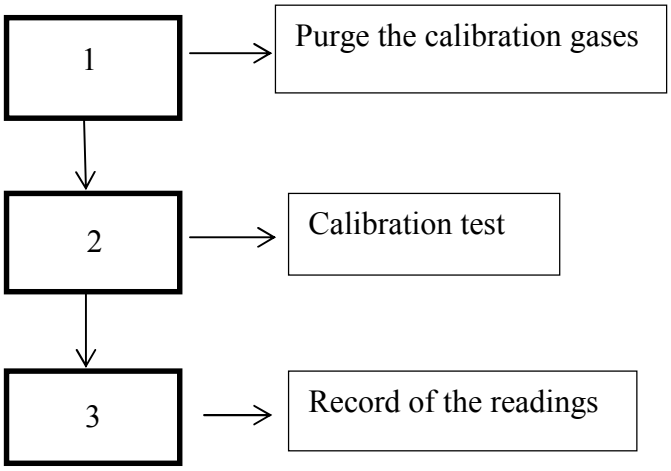

Figure 4.8: Calibration steps

4.6.4.2 Post-test calibration

After a maximum of three valid 20-minute emission tests, a post-test calibration was conducted for the HC, CO and NO calibration as per the following procedure:

(i) The analyzer was allowed to purge the gas sample until a stable zero reading is observed. This is recorded as zero reading.

(ii) The high range calibration gas to the analyzer and it is allowed to reach a stable reading before recording the analyzer reading.

(iii) The mid-range calibration gas is introduced into the analyzer and it is allowed to reach a stable reading. The analyser reading is recorded at this position.

(iv) The percentage difference with respect to the pre-test calibration value is calculated as:

$$\% \, Difference \; = \; \frac{a-b}{b} \times 100 \tag{4.20}$$

Where a = Post-test reading

b = Pre-test reading

If the difference is greater than ± 5% or 5 ppm, whichever is less restrictive, the emission test runs are invalid, and must be repeated. For zero gas, the post-test calibration error shall be not more than 10 ppm.

4.7 Smoke Measurement

4.7.1 General

Earlier, filtration type smoke-meters such as the white filter paper of specified quality were used. The degree of darkening of filter paper was evaluated by a light reflectance meter or visually, and was a measure of the exhaust smoke density. Opacimeters provide a more realistic measurement of the visible smoke emissions from diesel engines [118]. Presently, most smoke-meters or opacimeters use the light absorption principle.

4.7.2 Absorption Method

There are three main types of absorption viz., (i) light extinction type, (ii) continuous filtering type and (iii) spot filtering type. In light extinction type method, the intensity of a light beam is reduced by smoke which is a measure of the smoke intensity. Figure 4.9 shows the schematic diagram of the light extinction method.

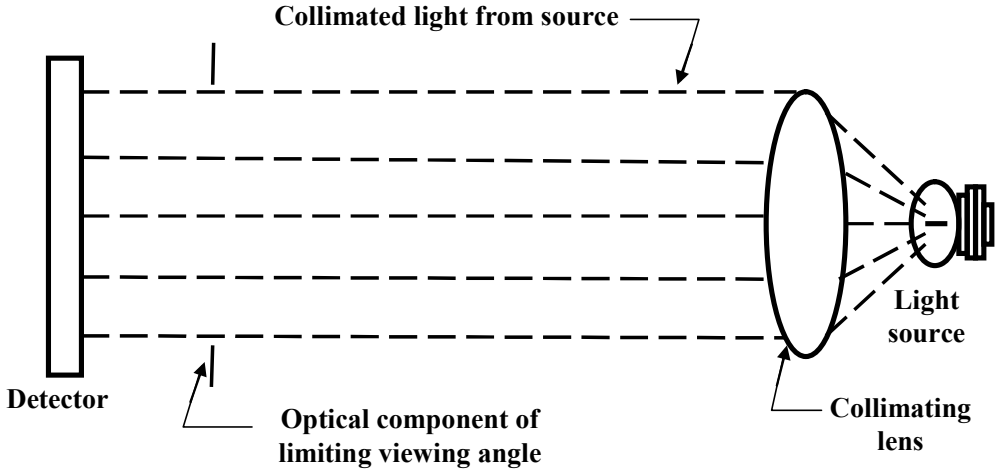

Figure 4.9: Light extinction method for measuring smoke

A continuously taken exhaust sample is passed through a tube of about 45 cm length, which has a light source at one end and a photocell at the other. The amount of light passed through this column is used as an indication of the smoke level or smoke density. The smoke level or smoke density is defined as the ratio of the electric output from the photocell when the sample is passed through the column to the electric output when clean air is passed through it.

Light from a source is passed through a standard length tube containing the exhaust gas sample from the engine and at its other end the transmitted light is measured by a suitable device. The fraction of the light transmitted through the smoke (T) and the length of the light path (L_e) are related by the Beer-Lambert law [111] as given below.

$$T = e^{-K_{ac} L_e} \tag{4.21}$$

where $K_{ac} = nA\theta$ = optical absorption coefficient of the obscuring matter per unit length, n = number of soot particles per unit volume, A = average projected area of each particle and θ = specific absorbance per particle.

The light source used in the absorption type smoke meter is an incandescent lamp with a colour temperature in the range of 2800 K to 3250 K or a green light emitting diode (LED) with a spectral peak between 550 nm and 570 nm. The receiver is a photocell or a photo diode (with filter, if spectral response similar to the photopic curve of the human eye i.e., maximum response should be in the range 550 nm to wavelength).

When light in the visible range from a source is transmitted through a definite path length of the exhaust gas, the smoke opacity is the fraction of light that is prevented from reaching the observer or the light detector of the smoke meter. The absolute smoke density is given by the absorption coefficient k, that is equal to the product c.d in the Equation (4.16), and has unit m^{-1}. The light absorption coefficient k, is given by Equation (4.22).

$$K = -\frac{1}{L\, ln\left(I / I_o \right)} \tag{4.22}$$

where L is length of the smoke column in meter, through which the light from the source is made to pass, I_o is the intensity of incident light and I is the transmitted light falling on the smoke meter receiver. The photographic view of the AVL Diesel smoke-meter is shown in Figure 4.9. The technical specification of the AVL437C Diesel smoke-meter is

given in Appendix IV. The exhaust gas sample is made to flow through a smoke measurement tube of fixed length. The pressure in the smoke tube should not differ by more than 75 Pa from the atmospheric pressure. Across the open ends of the smoke tube, the light source and detector are placed. The gas column absorbs part of the light from the source and the opacity is determined. In the full flow type, the light source and detector assembly are laced directly across the exhaust gas stream, usually at the end of the exhaust pipe. In this case, the path length of the smoke measurement varies with the cross sectional size of the exhaust gas stream or tail pipe. Hence, the conversion charts of the measured value to the absolute smoke density K for the different path lengths are made available for the full flow smoke meters.

Figure 4.9: Diesel smoke-meter

4.8 Combustion Parameter Measurement

4.8.1 Piezo electric pressure transducer

For acquiring the important combustion parameters, such as ignition delay, heat release rate, combustion duration, etc., the cylinder pressure and crank angle values are necessary. The cylinder gas pressure was measured using a Kistlerpiezo-electric transducer (model 5395A) in conjunction with a Kistler charge amplifier. The photograph of the pressure transducer used in this study is shown in Figure 4.10.

Figure 4.10: Photographic view of the Kistler pressure transducer

The quartz sensors can withstand a very high pressure varying from 0 to 250 bar. A hole was drilled on the dummy plug and the pressure sensor was placed in it. The drilled hole diameter was 5mm and an internal thread of pitch 1mm is made. The piezo-electric sensor was properly sealed so that there was no change in the compression ratio of the cylinder. The pressure produced by the engine cylinder was sensed by the pressure sensor placed on the dummy plug. The measured pressure acted through a diaphragm on the quartz crystal measuring elements, which transforms the pressure into an electrostatic charge Q in pico coulomb. The sensor was mounted on the combustion chamber plug end by a M5 tapping hole to accommodate the sensor. The complete specification of the Kistler make piezo quartz pressure sensor is given in Appendix V.

Figure 4.11 shows a photographic view of the location at which the pressure transducer is flush mounted at the top of of the engine head. The stainless steel diaphragm was welded hermetically to the stainless steel body. The quartz elements were mounted in a highly sensitive arrangement (transversal effect). The quartz element had a high natural frequency. Its connector was welded to the body, but its teflon insulator was not absolutely tight.

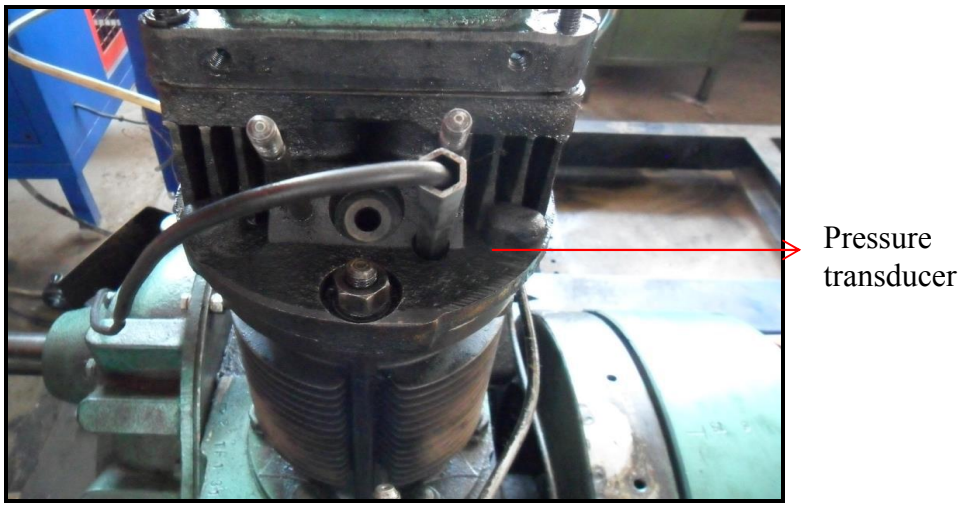

Figure 4.11: Photographic view of flush mounted transducer in engine cylinder head

The top dead centre (TDC) marker (Kistler model 5015A1000) was placed near the engine flywheel. At the TDC position, a small metallic deflector was fitted. The photographic view of the TDC marker and metallic deflector is shown in Figure 4.12. The setup was aligned in such a way that the sensor gives the output in the form of a square wave, exactly when the piston is at the TDC.

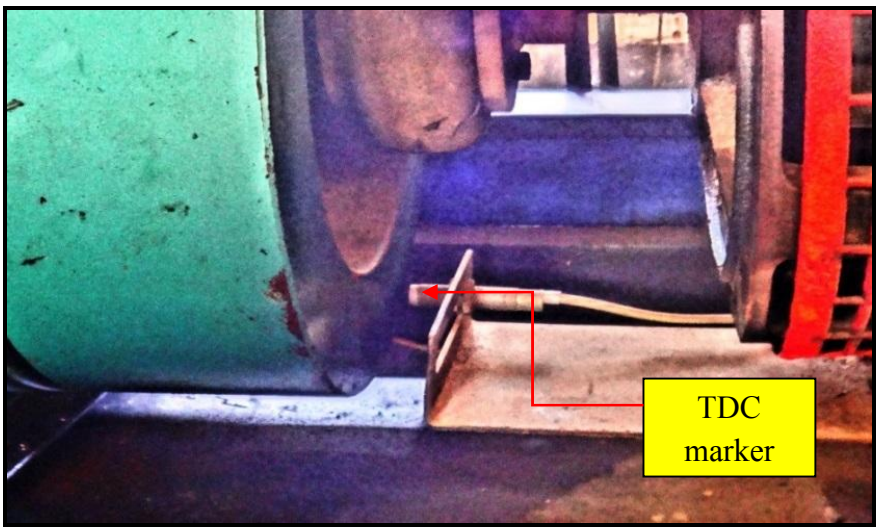

Figure 4.12: Photographic view of the TDC marker and deflector

In this research study, the gas pressure data was recorded as the average of 20 cycles of data, with a resolution of 0.5°CA, using a data acquisition system. From the average data of the pressure and crank angle values, the peak pressure, occurrence of the peak pressure, maximum rate of pressure rise and heat release rate were calculated, and stored in an excel file.

4.8.2 Pressure transducer calibration

The calibration of the pressure transducer was carried out to measure any differences in the output of the transducer for a known pressure. This was essential to minimize the combustion cylinder pressure measurement error, and was particularly important for the engine data. The calibration of pressure transducer is important, because it experiences thermal and mechanical stresses. The general procedure of calibration of the pressure transducer is described below.

The piezo-electric transducer signals naturally decay over time, and are therefore only suitable for dynamic measurements, like engine cylinder pressure measurements. Accordingly, they must be calibrated using a dynamic procedure. The Kistler piezo-electric transducer of model 5395A was subjected to a dynamic calibration procedure, using a standard dead weight tester. The dead weight tester generated the known pressure by hydraulically lifting precise weights with a piston, with an accurately known cross-sectional area. The charge output signal of these transducers was used as the input to a charge amplifier via a high impedance cable. The charge amplifier converts the low level charge (which is of the order of several picocoulomb) to a proportional voltage, which can be recorded with standard data acquisition equipment. In this procedure, a known pressure is applied to the transducer. Then, the output is grounded to zero volts, thereby eliminating signal decay. The pressure is then abruptly dropped to the atmospheric level, by rapidly releasing the hydraulic pressure holding up the weights and allowing them to fall. The resulting voltage change is recorded as a function of time, using a digital oscilloscope programmed to trigger on a voltage drop. The voltage change caused by the pressure change is determined, using a peak-to-peak calculation feature on the scope. Dynamic pressures are taken at intervals of 200 psi from 200 to 1000 psi. Readings are taken at each dynamic pressure. These are then averaged and a graph was plotted against the corresponding voltage output. The linearity of the transducer is found to be better than 1%. The repeatability is observed to be about 2 to 3%.

4.8.3 Charge amplifier

Figure 4.13 shows the charge amplifier circuit which was used to collect the output from the pressure transducer. The charge amplifier circuit was used to convert the obtained charge into an equivalent output voltage. It transferred the input charge to another

reference capacitor and produced an output voltage equal to the voltage across the reference capacitor.

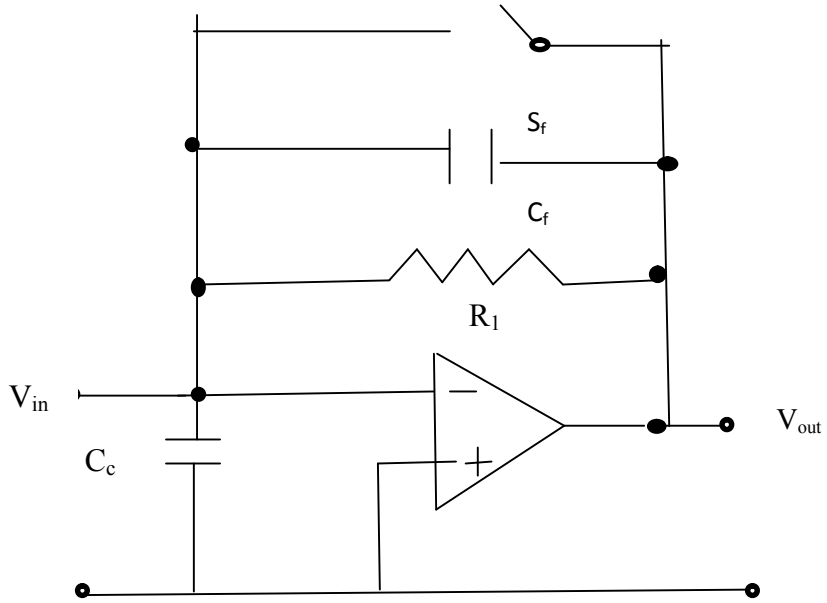

Figure 4.13: Charge amplifier circuit

Thus, the output voltage was proportional to the charge of the reference capacitor or the input charge; hence, the circuit acted as a charge to the voltage converter. The complete specification of the charge amplifier is given in Appendix VI. The input charge Q_{in} was applied to the summing point (inverting input) of the amplifier. It was distributed to the cable capacitance Q_c, the amplifier input capacitance Q_a and the feedback capacitor Q_f.

The node equation of the input is therefore: $Q_{in} = Q_c + Q_a + Q_f$ (4.23)

Using the electrostatic equation: $Q = U \times C$ and substituting Q_{in}, Q_c, Q_a and Q_f

$$Q_{in} = U_a x \left(C_c + C_a\right) + U_f x\ C_f \tag{4.24}$$

and solving the output voltage V_o:

$$V_o = V_f = \frac{Q_{in}}{C_f} \tag{4.25}$$

V_o is fed into the data acquisition system. The output of the Kistler charge amplifier lies within ± 10V DC.

4.8.4 Analog to Digital Converter

The analog signals from the sensors were fed into an Analog to Digital Converter (ADC) and then passed to a display unit, through a data acquisition card and micro controller. Both the pressure and proximity sensors were interfaced with the engine, and the output obtained was an analog signal. Further, the analog signal was converted into digital using the ADC, which was finally fed to a display unit through the data acquisition system. Using the data acquisition system, a graphical analysis evaluating the differential equation, computing the mathematical expression, display, control and recording were carried out for various engine operating parameters, like instantaneous pressure, crank angle, temperature and the heat release rate. From this, other combustion parameters, such as ignition delay, cumulative heat release rate, mass fraction burned and combustion duration were computed. A computer was used to process the data and store it during the investigation.

4.8.5 Necessity of the p-θ diagram

For studying engine behavior, measurement of pressure developed inside the cylinder with respect to every crank angle degree is very important, because both the values are used to calculate other combustion parameters such as ignition delay, heat release, rate of pressure rise, combustion duration etc., which are most important for the combustion analysis. The pressure inside the cylinder depends on the instantaneous cylinder volume, combustion, heat transfer to the combustion chamber walls, crevice regions and leakage. The p-θ diagram gives quantitative information on the progress of combustion. Valve timing, i.e., valve opening and closing, can be optimized based on this p-θ diagram. The determination of the other combustion parameters is described in the following subsections.

4.8.5.1 Ignition delay

The ignition delay of a CI engine is defined as the time (or crank angle) interval between the start of injection and the start of combustion. This delay is due to physical and chemical processes that take place before a significant fraction of the chemical energy of the injected liquid fuel is released. The physical processes are: atomization of the liquid fuel jet, evaporation of the fuel droplets and mixing of the fuel vapor with air. The chemical processes are precombustion reactions of the fuel, air and the residual gas mixture that leads to auto-ignition. These processes are affected by the engine design, operating variables and fuel characteristics. The start of combustion can also be

determined as the point at which the heat release rate curve deviates from the native axis to the positive [64].

Based on the crank angle, the ignition delay is determined with the following equation:

$$\text{Ignition delay in CA} = (CA)_{5\%} - (CA)_{inject} \quad (4.26)$$

where, $(CA)_{5\%}$= Crank angle at which 5% heat is released

$(CA)_{inject}$ = Crank angle at which fuel is injected into the combustion chamber.

4.8.5.2 Heat release rate

The heat release analysis can provide valuable information about combustion and its related parameters. It can also provide information about the effects of engine design changes, fuel injection system, fuel type, and engine operating conditions, on the combustion process and engine performance. The rate of heat release at each crank angle was determined by the following formula, derived from the first law of thermodynamics [119]:

$$\frac{dU}{dt} = Q - W \quad (4.27)$$

where, Q = the combination of the heat release rate and the heat transfer rate across the cylinder wall,

W = the rate of work done by the system due to the system boundary displacement.

U = Internal energy, t = time

Equation (4.27) can be simplified as

$$mC_v \frac{dT}{dt} = Q - p\frac{dV}{dt} \quad (4.28)$$

where m = mass of gas

C_v = Specific heat at constant volume of gas

T= Absolute temperature of gas

P = Gas pressure in cylinder

To simplify Eqn. (4.28) the following ideal gas assumption can be used.

$$pV = mRT \quad (4.29)$$

where p = Cylinder pressure

V= Volume of the cylinder

m = mass of gas

R = Gas constant

T = Absolute temperature

Eqn. (4.29) can be differentiated as (assuming a constant mass)

$$\frac{dT}{dt} = \frac{1}{mR}\left[P\frac{dV}{dt} + V\frac{dP}{dt}\right] \tag{4.30}$$

After combining Eqns.(4.28) and (4.30), the heat release equation becomes

$$Q = \left(\frac{C_v}{R} + 1\right)p\frac{dV}{dt} + \left(V\frac{C_v}{R}\right)\frac{dp}{dt} \tag{4.31}$$

After replacing time (t) with the crank angle (θ), the equation becomes

$$Q = \left(\frac{\gamma}{\gamma - 1}\right)p\frac{dV}{d\theta} + \left(\frac{1}{\gamma - 1}\right)V\frac{dp}{d\theta} \tag{4.32}$$

where, γ is the ratio of the specific heats $\left(\frac{C_p}{C_v}\right)$, p is the cylinder gas pressure and V is the instantaneous volume of the cylinder. The instantaneous cylinder volume can be obtained from the engine geometry and crank angle values.

4.8.5.3 Combustion duration

The crank angle duration for mass fraction burned from 10% to 90%, has been taken as the combustion duration [120].

4.8.5.4 Rate of pressure rise

The rate of pressure rise defines the load that is imposed by the combustion process on the cylinder head and block, and to a large extent, determines the structural design [117, 118]. Also, the rate of pressure rise is indicative of the noisy operation of the engine. The rate of pressure rise with respect to the crank angle ROPR is derived from the following expression:

$$ROPR = \frac{dp}{d\theta} \tag{4.33}$$

4.8.5.5 Mass fraction burned

Assuming that the pressure rise Δp_c is proportional to the heat added to the in-cylinder medium during the crank angle interval, the mass fraction burned (MFB) at the end of the considered i-th interval may be calculated as [121]:

$$MFB = \frac{m_b(i)}{m_b(total)} = \frac{\sum_0^i \Delta P_c}{\sum_0^N \Delta P_c} \tag{4.34}$$

where 0 and N denote the start and end of combustion respectively. N is also the total number of crank intervals.

4.9 Error Analysis

Uncertainty is a measure of the goodness of a result. Without such a measure, it is impossible to judge the fitness of a value. An uncertainty or error analysis is necessary to establish the bounds on the accuracy of the estimated parameters. Evaluations of some unknown uncertainties from known physical quantities were obtained, using the following general equation [122]:

$$\frac{U_Y}{Y} = \left[\sum_{i=l}^{n} \left(\frac{1}{y} \frac{\partial y}{\partial xi} U_{x_i} \right)^2 \right]^{\frac{1}{2}} \tag{4.35}$$

In the equation cited, Y is the physical parameter that is dependent on the parameter x_i. The symbol U_y denotes the uncertainty in Y. The total percentage uncertainty of this experiment is

$$= \sqrt{\%} \left\{ \begin{array}{l} \left(\text{Uncertainty of Temperature}\right)^2 + \left(\text{Uncertainty of Engine Load}\right)^2 + \\ \left(\text{Uncertainty of Specific Fuel Consumption}\right)^2 + \left(\text{Uncertainty of Engine Speed}\right)^2 \\ + \left(\text{Uncertainty of Cylinder Pressure}\right)^2 + \left(\text{Uncertainty of Crank Position}\right)^2 + \\ \left(\text{Uncertainty of NO}\right)^2 + \left(\text{Uncertainty of HC}\right)^2 + \left(\text{Uncertainty of CO}\right)^2 + \\ \left(\text{Uncertainty of Smoke Opacity}\right)^2 + \left(\text{Uncertainty of the Data Acquisition System}\right)^2 + ... \end{array} \right\} \tag{4.36}$$

$$= \sqrt{\%} \{ (\pm 0.15)^2 + (\pm 0.2)^2 + (\pm 0.5)^2 + \left(\pm 1\right)^2 + (\pm 0.15)^2 + \left(\pm 0.01\right)^2 + \left(\pm 1\right)^2 + \left(\pm 0.5\right)^2 + \left(\pm 1\right)^2 + \left(\pm 1\right)^2 + \left(\pm 0.001\right)^2 \} = \pm 2.14\%$$

As a result, the maximum uncertainty of the experimental results obtained was ± 2.14%. The instruments used in the present study and their uncertainties are given in Appendix VII.

4.10 Use of LFPO in a CI Engine

Year after year, the emission regulations for internal combustion engines are becoming more stringent in many countries. Engine manufacturers are very keen to manufacture their engines according to the emission regulations which are accepted universally. Although the legislations vary from country to country, there is a minimum level of

emissions set by each and every country in the world. The refineries and fuel producers are also trying to comply with the regulations, by improving the fuel quality as much as they can. At present, most of the diesel engine manufacturers produce engines to use diesel fuel only. In order to use alternative fuels, it is necessary to either make the fuel quality closer to diesel quality, or modify the engine hardware. Improving the fuel quality by different methods, such as modification of fuel structure, addition of high cetane fuels, and use of additives is much simpler and cheaper than the complexity and cost involved in engine modification. Many parameters, such as the cetane number, density, carbon-hydrogen structure and aromatic content are affected when fuel modification is carried out. Density and cetane number can be more easily altered by fuel modification than restructuring the carbon hydrogen chain or reducing the aromatic content. As per the ASME standards the ranges of the above mentioned parameters for diesel fuel are as follows:

(i) Kinematic viscosity 1.9-4.1 cSt at 40°C,

(ii) Cetane number 40-55, and

(iii) Maximum aromatic content 35% by vol.

In the context of utilizing low cetane alternative fuels in CI engines, several researchers improved the fuel quality by (i) blending high cetane fuels, particularly with diesel or biodiesel, (ii) adding small quantities of ignition improvers [123, 124], (iii) fumigating the ignition improvers [125] or gaseous fuels [126] in a dual fuel mode and (iv) using oxygenated additives [127]. In this research study a fewer fuel and a few engine modifications have been carried out to use LFPO as an alternative fuel for CI engines.

4.10.1 Fuel blending

Blending the alternative fuel with diesel in different proportions and using the blends is the simplest method of using an alternative fuel in IC engines, because it does not require any major change in the engine hardware [128].

In this study, 20% to 80% of LFPO in steps of 20% on volume basis was blended with diesel and the blends were used as fuels in the test engine. The blends were denoted as XLFPO where X indicates the percentage volume of LFPO in the LFPO-diesel blend. For example 40LFPO contains 40% LFPO and 60% diesel. Test properties of the tested fuels are listed in comparison with diesel properties and given in Table 4.1.

Table 4.1: Properties of diesel, TPO, LFPO and its diesel blends

Properties	ASTM Standard	Diesel	TPO	LFPO	20 LFPO	40 LFPO	60 LFPO	80 LFPO
Density (kg/m^3 @ 20 ^oC)	D1298	830	920	910	844.3	862	885	905
Kinematic viscosity (cSt@40^oC)	D 445	2.58	3.77	3.06	2.53	2.87	3.11	3.35
Lower heating value (MJ/kg)	D 4809	43.8	38	39.2	42.58	41.96	41.04	40.23
Flash point by Abel method (^oC)	D93	50	43	30	34	42	40	31
Fire point (^oC)	D92	56	50	50	62	60	58	56
Cetane number	D 613	50	-	32	43.38	41.17	38.27	35.14
Sulphur content (% wt)	D3177	0.3	-	0.70	0.72	0.87	1.58	1.80

The engine behavior in terms of the combustion, performance and emission characteristics of the diesel engine run on the proposed fuels was analyzed, and compared with that of diesel operation. Initially, the engine was run with diesel to obtain the reference data at no load, 25%, 50%, 75% and full loads. After conducting all the tests with the blends, the engine was again run on diesel to ensure that there was no fuel trace of the different blends.

4. 10.2 Change of injection timing

When the engine was able to run with different LFPO-diesel blends in a single cylinder, DI diesel engine, the engine exhibited inferior to those obtained with the diesel fuel operation. Due to the lower cetane number and higher density of the blends, the ignition of the 40LFPO blend started a little later, and the ignition delay was also found to be longer. Injection timing is an important factor that affects the engine behavior in all means [129]. Therefore, the engine run on the 40LFPO was subjected to different fuel injection timings by advancing and retarding the injection timing of maximum 3^oCA with respect to the original injection timings.

For this purpose, the fuel pump in the test engine was dismantled to change the injection timing. The static injection timing was changed, by adjusting the number of shims under the mounting flange of the fuel injection pump. The fuel injection timing was changed by adding or removing the number of shims fitted in the fuel injection pump. The standard fuel injection timing of the engine is 23^{o}CAbTDC which was set by the manufacturer, and there were three shims. The thickness of every shim was 0.3 mm. The shim with 0.3 mm thickness was added to get the retarded injection timing, while the shim was removed to get advanced injection timing. Each shim can either give 1.5^{o}CA advancement or retardation, according to the addition or removal of the shim in the pump.

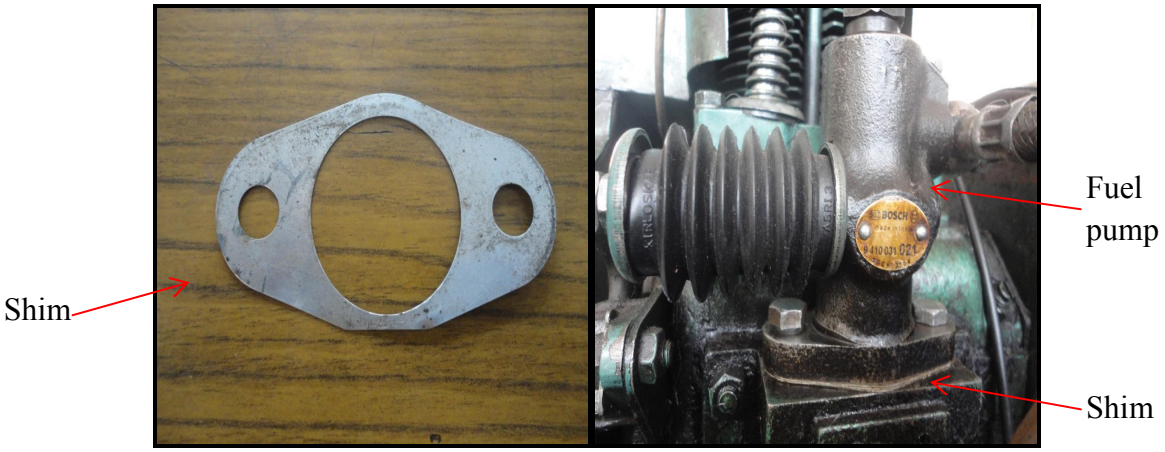

Figure 4.14: Photographic view of the (a) shim (b) shim fitted with fuel pump

Figures 4.14 (a) and (b) show the photographic view of the shim and the shim fitted with the fuel pump. In order to optimize the injection timing of the engine run on 40LFPO, experiments were conducted on the diesel engine with two different advanced injection timings and retarded injection timings from 20^{o}CAbTDC to 26^{o}CAbTDC at regular intervals of 1.5^{o}CA. The combustion, performance and emissions of the engine run on the 40LFPO blend were evaluated in the diesel engine at two advance injection timings (24.5^{o}CAbTDC and 26^{o}CAbTDC) and two retardation injection timings (20^{o}CAbTDC and 21.5 ^{o}CAbTDC) with the original injection timing (23^{o}CAbTDC). After finishing each set of experiment, the injection timing was restored to the original timing, and the next injection timing was set. The optimum injection timing was determined by analyzing the results of 40LFPO in comparison with the diesel data.

4. 10.3 Addition of cetane improver

Research reports indicate that the use of fuels with a high cetane number or ignition improver with a low cetane number fuel in the form of blends in CI engines would improve the engine behavior in terms of combustion and performance, while reducing the emissions in CI engines [130-133]. Running a CI engine fueled with a low cetane fuel in the dual fuel mode can also improve the combustion behavior of the engine [125]. Diethyl ether (DEE) is a good example of an ignition improver, whose cetane number is greater than 125, and it is an oxygenated fuel. It can be derived from various biomass materials at a cheaper cost [134]. Experimental investigations were carried out to study the effect of blending DEE in small quantities with diesel [135], ethanol-diesel blend [136], kerosene [137], orange oil [138], diesel water emulsion [139], bio-oil [89] and biodiesel obtained from Jatropha [140], Pongamia [141], Mahua [142], Palm oil [143], Cotton seed oil [144], Neem oil [145], and Soybean [146] on the engine behavior, in terms of the performance, emission and combustion parameters of DI diesel engines. Most of the investigation results suggested that there was a possibility of simultaneous reduction of NO_x and smoke emissions with improved performance. The main reasons stated for the reduction in the NO_x emission were improved cetane number, higher latent heat of vaporisation, and higher viscosity of the blend in some cases. The reduction in the smoke emission was attributed to the presence of oxygen, supplemented either by the DEE or the blend. In some experimental studies, DEE was fumigated in CI engines in which diesel [147], biodiesel [123], bioethanol-diesel blend [148] tyre pyrolysis oil [96] and orange oil [149] were used as pilot fuels. It was reported that the dual fuel mode offered improved brake thermal efficiency, and reduced smoke emission in comparison with those of neat diesel operation at part and full loads. The reason mentioned for the reduction in the smoke emission was the higher flame velocity of DEE and the presence of oxygen in it. DEE is a highly volatile flammable liquid [150]. It can easily catch fire and spread the flame very quickly [151]. Some researchers have reported that the NO_x emission was reduced, while some of them reported that the NO_x emission was higher than that of diesel operation at full load. The reason for reduced NO_x emission was the higher latent heat of vaporization, which reduced the maximum heat release rate in the premixed combustion phase. The reason for the higher NO_x stated by some of the researchers was the spontaneous ignition of DEE which enhanced the premixed combustion. Some researchers have used dimethyl

ether (DME) as an ignition improver with diesel [152], biodiesel [153] and diesel water emulsion [154]. They have also reported similar results.

Because of low cost and easy availability DEE was chosen as an ignition improver for this study. The effect of adding small quantities of DEE to the 40LFPO blend on the combustion, performance and emissions of the test engine was studied. In this investigation the DEE percentage was varied from 1 to 4%. Some important properties are listed in Table 4.2.

Table 4.2: Properties of diethyl ether

Properties	ASTM Method	DEE
Density (kg/m^3 @20 ^{o}C)	D1298	730
Kinematic viscosity (cSt@40 ^{o}C)	D445	0.23
Calorific value (MJ/kg)	D4809	33.9
Cetane number	D613	125
Flash point by Abel method (^{o}C)	D93	- 40
Fire point (^{o}C)	D92	44

The 40LFPO-DEE blend was stirred continuously with the help of a mechanical stirrer for about 30 minutes to ensure thorough mixing. The four test fuels namely, X1, X2, X3 and X4 were used in this investigation, where the numerical value indicates the percentage of DEE added to the 40LFPO blend. For example, X1 is a fuel that contains 40% LFPO, 1% DEE and 59% diesel. The compositions and designations of different 40LFPO-DEE blends are given in Table 4.3. The results of the combustion, performance and emission parameters of the engine run on these four blends were evaluated, compared with those of diesel operation under the same engine operating conditions, and discussed in Section 5.4.

Table 4.3: Composition of the test blends.

Designation	LFPO (%)	Diesel (%)	DEE (%)
Diesel	0	100	0
40LFPO	40	60	0
X1	40	59	1
X2	40	58	2
X3	40	57	3
X4	40	56	4

The physical properties of the 40LFPO and LFPO-DEE blends are listed in Table 4.4 in comparison with those of diesel and 40LFPO.

Table 4.4: Physical properties of diesel, 40LFPO, X1, X2, X3 and X4.

Properties	Diesel	40LFPO	X1	X2	X3	X4
Density (kg/m^3 @20 ^{o}C)	830	862	861	860	859	858
Kinematic viscosity (cSt@40 ^{o}C)	2.70	2.9	2.82	2.79	2.77	2.74
Lower heating value (MJ/kg)	43.8	41.9	41.8	41.7	41.6	41.5
Cetane number	50	41.2	41.9	42.6	43.4	44.2
Flash point (^{o}C)	50	42	41.9	41.8	41.7	41.6
Fire point (^{o}C)	56	60	53.5	53.4	53.2	53.1
Sulphur content (% wt)	0.3	0.87	0.48	0.48	0.47	0.47

4. 10.4 Addition of oxygenated additive

Many research works have been conducted to use low quality fuels with various oxygenated fuels or ignition improvers in diesel engines, after necessary engine or fuel modifications. The oxygenated additives used in the investigations included dimethyl carbonate (DMC), diethylene glycol dimethyl ether, diethyl succinate (DES), dimethoxymethane (DMM), diglyme, diethyl carbonate (DEC), diethyl adipate (DEA), dimethyl ether (DME), ethanol ethers, esters, alcohols butanol (Bu), n-pentanol, polyoxymethylene dimethyl ethers (PODE3-4), and acetates [155-165], etc. DMC is an attractive oxygenated fuel additive and has a very high percentage of oxygen, which helps to achieve a proper combustion in diesel engines. The transesterification process is used for the production of DMC. In this process, ethylene carbonate with methanol is transesterificated to produce DMC, which is cheaper [166].

In this module of research work, an attempt was made to study the effect of adding small quantities of an oxygenated additive DMC viz., 2, 4, 6, 8, 10 and 12% by volume, with the 40LFPO blend (i.e., Y1, Y2, Y3, Y4, Y5 and Y6 respectively) on the engine behavior in terms of the combustion, performance and emission characteristics. Table 4.5 gives the composition of the different 40LFPO-DMC blends. The properties of dimethyl carbonate in comparison with other additives or cetane improvers are given in Table 4.6.

Table 4.5: Composition of the test blends

Fuel	LFPO (%)	Diesel (%)	DMC (%)
Y1	40	58	2
Y2	40	56	4
Y3	40	54	6
Y4	40	52	8
Y5	40	50	10
Y6	40	48	12

The physico-chemical properties of diesel, 40LFPO and its DMC blends are listed in Table 4.6.

Table 4.6: Physical properties of diesel, DMC, 40LFPO, Y1, Y2, Y3, Y4, Y5 and Y6

Properties	**ASTM Method**	**Diesel**	**DMC**	**40LFPO**	**Y1**	**Y2**	**Y3**	**Y4**	**Y5**	**Y6**
Density (kg/m^3 @20^oC)	D1298	830	1079	862	867	872	877	882	887	891.88
Kinematic viscosity (cSt@40^oC)	D445	2-4	0.625	2.87	2.97	2.92	2.88	2.83	2.78	2.73
Calorific value (MJ/kg)	D4809	43.8	15.78	41.96	41.39	40.83	40.27	39.71	39.15	38.59
Cetane number	D613	40-55	35-36	41.17	41.72	41.44	41.16	40.88	40.6	40.32
Flash point by Abel method (^oC)	D93	50	18	32	41.36	40.72	40.08	39.44	38.8	38.16
Fire Point (^oC)	D92	56	-	60	70.48	69.36	68.24	67.12	66	64.88
Octane number	-	15-25	101-116	-	-	-	-	-	-	-
Oxygen (% wt)	-	0	53.3	14.39	15.46	16.52	17.59	18.66	19.72	20.79
Hydrogen (%wt)	D5291	13	6.7	8.65	8.52	8.39	8.27	8.14	8.02	7.89
Carbon (%wt)	D5291	87	40	75	74.26	73.31	72.37	71.43	70.49	69.55

The results of the performance, combustion and emissions of the diesel engine run on the proposed fuels were analyzed, compared with those of diesel operation.

4. 10.5 Improvement of turbulence by internal jet piston

There have been many methods used to improve the combustion behavior of a CI engine, by modifying the engine parameters or configuration, when fuel modification was not so effective. The methods adopted by the researchers include combustion chamber geometry [167-173], combustion chamber and nozzle geometry [174], combustion chamber, injector geometry [175], injection pressure [176], internal jet piston to induce turbulence [177], etc. Therefore, an attempt was made to study the effect of turbulence inducement in the

cylinder by providing two holes at different locations on the piston crown (internal jet piston). The test fuel 40LFPO10DMC (i.e., fuel containing 40% LFPO, 10% DMC and 50% diesel by volume) was tested without and with turbulent inducement in the test engine. For this purpose, the engine piston was provided with two internal jets. The method of providing internal jets is described in the following subsection.

4.10.5.1 Internal jet piston arrangement

There are different methods for creating a swirl motion or turbulence motion inside the combustion chamber, such as increasing the nozzle pressure, providing different shapes to the combustion chambers (hemispherical, cylinder, or radial shape) and mounting different types of piston heads (T, L or F type). Turbulence is necessary to break the flame front into pieces so that each and every part of the combustion chamber gets inflamed to ignite the homogeneous air fuel mixture. If there is an uneven flame distribution, then there will be an incomplete combustion, which gives less torque and also causes pollution.

In this study, more turbulence was induced by providing internal jets in the combustion chamber of the test engine. For this, the combustion chamber of the engine was modified by making two small micro-holes in the piston, which were used to create effective air motion in the combustion chamber. After assembling the piston into the engine, the 40LFPO was tested in the engine with the modified piston for determining the combustion, performance and emissions of the engine at different load conditions. Figures 4.15 (a) and (b) show the diagram of the piston without and with internal jet piston respectively. Figures 4.16 (a) and (b) show the photographic views of the base piston and turbulence induced (internal jet) piston respectively.

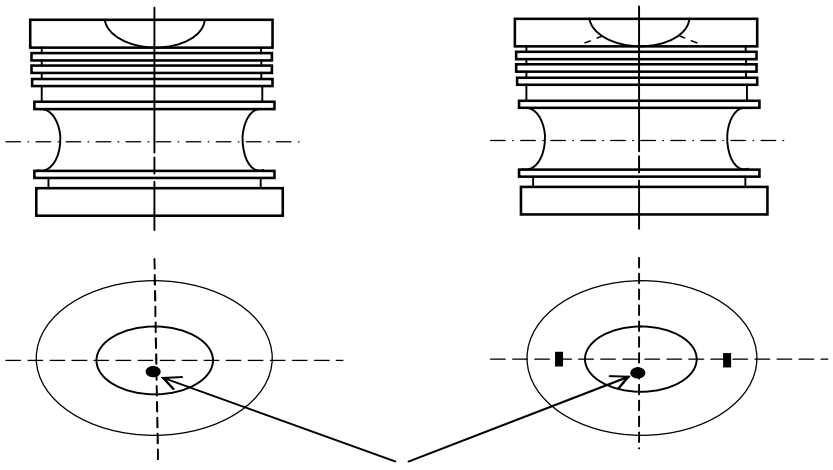

Figure 4.15: Pistons without and with internal jet piston

Two holes on the piston crown were provided for the turbulence to be induced in the cylinder. The holes of 3.0 mm diameter width and 7.0 mm depth were drilled diametrically opposite in the plane of the piston crown, parallel to the piston pin axis. The holes were drilled from the centre of the piston's flat surface such that the jets enter near the bottom of the cavity in the direction of the swirl. The angle of the holes drilled from the centre of the piston's flat surface towards the base of the bowl is 40° to the vertical axis of the piston [177].

(a) (b)

Figure 4.16: (a) Photographic view of the piston without an internal jet piston & (b) with internal jet piston.

The internal jet piston inserted in the engine cylinder is shown in Figure 4.17

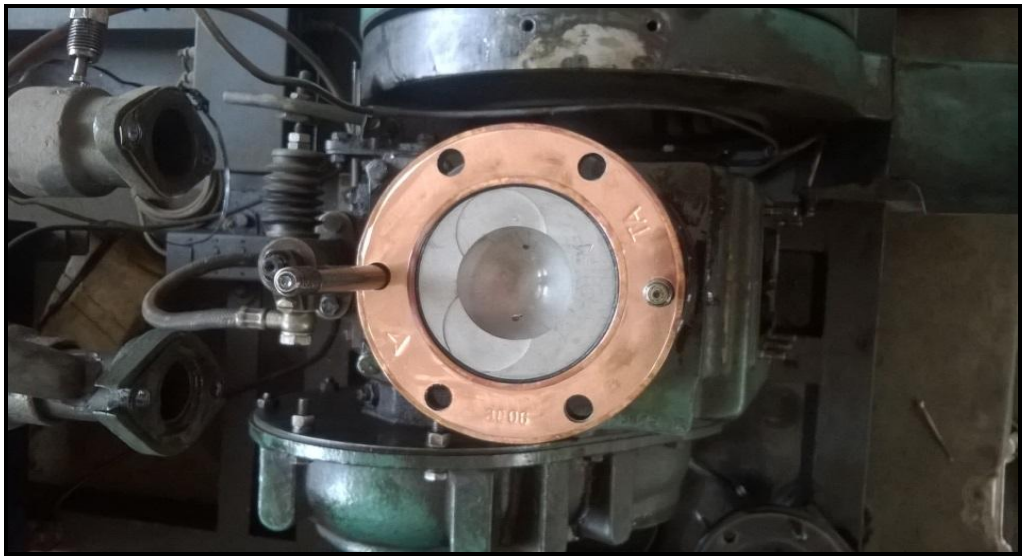

Figure 4.17: Photographic view of an internal jet piston assembled in a diesel engine

The combustion, performance and emission parameters of a 40LFPO10DMC with the internal jet piston were determined, analysed and compared with the results obtained for the diesel, 40LFPO and 40LFPO10DMC operations with a conventional piston. The results are discussed in Section 5.5.

4.10.6 Exhaust gas recirculation

The engine run on 40LFPO10DMC with an internal jet piston exhibited higher brake thermal efficiency compared to those of 40LFPO and diesel by about 5.3 and 4.5% respectively at full load. Similarly the nitric oxide (NO) emission of the engine running on 40LFPO10DMC with an internal jet piston was higher by about 90 and 6.5% respectively compared to those of 40LFPO and diesel at full load. The NO emission from the engine run on 40LFPO10DMC+IJP (i.e., fuel containing 40% LFPO, 10% DMC and 50% diesel and engine modified with internal jet piston) was found to be higher than that of diesel and 40LFPO10DMC was found to be lower than that diesel fuel at full load. The exhaust gas recirculation is an effective method to reduce the NO_x emission from CI engines [178]. The method of allowing CO_2 into the engine through the intake manifold to mix with the air fuel mixture is known as exhaust gas recirculation (EGR). In this method, the cylinder gas temperature is reduced by diluting the air fuel mixture with a non-reacting parasite gas. Since CO_2 is such type and significantly present in the exhaust gas itself, CO_2 is allowed to mix in lower percentages with the air fuel mixture. By doing this, CO_2 gas absorbs energy during combustion process resulting in lower cylinder gas temperatures. A maximum of 30% exhaust gas can be recirculated into the engine to reduce NO_x emission without much drop in the engine power output. There are two types of EGR adopted for reducing the NO_x emission which are: (i) hot EGR and (ii) cold EGR. In case of hot EGR, some portion of the exhaust gas is recirculated back with the fresh air into the cylinder. Exhaust consists of CO_2, N_2 and water vapor mainly. As the exhaust gas does not burn anymore so they can be recirculated back into cylinder. When a part of this exhaust gas is re-circulated to the cylinder, it acts as a diluent to the combusting mixture. This also reduces the oxygen concentration in the combustion chamber. The specific heat of exhaust gas is much higher than that of fresh air. Hence EGR increases the specific heat of the intake charge, thus decreasing the temperature rise for the same heat release in the combustion chamber and decreases the NO emission [179]. In the case of cold EGR, the exhaust gas is trapped and cooled by the heat exchanger or an inter cooler as required temperature and send back to the combustion chamber through inlet manifold. Cold EGR,

found to be more effective than hot EGR in NO_x reduction. This helps in attaining a lower intake air temperature, as compared to hot EGR. Cold EGR results in poor combustion in the engine cylinder and hence reduced peak temperature. Due to low temperature and less oxygen available in the engine cylinder during combustion, the NO_x emissions will reduce [180]. In this study, the heat exchanger consists of number of fins and air flow around the fins to cool the exhaust gases. The amount of exhaust gas recycling into the inlet manifold is controlled by means of two valves, one in the inlet pipe and other in the exhaust pipe line of the engine. The recirculated exhaust gas flows through another orifice box with inclined manometer for measuring the flow rate, before mixing with the fresh air. In this investigation, cold EGR was used. The arrangement of EGR used in this study is shown in Figure 4.18. The percentage of EGR recirculated in this study was 10, 20, 30, and 40%.

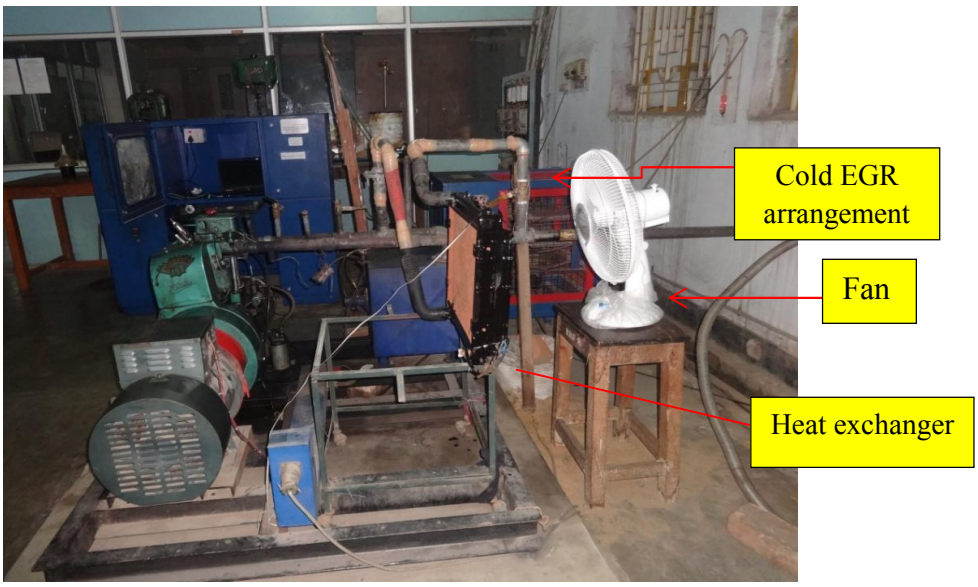

Figure 4.18: Photographic view of cold exhaust gas recirculation (EGR) arrangement.

4.10.7 Post-combustion CO_2 capture

Nowadays, due to the continuous increase in vehicle population, the carbon dioxide (CO_2) emission increases and leads to increase in global warming potential (GWP). As a result the climate of the earth is varying continuously. Factors, such as change in the earth's orbit, change in the sun's intensity, change in ocean currents, volcanic emissions and increase in greenhouse gas (GHG) concentrations affect the climate of the earth. Therefore, many researchers are carrying out investigation to control or capture CO_2. In this investigation, an attempt has been made to capture CO_2 from the exhaust gas of a diesel engine run on pyrolysis oil.

4.10.7.1. Carbon capture and storage

The carbon capture and storage (CCS) is the process of capturing waste CO_2 from sources like fossil fuel power plants and transporting into storage sites. Carbon capture and storage is mostly used to describe the methods of removing CO_2 emission from a large stationary source such as electricity generation and some industrial processes, and storing it away from the atmosphere. The aim is to prevent the release of large quantities of CO_2 into the atmosphere. The fossil fuels currently supply around 85 per cent of the world's energy needs, however, combustion of such fuels is a major source of emitting CO_2. It is a known fact that CO_2 is the most common greenhouse gas after water vapor and is contributing the most to global warming. CCS is one of the important technologies that will allow us to control or reduce the GHG emissions, while using fossil fuels and retaining our existing energy-distribution infrastructure.

4.10.7. 2 Various options for CO_2 capture

Depending upon different plant configurations, CO_2 emissions from heat engines can be reduced by any of the following methods [181]:

a) Pre-combustion capture
b) Post-combustion capture
c) Oxyfuel combustion

a) Pre-combustion capture

Figure 4.19 illustrates the principle of pre-combustion capture method. In pre-combustion the fossil fuel is partially oxidized to produce syngas (CO and H_2O), and then shifted to produce CO_2 and H_2. The CO_2 is then selectively removed, leaving only the hydrogen gas to support combustion. This method is most highly developed in commercial applications. In this method, exhaust gas is allowed to pass through a liquid solution in which CO_2 selectively dissolves and removes the carbon dioxide from the solution. This is generally done by heating the solution to remove the CO_2 for storage. But, this technique is applicable for small scale capture process and it is also difficult to use a liquid solution in the exhaust pipe.

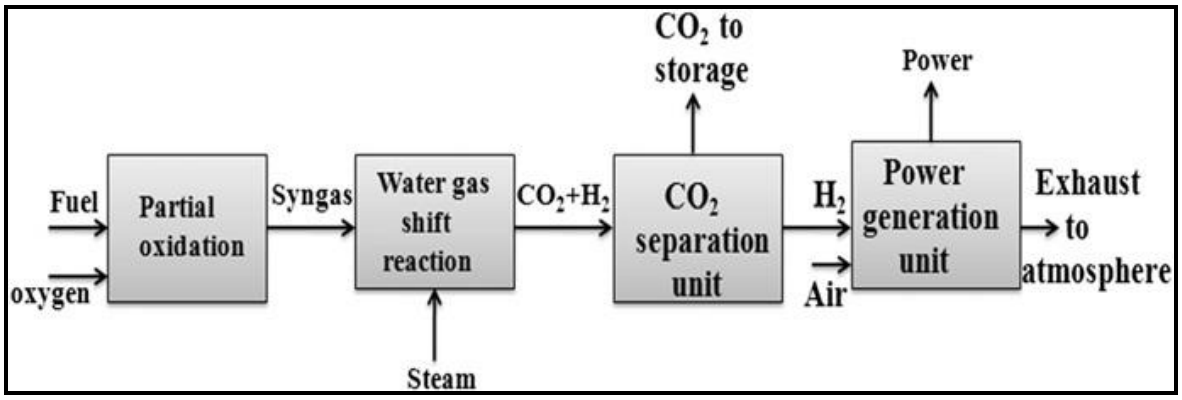

Figure 4.19: Principle of pre-combustion CO_2 capture

(b)Post-combustion capture

The principle of post-combustion CO_2 capture method is shown in Figure. 4.20. In this method, a mixture of CO_2, O_2, and N_2 gasses is produced, requiring a post-combustion separation process. In this process, exhaust gas is allowed to pass through solid adsorbents where the gas molecules in the exhaust are captured by pores present in the adsorbents. The mechanism involved in this process is known as adsorption. Post-combustion-capture method has an advantage that it may be more easily retrofitted to the existing combustion systems.

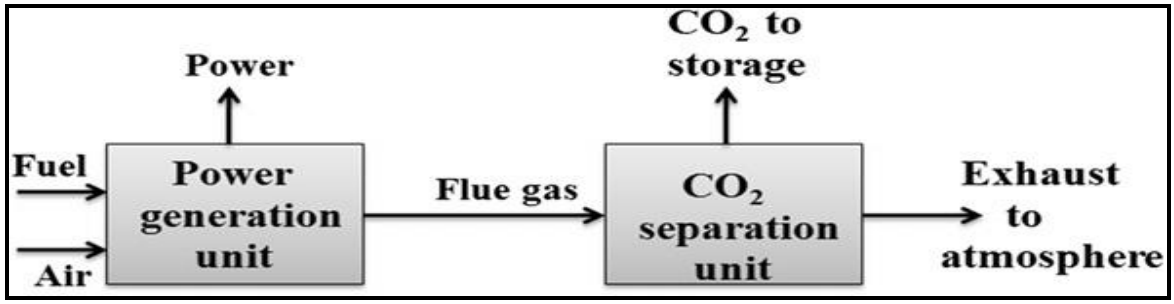

Figure 4.20: Principle of post-combustion CO_2 capture

(c) Oxyfuel combustion

Oxy-fuel combustion is a promising technology for capturing CO_2 from fuel gas or to modify the combustion process so that the flue gas has a high concentration of CO_2 for easy separation. In this process fuel is burned in the combustion chamber in the environment of pure O_2 (>95%) mixed with recycled flue gas (RFG) as shown in Figure. 4.21. In the most frequently proposed version of this concept, a cryogenic air separation unit is used to supply high purity oxygen. This high purity oxygen is mixed with RFG prior to combustion or in the boiler to maintain combustion conditions similar to an air fired configuration. This is necessary because currently available materials of construction cannot withstand at high temperatures resulting from coal combustion in pure oxygen. Flue gas stream from this system contains mainly CO_2 and water vapor. The water is

easily removed by condensation, and the remaining CO_2 can be purified relatively at a low cost.

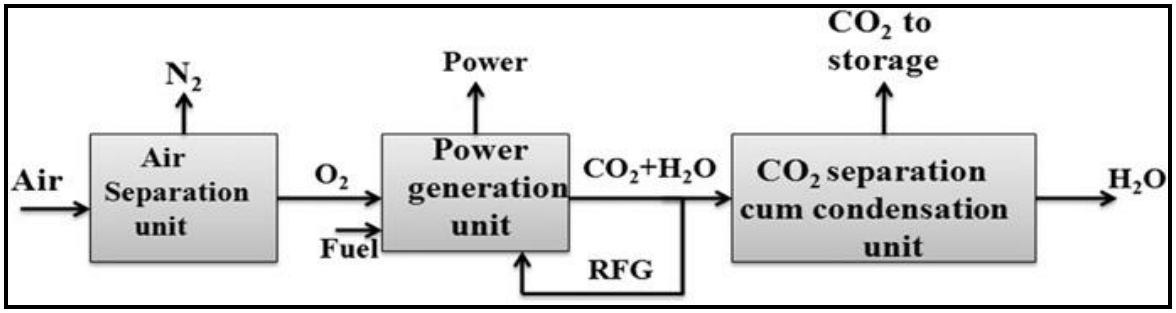

Figure 4.21: Principle of oxyfuel combustion CO_2 capture

4.10.7. 3 Material for CO_2 adsorption

The materials used for capturing CO_2 gas by adsorption are discussed below.

(i) Zeolite adsorbents

In CCS technology, various adsorbents, such as zeolite, membranes and activated carbons are used to control the CO_2 emission. Zeolite is the most effective and recent technology used to control CO_2. It is formed from ancient volcanic ash flows settling in seas and lakes. It is the world's only mineral with a naturally-occurring negative charge. It simply locks and holds many positive ions, absorbing a multitude of environmental contaminants, such as sodium, potassium, barium, calcium, and positively charged groups such as water and ammonia. Nearly every application of zeolites has been driven by environmental concerns, or plays a significant role in reducing toxic waste and energy consumption. It is the highly porous and consistent matrix of zeolite that provides the adsorption qualities. The high thermal and chemical stability of these inorganic crystals makes them ideal materials for use in high temperature applications, such as catalytic membrane reactors. Zeolite also has the potential to achieve precise and specific separation of gases, including the removal of H_2O, CO_2 and SO_2 from low-grade natural gas streams, as separation experiments through zeolite-containing membranes indicate that competitive adsorption can selectively separate light gas mixtures.

(ii) Zeolites 13X cylindrical pellets

Zeolite 13 X adsorbents played a major role in the development of adsorption technology. The three major areas of applications are:

i. Removal of trace or dilute impurities from a gas
ii. Separation of bulk gas mixtures
iii. Gas analysis

Commercial zeolites are generally available in bound forms where the zeolite crystals (1-5 mm) are formed in regular particle shapes (beads, pellets, cloverleaf design, etc.) using a binder material (clay, alumina, polymers, etc.). In this investigation, the zeolite 13X adsorbents were used which are 3mm size and cylindrical shape. Figure 4.22 shows the zeolite 13X pellets.

Figure 4.22: Zeolites 13X pellets

4.10.7. 4 Model construction of tail pipe with zeolite 13x adsorbents

The tail pipe had a length of 29 cm, width 16 cm and pipe inlet diameter is 4 cm. Zeolite 13X pellets were filled in the middle of two steel sheet meshes (trap). The inner section of the trap had steel mesh sheets of thickness 1 mm. Zeolite 13X pellets of 3 mm size and 800 gm were filled in the space between the two steel sheet meshes. The space was maintained, which were based on the size of the pellet. The size of the chosen zeolite pellets were in cylindrical shape, which had a maximum exposure of surface over the passing exhaust gas for CO_2 absorption. The tail pipe material is chosen as stainless steel to avoid corrosion of the material. The tail pipe is designed in such a way to minimize the back pressure. Conical sections are considered in designing the tail pipe to reduce the back pressure. The tail pipe is designed on the basis of previously designed models of catalytic converters for testing in the engines.

4.10.7.5. Working Principle

Figure 4.23 shows the photographic view of the tail pipe with zeolite 13X pellets. The exhaust was allowed to pass into the inlet of the tailpipe. Pressure of the exhaust gas got reduced and velocity of the gas increased because of the conical section. The flowing

exhaust gas was free to move in all directions inside the tailpipe. As the movement of exhaust gas was not abruptly obstructed anywhere in its path, the back pressure was limited to the minimum level. The maximum adsorption limit of zeolites depended on the amount of exhaust produced from the engine. The material for sheet mesh was considered as steel which has high thermal properties. The exhaust emissions of the engine were measured after the gas passed through the tail pipe.

Figure 4.23: Design of tailpipe with zeolite 13x pellets

4.11 Durability Tests

Before proposing an alternative fuel for commercialization, it is essential to conduct a durability test for long term use. The aim of the durability test is to evaluate the wear characteristics of the components and change in the lubricating oil properties of the engine.

In this study, the engine was subjected to a short term endurance test, in which the engine was run for 100 h for examining durability of engine, wear resistance and lubricating oil properties. The wear analysis was also done by the visual inspection. The lubricating oil samples collected during the engine durability test were analyzed using Atomic Absorption Spectroscopy (AAS) for determining the different metal traces present in the lubricating oil due to the engine wear and friction.

4.11.1 Short term endurance test

The main objective of the endurance test was to evaluate the wear characteristics of engine components and changes in lubrication oil properties of the test engine run with the fuel containing 40% LFPO, 10% DMC and 50% diesel, and the engine modified with internal jet piston and 20% exhaust gas recirculation (i.e., 40LFPO10DMC+IJP+20EGR). Since 40LFPO with 10DMC+IJP+20EGR operation exhibited the performance and emissions closer to that of the diesel operation, it was decided to ensure the long term utilization of 40LFPO in diesel engines. Therefore, a short term endurance test was conducted as per IS 10000 Part V-1980 method for 100 h. Before the start of the durability test, the existing fuel injection pump, fuel injector, fuel filter, oil filter was replaced with new one as recommended by the engine manufacturer. Before fitting the engine, the fuel injector and fuel injection pump was dismantled completely, and photographs were taken in order to compare the wear and deposits on them after the durability test. The used lubricating oil was drained completely and fresh lubricating oil of SAE 20-40 grade was filled in the oil sump up to its full capacity. The engine cylinder head was dismantled and the carbon deposits on the cylinder head and piston crown was completely cleaned using methanol. The cylinder head gasket was also changed with a new one and the cylinder head was fitted in the engine block. Once the engine was reassembled, it was allowed to run-in for 12 hours in the manner recommended by the manufacturer. Utmost care was take to prevent any misalignments occurring during dismantling and re-assembling of the engine.

4.11.2 Preliminary run for constant speed engine

The purpose of the preliminary run on the engine is to ensure that the engine can run trouble free, by operating both the engines for their running-in period. Under the preliminary run, the test speed engine was subjected to a preliminary run of 49 hours at the rated speed under the operating temperature specified by the manufacturer, in non-stop cycles of seven hours each, as given in Table 4.7. During the preliminary run, attention was paid to engine vibration and quietness. It was ensured that the temperature of the lubricating oil reached within 5^{o}C before starting the next cycle.

Table 4.7: Test cycle for preliminary run pattern of a constant speed engine

Load (Percent of rated load)	Running time (hour)
25	1.5
50	2
75	1.5
100	2

4.11.3 Short term test for constant speed engine

After the preliminary run, the engine was subjected to undergo the short term endurance test (load test) as recommended by IS Standard 1000, for 32 cycles (each of 16 hours continuous running) at a rated speed. In this study, the long term endurance test comprising 3 cycles was conducted. The test cycle followed is specified in Table 4.8.

Table 4.8: Test cycle for short term endurance test

Load (Percent of rated load)	Running time (hour)
100	4
50	4
100	1
No load	0.5
100	3
50	3.5

In this investigation, the short term endurance test was conducted using the 40LFPO10DMC+IJP+20EGR and at the end of each 16-hour cycle, the engine was stopped, and necessary servicing and minor adjustments were carried out in accordance with the manufacturer's schedule. Before starting the next cycle, it was ensured that the temperature of the engine sump oil had reached within 5K of the room temperature. The lubricating oil samples were collected from the engine after every 30 hours (from preliminary run onwards) for conducting various tribological studies. In the entire range of engine operation spread around 100 hours, there was no major breakdown noticed. After completion of the short term endurance test, the engine was completely dismantled, and the deposit formations on cylinder head, piston top and injector tip were investigated.

4.11.4 Lubrication oil analysis

The lubrication oil used in the diesel engine picks up the wear debris of various metals depending on the origin. The quantitative evaluation of wear particles present in oil gives the magnitude of engine component deterioration while qualitative analysis indicates its origin, i.e., wearing component. This ultimately provides adequate information about the components that are deteriorated and the incipient failure of the machine.

4.11.5 Determination of ash content

The lubricating oil samples were taken in a silicon crucible and kept in the furnace at 450°C for 4 hours, and then at 600°C for 2 hours to produce ash. The residual ash contains the wear debris of metal primarily. By weighing the crucible before and after the test, the weight percentage of ash was determined.

4.11.6 Atomic absorption spectroscopy test

The atomic absorption spectroscopy (AAS) works on the principle of absorption interaction, where atoms in the vapor state absorb radiation at a certain wavelength that are well defined and show the characteristics of a particular atomic element. The working principle of AAS is illustrated in Figure 4.24.

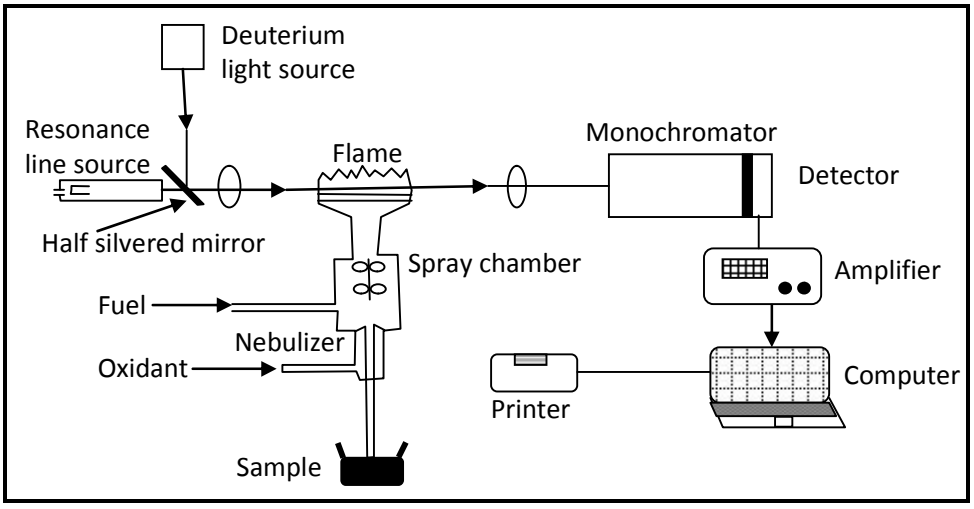

Figure 4.24: Principle of atomic absorption spectroscopy

In this process, the source of radiation projects a beam of a specific wavelength through a pure flame (air-acetylene) onto a sensor and the amount of radiation arriving at the photo sensor is recorded. The fluid sample is introduced into the flame and vaporized. The amount of radiation arriving at the photo sensor is reduced in proportion to the quantity of the specific element present in the sample. Hence, various elements such as Fe, Cu, Zn, Cr, Mg, Co and Pb were analyzed by AAS, and the results are discussed in Chapter 5. This

AAS test was conducted to evaluate the concentration of various metals present in the lubricating oil samples from the 40LFPO10DMC+IJP+20EGR fuelled test engine.

This gives a fair idea about the wear of different parts, material compatibility of the new fuel with the existing engines. In the present study, since many sliding components were involved, it was anticipated that the wear debris originating from different metallic parts appeared in the lubricating oil. The procedure followed is explained in the following steps:

a) Approximately 10 grams of oil sample was weighed in the silica crucible, and burnt at 450°C for 4 hours and at 650°C for 2 hours.
b) The ash was dissolved in concentrated HCl acid.
c) The mixture was diluted with distilled water to make 100 ml solution.
d) Standard solutions of various metals (concentrations ranging from 5 ppm to 20 ppm) were prepared.

Chapter 5

RESULTS AND DISCUSSION

5.1 General

Before the commercialization of any alternative fuel for CI engines, a deeper analysis is essential to ensure whether the fuel can exhibit the combustion, performance and emissions similar to those of a diesel fuelled engine. Otherwise, a suitable fuel or engine modification is done. The fuel modification technique includes blending, emulsification and adding additives, etc. Examples of varying compression ratio, varying nozzle opening pressure, injection timing, turbulence, etc. are observed to be adopted for attaining the desired engine performance. In this investigation, experiments were conducted in a single cylinder, four stroke, air cooled, DI diesel engine with a developing power of 4.4 kW at 1500 rpm, run on LFPO adopting fewer fuel and engine modifications. Three fuel modifications namely, blending diesel fuel, blending an ignition improver and blending an oxygenate additive were adopted in this study. Further, three engine modification techniques namely, change of injection timing, increasing the turbulence, and exhaust gas recirculation (EGR) were used. In all the methods considered in this study, the test fuels were taken on a volume basis only. Furthermore, a carbon capture method was used for absorbing CO_2 by using zeolite in the engine exhaust. A short term durability test was also carried out in the test engine which was run on 40LFPO with a necessary fuel and engine modification. All the results of the experimental investigations were analyzed and compared with those of diesel/40LFPO operation, and are presented in this chapter.

5.2 Fuel Blending with Diesel

In this section, the combustion, performance and emissions of the engine run on four different LFPO-diesel blends were, analyzed and compared to those of diesel operation in the same engine. The designation of the test fuels and their respective compositions are given below:

- 20LFPO = 20% LFPO+80% diesel
- 40LFPO = 40% LFPO+60% diesel

- 60LFPO = 60% LFPO+40% diesel
- 80LFPO = 80% LFPO+20% diesel

5.2.1 Combustion parameter

5. 2.1.1 Cylinder pressure history

The start of ignition of a CI engine fuel depends primarily on the cetane number and mixing ability of the fuel [121]. Figure 5.1 depicts the variation of the cylinder pressure with crank angle for diesel, 20LFPO, 40LFPO, 60LFPO and 80LFPO at full load condition.

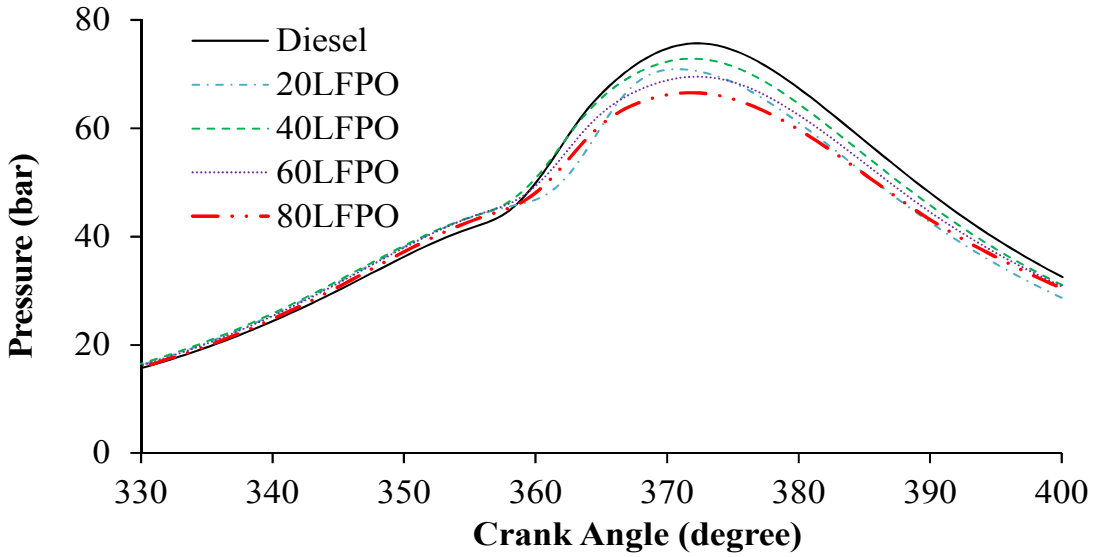

Figure 5.1: Variation of cylinder pressure with crank angle at full load

The change in the slope of the pressure-crank angle curve gives the start of combustion approximately [121]. The start of fuel injection (SOI) is set at 23^{o}CAbTDC. The commencement of ignition of diesel is the earliest among the fuels tested in this investigation, while the commencement of ignition of the 80LFPO is the farthest at full load. The early ignition of delay is due to its higher cetane number and lower density. It can be observed from the figure that the cylinder peak pressures for the 20LFPO, 40LFPO, 60LFPO and 80LFPO are found to be about 70.9, 72.9, 69.6 and 66.5 bar respectively, which is attained approximately at 371.7^{o}CA, 372.8^{o}CA, 373.1^{o}CA and 372.5^{o}CA respectively at full load, whereas for diesel, it is 75.7 bar at 370.4^{o}CA. Overall, the combustion of the LFPO-diesel blends starts a little later by about 1^{o}CA compared to that of diesel at full load. This may be due to the lower cetane number of the LFPO-diesel blends than that of diesel. Among the four blends, the ignition of 40LFPO starts earlier

than that of the other blends which is due to its higher cetane number as shown in Table 4.1.

5.2.1.2 Ignition delay

The crank angle duration between the beginning of injection and the ignition of fuel is called the ignition delay. The ignition ability of a diesel engine is mainly influenced by the chemical and physical properties of the fuel [182]. The ignition delay of the test blends in different engine operating conditions is shown in Figure 5.2.

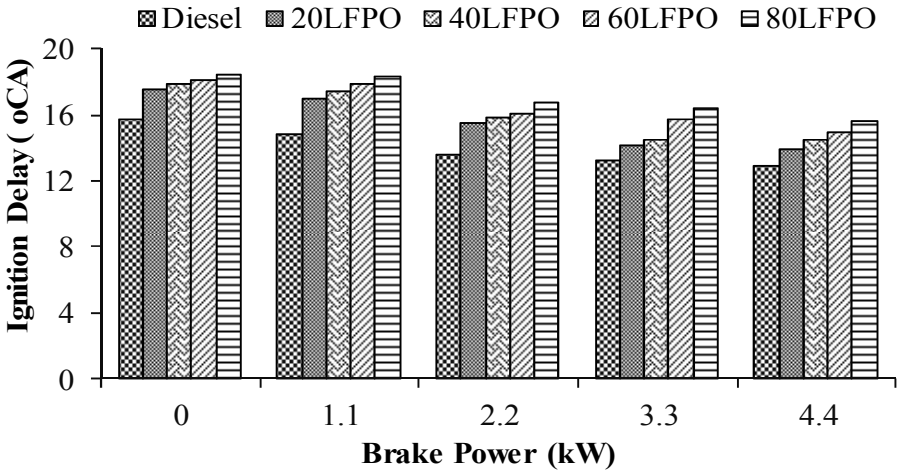

Figure 5.2: Ignition delay with brake power

The ignition delay is found to decrease with the increase in the engine load. This may be due to the higher combustion temperature at the time of injection and reduced exhaust gas dilution [64]. The values of the ignition delay for diesel, 20LFPO, 40LFPO, 60LFPO and 80LFPO at full load are found to be about 12.9, 13.9, 14.4, 14.9 and 15.6^{o}CA respectively. The ignition delays of the LFPO-diesel blends are longer compared to that of diesel at full load, which may be due to the lower cetane number and higher density of LFPO which takes more time for the ignition of the LFPO-diesel blends. In the entire range of engine operation, about 1-1.5^{o}CA difference is noticed between the diesel operation and the LFPO operation.

5.2.1.3 Cetane number determination

The cetane number is a very important parameter of the fuels [65]. It affects the behavior of the engine. In a particular diesel engine, higher cetane fuels will have shorter ignition delay periods than lower cetane fuels. The cetane numbers were calculated as a function of the ignition delay of the fuel which were described in Section 3.6.3 in chapter 3 [113].

The values of cetane number determined for different LFPO-diesel blends are given in Table 5.1.

Table 5.1: Cetane number at different loads

Load (%)	Cetane Number	Diesel	20LFPO	40LFPO	60LFPO	80LFPO
0	CN_0	47.87	38.31	36.78	35.56	33.91
25	CN_{25}	50.45	39.22	37.55	35.08	32.85
50	CN_{50}	53.89	42.73	40.31	39.27	35.29
75	CN_{75}	53.58	48.46	46.11	39.18	35.06
100	CN_{100}	54.48	48.17	45.12	42.24	38.58
Average cetane number	A_{CN}	52.05	43.38	41.17	38.27	35.14

It is seen from the table that the average cetane number of diesel is 52.05. Increasing the LFPO percentage in the blend decreases the cetane number. The average cetane number values of 20LFPO, 40LFPO, 60LFPO and 80LFPO are 43.38, 41.17, 38.27 and 35.14 respectively which are lower than that of diesel fuel.

5.2.1.4 Heat release rate and maximum heat release rates

Figure 5.3 illustrates the heat release rate pattern with the crank angle at full load for LFPO-diesel blends and diesel. The amount of heat release in the premixed combustion in a CI engine depends on the ignition delay, air fuel mixing rate and the heating value of the fuel [183]. It is apparent from the figure that the heat release rate is the highest for diesel at full load.

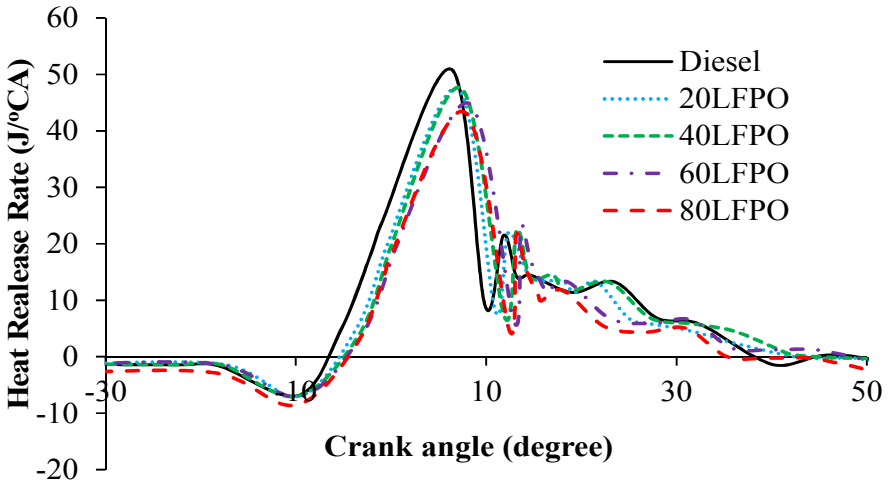

Figure 5.3: Variation of heat release rate with crank angle at full load

Diesel has a higher cetane number, better mixture formation of fuel with air, and higher calorific value than the LFPO-diesel blends. As a result, a higher heat release is noticed in diesel than that in the LFPO-diesel blends. Among the four different LFPO-diesel blends, the heat release for the 40LFPO blend is the highest at full load, which is due to lower density and higher calorific value. The maximum heat release rates for diesel, 20LFPO, 40LFPO, 60LFPO and 80LFPO are 52, 47.5, 47.6, 44.8 and 43.4 J/^{o}CA respectively at full load.

5.2.1.5 Combustion duration

Figure 5.4 depicts the variation of the combustion duration with brake power. Combustion duration is the difference in crank angle time between the start of combustion and the end of combustion [64]. From the heat release rate curve, the crank angle at which there is a sudden rise in the heat release was taken as the start of combustion. The end of the combustion was determined from the cumulative heat release rate curve. It was taken as the point where 90% of the heat release had taken place. It can be observed from the figure that the combustion duration increases with an increase in the brake power for all the tested fuels, which may be due to the increase in the quantity of fuel injected.

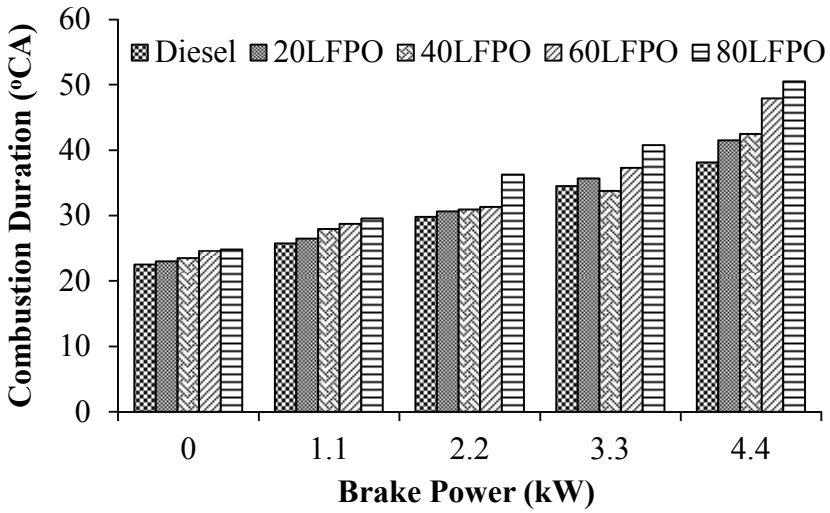

Figure 5.4: Variation of combustion duration with brake power

It can also be observed from the figure that the combustion duration is longer for all the blends in comparison with the diesel operation at full load. Increasing the LFPO percentage in the diesel blends results in longer combustion duration. This may be due to the high boiling point of the compounds present in the LFPO, and its lower cetane number, which takes more time for the chemical reaction. At full load, the value of the

combustion duration for diesel is found to be about 38.1°CA, and for 20LFPO, 40 LFPO, 60 LFPO and 80LFPO the values are 41.5, 42.5, 47.9 and 50.53°CA respectively.

5.2.1.6 Mass fraction burnt

Figure 5.5 depicts the variation of the mass fraction burnt (MFB) with crank angle at different brake power values. The mass fraction burnt is the percentage of fuel consumed by the mass to the total mass of fuel injected [184]. The crank angle for 100% MFB increases with increasing engine load, because a large quantity of fuel needs to be injected for higher engine loads. As the load increases, the crank angle at which 100% mass fraction is burnt also increases, due to more fuel being injected. The crank angle for 100% MFB is the lowest in the case of diesel, in comparison with the LFPO-diesel blends at full load.

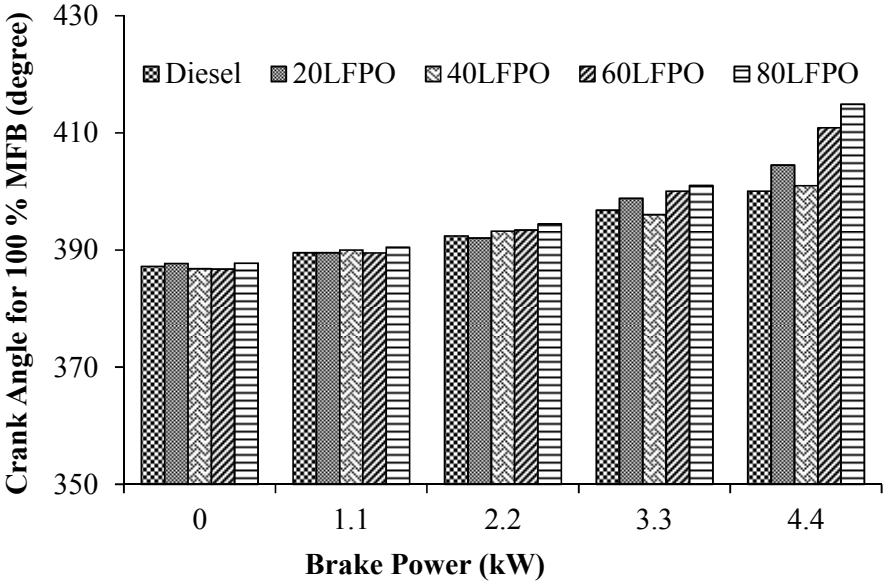

Figure 5.5: Variation of crank angle for 100% mass fraction burnt with brake power

A shorter ignition delay, and better mixing of fuel and air in the case of diesel is the reason for faster burning than the LFPO-diesel blends. It is also apparent from the figure that the 40LFPO blends exhibit higher mass fraction burnt than that of the other blends tested in this study, which is also evident from the heat release curve.

5.2.2 Performance parameters

5.2.2.1 Brake specific energy consumption

Figure 5.6 shows the variation of brake specific energy consumption (BSEC) for diesel and LFPO blends, with respect to brake power. The BSEC for diesel is 11.8 MJ/kWh at full load and it is approximately 12.6, 12.4, 12.7 and 13.67 MJ/kWh for the 20LFPO,

40LFPO, 60LFPO and 80LFPO blends respectively. As the load increases, the BSEC decreases for diesel and all the LFPO diesel blends, because of the increase in the cylinder temperature. The BSEC for the LFPO-diesel blends is found to be higher compared to that of diesel fuel tested in this study. This is attributed to the lower cetane number, lower heating value and higher density of the blends. The engine consumes more fuel with the LFPO-diesel blends than with diesel, to develop the same power output. The BSEC is the highest for the 80LFPO blend, viz, 13.67 MJ/kWh, due to its lower calorific value, among all the LFPO-diesel blends.

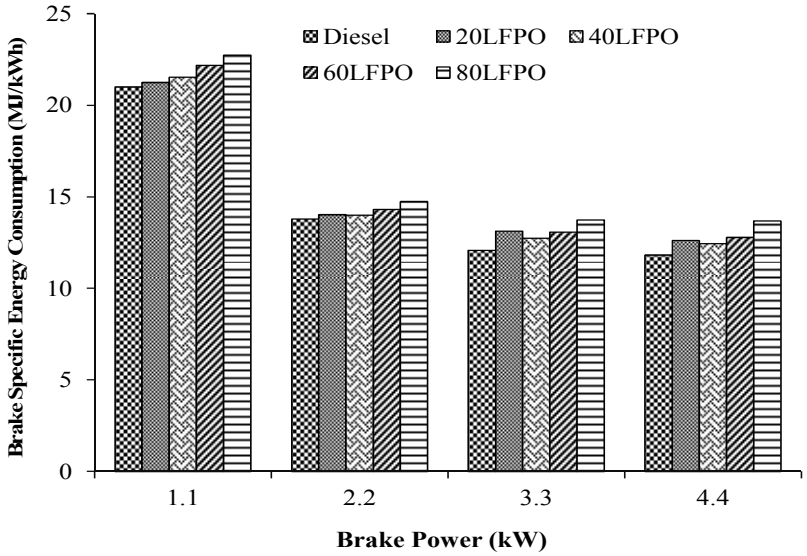

Figure 5.6: Variation of brake specific energy consumption with brake power

5.2.2.2. Thermal energy balance analysis

Figure 5.7 illustrates the variation of useful work with load for diesel and LFPO-diesel blends. It can be observed from the figure that the useful work and exhaust losses increase as the load increases, but other losses decrease.

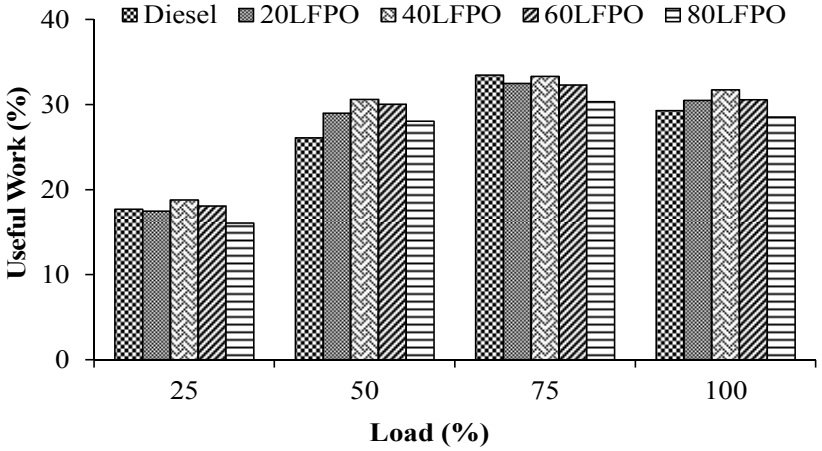

Figure 5.7: Variation of useful work with brake power

The useful work for diesel, 20LFPO, 40LFPO, 60LFPO and 80LFPO values are found to be about 29.2, 30.4, 31.7, 30.5 and 28.5% respectively. The 20LFPO, 40LFPO and 60LFPO values are higher by about 1.2, 2.4 and 1.2% in comparison with diesel at full load. This may be due to the higher percentage of LFPO and boiling point of the aromatic content present in the LFPO-diesel blends. It is evident from Figure 5.8 that at full load, the heat loss through the exhaust is found to be higher for 20LFPO, 40LFPO, and less for 60LFPO and 80LFPO compared to that of diesel.

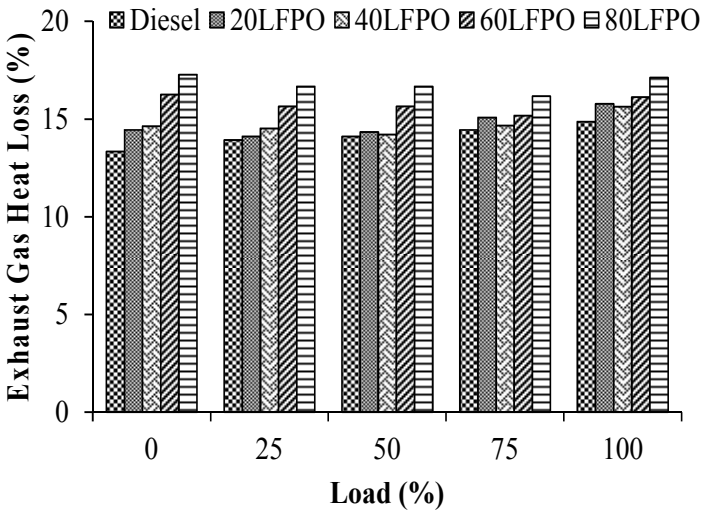

Figure 5.8: Variation of heat loss in the exhaust gas with brake power

The exhaust heat losses for diesel, 20LFPO, 40LFPO, 60LFPO and 80LFPO are found to be about 14.8, 15.8, 15.6, 16.1 and 16.9% at full load respectively. This may indicate that the 20LFPO and 40LFPO blends exhibit better combustion compared to that of 60LFPO and 80LFPO. Diesel shows lower unaccounted losses compared to those of the LFPO-diesel blends at full load. This may be due to the fact that diesel has higher useful work and lower heat loss in the exhaust gases compared to the other LFPO-diesel blends. The exhaust gas heat losses for diesel, 20LFPO, 40LFPO, 60LFPO and 80LFPO are found to be about 49.4, 53.7, 52.6, 55.7 and 57.26% at full load respectively.

5.2.3 Emission parameters

5.2.3.1 Nitric oxide emission

The parameters affecting the formation of NO_x in a CI engine are the combustion duration, temperature, compression ratio, pressure and the availability of oxygen [116]. Figure 5.9 depicts the variation of NO emission with brake power for diesel and the

LFPO-diesel blends. The NO emission per kWh for diesel and all the LFPO diesel blends decrease as the load increases. The value of NO emission is found to be the highest for diesel at full load among all the fuels tested in this study. LFPO-diesel blends have lower cetane numbers and higher density compared to that of diesel fuel and ignite later. The inferior combustion of LFPO results in lower peak pressure and temperature, leading to lower NO emission**.** Koc et al [98] also mentioned the similar reason for the results they obtained for tyre-biodiesel-diesel blend.

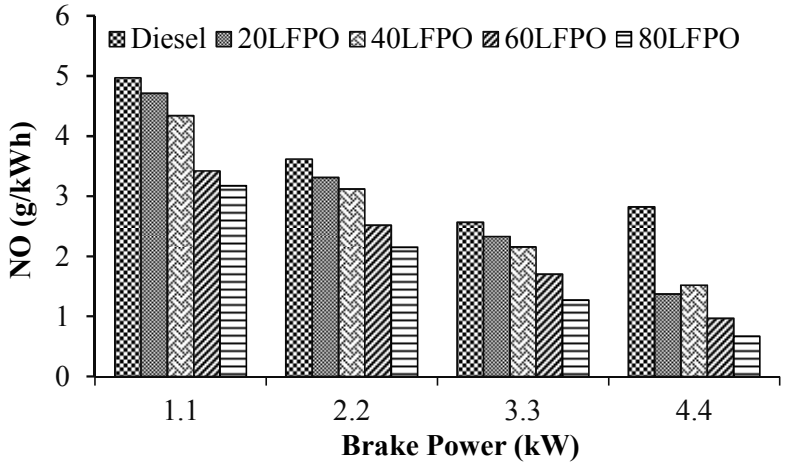

Figure 5.9: Variation of nitric oxide emission with brake power

The value of NO emission for diesel is 2.8 g/kWh at full load. While increasing the LFPO percentage, the NO emission decreases. The NO emission for the 20LFPO, 40LFPO, 60LFPO and 80LFPO blends are lower by about 51, 46.8, 68 and 76% compared to that of diesel at full load. The values of NO emission for diesel, 20LFPO, 40LFP, 60LFPO and 80LFPO are 2.8, 1.36, 1.5, 0.9 and 0.66 g/kWh respectively at full load operation.

5.2.3.2 Smoke emission

Figure 5.10 illustrates the smoke emission measured in the engine exhaust, for the fuels tested in this study. Smoke in a CI engine occurs due to the incomplete combustion in the combustion chamber and is normally formed in the rich zone [64]. With an increase in the load, the air fuel ratio decreases as the fuel injection increases, and hence, it results in higher smoke [183]. The smoke emission for diesel is found to be the lowest at full load among all the fuels used in this study. This is because of the better burning characteristics and the lower carbon to hydrogen ratio of diesel than those of LFPO-diesel blends. Among all the LFPO-diesel blends, 40LFPO exhibited lowest smoke emission in entire engine operation. The reason may be higher cylinder pressure and heat release rate compared to the other LFPO blends. The values of smoke emission for diesel, 20LFPO,

40LFPO, 60LFPO and 80LFPO are about 61.2, 82.2, 69.2, 80.5 and 85% respectively at full load operation.

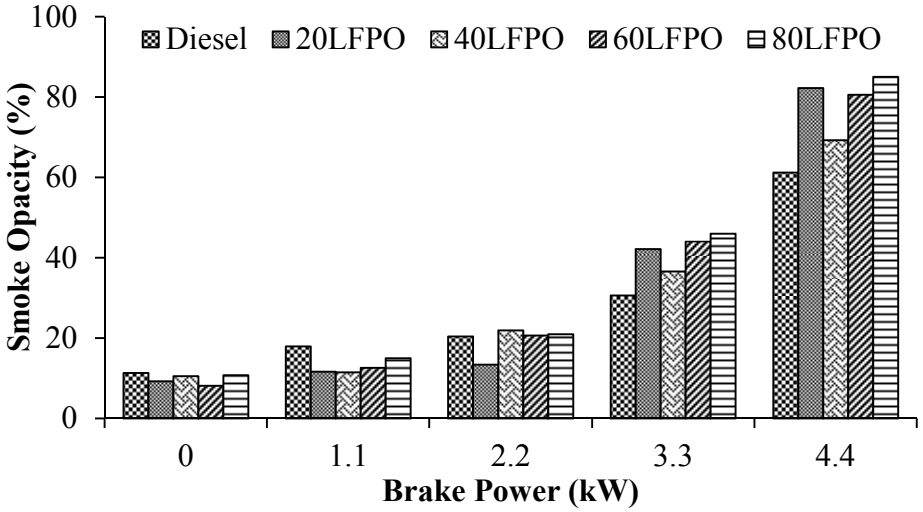

Figure 5.10: Variation of smoke emission with brake power

5.2.3.3 Carbon monoxide emission

Figure 5.11 shows the trend of CO emission for diesel and the LFPO diesel blends, with respect to brake power. Generally, the CO emission is formed due to the incomplete combustion of fuel [185].

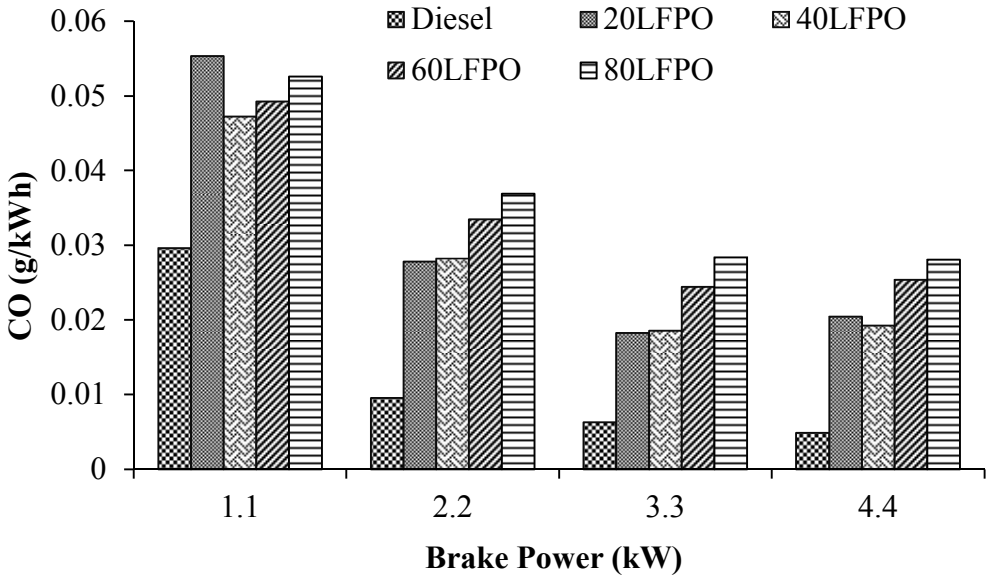

Figure 5.11: Variation of carbon monoxide with brake power

However, if the combustion is complete, CO will be oxidized into CO_2. It can be observed from the figure that the CO emission decreases with increasing loads. For the LFPO-diesel blends, the CO emissions are found to be higher in comparison with diesel

throughout the engine operation. The reason may be their higher density, longer ignition delay (low cetane number), higher sulphur content and high volatility (lower flashpoint) that generate a cooling effect and incomplete combustion [98]. The CO emission of 40LFPO is lowest among the other LFPO blends, this may be due to the higher cylinder pressure and temperature for compete combustion inside the cylinder. The CO emissions for diesel, 20LFPO, 40LFPO, 60LFPO and 80LFPO are to be found 0.0048, 0.020, 0.0192, 0.025 and 0.028 g/kWh respectively at full load operation.

5.2.3.4 Unburnt Hydrocarbon Emission

Figure 5.12 shows the trend of HC emission for diesel and the LFPO diesel blends, with respect to brake power. The HC emission of the diesel engine is primarily influenced by the fuel quality or oxygen availability. The HC emission generally occurs due to the incomplete combustion of the engine. It can be observed that the HC emission decreased with increased load. This is due to the higher cylinder temperature at full load.

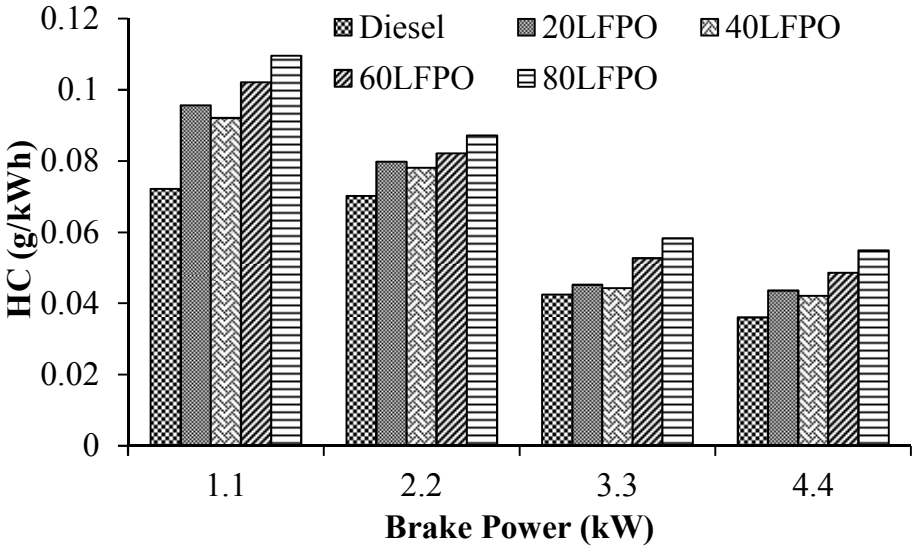

Figure 5.12: Variation of HC emission with brake power

The HC emission for diesel was the lowest among all the fuels tested in this investigation. The reason may be higher heating value and lower density among all the tested fuels. The HC emission for 80LFPO is the highest among all fuels. This may be lower cetane number, lower heating value and higher density among all fuels. The other reasons may be longer ignition delay and presence of higher proportion of aromatic content, which cause incomplete combustion in the combustion chamber. It can also be observed from the figure that the HC emission of 40LFPO is the lowest i.e., about 0.042 g/kWh among all the LFPO-diesel blends, the reason may be higher cylinder temperature among all

blends, which provides complete combustion. The HC emission for diesel, 20LFPO, 40LFPO, 60LFPO and 80LFPO are to be found 0.0360, 0.0435, 0.0420, 0.0486 and 0.0548 g/kWh at full load respectively.

5.2.4. Summary

It is understood from the results that the light fraction pyrolysis oil (LFPO) obtained from a commercial tyre pyrolysis plant can be used in the form of diesel blends in a DI diesel engine. The following conclusions are drawn based on the effects of blending diesel with various percentage of LFPO.

- The cetane numbers of LFPO-diesel blends are found to be lower than that of diesel as a result of mixed hydrocarbons present in it.
- The BSEC is the highest for the 80LFPO blend viz., 12.7 MJ/kWh, due to the lower calorific value, among all the LFPO-diesel blends. The BSEC of 40LFPO is found to be the lowest among all the blends and by about 5.33% higher than that of diesel at full load.
- The NO emissions for the 20LFPO, 40LFPO 60LFPO and 80LFPO blends are about 51, 46.8, 68 and 76% lower compared to that of diesel fuel at full load. The CO emissions for the 20LFPO, 40LFPO 60LFPO and 80LFPO blends are noticed higher by approximately about 61%, 59%, 67% and 82.8% compared to that of diesel fuel at full load.
- The values of smoke emission for diesel, 20LFPO, 40LFPO 60LFPO and 80LFPO are about 61.2%, 82.2%, 69.2% and 80.5% respectively, at full load operation. The 40LFPO gave better results in terms of performance, combustion and lower emissions compared to that of 20LFPO, 60LFPO and 80LFPO blends.
- A maximum of 80% LFPO can be used in the form of a blend without any engine modification. The 40LFPO blend gave better performance and lower emissions than those of the other blends. However, the performance of the LFPO blend is lower, and the emissions are higher than those of diesel fuel operation in the same engine at all loads.

The results of some of the important parameters of the engine run on the LFPO-diesel blends in comparison with diesel operation are listed in Table 5.2.

Table 5.2: Summary of values of important parameters for LFPO-diesel blends and diesel at full load

Sl No.	Parameter	Diesel	20LFPO	40LFPO	60LFPO	80LFPO
	Combustion parameters					
1	Maximum cylinder pressure (bar)	75.7	70.9	72.9	69.6	66.5
2	Maximum heat release (J/^{o}CA)	52	47.5	47.6	44.8	43.4
3	Ignition delay (^{o}CA)	12.9	13.9	14.4	14.9	15.6
4	Occurrence of maximum pressure (^{o}CA)	370.4	371.7	372.8	373.1	372.5
5	Combustion duration (^{o}CA)	38.1	41.5	42.5,	47.9	50.53
	Performance parameters					
6	Brake specific energy consumption (BSEC) MJ/kW	11.8	12.6	12.4	12.7	13.67
7	Brake Work (%)	29.2	30.4	31.7	30.5	28.5
8	Exhaust Gas Heat Losses (%)	49.4	53.7	52.6	55.7	57.3
	Emission parameters					
9	NO emission (g/kWh)	2.8	1.36	1.5	0.9	0.66
10	Smoke opacity (%)	61.2	82.2	69.2	80.5	85
11	CO emission (g/kWh)	0.0048	0.020	0.0192	0.025	0.028
12	HC emission (g/kWh)	0.0360	0.0435	0.0420	0.0486	0.0548

5.3 Effect of Injection Timing

5.3.1 General

This investigation was aimed to study the effect of varying the injection timing on the combustion, performance and emission characteristics of the same test engine, when it was run with 40LFPO blend. The designations given for the different injection timing of engine operated with 40LFPO blend in this study are as follows;

a. 40LFPO - 20bTDC,
b. 40LFPO - 21.5bTDC,
c. 40LFPO - 23bTDC,
d. 40LFPO - 24.5bTDC and
e. 40LFPO -26TDC.

For example, 40LFPO-20bTDC represents a test condition where 40LFPO is the fuel and fuel injection takes place at 20^{o} crank angle before top dead centre. The results of the performance, combustion and emissions of the diesel engine run on the 40LFPO before and after varying the injection timing were analyzed and compared with those of diesel operation, and are presented in this section.

5.3.2 Combustion parameters

5.3.2.1 Cylinder pressure and heat release rate

The variations of the cylinder pressure, and the heat release rate with crank angle are presented for diesel, 40LFPO, 40LFPO with advanced and retarded injection timings in Figure 5.12. The 40LFPO blend has a low cetane number and density compared to that of diesel. As a result the ignition is the farthest from the diesel curve. Advancing injection timing for the 40LFPO blend results in an early start of ignition, while retardation results in a delay in the start of combustion. It can be observed from the figure that the cylinder peak pressures for diesel and 40LFPO are found to be about 75.7 and 72.9 bar respectively at full load, and they are attained for diesel and 40LFPO at about 370.4 and 372.8 bar respectively at full load. The lower peak cylinder pressure for 40LFPO attained at a later crank angle is a result of its lower cetane number and higher density than that of diesel. By advancing the injection timing to a maximum of 26^{o}CA, the peak cylinder pressure is overall increased by about 2 bar at full load over those of the 40LFPO and diesel operations, which are attained marginally closer to that of 40LFPO. The cylinder

peak pressure for the advanced injection timing of 26°CA is higher by about 2.5 and 6.5% compared to that of diesel and 40LFPO respectively, at full load. This is due to more fuel accumulated and its consequent burning in the premixed combustion stage [121].

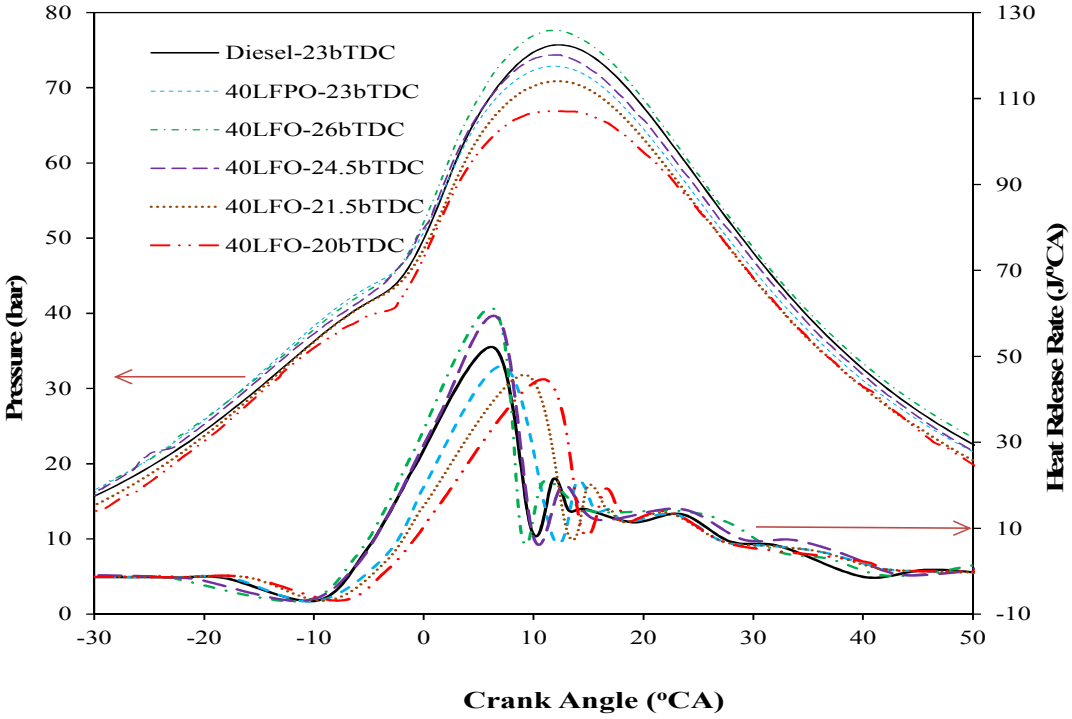

Figure 5.13: Variation of cylinder pressure and HRR with CA at full load

For the retarded injection timing, the peak pressure shift was approximately 1.8°CA away from the top dead centre (TDC) with an overall reduction in the peak cylinder pressure of about 2 bar compared to those of diesel and 40LFPO operations. It is apparent that the heat release rate (HRR) and the maximum HRR occur for the diesel operation close to the top dead centre (TDC), and it is 52 J/°CA for the diesel operation at full load. This is attributed to its higher cetane number and lower density than that of 40LFPO. The HRR for the advanced injection timing is higher than those of the original and retarded injection timings. This is because more amount of fuel gets accumulated in the early stage of the combustion phase as a result of the longer ignition delay. At full load, the heat release rate decreases with retardation of the injection timing of 40LFPO. With advanced injection timings, the maximum rates of heat release for 40LFPO are higher than those of the retarded injection timings. Overall, by advancing the injection timing, a maximum increase in the HRR value of about 6J/°CA is noticed for the 40LFPO blend than that of 40LFPO at the original injection timing at full load. Similarly, at full load there is a drop of about 5-6 J/°CA in the value of the maximum HRR noticed when the injection timing is retarded for the 40LFPO.

5.3.2.2 Ignition delay

The ignition ability of a diesel engine is mainly influenced by the chemical and physical properties of the fuel [182]. The ignition delay of diesel and 40LFPO with different injection timings (advanced, original and retarded) are depicted in Figure 5.13.

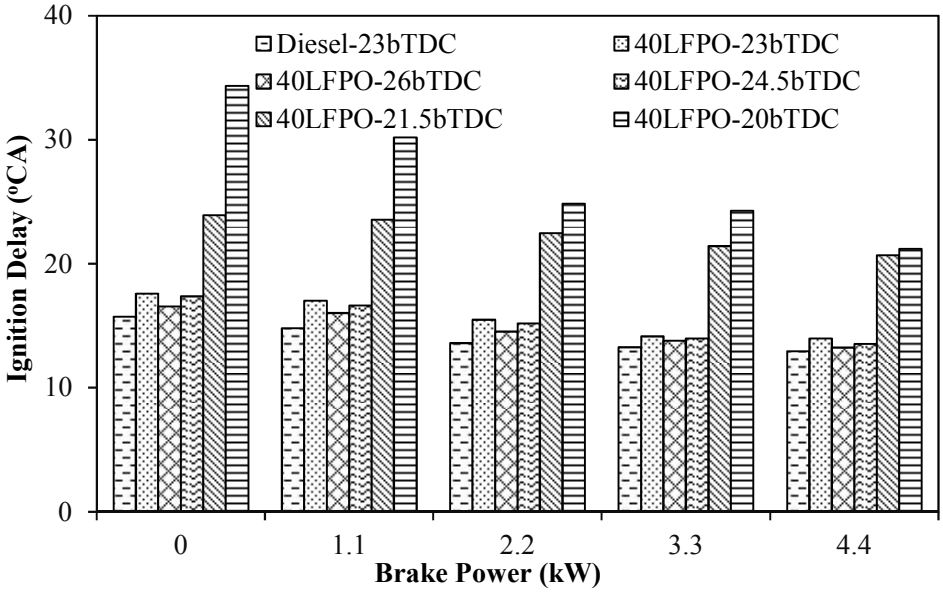

Figure 5.14: Variation of ignition delay with brake power

It can be observed from the figure that the ignition delay decreases with the increase in the load, which is due to the increase in the cylinder temperature. The ignition delay of diesel is found to be the shortest among all the injection timings studied, which is due to its higher cetane number compared to that of the 40LFPO blend. It can also be observed that by advancing the injection timing to a maximum of 3^{o}CA the ignition delay decreases in the entire engine operation, which is due to the better air-fuel mixture formed during the delay period, and rapid burning in the premixed combustion phase [186, 187]. By retarding the injection timing to a maximum of 3^{o}CA the delay increases in the entire load spectrum. The values of ignition delay at 23^{o}bTDC for diesel and 40LFPO at full load are approximately 12.9 and 13.9^{o}CA respectively. At full load, for the 40FLPO operation, about 2-3^{o}CA is reduced during advancing the injection timing, while about 4-5^{o}CA is increased in the delay during retardation than those of 40LFPO operation. The reduction in the ignition delay while advancing is due to the early injection of fuel and the increase in the ignition delay while retardation is due to the late injection of fuel for the 40LFPO blend.

5.3.2.3 Combustion duration

The variations of combustion duration with the load for diesel, 40LFPO and 40LFPO-20bTDC, 40LFPO-21.5bTDC, 40LFPO-24.5bTDC, 40LFPO-26bTDC, are depicted in Figure 5.14.

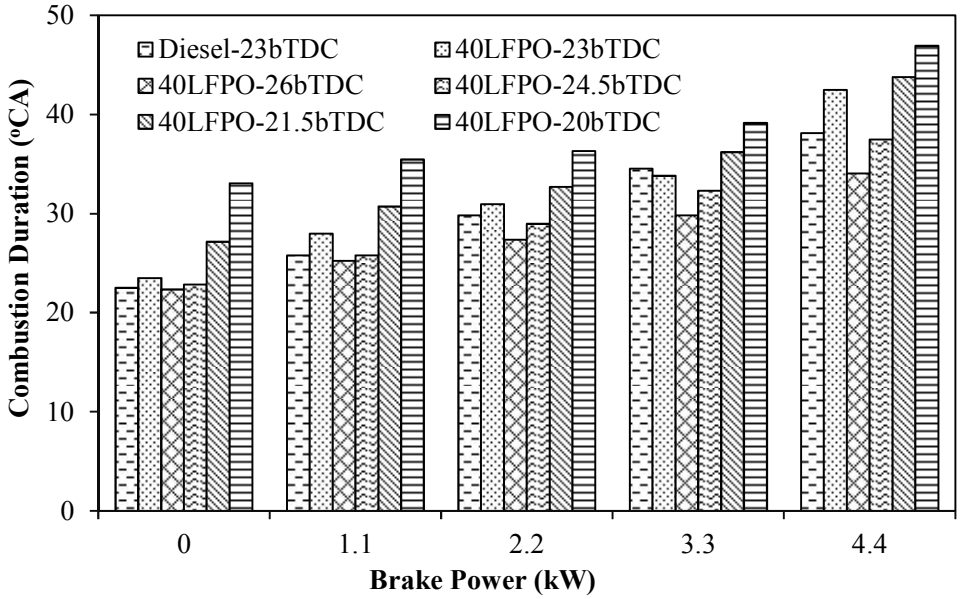

Figure 5.15: Variation of combustion duration with brake power

It can be observed from the figure that the combustion duration increases with the increase in the load for all the test conditions, as a result of more quantity of fuel injected. It is also apparent from the figure that the combustion duration of the 40LFPO blend at the original injection timing is longer compared to that of diesel fuel at all loads. This may be due to the slow combustion, as a result of the higher density and poor volatility of the blend. For advanced injection timing, the combustion duration is decreased and for retarded injection timing the combustion duration is increased. The reason may be the early and late start of combustion in the premixed combustion phase. The combustion duration was in the range 20-35^{o}CA from no load to full load for all the test conditions.

5.3.3 Performance parameters

5.3.3.1 Brake specific energy consumption

The variation of BSEC with respect to brake power is shown in Figure 5.15. It can be observed from the figure that as load increases BSEC decreases for all the test conditions in this study [121]. This may be due to the increase in the cylinder gas temperature as expected.

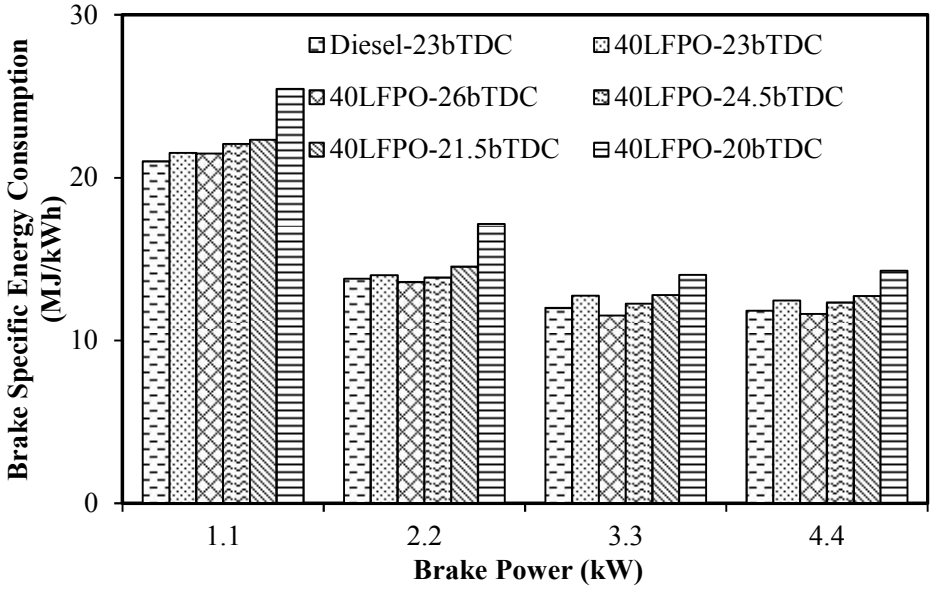

Figure 5.16: Variation of brake specific energy consumption with brake power

BSEC decreases when the injection timing is advanced and increases when the injection timing is retarded. On advancing the injection timing from 23^{o}bTDC to a maximum of 3^{o}CA, the ignition delay is reduced due to the early commencement of ignition and hence, results in less BSEC [129]. The minimum BSEC is noticed for the advanced injection timing of 26^{o}bTDC for 40LFPO at full load, compared to all the injection timings in this study. Retarded injection timing means late combustion and the peak pressure occurs away from the TDC, and results in a reduced effective pressure to do the work. Similar reason was reported by Khabbaz and Mobasheri [188] when they carried out an investigation of the effects of triaromatic utilisation on performance, combustion and emission with diesel engine. By advancing the injection timing using 40LFPO an overall reduction by about 6.5% and 1.5% compared to 40LFPO and diesel respectively both at original fuel injection timing 23^{o} before top dead centre.

5.3.3.2 Exhaust gas temperature

Figure 5.16 illustrates the variation of the exhaust gas temperature for different injection timings of 40LFPO and diesel with brake power. The exhaust gas temperature gives an indication of the conversion of heat into work [189].

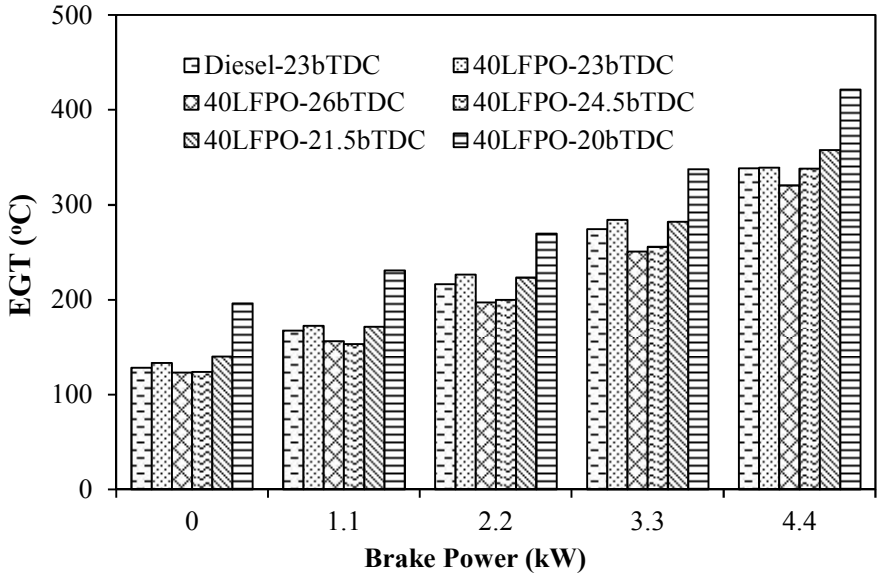

Figure 5.17: Variation of EGT with brake power

EGT is found to be lower for advanced injection timings due to more heat release occurring closer to the TDC in the expansion stroke, which provides enough time for the hot gases to expand and cool down before the exhaust valves were opened. This causes better heat utilization and more cooling of the combustion products, and hence, reduced exhaust gas temperature [190]. The EGT of advanced injection timing at 26^{o}bTDC using 40LFPO is found to be lower by about 5.3% and 5.5% compared to that of diesel and 40LFPO both at the original injection timing (i.e., 23^{o} CAbTDC) at full load.

5.3.4 Emission parameters

5.3.4.1 Hydrocarbon emission

The variations of the hydrocarbon (HC) emission with brake power for diesel and 40LFPO, with advanced and retarded injection timings, are shown in Figure 5.17. The HC emission decreases with the increase in the engine load without and with change in the injection timings. It happens due to the increase in the cylinder gas temperature. For advanced injection timing, combustion is improved due to the availability of more time for the mixing process. Therefore, this leads to a lower HC mass emission compared to that of retarded injection timing at all load conditions [191]. The HC emissions for advanced injection timings are about 0.017 and 0.02 g/kWh, and for the retarded injection timing 0.043 and 0.048 g/kWh at full load respectively.

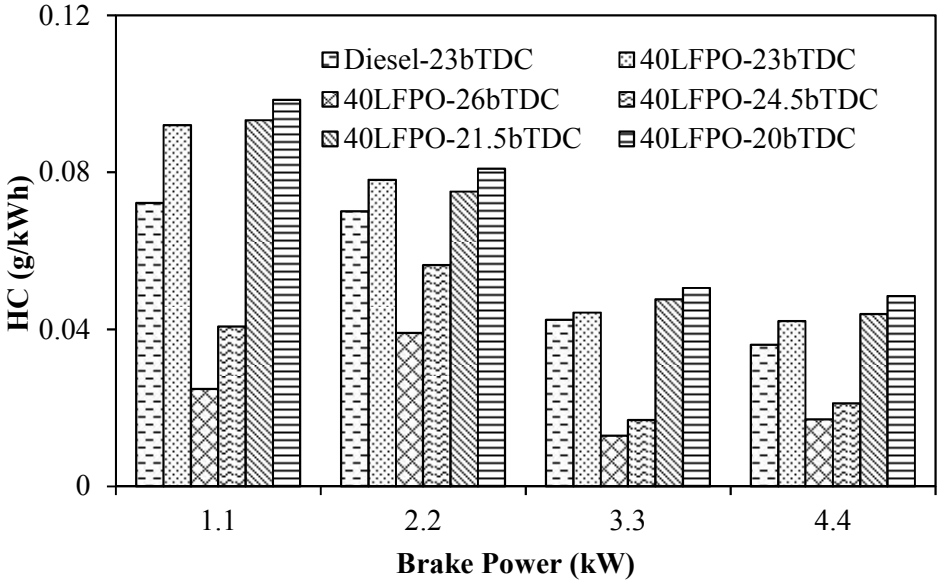

Figure 5.18: Variation of hydrocarbon with brake power

It can also be observed that the HC emission with advanced injection timing for 40LFPO-26^{o}CAbTDC is the lowest among all the tested injection timings. At an advanced injection timing of 26 ^{o}bTDC for 40LFPO, the HC emission is lower by about 52 and 59% compared to that of diesel and 40LFPO respectively with the original injection timing at full load.

5.3.4.2 Carbon monoxide emission

The CO emission generally occurs due to the non-availability of oxygen, poor mixture formation and ignition delay. Diesel engines produce less CO emission as they run on the lean mixture. The CO emission is generated when an engine is operated with a rich mixture [191]. It can be observed from Figure 5.18 that for the original injection timing, the CO emission of 40LFPO is higher by about 74% than that of diesel at full load. This is due to the longer ignition delay and poor mixture formation. It can also be observed that the retarded injection timings exhibit a higher CO emission than those of the original and advanced injection timings at full load.

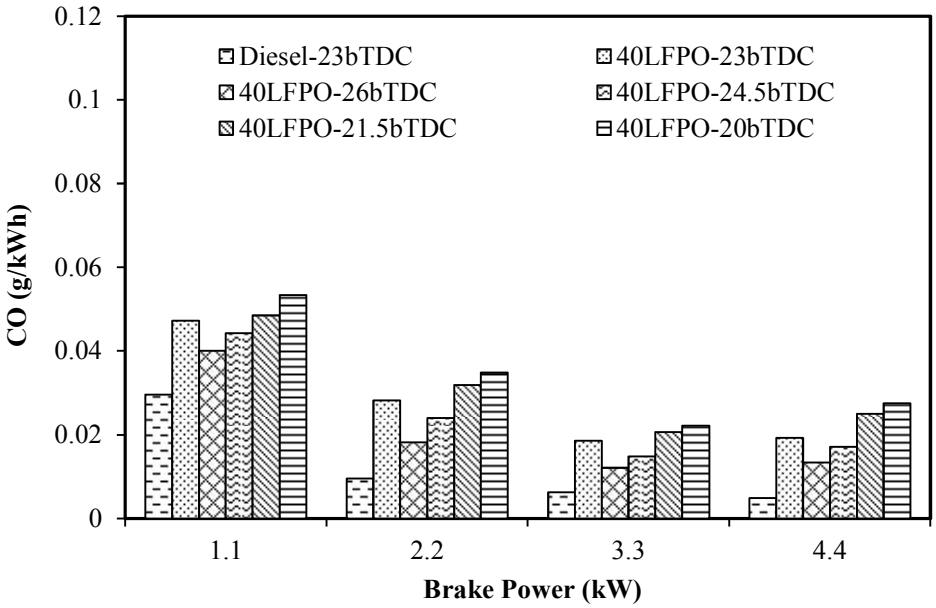

Figure 5.19: Variation of carbon monoxide with brake power

For advanced injection timings, the CO emission is less compared to the retarded injection timings, due to a higher cylinder temperature longer time duration for oxidation between carbon and oxygen molecules, and their conversion into carbon dioxide [188,189]. The CO emission was found to be about 0.0048, 0.019, 0.013, 0.017, 0.025, 0.027 and 0.016 g/kWh for diesel, LFPO, 40LFPO-26^{o}bTDC, 40LFPO-24.5^{o}bTDC, 40LFPO-21.5^{o}bTDC and 40LFPO-20^{o}bTDC at full load respectively.

5.3.4.3 Nitric oxide emission

The variations of nitric oxide (NO) emission with brake power for the fuels tested in this study are illustrated in Figure 5.19. The formation of NO emission is highly dependent on the maximum temperature of the burning gases, oxygen content and residence time available for the reactions to take place at these extreme conditions [192]. Similar reason is reported by Wei et al [193] for the study they carried out effects of methanol to diesel ratio and diesel injection timing on combustion, performance and emissions of a methanol port premixed diesel engine. It can be observed from the figure that diesel exhibits the highest NO emission among all the fuels tested in this study. This is because of the highest maximum heat release rate developed in the premixed combustion, and its better fuel characteristics in comparison with the 40LFPO blend.

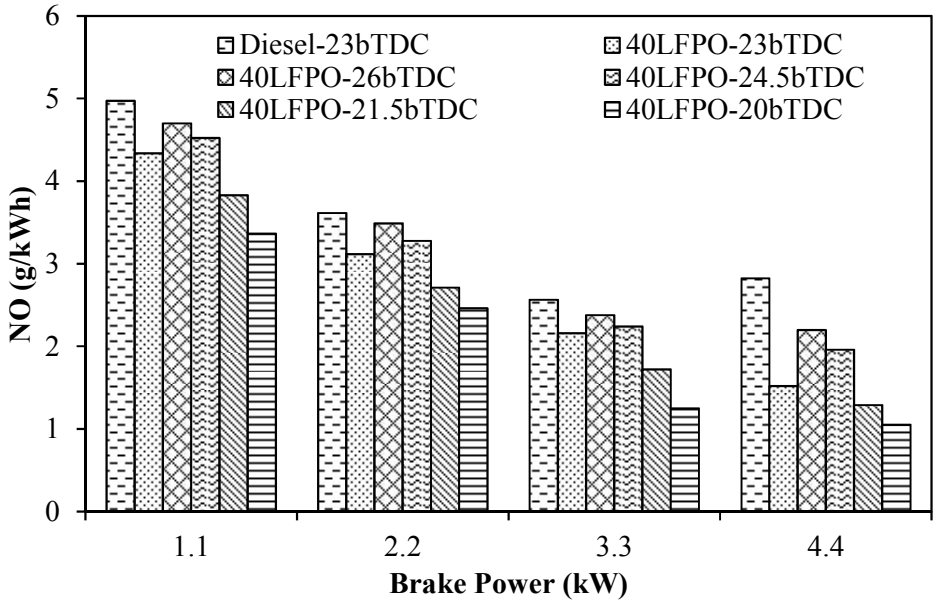

Figure 5.20: Variation of nitric oxide with brake power

The NO emission is found to be the lowest for the retarded injection timings of 21.5^{o}CAbTDC and 20^{o}CAbTDC for 40LFPO; that is about 1.28 and 1.05g/kWh respectively at full load. This is attributed to the lower heat released in the premixed combustion phase. Advancing the injection time increases the NO emission, which is due to more time being available for a better air-fuel mixture that results in an increase in the HRR. The HRRs for the advanced injection timings of 26^{o}CAbTDC and 24.5^{o}CAbTDC are higher about 44 and 28% compared to that of 40LFPO with the original injection timing at full load.

5.3.4.4 Smoke emission

Figure 5.20 illustrates the variation of smoke emission with brake power for different injection timings and the original injection timing of diesel and 40LFPO. In general, the smoke emission occurs due to the incomplete combustion in the combustion chamber of the CI engine. As the load increases more fuel is injected, and this increases the formation of smoke for diesel and 40LFPO at all injection timings. This reason is supported by Sayin et al [194] for the results they obtained from diesel engine run on diesel-methanol blends for effect of injection timing**.** The smoke emission value of diesel is found to be about 61.2% at the original injection timing at full load. The smoke emission of 40LFPO is lower with advanced injection timings as a result of increased NO emission.

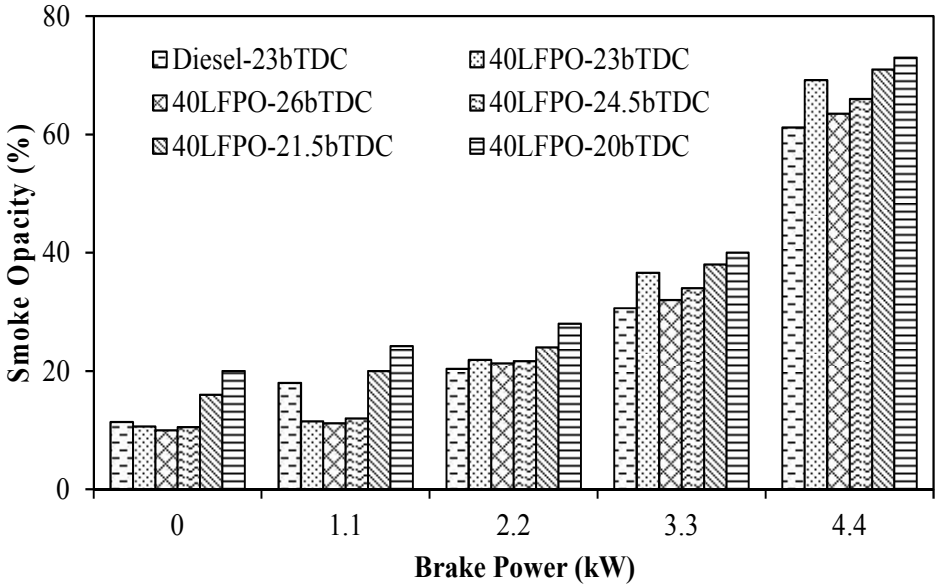

Figure 5.21: Variation of smoke emission with brake power

The smoke emission is higher with retarded injection timings. This is due to the lack of time for the air-fuel mixture leading to incomplete combustion resulting in the smoke emission. The smoke emission values of 40LFPO at the advanced injection timings of 26^{o}CAbTDC and 24.5^{o}CAbTDC at full load are found to be lower by about 5.7 and 3.2% compared to those of diesel and 40LFPO at the original injection time respectively.

5.3.5 Summary

The combustion, performance and emission characteristics of a single cylinder, four stroke, air-cooled, direct injection, diesel engine developing a power output of 4.4 kW at a constant speed of 1500 rpm run on the 40LFPO, without and with the change in its injection timing, were analyzed and compared to those of diesel operation. The following conclusions are drawn based on the experimental results:

- A maximum of about 17-12^{o}J/CA increases in the HRR by advancing the injection timing for the 40LFPO blend compared to that of diesel fuel and 28-23^{o}J/CA increases in the HRR for 40LFPO at the original injection timing.
- At full load, the overall ignition delay increases to a maximum of 8^{o}CA for advancement of fuel injection timing for 40LFPO, while it is increased to a maximum of 1^{o}CA for retardation.
- The BSEC is lower by about 6.5% and 1.5% on advancing the injection timing of 26^{o}CAbTDC and 23^{o}CAbTDC compared to that of diesel at full load.

- The EGT for the advanced injection timing of 26bTDC is lower by about 5.3% and 5.5% compared to those of diesel and 40LFPO at the original injection timing at full load.
- The HC and CO emissions decrease with the advanced injection time compared to the retarded injection timings at all load conditions.
- The NO emissions are found to be higher by about 44% and 28% at advanced injection timings than those of 40LFPO and diesel at the original injection timings respectively at full load.
- The smoke emission is found to be lower by about 5.7% and 3.2% than that of 40LFPO for the original injection timing at full load.

From this experimental investigation, it is concluded that the advanced injection timing of 26^{o}CA improved the performance and reduced the emissions of the diesel engine run on the 40LFPO blend. Table 5.3 provides the values of some of the important parameters of the engine operated with 40LFPO at different injection timings and diesel at full load.

Table 5.3: Summary of values of parameters for diesel and 40LFPO with different injection timings at full load.

Sl No	Parameter	Diesel	40LFPO-20bTDC	40LFPO-21.5b TDC	40LFPO-23b TDC	40LFPO-24.5b TDC	40 LFPO-26bTDC
	Combustion parameters						
1	Maximum cylinder pressure (bar)	75.7	66.8	70.8	72.9	74.3	77.62
2	Maximum heat release (J/^{o}CA)	52	44.6	45.6	47.6	58.7	61.02
3	Ignition delay (^{o}CA)	12.90	21.2	20.7	14.4	13.53	13.23
4	Occurrence of maximum pressure (^{o}CA)	370.4	373	372.9	372.8	372.1	371.5
5	Combustion duration (^{o}CA)	38.1	46.9	43.8	42.5	37.6	34.0
	Performance parameters						
6	Specific fuel consumption (kg/kWh)	11.8	14.3	12.7	12.4	12.3	11.6
7	Exhaust gas temperature (^{o}C)	338.5	421.4	357.6	339.20	338.2	320.5
	Emission parameters						
8	HC emission (g/kWh)	0.036	0.048	0.043	0.042	0.021	0.017
9	CO emission (g/kWh)	0.004	0.027	0.025	0.019	0.017	0.013
10	NO emission (g/kWh)	2.82	1.05	1.28	1.52	1.95	2.19
11	Smoke opacity (%)	61.2	73	71	69.2	66	63.5

5. 4 LFPO-DEE Blends

5.4.1 General

The effects of adding small quantities of Diethyl ether (DEE), an ignition improver, to the 40LFPO blend on the combustion, performance and emissions of the test diesel engine were evaluated. Diethyl ether whose cetane number is greater than that of diesel was added to the 40LFPO. The percentage of DEE was varied from 1% to 4% in steps of 1% on a volume basis. The designation and composition of the 40LFPO based test fuels used in this module are given below;

a) 40LFPO (40% LFPO + 60% Diesel)
b) X1 (40% LFPO + 59% Diesel + 1% DEE)
c) X2 (40% LFPO + 58% Diesel + 2% DEE)
d) X3 (40% LFPO + 57% Diesel + 3% DEE)
e) X4 (40% LFPO + 56% Diesel + 4% DEE)

The results of the combustion, performance and emission parameters of the engine run on the 40LFPO-DEE blends were evaluated, compared with those of the diesel operation of the same engine, and presented in this section.

5.4.2 Combustion parameters

5.4.2.1 Pressure crank angle diagram

The variations of cylinder pressure and heat release rate with respect to the crank angle at full load for 40LFPO and its DEE blends, in comparison with those of diesel, are depicted in Figure 5.21. In each test, the combustion pressure was obtained for every 0.6^{o}CA interval by the data acquisition system. The start of ignition for diesel at full load is the earliest among all the fuels tested in this study, which is due to its higher cetane number. The ignition of 40LFPO commenced a little later than diesel ignition, which is about 2^{o}CA at full load. This is attributed to its lower cetane number than that of diesel.

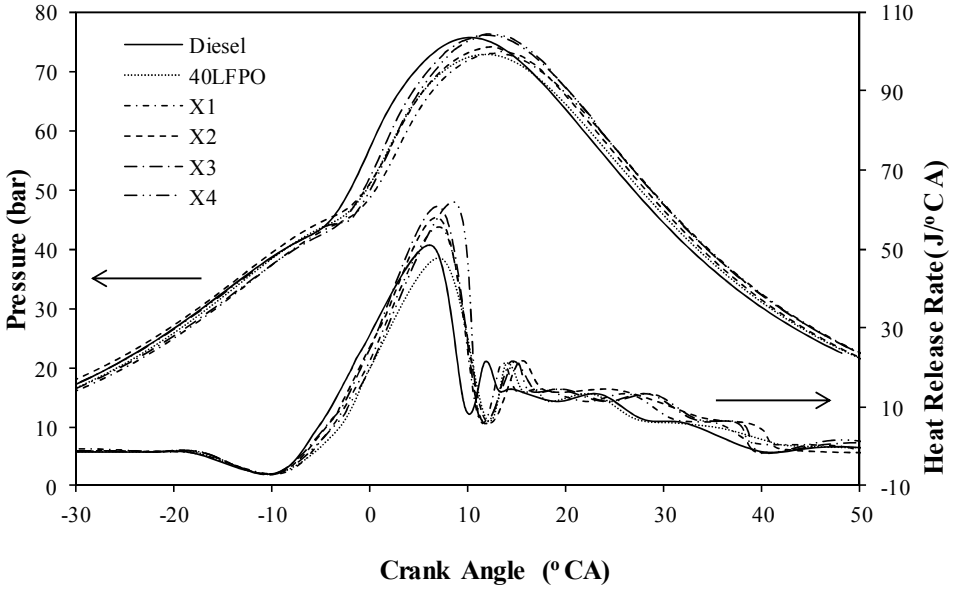

Figure 5.22: Variation of cylinder pressure and HRR with CA at full load.

By adding the ignition improver to the 40LFPO blend, the start of ignition is advanced closer to that of diesel by about 1°CA at full load. The advancement is attributed to the increase in the cetane number of 40LFPO. As a result of the early start of ignition, the peak pressure of diesel attained is closer to the top dead centre (TDC). The peak pressure of the 40LFPO blend is attained later by about 11.7°CA from the TDC at full load. The 40LFPO has a lower cylinder peak pressure, which is attributed to the poor mixture formation, and with the DEE addition the peak pressure increases for the X1, X2, X3 and X4 operations. The peak pressures of diesel, 40LFPO, X1, X2, X3 and X4 are about 75.70, 72.9, 73.4, 74.0, 75.4 and 76.3 bar, which are attained at 370.4, 371.8, 373.4, 372.9, 372.42 and 372.0°CA at full load respectively. This is because DEE offers additional oxygen to the 40LFPO blend, which leads to more complete combustion. With 4% DEE addition, the peak pressure of X4 is found to be the highest among all the fuels. This may be mainly due to the heat release rate in the premixed combustion phase than that of the X1, X2 and X3 blends. The difference in the peak pressure value between diesel and X4 is about 0.6 bar at full load.

5.4.2.2 Heat release rate

The maximum heat release rate (HRR) for the 40LFPO blend at full load is attained by about 1°CA, which is much later than that of diesel, as a result of lower ignition delay. The maximum HRR for the 40LFPO blend is lower than that of diesel, due to its longer ignition delay and poor mixture formation in the premixed combustion phase. By adding DEE with the 40LFPO blend, the maximum HRR is increased. The increase in the

maximum HRR after the addition of DEE, to the 40LFPO blend is about 61.8 J/^{o}CA at full load. This is due to the instantaneous heat release of DEE. The maximum heat release rates for X1, X2, X3 and X4 are approximately 55.5, 57.5, 60.6 and 61.8J/^{o}CA respectively, at full load.

5.4.2.3 Ignition delay

The variations of the ignition delay with brake power for diesel and 40LFPO, without and with the addition of the ignition improver, are depicted in Figure 5.22.

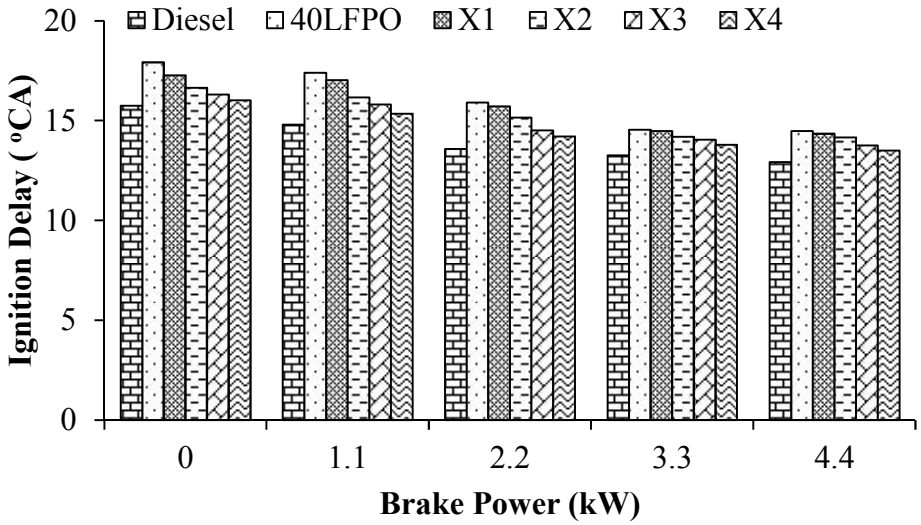

Figure 5.23: Variation of ignition delay with brake power

It is apparent from the figure that the ignition delay decreases with the increase in the load which is due to the increase in the cylinder temperature. The ignition delay of diesel is found to be the lowest among all the fuels tested in this investigation, because of its higher cetane number, while the ignition delay of the 40LFPO blend is found to be the longest throughout the engine operation, due to its lower cetane number. Adding DEE to the 40LFPO blend reduces the ignition delay by about 1-3 ^{o}CA throughout the load spectrum.

A maximum reduction of about 1.6^{o}CA is achieved with 4% DEE addition (X4) at no load, and 1.35^{o}CA is achieved at full load. The values of ignition delay for X1, X2, X3 and X4 are about 14.4, 14.1, 13.8 and 13.5^{o}CA respectively at full load.

5.4.2.4 Maximum cylinder pressure

Figure 5.23 shows the variation of the maximum cylinder pressure with brake power for diesel, 40LFPO without and with DEE addition in different quantities.

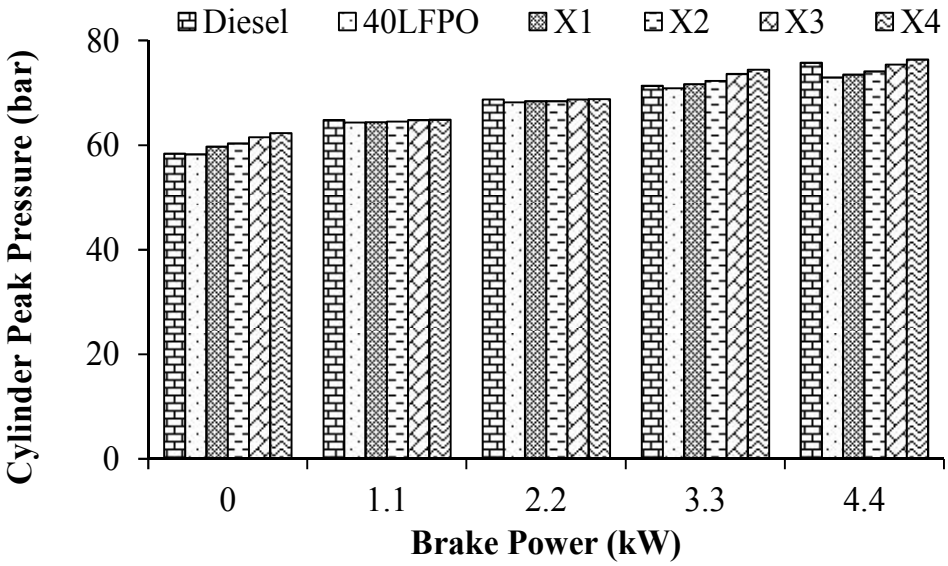

Figure 5.24: Variation of cylinder peak pressure with brake power

As evidenced from the heat release rate curves, the peak pressure is found to be the lowest in the entire engine operation in case of diesel. This is due to the higher cetane number of diesel. The peak pressure of 40LFPO is lower due to poor mixture formation as a result of lower cetane number, higher viscosity and less volatility. The peak cylinder pressure increases with the increase in the DEE i.e., from X1 to X4. The peak cylinder pressure values for diesel, 40LPFO, X1, X2, X3 and X4 are found to be about 75.7, 72.9, 73.4, 74.0, 75.4 and 76.3 bar respectively, at full load. The increase in the maximum cylinder pressure is attributed to the higher heat release in the premixed combustion.

5.4.2.5 Combustion duration

The combustion durations for diesel and 40LFPO, without and with DEE addition in different quantities are portrayed in Figure 5.24.

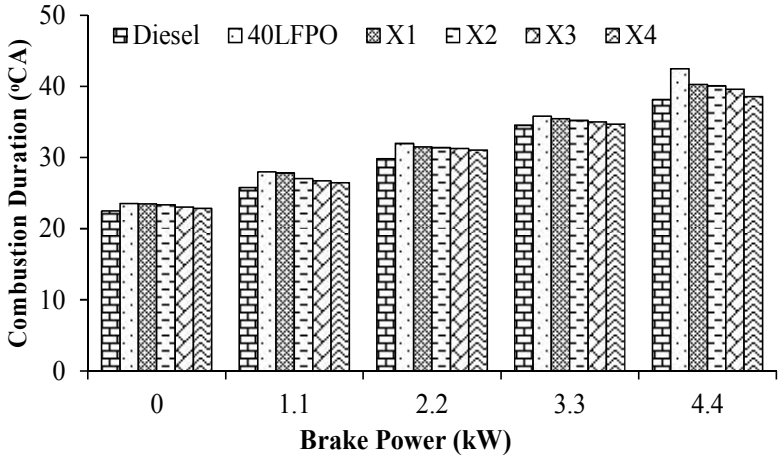

Figure 5.25: Variation of combustion duration with brake power

The combustion duration for diesel is found to be the lowest among all the fuels tested in this study in the entire range of engine operation, as a result of better mixture formation and faster burning. The slow combustion, as a result of poor mixture formation of 40LFPO leads to a longer combustion duration in the entire range of operation. The combustion is found to decrease with the increase in the ignition improver from 1 to 4%. The combustion duration of diesel is 38.1^{o}CA and for the 40LFPO, it is 42.5 ^{o}CA at full load. In the case of X1, X2, X3 and X4, the values of combustion duration are by about 40.3, 41.9, 39.6 and 40^{o}CA respectively.

5.4.2.6 Maximum rate of pressure rise

Figure 5.25 illustrates the variation of maximum rate of pressure rise with brake power for diesel and 40LFPO, without and with the DEE addition in different proportions. The rate of pressure rise is the first derivative of cylinder pressure that relates to the smoothness of the engine operation. It can be observed from the figure that the maximum rate of pressure rise of diesel increases initially with load, and then decreases due to the prominent influence of the premixed phase at lower loads, while the role of the diffusion phase of combustion remains significant at higher loads. Similar reason is reported by Yoshiyuki et al [195]. They investigated the effect of cetane number and aromatics content on combustion process and emission in diesel engine.

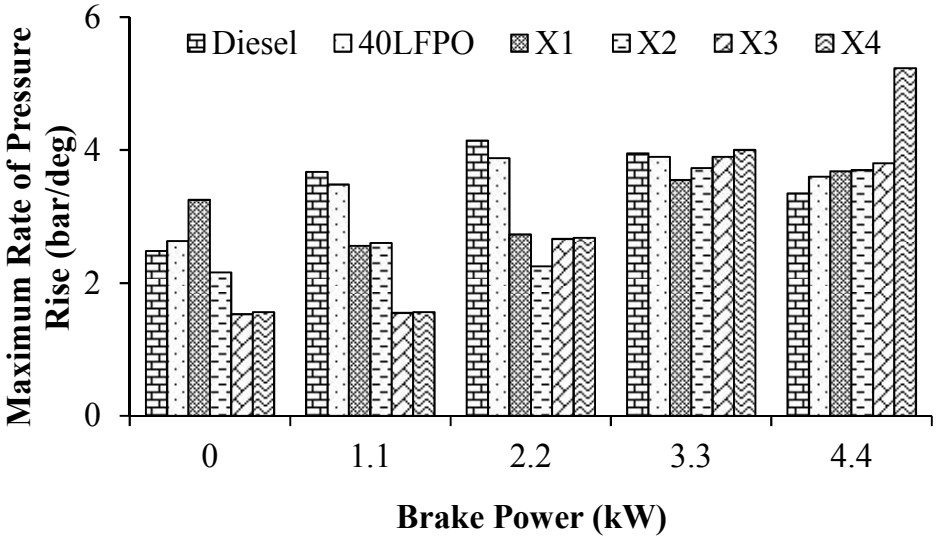

Figure 5.26: Variation of maximum rate of pressure rise with brake power

The maximum rate of pressure rise is the highest for X4 at full load. The reason may be the higher quantity of DEE, which provides oxygen and volatility to the fuel, and improved combustion. The values of the maximum rate of pressure rise at full load for

diesel, 40LFPO, X1, X2, X3 and X4 blends are by about 3.4, 3.6, 3.9, 3.7, 3.8 and 5.2 bar/deg respectively.

5.4 2.7 Combustion efficiency

The combustion efficiency indicates the amount of energy left for the unburned combustible products. The combustible products left in the exhaust gas are CO, unburned hydrocarbons and particulates [196]. The higher amounts of these products reflect the lower combustion efficiency. The combustion efficiency (η_c) can be calculated using the equation given below [197].

$$\eta_c = \left(1 - \frac{\sum X_i Q_{cvi}}{\left(\frac{m_f}{m_a + m_f} \right) Q_{cvf}} \right) \times 100 \qquad (5.1)$$

where η_c= combustion efficiency

X_i = mass fractions of CO and HC

Q_{cvi} = lower heating values of CO and HC

m_a = mass of air

m_f = mass of fuel

Q_{cvf} = lower heating value of fuel

Figure 5.26 portrays the variation in the combustion efficiency with different load conditions of the engine. It is seen that the combustion efficiency increases with the increase in the brake power. The combustion efficiency of diesel is higher than those of all the tested fuels in this study.

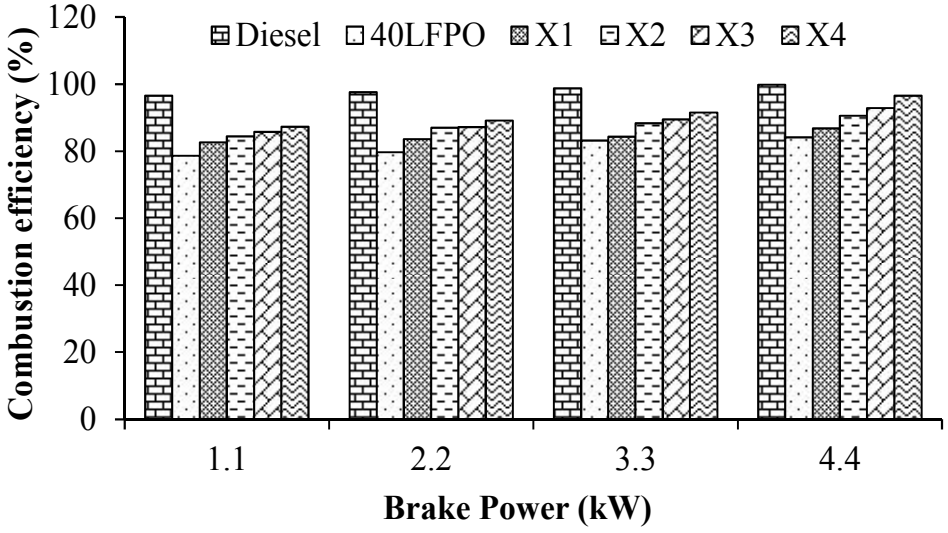

Figure 5.27: Variation in the combustion efficiency with brake power

The combustion efficiency is more than 99% for diesel in a diesel engine, because diesel has a higher calorific value and is a cleaner fuel, which causes complete combustion in the combustion chamber. The combustion efficiencies of the 40LFPO, X1, X2, X3 and X4 blends at full load, i.e., 4.4 kW are found to be about 84, 86.7, 90.5, 92.8 and 96.5% respectively, due to less complete combustion than that of diesel, and the presence of aromatic compounds present in these fuels.

5.4.3 Performance parameters

5.4.3.1 Brake specific energy consumption

The variation of brake specific energy consumption (BSEC) for diesel, 40LFPO and its DEE blends with respect to load are plotted and shown in Figure 5.27. It can be observed from the figure that as the load increases the BSEC decreases for all the fuels tested in this study. This is due to more amount of fuel being consumed to produce the same power output. The BSEC for diesel is the lowest among all the fuels tested in this study in the entire range of engine operation, because of its higher heating value, lower density and fuel composition.

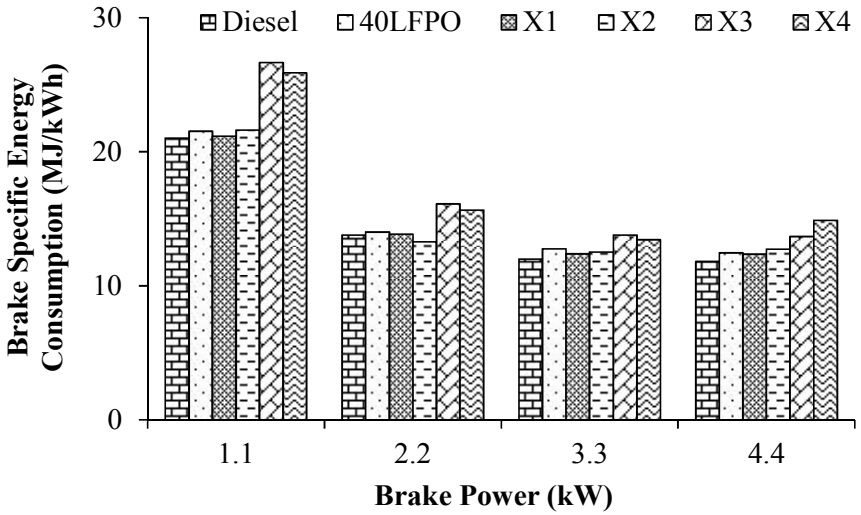

Figure 5.28: Variation of brake specific energy consumption with brake power

The BSEC of the 40LFPO blend is marginally higher than that of diesel throughout the load spectrum. This is due to the higher density and lower heating value of the blend. Adding 1-2% of DEE to 40LFPO reduces the BSEC to a maximum of 1 and 3% than that of diesel and 40LFPO respectively, at full load. Beyond 2%, the addition of DEE increases the BSEC of the blend over that of diesel and 40LFPO. The reason may be the higher latent heat of vaporization of DEE that absorbs the heat of combustion. Similar

reason was supported by Ali et al [198]. The BSEC of X4 is 16.9 M J/kWh higher i.e., about 25% than that of diesel at full load. The BSEC of diesel, 40LFPO, X1, X2, X3 and X4 are about 11.8, 12.6, 12.4, 12.7, 14.7 and 16.9 MJ/kWh respectively.

5.4.3.2 Exhaust gas temperature

Figure 5.28 illustrates the variation of the exhaust gas temperature (EGT) for diesel, and with and without the addition of diethyl ether (DEE) with 40LFPO. It can be observed from the figure that as the load increases, the EGT increases throughout the load spectrum for diesel, 40LFPO X1, X2, X3 and X4 due to the increase in the quantity of fuel injected. The EGT varies from 338 to 339^{o}C at full load for all the blends. The EGT reduces with the addition of DEE. This may be due to a reduced ignition delay as a result of the increase in the cetane number.

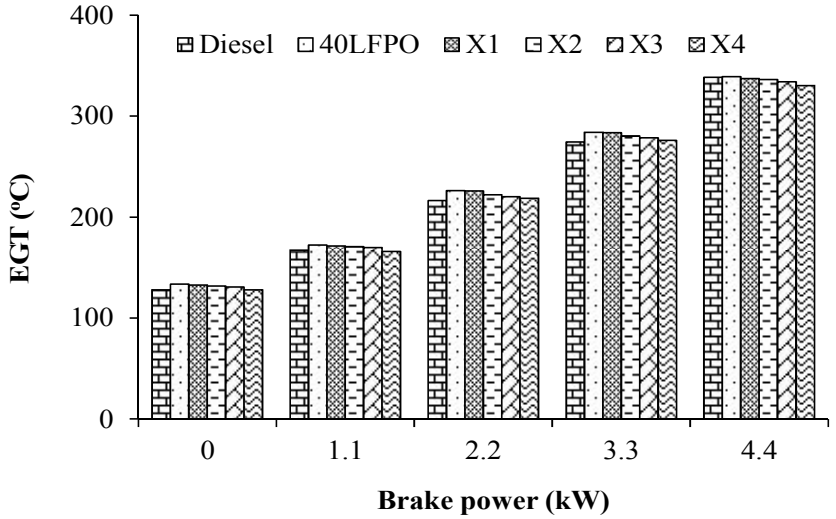

Figure 5.29: Variation of exhaust gas temperature with brake power

Similar reason is supported by Cinar et al [147], for the results obtained in a single cylinder four stroke CI engine, which was run by diesel doped with carbon black. The EGT for X4 is lower compared to other blends, the reason of which may be the highest percentage of DEE compared to the other blends. The values of the exhaust gas temperatures of diesel, 40LFPO, X1, X2, X3 and X4 are about 338.5, 339.2, 337.3, 336. 4,334.2 and 330.5^{o}C respectively.

5.4.4 Emission parameters

5.4.4.1 Nitric oxide emission

The variations of NO emissions with load for the fuels tested in this study are depicted in Figure 5.29. It can be observed from the figure that diesel operation exhibits the highest

NO emission among all the fuels tested in this study. Diesel has better fuel characteristics in comparison with 40LFPO and its DEE blends. Due to the higher density of 40LFPO, the combustion is incomplete and results in a lower NO emission for the given power output. The addition of more DEE percentage might reduce the cylinder temperature as a result of its higher latent heat of vaporization which results in lower NO emission than that of diesel operation for the given power output. This reason can be supported by the results reported by in the literature for the effect of DEE used in diesel engine respectively [199].

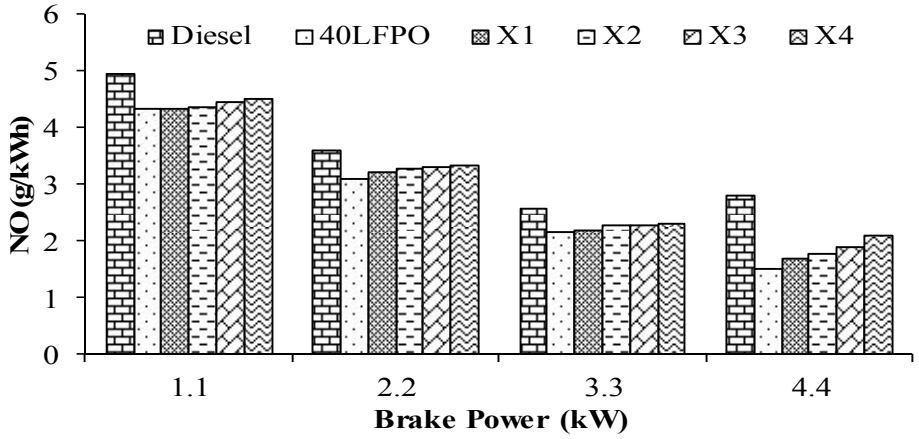

Figure5.30: Variation of nitric oxide emission with brake power

However, the NO emission of the 40LFPO-DEE blend increases with an increase in DEE percentage at all loads. It can also be observed from the figure that the NO emission is increased by the addition of DEE in 40LFPO and diesel blends for the entire load spectrum. The reason may be due to DEE, which has high volatility and oxygen that provides complete combustion. The NO emission of X4 is higher by about 2.09 g/kWh among the other 40LFPO-DEE blends at full load. The NO emission of X4 is approximately about 25% lower compared to that of diesel, and about 20% higher compared to that of 40LFPO blend at full load.

5.4.4.2 *Carbon dioxide emission*

Carbon dioxide (CO_2) emission indicates complete combustion, due to sufficient amount of oxygen being available in the air-fuel mixture, or sufficient time in the cycle for complete combustion [200]. Figure 5.30 portrays the variation of CO_2 emission with respect to load for diesel, 40LFPO and its DEE blends. It can be observed from the figure that the diesel operation produces the highest CO_2 emission among all the fuels tested in this study, as a result of more complete combustion of fuel. The higher density and lower

volatility of 40LFPO result in lower CO_2 emission throughout the engine operation in comparison with diesel operation. When DEE is added to the 40LFPO blend, the CO_2 emission is increased in the entire load spectrum. The CO_2 emission for X4 is higher by about 1.3 g/kWh compared to the X1, X2 and X3 blends. The oxygen present in the DEE may promote the combustion of the LFPO-DEE blend, and hence, a marginally higher amount of CO_2 is produced than that of 40LFPO.

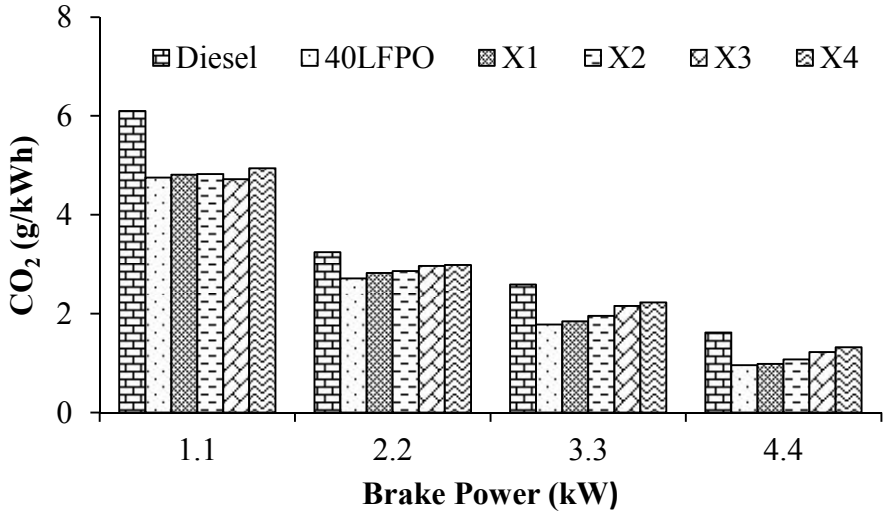

Figure 5.31: Variation of carbon dioxide emission with brake power

The CO_2 emission for X4 is approximately about 18% lower compared to that of diesel, and about 22% higher compared to that of 40LFPO blend at full load.

5.4.4.3 Hydrocarbon emission

The HC emission occurs in a CI engine due to incomplete combustion and the variation of HC emission levels, with respect to equivalence ratio and deposits on the wall. The HC emission of the diesel engine is primarily influenced by fuel quality and the oxygen availablity for complete combustion. It is also influenced by the ignition delay, rate of reaction and engine design. Figure 5.31 depicts the variation of HC emission with load for the different fuels tested in this study. The 40LFPO operation exhibits higher HC emission than that of diesel operation throughout the load spectrum. The higher aromatic content and poor mixture formation may be the reasons for the higher HC emission**.** With the 40LFPO blend, the HC concentration ranges from 0.036 to 0.037g/kWh at full load operation. It can also be observed that the HC concentration with 4% addition of DEE is lower compared to that of all the blends throughout the engine operation. The reason may be the addition of DEE, which provides oxygen to improve the oxidation. The similar reason is supported by Edwin et al [201]. The HC emissions for diesel, 40LFPO, X1, X2

and X3 are about 0.036, 0.042, 0.041, 0.040, 0.038 and 0.037g/kWh at full load respectively.

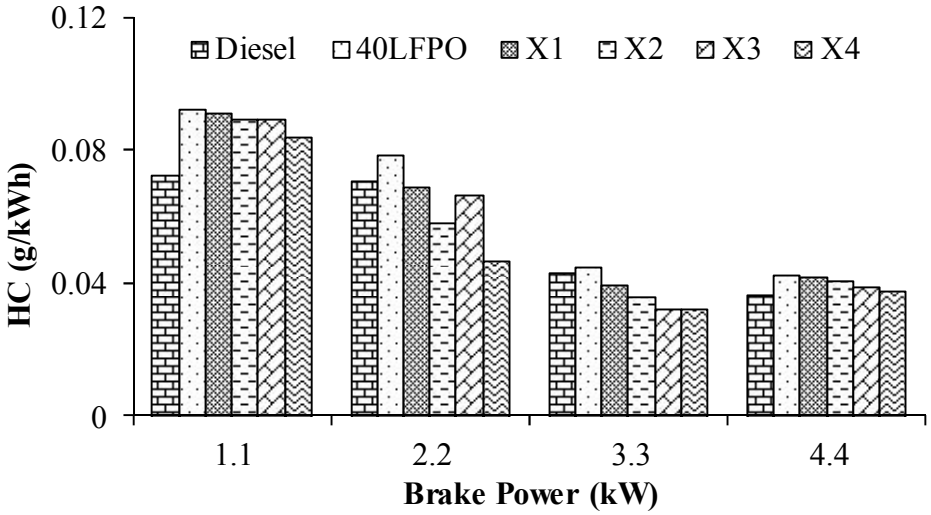

Figure 5.32: Variation of hydrocarbon emission with brake power

The HC emission of X4 is approximately about 2.7% higher compared to that of diesel and about 14% lower compared to that of the 40LFPO blend.

5.4.4.4 Carbon monoxide emission

The carbon monoxide (CO) emission is an indication of the incomplete combustion of the fuel air mixture that takes part in the combustion process.

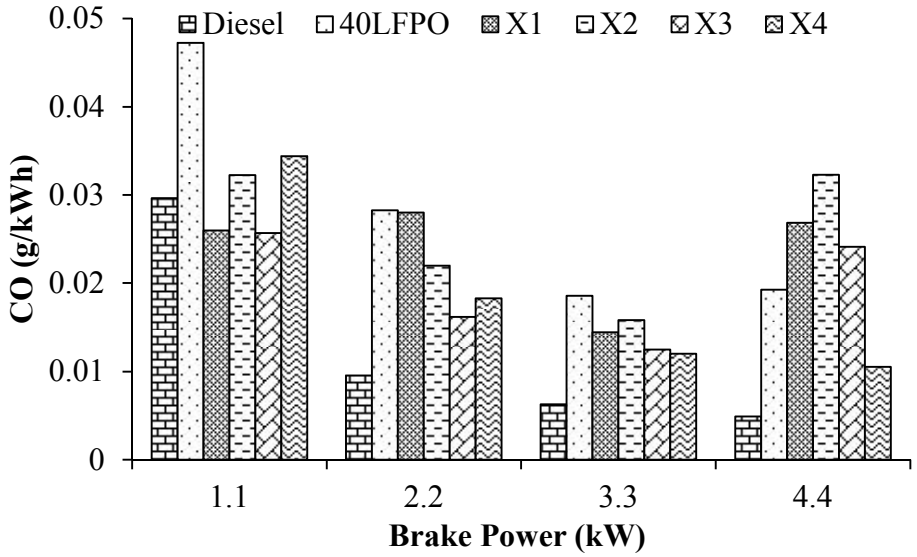

Figure 5.33: Variation of carbon monoxide emission with brake power

CO is generated, when an engine is operated with a rich mixture. Diesel engines generally produce lower CO emission as they run on lean mixture. Figure 5.32 illustrates the variation of CO emission with brake power for diesel, 40LFPO and its DEE blends. It

can be observed from the figure that as the load increases the CO emission decreases but at full load it again increases. This is due to maximum fuel supply at full load to overcome the higher load, which provides rich mixture and therefore, CO emission occurred. Barik and Murugan [200] indicated the same reason for investigation of emission parameters in diesel engine. The CO emission is the highest for 40LFPO in this study. However, the addition of DEE with the 40LFPO-diesel blends results in reduced CO emission, which is due to more oxygen being available for combustion than in 40LFPO. The similar result is supported [201]. At full load, X4 gives lower CO emission of about 45% for the 40LFPO blend.

5.4.4.5 Smoke emission

The variation of smoke emission, with brake power for diesel, 40LFPO and its DEE blends are depicted in Figure 5.33.

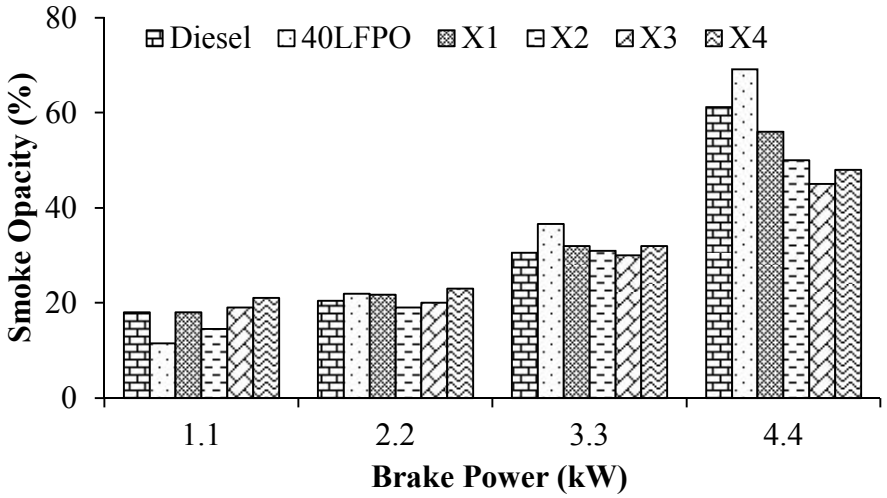

Figure 5.34: Variation of smoke emission with brake power

The smoke emission increases with an increase in the load. This is due to the increase in the mass of fuel consumed when brake power is increased. The smoke emission for the 40LFPO blend is found to be the highest at full load. The value of smoke emission for diesel and 40LFPO are 61.2 and 69.2% respectively at full load. Adding DEE to 40LFPO blend, the smoke emission reduces, and the values for X1, X2, X3 and X4 are 56, 50, 45, 48% are respectively at full load. The smoke emission for X3 is found to be the lowest in this investigation. The volatility and oxygen enrichment provided by DEE is beneficial in improving the fuel evaporation and smoke reduction [202]. The smoke emissions of X3, X4 are approximately 26 and 21% lower compared to that of diesel, and about 39%, 34% lower compared to that of the 40LFPO blend at full load.

5.4.5 Summary

The combustion, performance and emission parameter characteristics of the test engine run on 40LFPO and its different DEE blends were evaluated, analyzed and compared with those of diesel operation. The following conclusions are drawn from the present investigation:

- The addition of DEE improves the performance, combustion and reduces the smoke emission.
- The BSFC of the X4 blend is 6% lower compared to that of diesel at full load.
- The ignition delay of the 40LFPO-DEE blends is reduced by about 1-2^{o}CA at full load.
- The values of the peak cylinder pressures for X1, X2, X3 and X4 are 73.5, 74.2, 75.9 and 76.9 bar respectively at full load.
- The addition of 4% DEE to the 40LFPO diesel blend, gives better results in terms of combustion and lower CO emission compared to all the blends studied. The 3% DEE for smoke emission is the lowest among all the fuels studied.
- The NO emission of X4 is approximately 25% lower compared to that of diesel and about 20% higher compared to that of the 40LFPO blend at full load.
- The smoke emissions of X3 and X4 are found to be approximately 26 and 21% lower compared to that of diesel, and about 39 and 34% lower compared to that of the 40LFPO blend at full load.

The values of important parameters related to combustion, performance and emission for the single cylinder direct injection CI engine run diesel, 40LFPO and 40LFPO blend with various percentage DEE are summarized in Table 5.4.

Table 5.4: Summary of values of important parameters for the engine run on 40LFPO and its diesel blends and diesel at full load

Sl No	Parameter	Diesel	40LFPO	X1	X2	X3	X4
	Combustion parameters						
1	Maximum cylinder pressure (bar)	75.7	72.9	73.4	74.0	75.4	76.3
2	Maximum heat release (J/^{o}CA)	52	47.6	55.5	57.5	60.6	61.8
3	Ignition delay (^{o}CA)	12.9	14.4	14.4	14.1	13.8	13.5
4	Occurrence of maximum pressure (^{o}CA)	370.4	372.8	373.4	372.9	372.42	372.0
5	Combustion duration (^{o}CA)	38.1	42.50	40.3	41.9	39.6	40
	Performance parameters						
6	Brake specific energy consumption (MJ/kW)	11.8	12.44	12.4	12.7	14.7	16.9
7	Exhaust Gas Temperature (^{o}C)	338.5	339.20	337.3	336.4	334.2	330.5
	Emission parameters						
8	HC emission (g/kWh)	0.036	0.042	0.041	0.040	0.038	0.037
9	CO emission (g/kWh)	0.0048	0.019	0.026	0.032	0.024	0.010
10	NO emission (g/kWh)	2.8	1.52	1.68	1.77	1.91	2.09
11	Smoke opacity (%)	61.2	69.2	56	50	45	48

5.5 Effect of Dimethyl Carbonate

5.5.1 General

This chapter discusses the results of the combustion, performance and emission parameters obtained from the same diesel engine run on 40LFPO without and with its oxygenate additive blends in comparison with diesel. As oxygenate additive dimethyl carbonate (DMC) was added in small quantities of 2, 4, 6, 8, 10 and 12% by volume to the 40LFPO blend for the investigation. The designations for test fuels used in this module are given below;

a) 40LFPO (40% LFPO + 60% Diesel)
b) Y1 (40% LFPO + 2% DMC + 58% Diesel)
c) Y2 (40% LFPO + 4% DMC + 56% Diesel)
d) Y3 (40% LFPO + 6% DMC + 54% Diesel)
e) Y4 (40% LFPO + 8% DMC + 52% Diesel)
f) Y5 (40% LFPO + 10% DMC + 50% Diesel)
g) Y6 (40% LFPO + 12% DMC + 48% Diesel)

The results of the combustion, performance, and emissions of the same test engine run on the proposed fuels were evaluated, analyzed and compared with those of diesel operation.

5.5.2 Combustion parameters

5.5.2.1 Cylinder pressure and heat release rate

The variations of the cylinder pressure and the heat release rate with respect to the crank angle for diesel and 40LFPO, without and with the addition of DMC are depicted in Figure 5.34. It is apparent from the figure that the start of ignition is the earliest for diesel due to its high cetane number and better fuel air mixing characteristics. The ignition of the 40LFPO blend is the farthest from the diesel curve as a result of its lower cetane number and higher density. By adding the DMC, the ignition quality of the blend is improved, and hence, the curves for Y1-Y6 lie between the diesel and 40LFPO diesel blend curves. It can be observed from the figure that the cylinder peak pressures for diesel, 40LFPO, Y1, Y2, Y3, Y4, Y5 and Y6 are about 75.7, 72.9, 74.70, 75.90, 76, 76.5, 77.4 and 76.4 bar respectively at full load. The cylinder peak pressures for 40LFPO, Y1, Y2, Y3, Y4, Y5

and Y6 are attained at about 370.4, 372.8, 372.4, 372.5, 372.3, 372.2, 372 and 372.8°CA respectively, at full load.

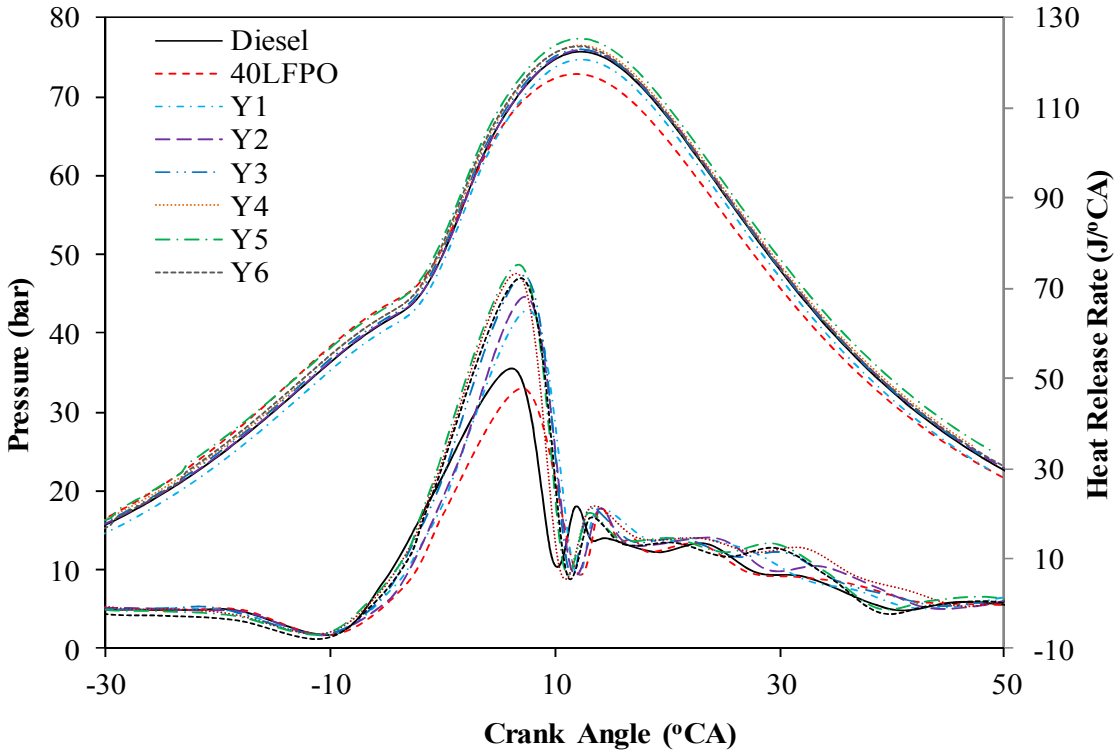

Figure 5.35: Variation of cylinder pressure and HRR with CA at full load

The cylinder peak pressure for Y5 is higher by about 3-4 bar compared to all the fuels tested in this study [203]. This is because of the higher heat release rate in the premixed combustion phase. But, the maximum cylinder pressure is decreased for Y6, at full load. It is apparent from the heat release rate (HRR) curve that the maximum HRR occurs close to the top dead centre (TDC), and it is 52 J/°CA for diesel operation at full load. The maximum HRR for the Y5 blend is higher than that of diesel at full load because of its complete combustion. By adding DMC to the 40LFPO blend, the HRR is increased [187, 203-205]. The maximum HRR for diesel, 40LFPO, Y1, Y2, Y3, Y4, Y5 and Y6 are approximately 52, 47.63, 65.02, 67.78, 72.61, 73.01, 75.08 and 72.08 J/°CA respectively, at full load.

5.5.2.2 Ignition delay

The ignition delays of diesel, 40LFPO and 40LFPO-diesel-DMC blends are depicted in Figure 5.35. It can be observed from the figure that the ignition delay decreases with the increase in the load, which is due to the increase in the cylinder temperature. The ignition delay of diesel is found to be the shortest among all the fuels studied in this investigation,

which is due to its higher cetane number. The ignition delays of the 40LFPO-diesel-DMC blends (Y1-Y6) decrease and the delay curves shift towards the diesel operation, as a result of lower viscosity and oxygen content**.** This reason may be supported by Hu et al [205] for experimental analysis of ignition delay times of dimethyl carbonate at high temperature in diesel engines.

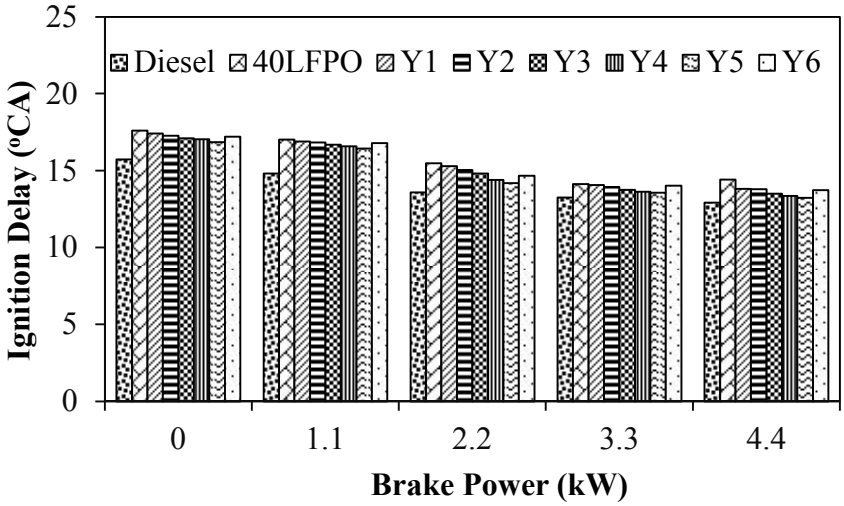

Figure 5.36: Ignition delay with brake power

The values of ignition delay for diesel, 40LFPO, Y1, Y2, Y3, Y4, Y5 and Y6 are about 12.9, 14., 13.4, 13.8, 13.5, 13.4, 13.2 and 13.7^{o}CA at full load respectively. Overall about 1-2^{o}CA is decreased when DMC is added to the 40LFPO blend.

5.5.2.3 Combustion duration

Figure 5.36 depicts variation of the combustion duration of 40LFPO with DMC blends. It is apparent from the figure that the combustion duration of 40LFPO blend is the longest followed by diesel, 40LFPO and its oxygenate additive blends (Y1-Y6). The longest combustion duration of 40LFPO is a result of slow or sluggish combustion. By adding the oxygen additive to 40LFPO, the blend marginally improves the mixture formation and the oxygen availability. Xiaolu et al [162] have also got similar results, by investigation of characterization of a diesel engine operated with dimethyl carbonate. However, the combustion duration decreases up to Y5 and then increases. The increase in the combustion duration of Y6 is due to a poor mixture formation resulting from its higher density, which is a dominating factor.

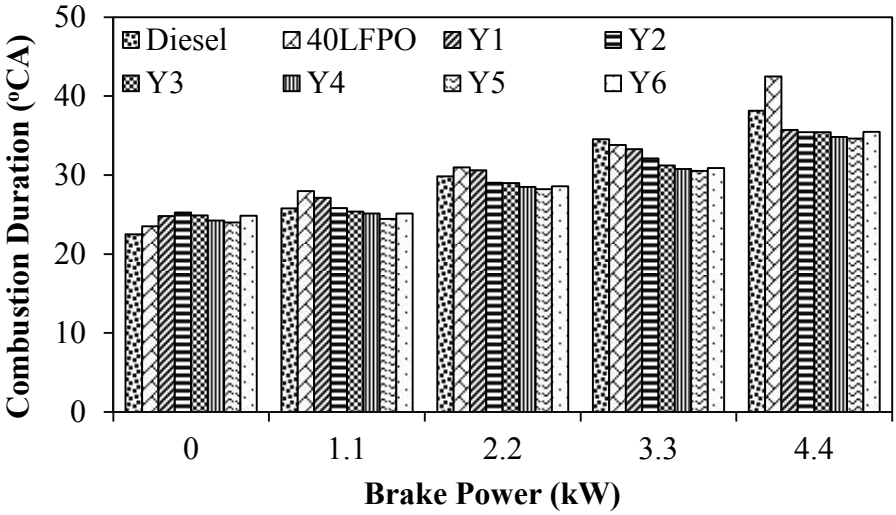

Figure 5.37: Variation of combustion duration with brake power

The values of combustion duration of diesel, 40LFPO, Y1, Y2, Y3, Y4, Y5 and Y6 are about 38.1, 42.5, 35.7, 35.4, 35.40, 34.8, 34.60 and 35.5 ^{o}CA respectively, at full load. It is apparent that the combustion duration is overall decreased by about 6-7^{o}CA from the 40LFPO curve in the entire range of engine operation.

5.5.2.4 Peak cylinder pressure

Figure 5.37 depicts the variation of peak cylinder pressure with brake power for diesel, 40LFPO and its DMC blends. The peak cylinder pressure of a CI engine is influenced by the cetane number of the fuel used and the heat release during the premixed combustion phase [206]. The peak cylinder pressure generally increases with load as a result of increased gas temperature. The peak cylinder pressure of 40LFPO is lower, because of its lower heat release rate in the premixed combustion phase. This is also evidenced from the heat release rate curves. This may be attributed to the increase in the maximum heat release rate in the premixed combustion phase. The maximum cylinder pressure is found to be lower for the Y6 blend as a result of lower heat released in the premixed combustion phase. Overall, about 2.7 bar is increased from Y1 to Y6 from no load to full load. The peak cylinder pressure marginally increases with the increase in the oxygenated additive DMC percentage. The reason may be the increase in the heat release rate as a result of enhanced combustion [205]. The cylinder peak pressure values for diesel, 40LPFO, Y1, Y2, Y3, Y4, Y5 and Y6 are found to be about 75.7, 72.8, 74.70, 75.90, 76.0, 76.5, 77.4 and 75.8 bar respectively, at full load.

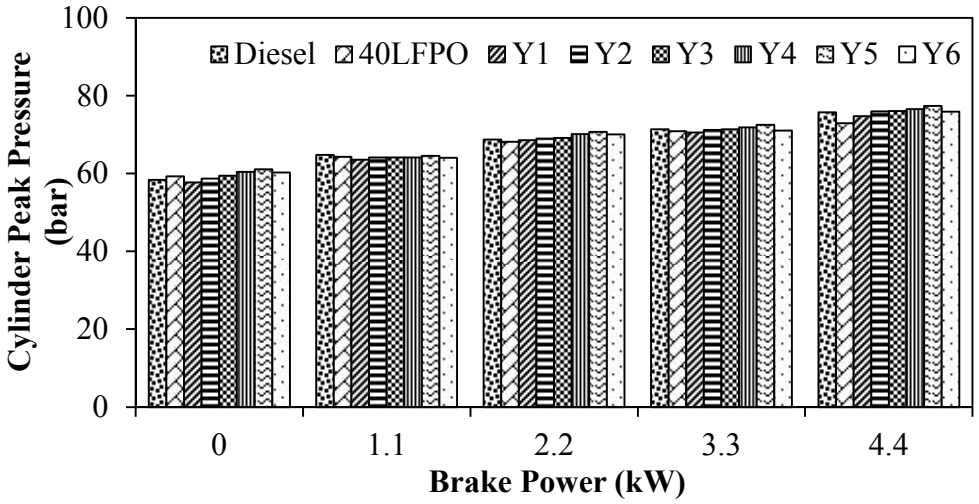

Figure 5.38: Variation of cylinder peak pressure with brake power

5.5.2.5 Maximum pressure rise rate

The variation of maximum rate of pressure rise with brake power for diesel, 40LFPO and its DMC blends are illustrated in Figure 5.38. It can be observed from the figure that the maximum rate of pressure rise increases with the increase in load as expected [195]. The maximum rate of pressure rise is the lowest for 40LFPO as reflected in the cylinder pressure. The maximum rate of pressure rise increases when the DMC is added to the 40LFPO blend. The maximum rate of pressure rise for the Y5 blend is the highest among the fuel tested in the study. The reason may be due to the high peak cylinder pressure attained. The values of maximum rate of pressure rise for diesel, 40LFPO, Y1, Y2, Y3, Y4, Y5 and Y6 are approximately 3.4, 3.6, 3.56, 3.8, 3.9, 4.09, 4.2 and 4.05 bar/ ^{o}CA respectively at full load.

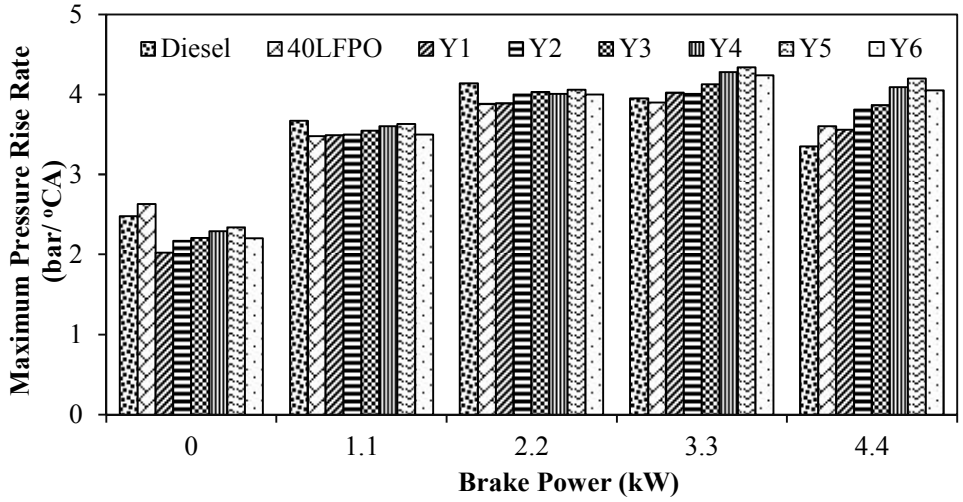

Figure 5.39: Variation of the maximum pressure rise rate with brake power

5.5.3 Performance parameters

5.5.3.1 Brake specific energy consumption

The variation of BSEC with respect to brake power is shown in Figure 5.39. It can be observed from the figure that as the load increases the BSEC decreases for all the fuels tested in this study. This may be due to the increase in the cylinder gas temperature as expected. The BSEC for diesel is the lowest among all the fuels tested in this study in the entire range of engine operation, because of its higher heating value, lower density and more complete combustion. The BSEC of all the 40LFPO-DMC blends are higher than that of diesel operation at all loads, because of the lower heating value, higher density and poor combustion attributes of the blends [207]. The BSEC of the 40LFPO-DMC10 (Y5) blend is lower compared to that of all other fuels at 25% load, and lower compared to those of the other 40LFPO-DMC blends at full load. The reason may be improved combustion by providing more oxygen to the combustion. Zhang and Balasubramanian [208] have got similar results by investigation of effects of oxygenated fuel blends on carbonaceous particulate composition and particle size distributions from a stationary diesel engine.

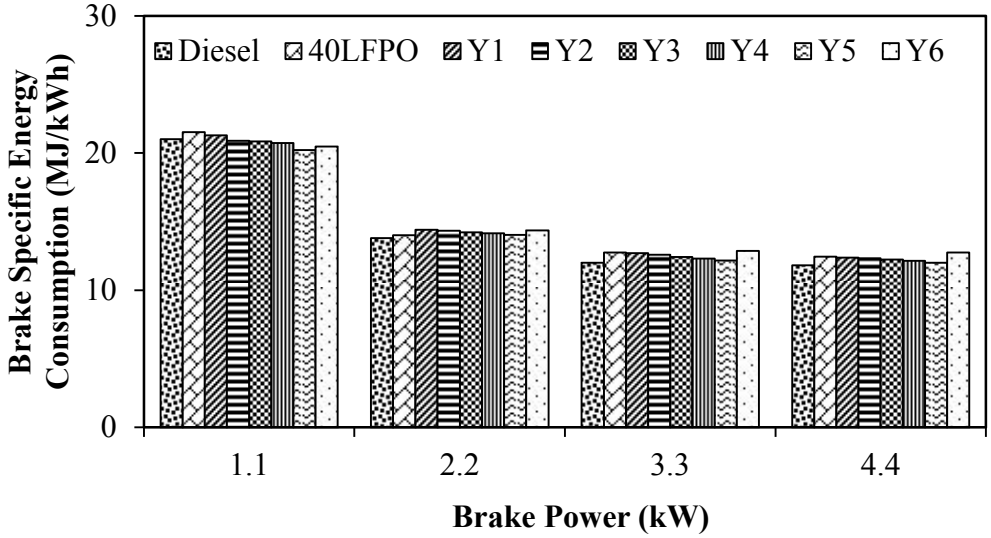

Figure 5.40: Variation of brake specific energy consumption with brake power

By increasing the percentage of DMC beyond 40% to the Y5 blend, the BSEC of Y6 increases. This may be due to the marginally higher density and lower calorific value of the DMC compared to that of diesel fuel. The BSEC of diesel, 40LFPO, Y1, Y2, Y3, Y4, Y5 and Y6 are about 11.8, 12.4, 12.4, 12.3, 12.2, 12.1, 12.0 and 12.7 (MJ/kWh) respectively at full load.

5.5.3.2 Exhaust gas temperature

Figure 5.40 illustrates the variation of the exhaust gas temperature (EGT) for diesel without and with the addition of dimethyl carbonate (DMC) to the 40LFPO blend. It can be observed from Figure 5.40 that EGT increases with load as a result of increased cylinder gas temperature. Better conversion of heat into work is achieved by adding the oxygenated additive to the LFPO-diesel blend, and it exhibits a lower EGT than that of 40LFPO. Further, by increasing the DMC percentage in the blend, the EGT increased. This may be due to the effect of the higher density of the blends. The values of EGT for diesel, 40LFPO, Y1, Y2, Y3, Y4, Y5 and Y6 are about 338.5, 339.2, 330, 328, 326, 322.7, 320.7 and 325.32 ^{o}C at full load respectively.

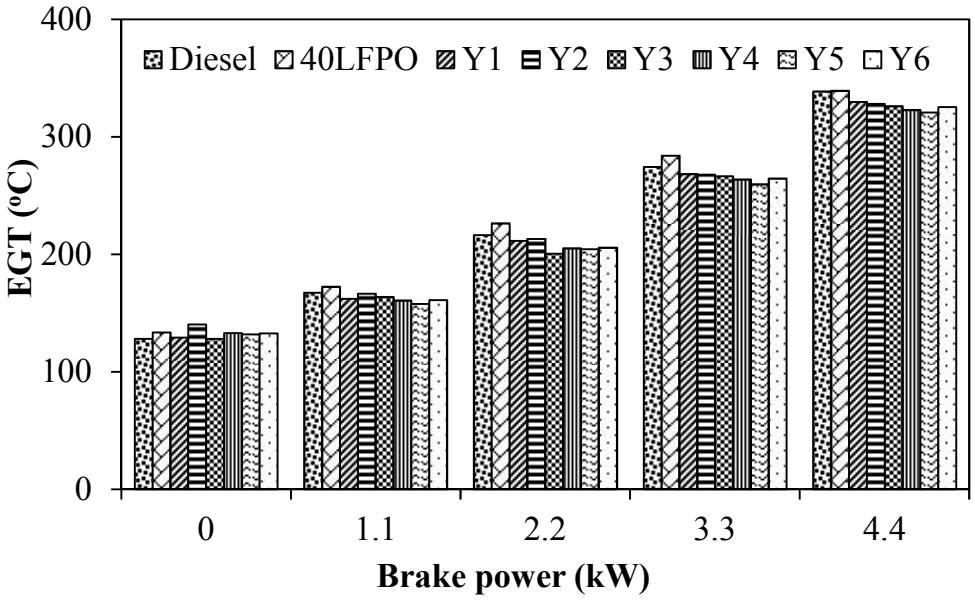

Figure 5.41: Variation of EGT with brake power

5.5.4 Emission parameters

5.5.4.1 Hydrocarbon emission

Figure 5.41 depicts the variation of hydrocarbon (HC) emission for diesel, 40LFPO and its DMC blends with brake power. The HC emission for the 40LFPO blend is the highest among all the fuels studied. More incomplete combustion is the reason for the higher HC emission. For the 40LFPO blend, the HC concentration ranges from 0.036 at no load to 0.037 g/kWh at full load. By offering supplementary oxygen through the addition of DMC to the 40LFPO blend, the HC emission is found to decrease significantly [131].

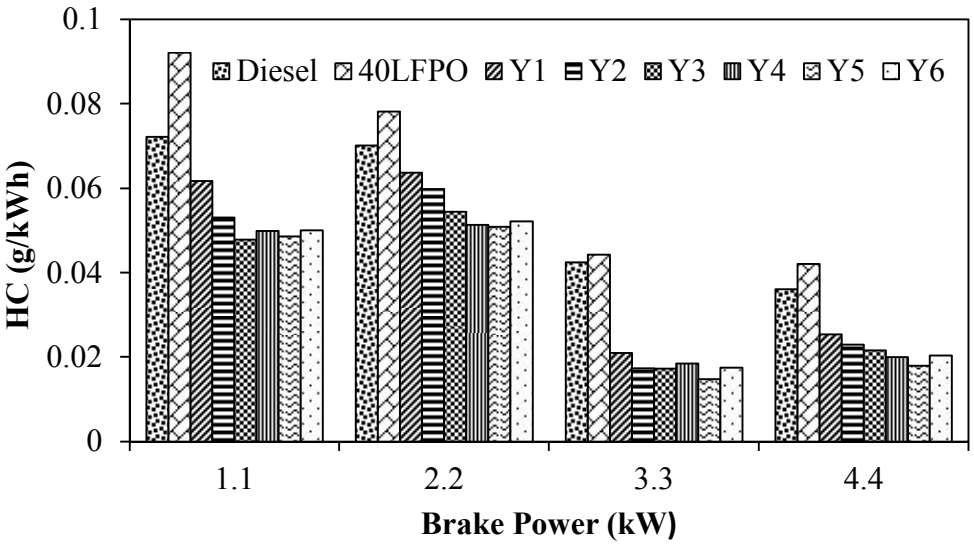

Figure 5.42: Variation of hydrocarbon with brake power

It is also seen that the HC concentration in Y5 operation is lower, compared to all other blends throughout the engine operation. The HC emissions for diesel, 40LFPO, Y1, Y2, Y3, Y4, Y5 and Y6 are approximately 0.036, 0.042, 0.025, 0.022, 0.021, 0.020, 0.0178 and 0.0203 g/kWh at full load respectively. The HC emission for Y5 is approximately 50% lower compared to that of diesel and 57% lower compared to that of 40LFPO blend.

5.5.4.2 Carbon monoxide emission

The trend of CO emission with brake power for diesel, 40LFPO and its DMC blends are depicted in Figure 5.42. It is seen that as the load increases the CO emission decreases. This is because of the longer combustion duration as seen in the heat release curve. By adding DMC in small quantity to the 40LFPO blend, the CO emission is reduced.

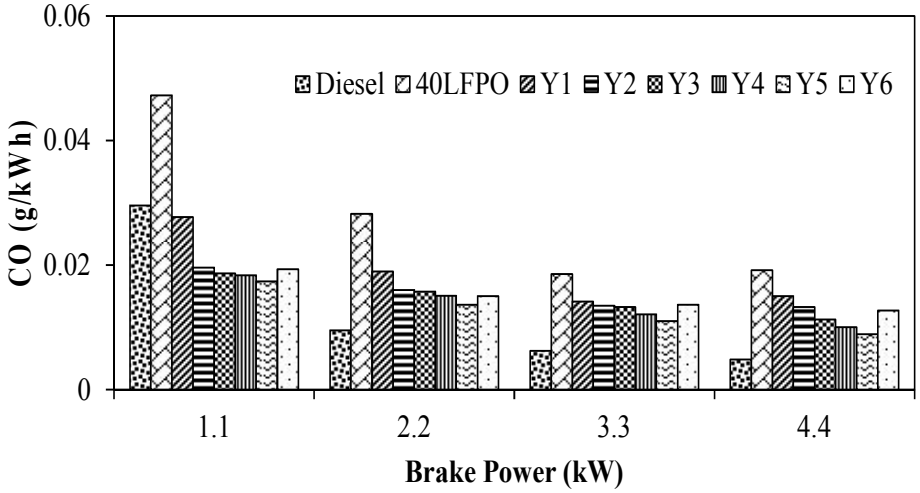

Figure 5.43: Variation of carbon monoxide with the brake power

This is attributed to the supplement of oxygen by the DMC [157]. The CO emission for the Y5 blend is about 53% lower than that of 40LFPO blend and 83% higher than that of diesel. The CO emission for diesel, 40LFPO, Y1, Y2, Y3, Y4, Y5 and Y6 are approximately 0.004, 0.019, 0.015, 0.013, 0.011, 0.01, 0.009 and 0.013 g/kWh respectively at full load.

5.5.4.3 Carbon dioxide emission

Figure 5.43 depicts the variation of carbon dioxide (CO_2) emission with brake power for diesel and 40LFPO without and with DMC addition.

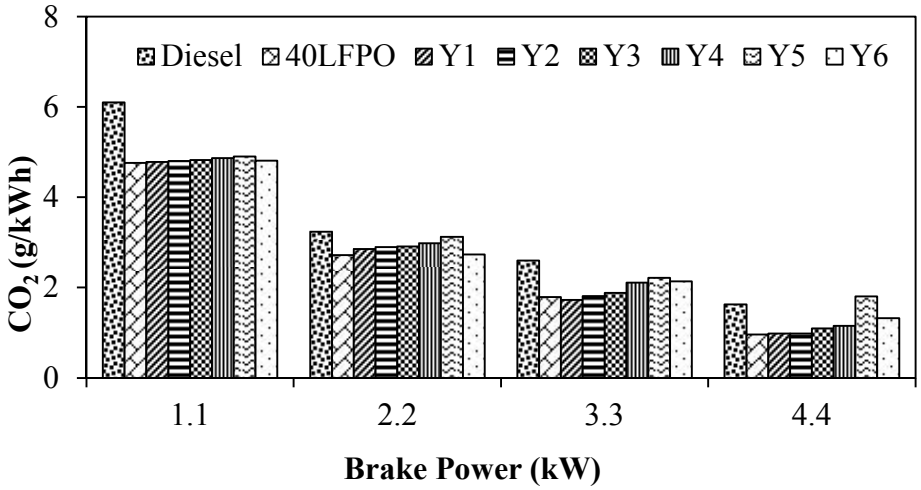

Figure 5.44: Variation of carbon dioxide with brake power

Diesel shows the highest CO_2 emission, among all the fuel tested in the study, as a result of more complete combustion. The CO_2 emission is found to be the lowest for the 40LFPO blend throughout the load spectrum, because of incomplete combustion. This is also evidenced from Figure 5.43. Diesel shows the highest value of CO_2 emission throughout the load spectrum in this study. The CO_2 emission for Y5 is higher by about 11% compared to that of diesel and 88% compared to the 40LFPO blend at full load. The CO_2 emission for diesel, 40LFPO, Y1, Y2, Y3, Y4, Y5 and Y6 are about 1.62, 0.95, 0.97, 0.98, 1.09, 1.15,1.80 and 1.32 g/kWh respectively, at full load.

5.5.4.4 Nitric oxide emission

The variation of nitric oxide (NO) emissions with load for the fuels tested in this study are illustrated in Figure 5.44. It can be observed from the figure that diesel exhibits the highest NO emission among all the fuels tested in this study. This is because of the highest maximum heat release rate developed in the premixed combustion, which is

evidenced from Figure 5.44. Diesel has better fuel characteristics in comparison with the 40LFPO blend and its DMC blends [209].

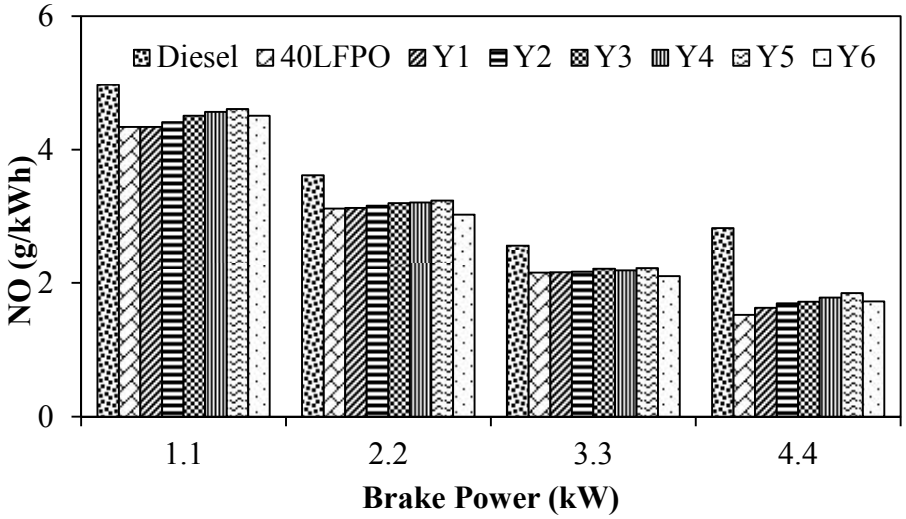

Figure 5.45: Variation of nitric oxide emissions with brake power

The NO emission is found to be the lowest for the 40LFPO blend, which is due to lower heat release rate developed in the premixed combustion phase, as a result of the longer ignition delay. By adding DMC to the 40LFPO blend, the NO emission increases up to Y5 and then declines [210]. The NO emission of Y5 is lower by about 34% compared to that of diesel fuel and 21% higher than that of the 40LFPO blend at full load. The NO emission for diesel, 40LFPO, Y1, Y2, Y3, Y4, Y5 and Y6 are about 2.82, 1.52, 1.62, 1.69, 1.71, 1.78, 1.85 and 1.72 g/kWh at full load respectively.

5.5.4.5 Smoke emission

Figure 5.45 illustrates the variation of smoke emission with brake power for the fuels tested in this study. With an increase in the load, the smoke emission increases as a result of the increase in the mass of fuel consumption [183]. The smoke emission of 40LFPO blend is the highest among all the fuels tested in this study. With an increase in the percentage of DMC in the blend, the smoke emission is reduced. The reason may be reduced ignition delay, volatility, and availability of oxygen, which improved the combustion [210, 211]. The values of smoke emission for diesel, 40LFPO, Y1, Y2, Y3, Y4, Y5 and Y6 are about 61.2, 69.2, 65.0, 62.0, 60, 55.0, 53.0, and 54.0% respectively at full load operation.

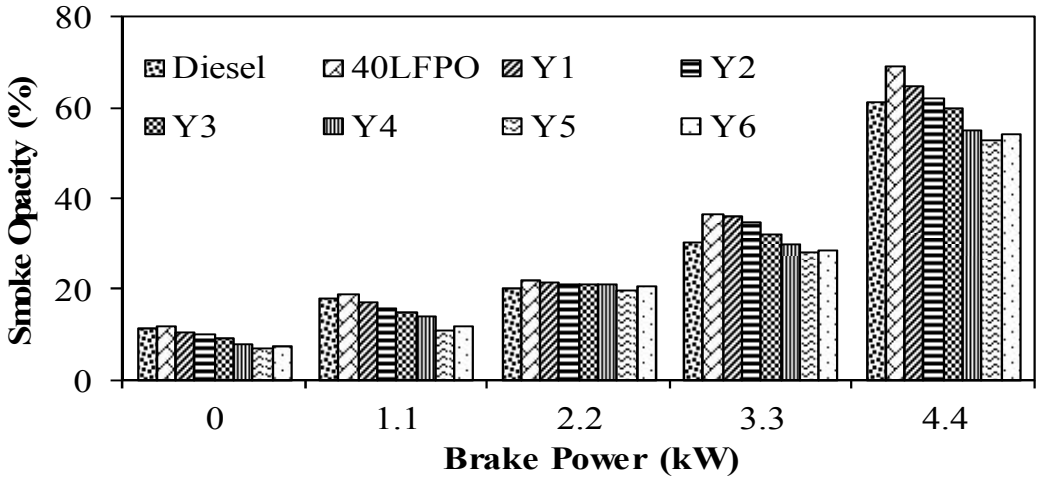

Figure 4.46: Variation of smoke emission with brake power

The smoke emission for the Y5 blend is about 13% lower than that of diesel fuel and 23% less than that of the 40LFPO blend at full load operation.

5.5.5 Summary

The performance, combustion and emission characteristics of the test engine run on 40LFPO and its DMC blends, and diesel, as fuels were assessed, and compared with those of diesel operation.

The addition of an oxygenated additive DMC in the range 1-10% to the 40LFPO blend improves the performance and combustion. The Y5 blend gave better results in terms of performance, combustion and emissions compared to all the blends studied. The addition of more than 12% DMC to the 40LFPO blend produced a negative impact on the engine behavior. The BSEC is decreased by the addition of DMC by 1-10%, but it increased when more than 10% DMC was added. Such variation of BSEC is because of the reduced calorific value, increased density and incomplete combustion of the resultant blend. The BSEC of the Y5 blend is 3.8% higher than that of diesel fuel and 1.4% lower than that of the 40LFPO blend at the full load. The ignition delay and combustion duration also marginally decrease by the addition of DMC to the 40LFPO blend and shift the curves towards the diesel operation. The ignition delay of Y6 is about 0.3^{o}CA longer than that of diesel fuel and 0.73^{o}CA shorter than that of the 40LFPO blend at full load. The NO emission of the Y5 blend is lower by about 34% compared to that of diesel fuel, and 21% higher than that of the 40LFPO blend at full load. The HC and CO emissions are also decreased in this study. The smoke emission for the Y5 blend is about 13% lower than that of diesel fuel and 23% lower than that of the 40LFPO blend at full load operation.

Table 5.5 gives the important parameters of the engine run under diesel, 40LFPO and its DMC blends at full load.

Table 5.5: Summary of values important parameters for diesel, 40LFPO and its DMC blends at full load

Sl No	Parameter	Diesel	40LFPO	Y1	Y2	Y3	Y4	Y5	Y6
	Combustion Parameter								
1	Maximum cylinder pressure (bar)	75.7	72.9	74.70	75.90	76	76.5	77.4	76.4
2	Maximum heat release (J/^{o}CA)	52	47.63	65.02	67.78	72.61	73.01	75.08	72.08
3	Ignition delay (^{o}CA)	12.9	14.4	13.8	13.8	13.5	13.4	13.2	13.7
4	Occurrence of maximum pressure (^{o}CA)	370.4	372.8	372.4	372.5	372.3	372.2	372	372.8
5	Combustion duration (^{o}CA)	38.1	42.50	35.7	35.4	35.40	34.8	34.6	35.5
	Performance parameters								
6	Brake specific energy consumption (MJ/kWh)	11.8	12.44	12.4	12.3	12.2	12.1	12.0	12.7
7	Exhaust Gas Temperature (^{o}C)	338.5	339.20	330	328	326	322.7	320.71	325.32
	Emission parameters								
8	HC emission (g/kWh)	0.036	0.042	0.025	0.022	0.021	0.020	0.017	0.020
9	CO emission (g/kWh)	0.0048	0.019	0.015	0.013	0.011	0.01	0.009	0.013
10	NO emission (g/kWh)	2.8	1.52	1.62	1.69	1.71	1.78	1.85	1.72
11	Smoke opacity (%)	61.2	69.2	65.0	62.0	60	55.0	53.0	54.0

5.6 Effect of Internal Jet Piston Geometry

5.6.1 General

From the previous experimental results, it was understood that even with the oxygenated additive, the 40LFPO blend exhibited inferior performance and higher smoke emission than those of diesel operation at full load in the same engine. Hence, turbulence was created in the combustion chamber by providing an internal jet in the piston for the engine run with 40LFPO10DMC. It is to be noted that in all the previous sections the experiments were conducted on the engine had no modification in the geometry of any of its components. The notations used in this module of the experiment are given below

a) Diesel (100% Diesel, unmodified engine)
b) 40LFPO (40% LFPO + 60% Diesel, unmodified engine)
c) 40LFPO10DMC (40% LFPO + 50% Diesel + 10% DMC, unmodified engine)
d) 40LFPO10DMC + IJPG (40% LFPO + 50% Diesel + 10% DMC + IJPG, engine modified with internal jet piston (IJP))

The investigation results in terms of combustion, performance and emissions are compared with those of the engine run with the conventional diesel fuel, with and without turbulence inducement, and presented in this section.

5.6.2 Combustion parameters

5.6.2.1Cylinder pressure and heat release rate

Figure 5.46 depicts the variations of the cylinder pressure and the heat release rate (HRR) with the crank angle for the diesel, 40LFPO with the conventional piston, and 40LFPO10DMC, without and with internal jet piston operations at full load. It can be observed from the figure that the cylinder peak pressures for the engine run on diesel, 40LFPO, 40LFPO10DMC and 40LFPO10DMC+IJP are about 75.7, 72.9, 77.4 and 78.8 bar respectively at full load. The cylinder peak pressures for diesel, 40LFPO, 40LFPO10DMC and 40LFPO10DMC+IJP are attained at about 370.4, 372.8, 372.03 and 372.6^{o}CA at full load respectively. The combustion of 40LFPO10DMC with IJP starts little earlier than that of 40LFPO, but little later than diesel operation at full load. The reason may be the enhanced air turbulence motion caused by providing two holes on the piston crown [2]. The cylinder peak pressure of the 40LFPO10DMC+IJP blend is the highest, which is about 78.4 bar in this investigation. This is because DMC has oxygen

and better air fuel mixing provided by the internal jet piston for complete combustion. Similar reason is reported by Lu et al [203] for the results they obtained from a diesel engine running on oxygenated fuel additives combined with a cetane number improver. It can be observed from the HRR curves that the maximum HRR for the diesel operation occurs close to the top dead centre (TDC) and it is 52.0 J/^{o}CA at full load. The maximum HRRs for diesel, 40LFPO, 40LFPO10DMC and 40LFPO10DMC+IJP are about 52.0, 47.6, 75.08 and 78.50 J/^{o}CA respectively, at full load.

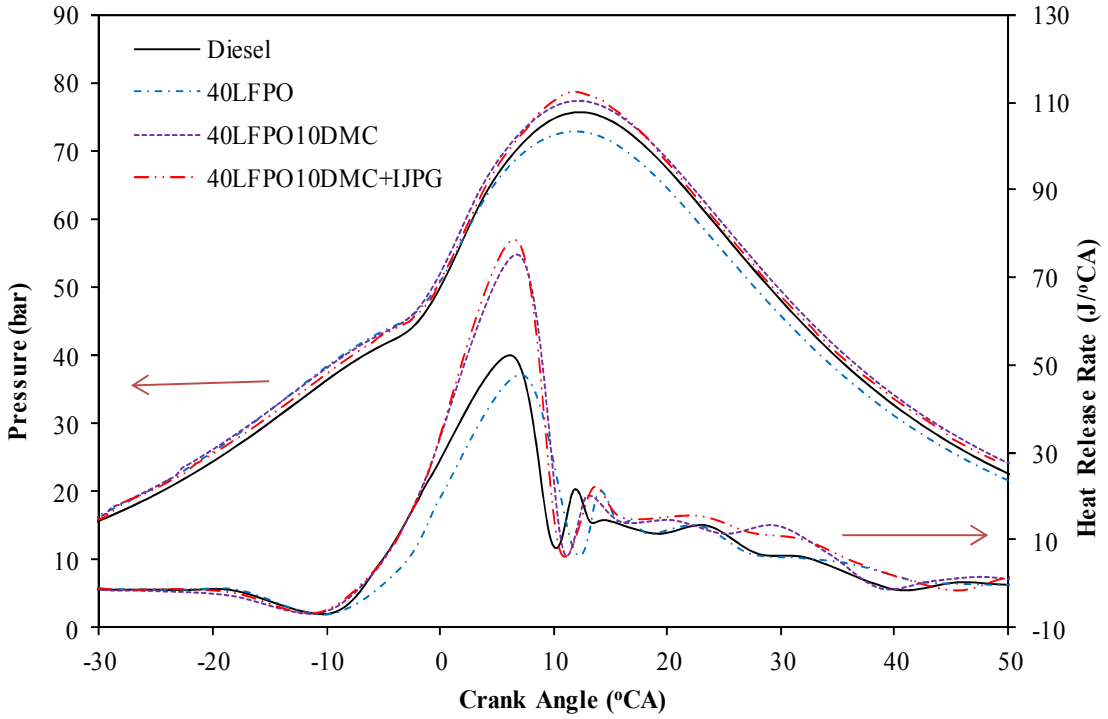

Figure 5.47: Variation of cylinder pressure and HRR with crank angle at full load

In the premixed combustion phase, the heat release rate is increased by the homogeneous air fuel mixture, volatility of the fuel, the availability of oxygen and better atomization in case of the 40LFPO10DMC+IJP. The high viscous fuel affects the spray formation and atomization of fuel during the ignition delay period. Hence, the heat release rate for 40LFPO is lower compared to that of the 40LFPO10DMC blend.

5.6.2.2 Ignition delay

The ignition delays of diesel, 40LFPO, 40LFPO10DMC and 40LFPO10DMC+IJP operations with brake power are depicted in Figure 5.47. The ignition delay decreases with the increase in the load which is due to the increase in the cylinder temperature. Generally, the ignition delay is reduced by increasing the factors such as, fuel cetane

number, fuel atomization, oxygen concentration, fuel quality and swirl motion etc. inside the combustion chamber. The ignition delay of 40LFPO is longer compared to that of diesel fuel and 40LFPO10DMC, with and without the internal jet piston, due to its lower cetane number.

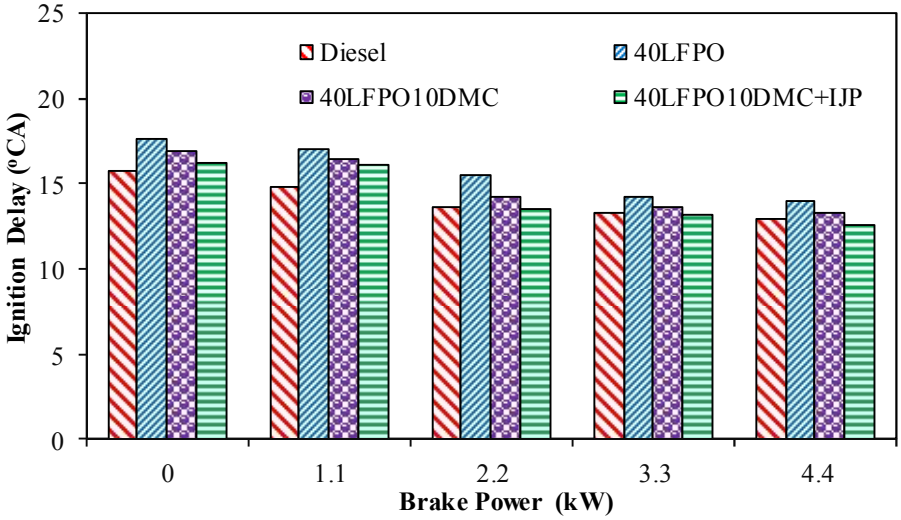

Figure 5.48: Ignition delay with brake power

The ignition delay of 40LFPO10DMC+IJP is the shortest and closer towards the diesel curve, because the blend has a lower viscosity, and the internal jet piston provides better air fuel mixture and fuel spray for a more complete combustion. Hu et al [155] have documented the similar reason by running the diesel engine fuel with dimethyl carbonate at high temperature. The values of the ignition delay for diesel, 40LFPO, 40LFPO10DMC and 40LFPO10DMC+IJP are about 12.9, 13.9, 13.2 and 12.5 ^{o}CA respectively at full load.

5.6.2.3 Combustion duration

Figure 5.48 shows variation of the combustion duration with brake power for diesel, 40LFPO, 40LFPO10DMC and 40LFPO10DMC+IJP. It can be observed from the figure that the combustion duration increases with an increase in the load. This is because as load increases the amount of fuel consumption increases and therefore, a longer time is required for the combustion of fuel. The combustion of the engine depends upon the air fuel mixture, availability of oxygen, etc. The combustion duration of 40LFPO is longer than that of diesel, because of its sluggish combustion. However, the combustion duration is shortened a little by adding DMC to 40LFPO.

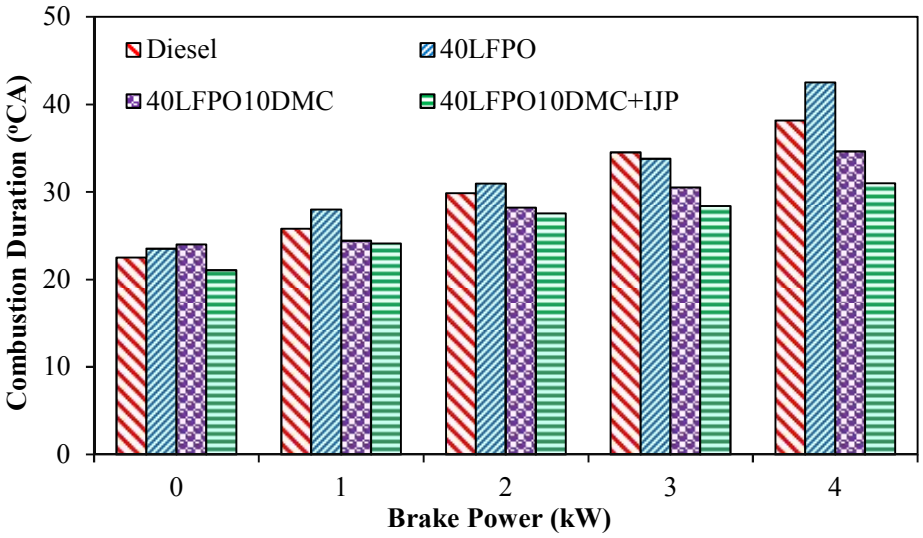

Figure 5.49: Variation of combustion duration with brake power

The combustion duration is shortened for 40LFPO10DMC with the internal jet piston. This may be due to a higher turbulent motion of air in the combustion chamber caused by the internal jets. The combustion duration of 40LFPO10DMC+IJP blend is about 31.41 ^{o}CA, which is the lowest among all the fuels tested in this study in the entire range of engine operation. The values of combustion duration of diesel, 40LFPO, 40LFPO10DMC and 40LFPO10DMC+IJP are about 38.1, 42.5, 34.60 and 31.01^{o}CA at full load, respectively.

5.6.2.4 Cylinder peak pressure

The trend of cylinder peak pressures with brake power for diesel, 40LFPO10DMC without and with turbulent inducement are depicted in Figure 5.49. It can be observed that the peak cylinder pressure increases with increase in brake power due to the consumption of more fuel at higher loads to meet the power requirements. The cylinder peak pressure for the 40LFPO blend is less than that of diesel because of the aromatic content present in the 40LFPO blend, which may affect during the premixed combustion phase. The other cause may be that 40LFPO has a lower heating value, lower cetane number and higher denser fuel compared to those of diesel fuel. The cylinder peak pressure of 40LFPO10DMC+IJP is found to be the highest in this study, which is 3.7% higher than that of diesel fuel and 7.73% higher than that of 40LFPO blend at full load.

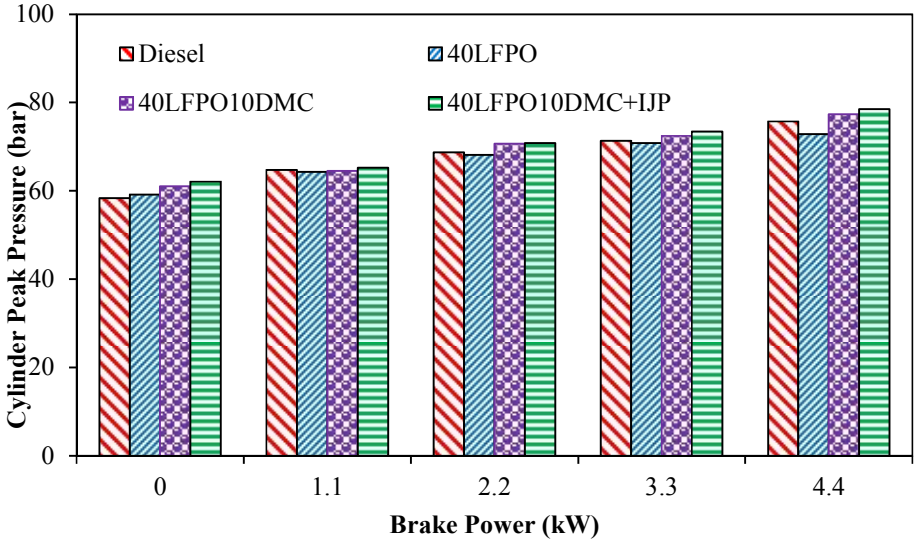

Figure 5.50: Variation of cylinder peak pressure with brake power.

The reason may be that 40LFPO10DMC+IJP has a higher heat release rate due to the homogeneous air fuel mixture and better fuel atomization by the turbulence air motion of the internal jets. Another reason may be that 40LFPO10DMC+IJP has a lower density, high oxygen concentration and higher volatility compared to that of diesel fuel, which shorten the ignition delay period of the fuel. The cylinder peak pressure values for diesel, 40LFPO, 40LFPO10DMC and 40LFPO10DMC+IJP are found to be about 75.70, 72.8, 77.4 and 78.50 bar at full load respectively.

5.6.3 Performance parameters

5.6.3.1 Brake thermal efficiency

Figure 5.50 depicts the variation of the brake thermal efficiency (BTE) with brake power. It can be observed from the figure that BTE increases with an increase in load due to more fuel being consumed. The brake thermal efficiency of 40LFPO blend is the lowest among all the operations, followed by diesel and 40LFPO10DMC at full load. The lowest brake thermal efficiency of the 40LFPO operation is due to its higher density and lower heating value compared to that of diesel and 40LFPO10DMC, which affect the spray formation for combustion. The brake thermal efficiency of 40LFPO10DMC with the internal jet piston is increased by about 4.5 and 5.3% over that of diesel fuel and 40LFPO blend respectively, at full load. This may be due to the higher turbulence motion of air in the combustion chamber offered by the internal jets, which leads to a better mixture formation of 40LFPO10MC [212]. Rajan and Senthil kumar [176, 177] have also reported similar reason by investigating the characteristics of a diesel engine

with internal jet piston using biodiesel. The brake thermal efficiency values of diesel, 40LFPO, 40LFP10DMC and 40LFP10DMC+IJP are about 32.47, 31.71, 33.01 and 37.03% respectively at full load.

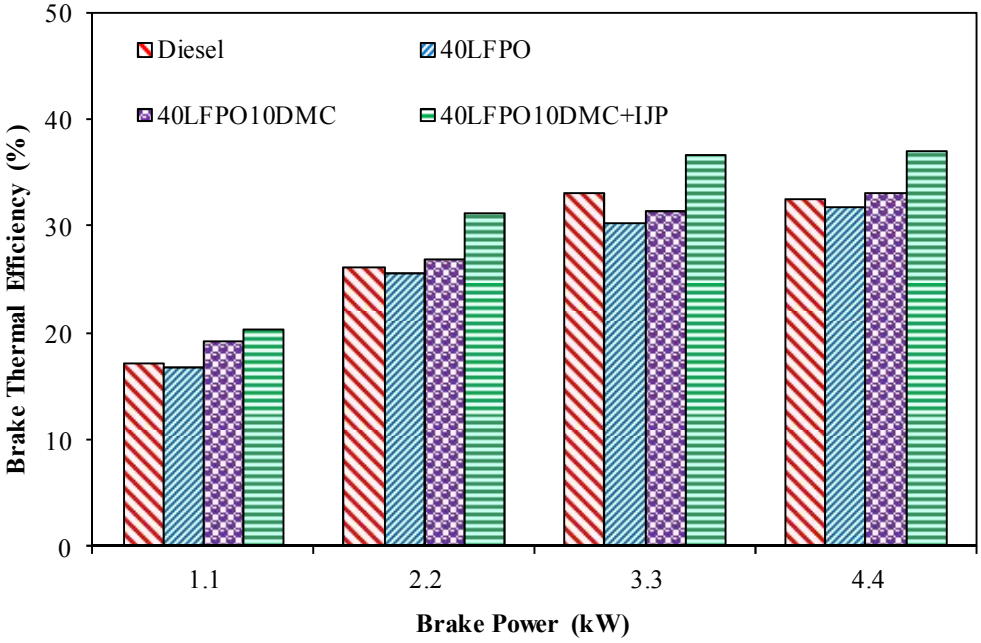

Figure 5.51: Variation of brake thermal efficiency with brake power

5.6.3.2 Exhaust gas temperature

Figure 5.51 illustrates the variation of the exhaust gas temperature (EGT) for the diesel, 40LFPO and 40LFPO10DMC operations, when the engine was run with and without the internal jet piston. It can be observed from the figure that the EGT increases with load, which is due to the increase in the fuel consumption. The EGT of 40LFPO10DMC declined with the internal jet piston. The EGT of 40LFPO10DMC+IJP is reduced by about 8.9 and 9.2% over that of diesel fuel and the 40LFPO blend respectively. This may be due to more complete combustion resulting from a better air fuel mixing and the presence of oxygen in the DMC. The EGT values of diesel, 40LFPO, 40LFPO10DMC and 40LFPO10DMC+IJP are about 338.5, 339.2, 320.7 and 308.0 ^{o}C at full load, respectively.

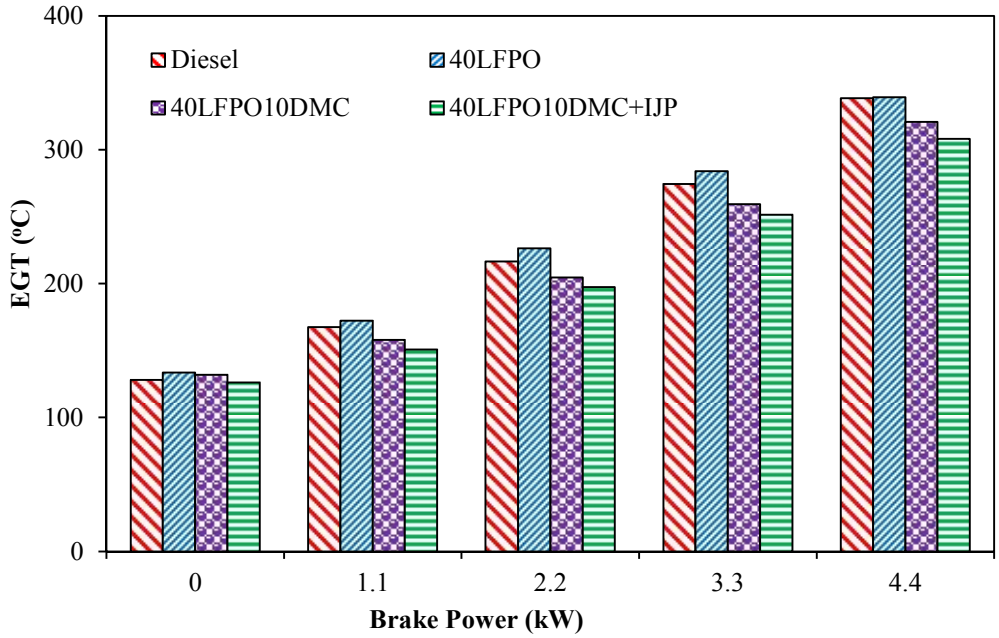

Figure 5.52: Variation of EGT with brake power

5.6.4 Emission parameters

5.6.4.1 Hydrocarbon emission

The hydrocarbon emission (HC) from a diesel engine is primarily influenced by the fuel quality and the oxygen available for complete combustion.

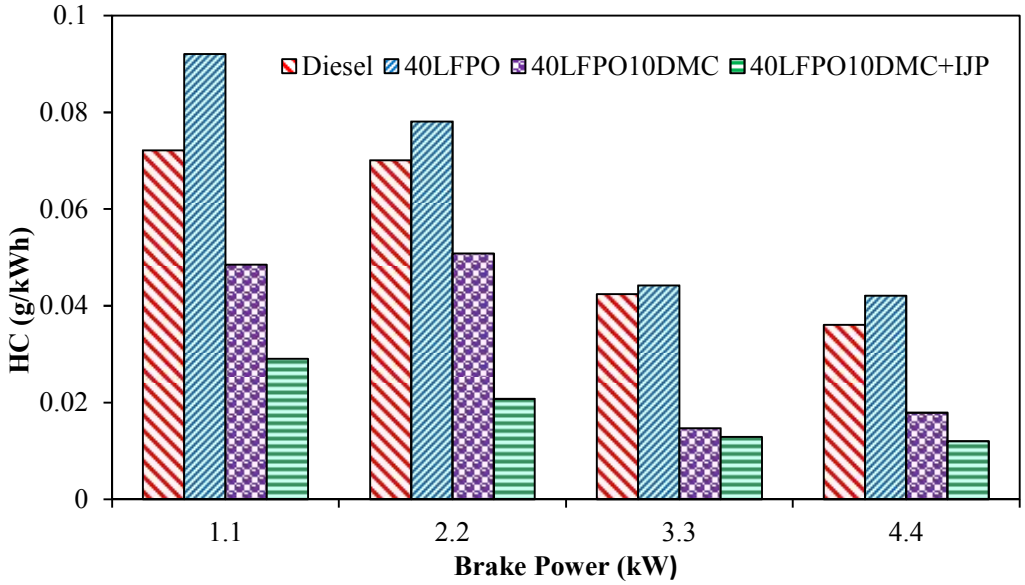

Figure 5.53: Variation of hydrocarbon with brake power

Figure 5.52 depicts the variation of HC emission with brake power when the engine was operated on diesel, 40LFPO, 40LFPO10DMCand 40LFPO10DMC+IJP. The HC emission for the 40LFPO blend is the highest among all the operations in this

investigation. Poor mixture formation is the reason for the higher HC emission. With the 40LFPO blend, the HC concentration ranges from 0.0420 at no load to 0.092 g/kWh at full load operation. The HC emission for the 40LFPO10DMC blend is reduced by about 57% over that of 40LFPO, which is due to the high oxygen concentration, higher volatility and lower density compared to the 40LFPO blend. It can also be observed that the HC emission for 40LFPO10DMC+IJP is the lowest among all the tested fuels in this investigation. The reason may be that the internal jet piston provides the turbulence in air motion inside the combustion chamber, which helps to develop a homogeneous air fuel mixture resulting in complete combustion [213]. The HC emission for 40LFPO10DMC+IJP is lower by about 32.9% compared to that of the 40LFPO10DMC blend at full load operation. The HC emission of 40LFPO10DMC+IJP is the lowest in this study, and they are 66.6% lower compared to that of diesel and 71.4% lower compared to that of 40LFPO. The HC emissions for diesel, 40LFPO, 40LFPO10DMC and 40LFPO10DMC+IJP are about 0.036, 0.04, 0.018 and 0.012 g/kWh at full load respectively.

5.5.4.2 Carbon monoxide emission

Figure 5.53 portrays the variation of carbon monoxide with brake power for diesel, and 40LFPO10DMC without and with turbulent inducement.

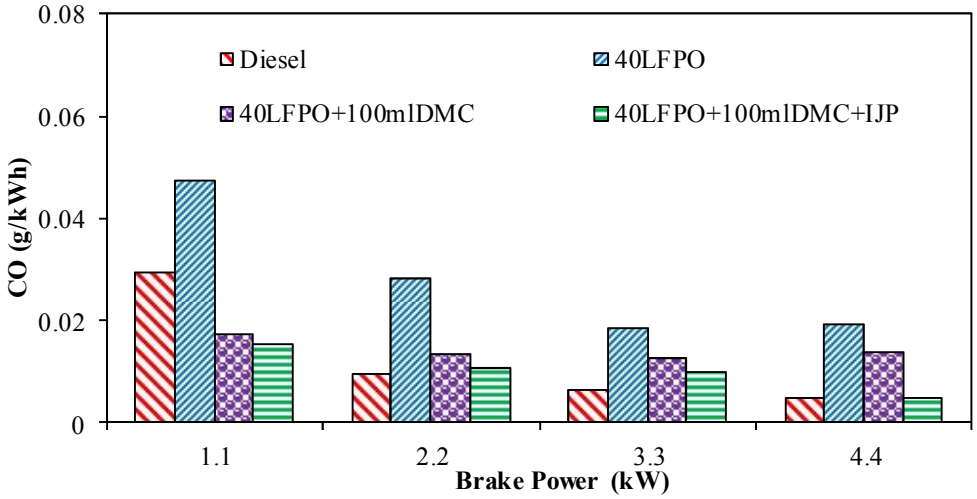

Figure 5.54: Variation of carbon monoxide with brake power

The CO emission for the 40LFPO blend is the highest among all the fuels tested in this study. This is due to the less availability of oxygen and poorer fuel air mixture formation. The CO emission of 40LFPO10DMC+IJP is the lowest in this study. This is due to the 40LFPO10DMC+IJP blend's fast burning compared to the other fuels tested in this

study. The other reason may be that the DMC provides the oxygen and the turbulent motion by the internal jet helps the homogeneous air-fuel mixture inside the combustion chamber, which leads to complete combustion [213]. The CO emissions for 40LFPO10DMC+IJP is about the 2.2, 75 and 66% lower compared to those of diesel, 40LFPO and 40LFPO10DMC at full load respectively.

5.6.4.3 Carbon dioxide emission

Figure 5.54 shows the variation of carbon dioxide (CO_2) with brake power. The CO_2 emission for 40LFPO10DMC with the internal jet piston is increased by about 16.68% with the base engine operation at full load.

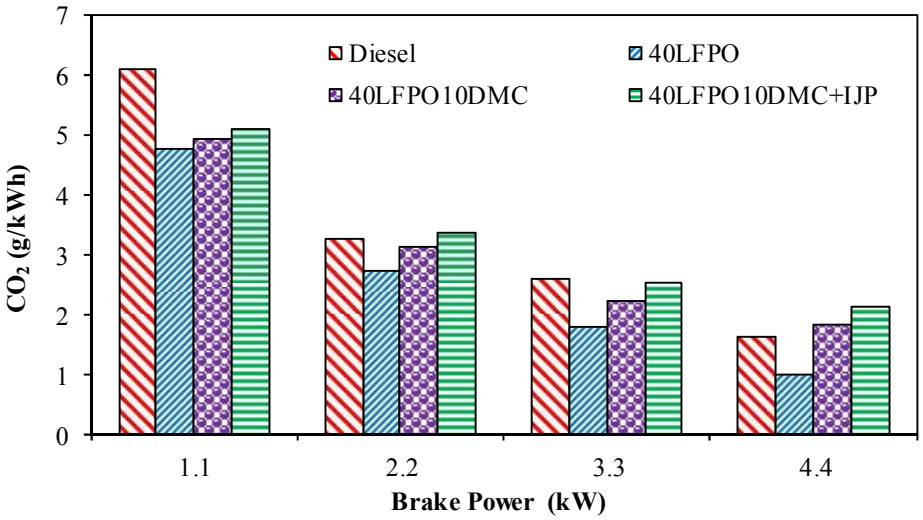

Figure 5.55: Variation of carbon dioxide with brake power

It can be observed from the figure that the 40LFPO blend exhibited lower CO_2 emission among all the test fuels in this study. This is because of its higher density, poor volatility and physicochemical properties. It can be observed that CO_2 emission for the 40LFPO10DMC+IJP is the highest among all the test fuel conditions and increased by about 16.7% from the engine run without the internal jet piston. This is because DMC provides higher oxygen and better air fuel mixture developed by the internal jet turbulence motion of the piston. The CO_2 emission values for diesel, 40LFPO, 40LFPO10DMC and 40LFPO10DMC+IJP are about 1.62, 0.95, 1.80 and 2.07 g/kWh at full load, respectively.

5.6.4.4 Nitric oxide emission

The variation of nitric oxide (NO) emission with brake power for the fuels tested in this study is illustrated in Figure 5.55. It can be observed from the figure that the diesel

operation exhibits the highest NO emission in this study. The reason may be its higher combustion temperature as a result of more complete combustion compared to those of 40LFPO and 40LFPO10DMC blends, which affect the ignition delay and enhance the heat release rate of the combustion chamber [176].

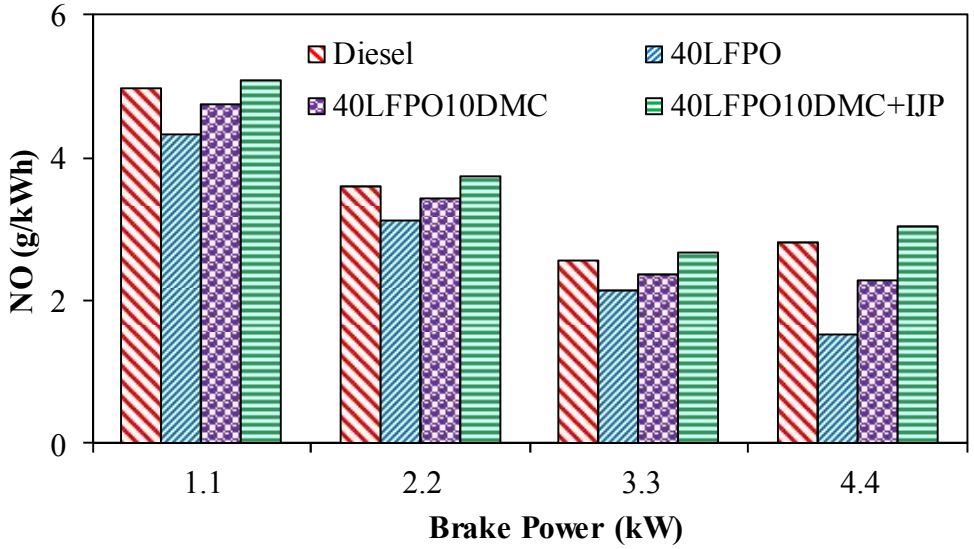

Figure 5.56: Variation of nitric oxide with brake power.

The NO emission for 40LFPO10DMC with the internal jet piston is higher by about 7.5% compared to that of diesel fuel operation at full load. The NO emission for the 40LFPO10DMC+IJP blend is the highest among the 40LFPO and 40LFPO10DMC blends. This is due to the higher combustion temperature among the 40LFPO and 40LFPO10DMC blends. The other reason may be a shorter ignition delay compared to the 40LFPO and 40LFPO10DMC blends. The NO emissions for diesel, 40LFPO, 40LFPO10DMC and 40LFPO10DMC+IJP are about 2.82, 1.52, 2.28 and 3.03 g/kWh respectively at full load.

5.6.4.5 Smoke emission

Figure 5.56 illustrates the variation of smoke emission with brake power for the fuels tested in this study. With an increase in the load, the air fuel ratio decreases as the fuel injection increases and hence, results in higher smoke emission [183].

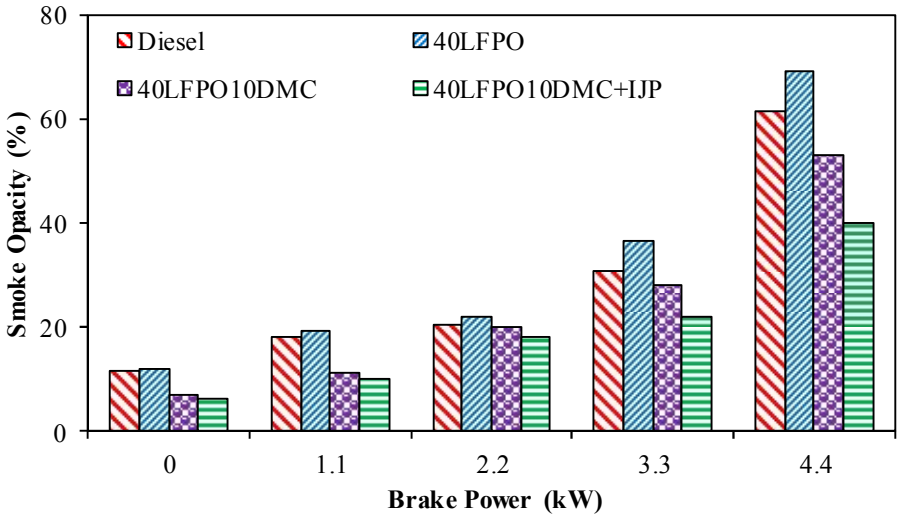

Figure 5.57: Variation of smoke emission with brake power

The values of the smoke emission for the diesel, 40LFPO, 40LFPO10DMC and 40LFPO10DMC+IJP operations are about 61.2, 69.2, 53 and 40% respectively, at full load operation. The smoke emission for 40LFPO is the highest in the entire range of engine operation because it has higher density, higher aromatic content and lower oxygen concentration. By adding 10% DMC with 40LFPO, the smoke emission is reduced by about 16.2% because of better combustion than that of 40LFPO. The smoke emission with the internal jet piston for the 40LFPO10DMC operation is lower by about 32.5% in comparison with the base engine operation at full load condition. This may be due to more complete combustion offered by the turbulent air motion of the internal jets inside the piston crown for better fuel atomization [214]. The smoke emission for 40LFPO10DMC+IJP is the lowest among all the tested fuels in this study and 21.2% lower compared to that of diesel fuel at full load.

5.6.5 Summary

The performance, combustion and emission characteristics of the test engine run on the 40LFPO10DMC blend, with and without an internal jet piston, were evaluated, analyzed and compared to those of diesel and 40LFPO blend operations. The important points noted in the present investigation are listed below.

- The BTE obtained for 40LFPO10DMC with the internal jet piston is increased by about 4.02% compared to that of base engine operation at full load. The BTE of 40LFPO10DMC with the internal jet piston has increased by about 4.5% compared

to that of diesel fuel, and by about 5.3% compared to that of the 40LFPO blend at full load.

- The values of ignition delay for diesel, 40LFPO, 40LFPO10DMC and 40LFPO10DMC+IJP are about 12.9, 13.9, 13.2 and 12.5^{o}CA respectively at full load.
- The 40LFPO10DMC+IJP blend shows a HRR of about 78.5 J/^{o}CA at full load which is the highest in this investigation.
- The combustion duration for the 40LFPO10DMC blend with the internal jet piston has decreased by about 10.4% compared to the base engine operation at full load.
- The NO emission for the 40LFPO10DMC+IJP operation is higher than that of all the fuels in this study and 21.3% lower compared to that of diesel fuel at full load.
- The smoke emission for the engine run with the internal jet piston for 40LFPO10DMC is about 13% lower compared to that of the base engine operation. The smoke emission for 40LFPO10DMC+IJP is the lowest among all the tested fuels in this study and 21.2% lower compared to that of diesel fuel at full load operation.

Table 5.6 gives the summary of the values of some of the important parameters of the engine run under 40LFPO10DMC+IJP condition in comparison to the diesel at full load.

Table 5.6: Values of some of the important parameters of the engine run on diesel, 40LFPO, 40LFPO10DMC and 40LFPO10DMC+IJP at full load.

Sl No	Parameter	Diesel	40LFPO	40LFPO10 DMC	40LFPO10D MC+IJP
	Combustion parameters				
1	Maximum cylinder pressure (bar)	75.7	72.9	77.4	78.8
2	Maximum heat release (J/^{o}CA)	52	47.63	75.08	78.50
3	Ignition delay (^{o}CA)	12.9	14.4	13.2	12.5
4	Occurrence of maximum pressure (^{o}CA)	370.4	372.8	372	372.58
5	Combustion duration (^{o}CA)	38.1	42.50	34.6	31.01
	Performance parameters				
6	Brake thermal efficiency (%)	32.47	31.71	33.01	37.03
7	Exhaust gas temperature (^{o}C)	338.5	339.20	320.71	308.0
	Emission parameters				
8	HC emission (g/kWh)	0.036	0.042	0.017	0.012
9	CO emission (g/kWh)	0.0048	0.019	0.009	0.005
10	NO emission (g/kWh)	2.8	1.52	1.85	3.03
11	Smoke opacity (%)	61.2	69.2	53.0	40

5.7 Effect of Exhaust Gas Recirculation

5.7.1 General

In the previous section, it is seen that with the addition of 10% DMC to the 40LFPO blend, and with the incorporation of internal jet piston in the engine, gave better results in terms of performance, combustion and emissions compared to all the other blends studied. However, the NO_x was noticed higher, when turbulence was induced due to engine modification in the form of internal jet piston. The exhaust gas recirculation technique was further used in the investigation to reduce NO emission. During this investigation, four exhaust gas recirculation (EGR) rates (10%, 20%, 30%, and 40%) were used with an intention to reduce the NO emission of the engine run on 40LFO10DMC. The designations of different fuel and engine modifications adopted in this study are given below:

a) 40LFPO (40% LFPO + 60% Diesel, unmodified engine, no EGR)
b) 40LFPO10DMC+IJP = M (40% LFPO + 10% DMC + 50% Diesel, engine modification with internal jet piston
c) M+10EGR (40LFPO10DMC fuel, IJP engine, 10% EGR)
d) M+20EGR (40LFPO10DMC fuel, IJP engine, 20% EGR)
e) M+30EGR (40LFPO10DMC fuel, IJP engine, 30% EGR)
f) M+40EGR (40LFPO10DMC fuel, IJP engine, 40% EGR)

The engine behavior in terms of the performance, combustion and emission parameters of the engine run on these different EGR rates were evaluated and compared with those of diesel operation in the same engine, and presented in this investigation.

5.7.2 Performance parameters

5.7.2.1 Specific fuel consumption

The variations of specific fuel consumption with brake power are depicted in Figure 5.57. It can be observed from the figure that the SFC decreases with increase in load. Because, less energy from the fuel is required at full load compared to no load, due to the increased cylinder temperature at full load. The similar reason was also documented by Kumar et al [215] when they run the diesel engine using poon oil-based fuels. The SFC of 40LFPO blend is higher at all loads among the diesel and 40LFPO10DMC+IJP, the reason of which may be that the density of 40LFPO is higher compared to that of diesel and

40LFPO10DMC+IJP, which affect the mixture of air fuel ratio and fuel spray characterization.

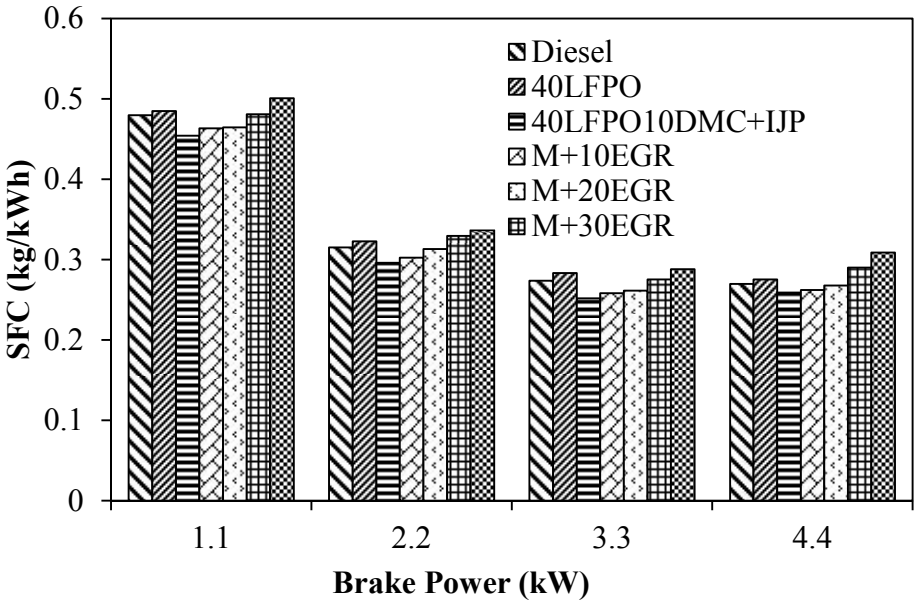

Figure 5.58: Variation of specific fuel consumption with brake power

It can also be observed from the figure that the SFC of 40LFPO10DMC+IJP is the lowest among all the fuels tested in this present study. The reasons are effect of DMC and IJP, where DMC provides oxygen and IJP helps in achieving more homogeneous air fuel mixture. The SFC of diesel and 40LFPO10DMC+IJP with different EGR rates are not significant at different loads, but 40LFPO10DMC+IJP with increasing EGR rates are increased compared to all tested fuels. This may be reduction in cylinder temperature by the EGR dilution [215, 216]. At full load, the SFC for diesel, 40LFPO, 40LFPO10DMC+IJP, M+10EGR, M+20EGR, M+30EGR and M+40EGR are about 0.269, 0.275, 0.258, 0.262, 0.267, 0.289 and 0.308 kg/kWh respectively. Up to 20%, the SFC is less or close to diesel fuel consumption. By increasing the EGR beyond 20%, the SFC increases. Although the thermal energy shared by the exhaust gas to the fresh charge is higher, in case of 30% EGR with the fresh air, more dilution of EGR increases SFC.

5.7.2.2 Brake thermal efficiency

The variations of brake thermal efficiency (BTE) for diesel, 40LFPO, 40LFPO10DMC without and with different values of EGR with brake power are depicted in Figure 5.58. It can be observed from the figure that the BTE increases with increase in load. The high cylinder temperature causes higher BTE. It can also be observed from the figure that the BTE of 40LFPO blend is the lowest among all the tested fuels. The reason may be more

aromatic content present in the blend fuel, which is a cause for incomplete combustion. Again, this figure shows that the BTE of 40LFPO10DMC+IJP is the highest among the all tested fuels, which is due to swirled motion by IJP and complete combustion.

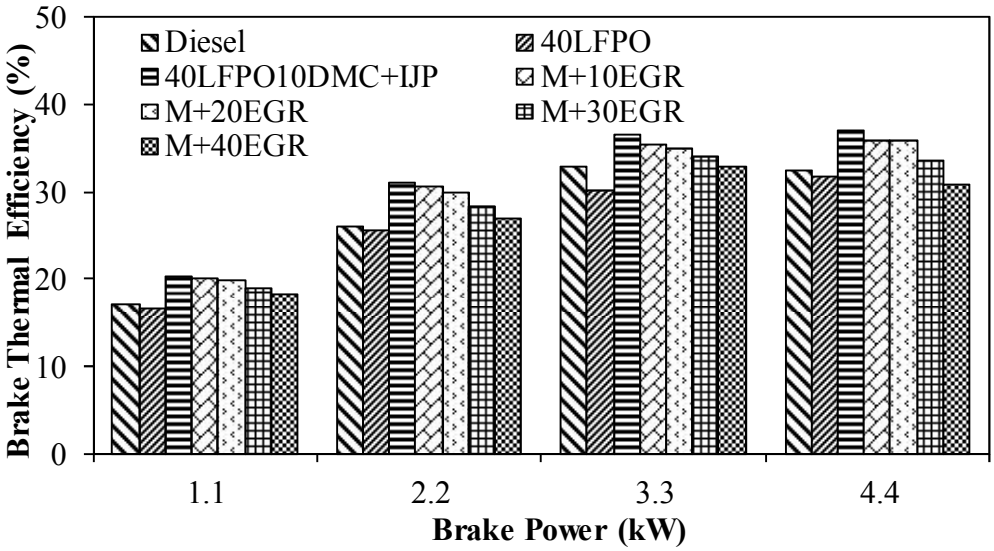

Figure 5.59: Variation of brake thermal efficiency with brake power

The BTE of diesel, 40LFPO, 40LFPO10DMC+IJP, M+10EGR, M+20EGR, M+30EGR and M+40EGR are about 32.5, 31.7, 37.0, 36.01, 35.8, 33.7 and 30.8% at full load respectively. It can be observed from figure that the brake thermal efficiency decreases with the addition of EGR rate with the 40LFPO10DMC+IJP. The reason may be the increase in incomplete combustion by decreasing the oxygen concentration in the combustion chamber. Can et al [217] have reported similar results by investigating the effect of EGR application on the combustion and exhaust emissions in a diesel engine with soybean biodiesel fuel.

5.7.3.3 Exhaust gas temperature

Figure 5.59 illustrates the variations of the exhaust gas temperature (EGT) with brake power for diesel, and 40LFPO10DMC+IJP with different EGR rates. The EGT increases with increase in load, as a result of increase in the fuel consumption. It can be observed from the figure that EGT of 40LFPO is the highest among all tested fuels. Longer ignition delay and poor volatility of LFPO take more time for combustion and maximum HRR occurs away from the TDC. So, here all heat energy cannot convert into the useful work. The EGTs of diesel, 40LFPO, 40LFPO10DMC+IJP, M+10EGR, M+20EGR, M+30EGR and M+40EGR are about 338.4, 339.2, 308.0, 303.0, 301.4, 295.3 and 290.1^{o}C at full load

respectively. It can also be seen that while increasing the EGR flow rate, the EGT is decreased throughout the load. The reason may be the result of peak combustion temperature reduction and the effect of cold EGR. Similar reason is mentioned by Kumar and Saravanan [178] for the results they obtained from a diesel engine run with pentanol/diesel blends with EGR.

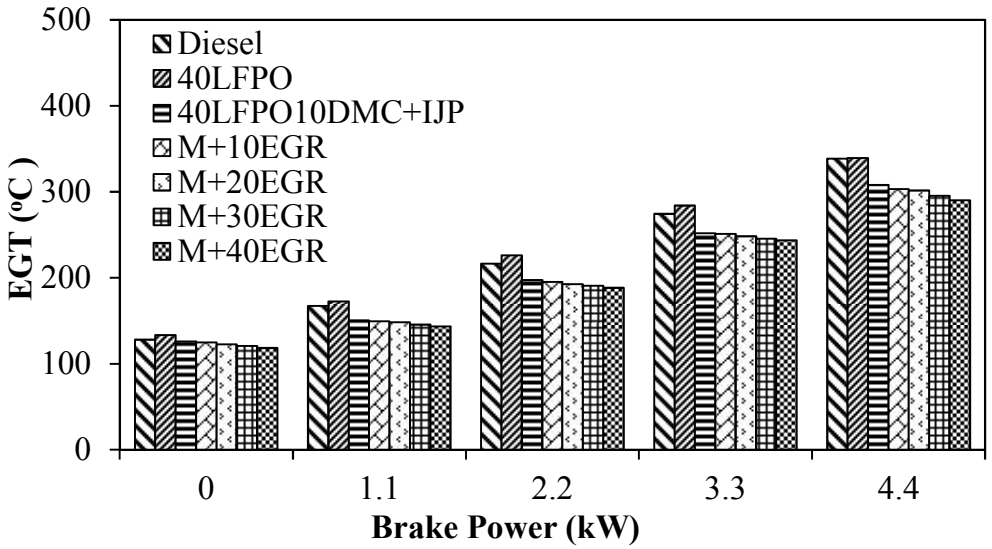

Figure 5.60: Variation of EGT with brake power

5.7. 3 Combustion parameters

5.7.3.1 Cylinder pressure and heat release rate

Figure 5.60 shows the variations of the cylinder pressure and heat release rate with respect to the crank angle for diesel, 40LFPO, 40LFPO10DMC+IJP, M+10EGR, M+20EGR, M+30EGR and M+40EGR at full load condition. It can be observed from the figure that the 40LFPO10DMC+IJP blend has the highest peak cylinder pressure, which is about 78.4 bar in this investigation compared to all tested fuels studied in this investigation. This is because DMC has oxygen and better air fuel mixing provided by the internal jet piston for complete combustion. The cylinder peak pressures for the 40LFPO, 40LFPO10DMC+IJP, M+10EGR, M+20EGR, M+30EGR and M+40EGR are about 72.9, 78.8, 77.8, 77.0, 73.8 and 69.8 bar respectively. The cylinder pressure of the combustion chamber marginally reduces by adding higher percentage EGR to the combustion chamber. Similar reason was reported by Can et al [217] for the results they obtained by combined effects of soybean biodiesel fuel addition and EGR application on the combustion and exhaust emissions in a diesel engine. The peak cylinder pressure declined because of the introduction of cold EGR to the combustion chamber. The reason may be that specific heat of air-fuel mixture

is higher for combustion due to cold EGR. Similar reason was reported by Abdelaal and Hegab [218] for the results they obtained by combustion and emission characteristics of a natural gas-fuelled diesel engine with EGR. The other reasons may be reduced availability of oxygen content and deteriorated combustion with high EGR flow rates. Similar reason was reported by Zhao et al [219] for the results they obtained by ccombustion and emission characteristics of a DME (dimethyl ether)-diesel dual fuel premixed charge compression ignition engine with EGR.

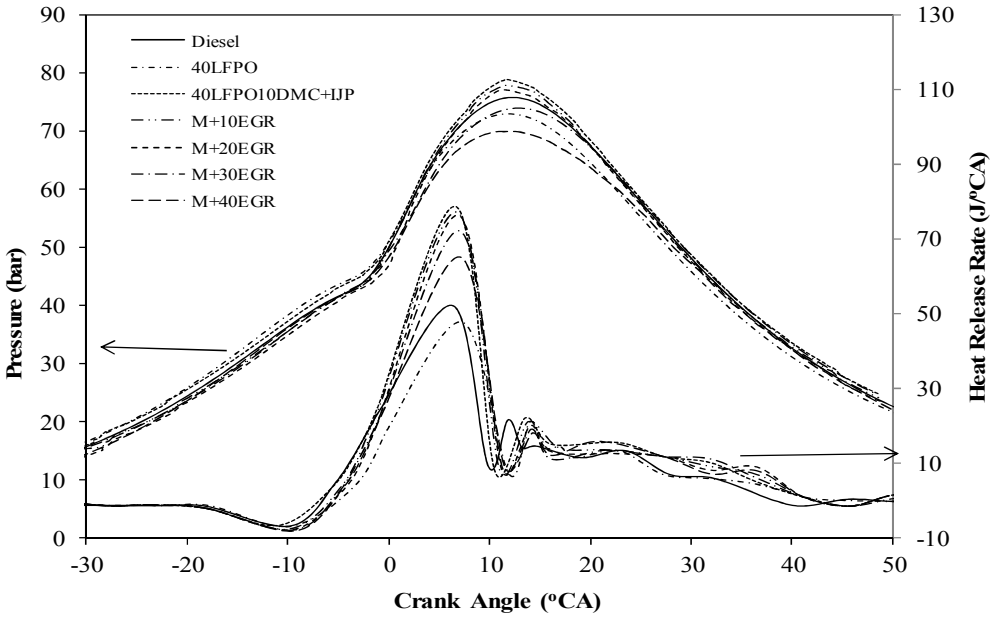

Figure 5.61: Variation of cylinder pressure and HRR with crank angle at full load

It can be observed from Figure 5.60 that 40LFPO10DMC+IJP blend has maximum HRR about 78.5 J/^{o}CA compared to the other tested fuels. The heat release rate is increased by the homogeneous air fuel mixture, volatility of the fuel, the availability of oxygen and better atomization of the 40LFPO10DMC+IJP operation. The maximum HRRs for diesel, 40LFPO, 40LFPO10DMC+IJP, M+10EGR, M+20EGR, M+30EGR and M+40EGR are found to be 50.8, 47.6, 78.5, 77,76.2, 72 and 65 J/^{o}CA respectively at full load. By increasing the EGR flow rate, the HRR is decreased. The cold EGR enters into the combustion chamber, which increases the specific heat of air fuel mixture and decreases the oxygen availability inside the combustion chamber, and results in incomplete combustion. This reason can be supported by the reasons indicated by Zhao et al and Lattimore et al [219, 220]. Also, the ignition delay increases due to the presence of the inert gas of EGR and decreases the oxygen concentration. More amount of fuel is

accumulated with the EGR dilution that affects the combustion of the engine. This reason can be supported Figure 5.60 that HRR and cylinder pressure also marginally decline with the lower EGR flow rate.

5.7.3.2 Ignition delay

The ignition delay for the diesel, 40LFPO 40LFPO10DMC+IJP, M+10EGR, M+20EGR, M+30EGR and M+40EGR in different engine operating conditions are depicted in Figure 5.61.

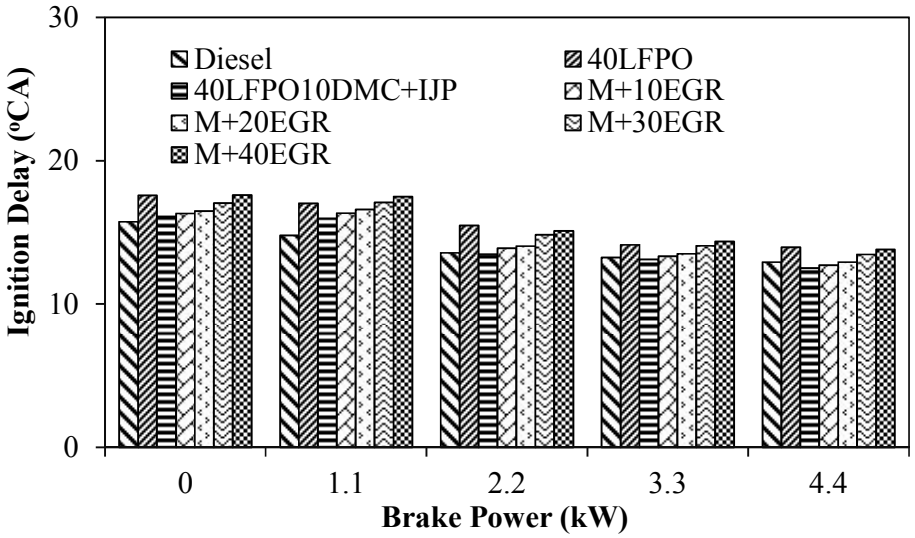

Figure 5.62: Ignition delay with brake power

It can be observed from the figure that the ignition delay decreases with the increase in the load which is due to the increase in the cylinder temperature. It can also be observed that the 40LFPO blend has a higher ignition delay at all loads compared to the fuels tested in the present study. This is due to the lower cetane number compared to diesel fuel and higher density among the all tested fuels. The ignition delay of 40LFPO10DMC+IJP is found to be the shortest among all the fuels studied in this investigation at full load, because IJP provides a good air fuel mixture and there is no EGR dilution in the combustion chamber. The ignition delays of 40LFPO10DMC+IJP with different EGR rates are increased. The reason may be that the oxygen supply is replaced by CO_2 and cold EGR causes delay in ignition of air fuel mixture [221]. The values of ignition delay for diesel, 40LFPO, 40LFPO10DMC+IJP, M+10EGR, M+20EGR, M+30EGR and M+40EGR are about 12.9, 14.4, 12.5, 12.7, 12.9, 13.5 and 13.8^{o}CA respectively at full load.

5.7.3.3 Combustion duration

The variations of combustion duration for diesel, 40LFPO, 40LFPO10DMC+IJP without and with EGR flow rates are depicted in Figure 5.62. It can be observed from the figure that the combustion duration increases with increase in load. This is because more amount of fuel accumulated with increasing load and took more time for combustion.

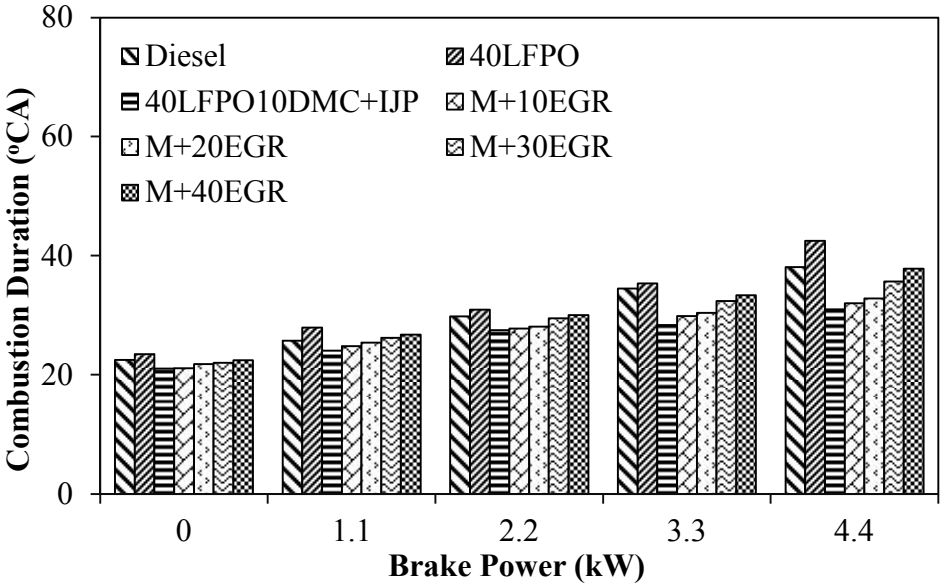

Figure 5.63: Variation of combustion duration with brake power

It can also be observed that combustion duration of 40LFPO is the highest among all the fuels tested at all loads. The reason is presence of aromatic hydrocarbons in 40LFPO, which have higher boiling point temperature for combustion, and another reason may be poor atomized character because of high density fuel. The slow combustion, as a result of poor mixture formation of 40LFPO, leads to a longer combustion duration. The combustion duration for the 40LFPO10DMC+IJP blend is the lowest among all the tested fuels. This may be because the density and viscosity of DMC are lower compared to that of other LFPO based fuels, and it also provides the oxygen. Better fuel spray leads to homogeneous air/fuel mixture that provides a faster combustion. The combustion duration of 40LFPO10DMC+IJP with EGR is increased with the increase in EGR flow rate. The reason may be that EGR introduces inert gas at low temperature into the combustion chamber, which will take little more time to get ignited to the fresh air. Similar results were indicated by Kumar and Saravanan [178]. The values of combustion duration of diesel, 40LFPO, 40LFPO10DMC+IJP, M+10EGR, M+20EGR, M+30EGR and M+40EGR are about 38.1, 42.5, 31.0, 32.0, 32.8, 35.7 and 37.8^{o}CA at full load respectively.

5.7.3.4 Peak cylinder peak pressure

Figure 5.63 depicts the trend of cylinder peak pressure for diesel, 40LFPO, and 40LFPO10DMC+IJP without and with EGR.

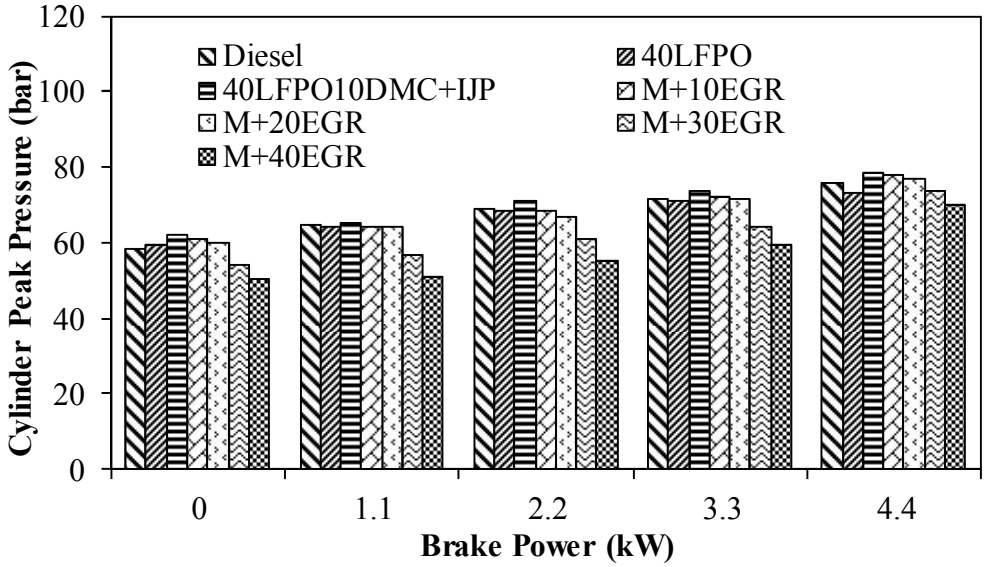

Figure 5.64: Variation of cylinder peak pressure with brake power

It can be observed from the figure that cylinder peak pressure increases with load. The reason may be that more amount of fuel is accumulated at full load, which enhances the cylinder temperature. The peak pressure of 40LFPO is lower due to poor mixture formation as a result of higher viscosity. The peak cylinder pressure of 40LFPO10DMC+IJP blend is the highest compared to all tested fuels. This is because the oxygenated additive DMC, which is highly volatile and it helps for homogeneous air fuel mixture. The reason may be the availability of oxygen content, which gives the better reaction with fuel and enhances the combustion. The IJP also provides the swirl motion, which helps for complete combustion, resulting in higher cylinder peak pressure for 40LFPO10DMC+IJP blend. The cylinder peak pressures of 40LFPO10DMC+IJP with various cold EGR flow rates are decreased. The reason is that latent heat of combustible air fuel mixture is higher, because cold EGR affects the combustion. The cylinder peak pressure values for diesel, 40LPFO, 40LFPO10DMC+IJP, M+10EGR, M+20EGR, M+30EGR and M+40EGR are found to be about 73.2, 72.9, 78.8, 77.8, 77.0, 73.8 and 69.8 bar respectively at full load.

5.7.4 Emission parameters

5.7.4.1 Hydrocarbon emission

Figure 5.65 depicts the variation of hydrocarbon (HC) emission with brake power for different fuel and engine modifications performed in this study, when 40LFPO was used as an alternative fuel. The HC emission for the 40LFPO blend is the highest among all the fuels tested in this study. The poor mixture formation is the reason for the higher HC emission. With the 40LFPO blend, the HC concentration ranges from 0.036 at no load to 0.037 g/kWh at full load operation.

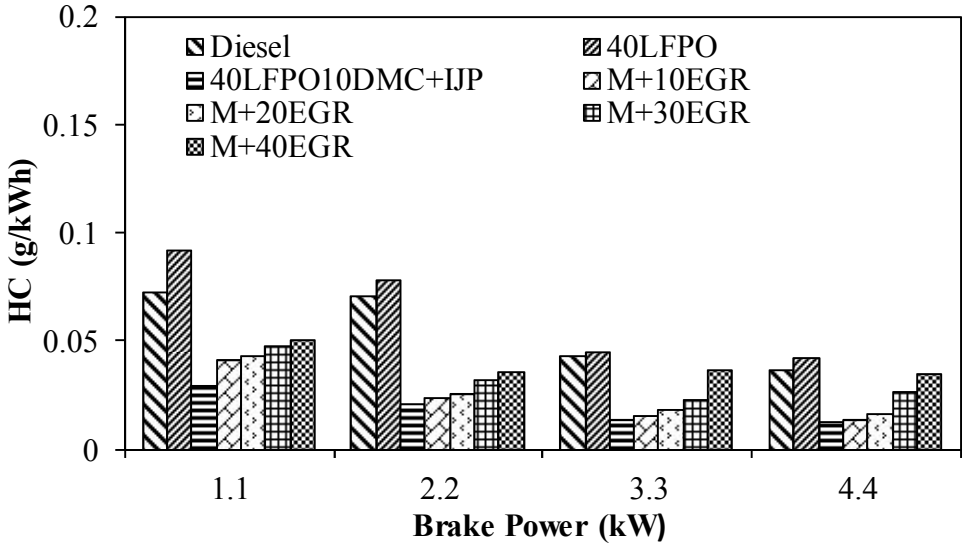

Figure 5.65: Variation of hydrocarbon with brake power

The HC emission for the 40LFPO10DMC+IJP with different EGR rates, increases and the reason may be more incomplete combustion in the combustion chamber by the inert gas of EGR. Similar reason was reported by Rajesh kumar and Saravanan [178] for the results they obtained by studying the effect of exhaust gas recirculation on performance and emissions of a constant speed DI diesel engine fuelled with pentanol/diesel blends. The HC emissions for diesel, 40LFPO, 40LFPO10DMC+IJP, M+10EGR, M+20EGR, M+30EGR and M+40EGR are about 0.036, 0.042, 0.012, 0.013, 0.015, 0.025 and 0.034 g/kWh at full load respectively.

5.7.4.2 Carbon monoxide emission

The trends of CO emission with brake power for diesel, 40LFPO, 40LFPO10DMC+IJP without and with EGR flow rates are depicted in Figure 5.66.

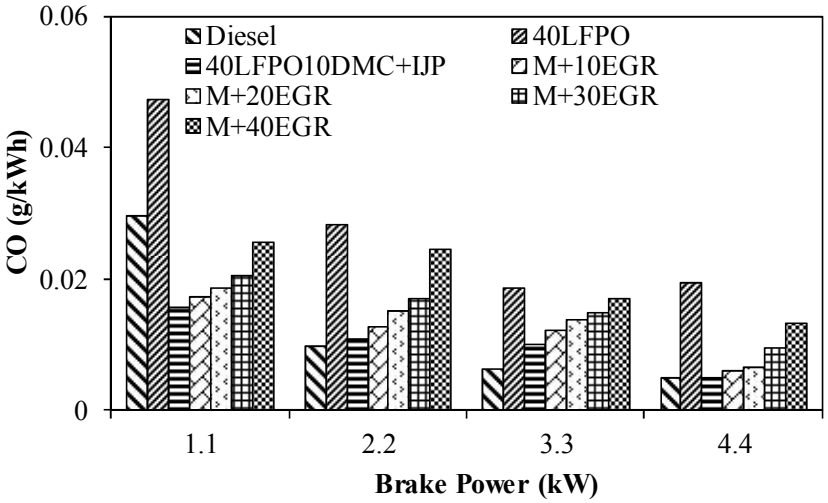

Figure 5.66: Variation of carbon monoxide with brake power

It can be observed that, as the load increases the CO emission decreases. The CO emission for 40LFPO is the highest among all the fuels tested in this study. The reason may be higher velocity among all fuels, which leads to incomplete combustion. However, the addition of oxygenated additive DMC to the 40LFPO-diesel blends results in reduced CO emission, which is due to availability of more oxygen for combustion than in 40LFPO. Introduction of EGR prevents CO oxidation due to lower oxygen concentration and as a result, CO emission marginally increases with the increase in EGR rates as seen in Figure 5.66. The CO emissions for diesel, 40LFPO, 40LFPO10DMC+IJP, M+10EGR, M+20EGR, M+30EGR and M+40EGR are about 0.0048, 0.0192, 0.0047, 0.0058, 0.00631, 0.0093 and 0.0130 g/kWh at full load respectively.

5.7.4.3 Carbon dioxide emission

The trends of CO_2 emission with brake power for diesel, 40LFPO, 40LFPO10DMC+IJP without and with EGR flow rates are depicted in Figure 5.67. It is apparent from figure that the CO_2 emission is marginally increased with increase in the EGR flow rate. This is because EGR mainly consists of CO_2 and H_2O, and at higher engine load, the percentage of CO_2 in EGR becomes higher [216, 222]. The CO_2 emissions for diesel, 40LFPO, 40LFPO10DMC+IJP, M+10EGR, M+20EGR, M+30EGR and M+40EGR are about 1.612, 0.96, 2.10, 2.30, 2.38, 2.756 and 2.99 g/kWh at full load respectively. The CO_2 emission with different EGR flow rates such as M+10EGR, M+20EGR, M+30EGR and M+40EGR are increased about 42, 47, 70 and 85% compared to diesel fuel operation.

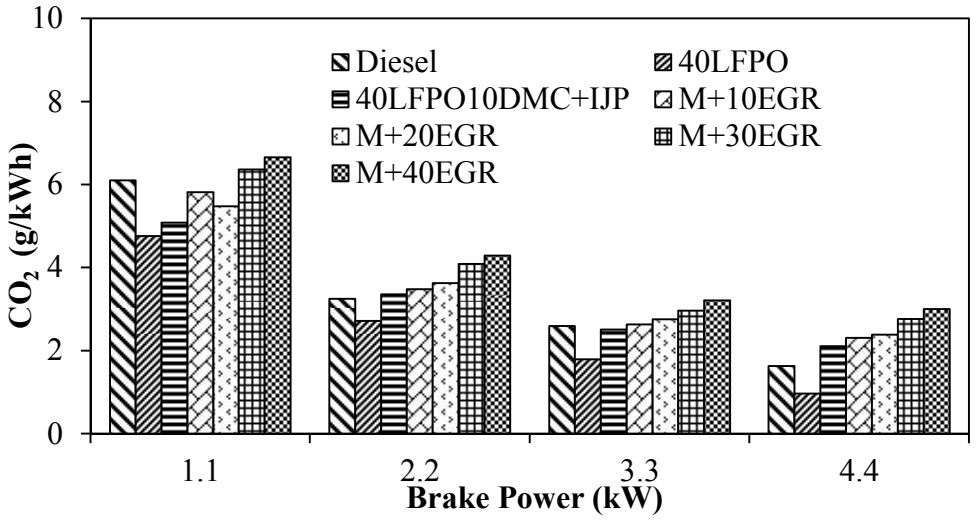

Figure 5.67: Variation of carbon dioxide with brake power

5.7.4.4 Nitric oxide emission

The variation of nitric oxide (NO) emission with load for different fuels without and with EGR tested in this study is illustrated in Figure 5.68. The NO emission for diesel, 40LFPO, 40LFPO10DMC+IJP, M+10EGR, M+20EGR, M+30EGR and M+40EGR are about 2.82, 1.5, 3.03, 2.73, 1.9, 1.63 and 1.3g/kWh at full load respectively. It can be observed from the figure that by introducing more EGR, the NO emission decreases up to 30% EGR. This is due to lower heat release rate that causes reduced cylinder temperature. Also, the oxygen availability decreases with the increase in EGR flow rates. This is also another reason for the reduced NO emission with the EGR operation throughout all loads. Zamboni et al and Verschaeren et al [223, 224] have also reported similar results.

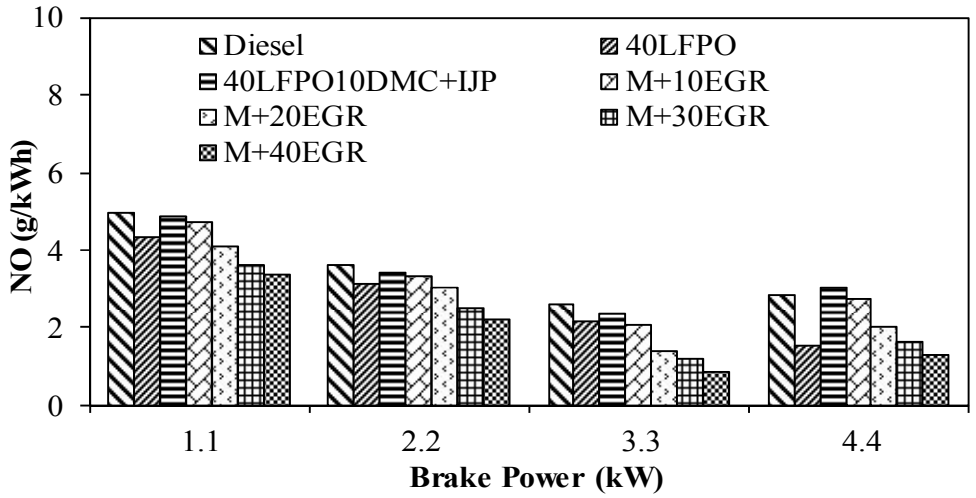

Figure 5.68: Variation of nitric oxide with brake power

5.7.4.5 Smoke emission

Figure 5.69 illustrates the variation of smoke emission with brake power for fuels tested in this study. With an increase in the load, the air fuel ratio decreases as the fuel injection increases, and hence, it results in higher smoke [218].

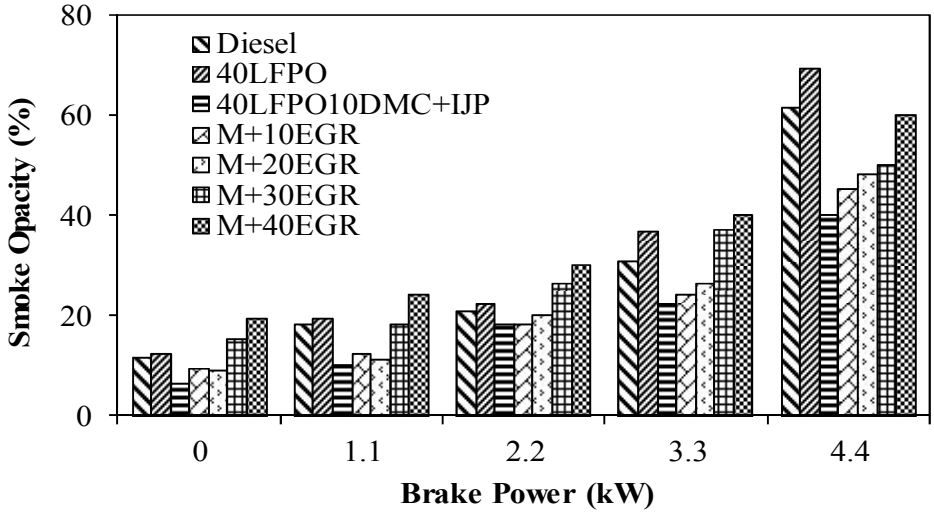

Figure 5.69: Variation of smoke emission with brake power

By adding DMC with the 40LFPO blend, the smoke emission is reduced at all loads. The reason may be the reduced density and increased availability of oxygen that promote the combustion of the 40LFPO-DMC blends. It can be observed from figure that with increase in EGR rate, the smoke emission increases at all loads. The reason is due to more incomplete combustion and reflects trade-off between NO and smoke emissions. The reason can be supported by Zhao et al [219], Chen et al [221] and Zamboni et al [223]. However, the smoke emissions for all the EGR flow rates are lower than those of diesel and 40LFPO10DMC+IJP. The similar results are reported in the literature [178, 125]. The values of smoke emission for diesel, 40LFPO, 40LFPO10DMC+IJP, M+10EGR, M+20EGR, M+30EGR and M+40EGR are about 61.2, 69.2, 40, 45, 48, 50 and 60% respectively at full load.

5.7.5 Conclusions

The performance, combustion and emission characteristics of the test engine run on the 40LFPO10DMC+IJP with different EGR rates were determined, analyzed and compared with those of diesel and 40LFPO operations. The following conclusions are made from the present investigation:

- The M+20EGR gave better results in terms of performance, combustion and lower emission compared to all the EGR rates studied.
- With EGR rates, the SFC marginally increased and the BTE declined.
- The SFCs of diesel, 40LFPO, 40LFPO10DMC+IJP, M+10EGR, M+20EGR, M+30EGR and M+40EGR are about 0.26, 0.27, 0.25, 0.26, 0.26, 0.28 and 0.30kg/kWh respectively.
- The cylinder peak pressures for the 40LFPO, 40LFPO10DMC+IJP, M+10EGR, M+20EGR, M+30EGR and M+40EGR are about 72.9, 78.8, 77.8, 77.0, 73.9 and 69.9 bar respectively at full load.
- The ignition delay period got prolonged with increased EGR. The values of ignition delay for diesel, 40LFPO, 40LFPO10DMC+IJP, M+10EGR, M+20EGR, M+30EGR and M+40EGR are about 12.9, 13.9, 12.5, 12.7, 12.9, 13.5 and 13.8^{o}CA respectively at full load.
- The addition of EGR rates decreases the NO emission, and HC, CO and smoke opacity are marginally increased.
- The NO emission for diesel, 40LFPO, 40LFPO10DMC+IJP, M+10EGR, M+20EGR, M+30EGR and M+40EGR are about 2.8, 1.5, 3.03, 2.7, 1.9, 1.6 and 1.3 g/kWh at full load, respectively.
- The values of smoke emission for diesel, 40LFPO, 40LFPO10DMC+IJP, M+10EGR, M+20EGR, M+30EGR and M+40EGR are about 61.2, 69.2, 40, 45, 48, 50 and 60% at full load respectively.

  The important values of combustion, performance and emission parameters at full load for 40LFPO with and without different cold EGR flow rates are given in Table 5.7.

Table 5.7: Summary of important values of parameters for 40LFPO with and without different cold EGR flow rates at full load.

Sl No.	Parameter	Diesel	40LFPO	40LFPO 10DMC +IJP	M+10 EGR	M+20 EGR	M+30 EGR	M+40 EGR
	Combustion parameters							
1	Maximum cylinder pressure (bar)	75.7	72.9	78.8	77.8	77.0	73.8	69.8
2	Maximum heat release (J/^{o}CA)	52	47.63	78.50	77	76.2	72	65
3	Ignition delay (^{o}CA)	12.9	14.4	12.5	12.7	12.9	13.5	13.8
4	Occurrence of maximum pressure (^{o}CA)	370.4	372.8	372.58	372.7	372.80	372.82	373
5	Combustion duration (^{o}CA)	38.1	42.50	31.01	32.0	32.8	35.7	37.8
	Performance parameters							
6	Specific fuel consumption (SFC) (kgs/kwh)	0.26	0.27	0.25	0.26	0.27	0.29	0.30
7	Brake thermal efficiency	32.478	31.715	37.032	36.012	35.837	33.663	30.802
8	Exhaust gas temperature (^{o}C)	338.5	339.20	308.0	303.0	301.4	295.3	290.1
	Emission parameters							
9	HC emission (g/kWh)	0.036	0.042	0.012	0.013	0.015	0.025	0.034
10	CO emission (g/kWh)	0.0048	0.019	0.005	0.005	0.006	0.009	0.013
11	NO emission (g/kWh)	2.8	1.52	3.03	2.73	1.98	1.63	1.27
12	Smoke opacity (%)	61.2	69.2	40	45	48	50	60

5.8 Post-combustion CO_2 Capture

5.8.1 General

In the previous section, the results of the combustion, performance and emission parameters of the test engine run on 40LFPO10DMC+IJP without and with EGR were discussed. It was found that when EGR was adopted, 20% EGR gave better performance and lower emissions compared to those of other EGR flow rates. In this section, an attempt was made to study the effect of capturing CO_2 in the tailpipe in 40LFPO10DMC+IJP without and with 20EGR. Zeolite 13X pellets were used for capturing in the tail pipe of the engine exhaust. The results of the combustion, performance and emission parameters of 40LFPO based engine operation were evaluated and compared with that of diesel operation, and presented in the following sections. In this investigation, CO_2 is captured from the exhaust gas of the same diesel engine run on 40LFPO based fuel. The fuel test conditions followed in this study are given below;

(i) Diesel

(ii) 40LFPO10DMC+IJP

(iii) 40LFPO10DMC+IJP+Z

(iv) 40LFPO10DMC+IJP+20EGR

(v) 40LFPO10DMC+IJP+20EGR+Z

The notations used to denote the above five test environments are same as that followed in earlier section except Z. Z means capture of CO_2 gas with zeolite 13X pellets in the exhaust tail pipe.

5.8.2 Combustion parameters

5.8.2.1 Cylinder pressure and heat release rate

Figure 5.68 illustrates the variations of the cylinder pressure and heat release rate with respect to the crank angle for diesel, 40LFPO10DMC+IJP, 40LFPO10DMC+IJP+Z, 40LFPO10DMC+IJP+20EGR and 40LFPO10DMC+IJP+20EGR+Z at full load condition. It can be observed from the figure that the cylinder peak pressures for the diesel, 40LFPO10DMC+IJP, 40LFPO10DMC+IJP+Z, 40LFPO10DMC+IJP+20EGR and 40LFPO10DMC+IJP+20EGR+Z are approximately 75.70, 78.8, 76.8, 77.0 and 76.42 bar respectively. Also, the peak cylinder temperature for 40LFPO10DMC+IJP is higher than that for the diesel. This may be because DMC provides oxygen to the combustion

chamber and IJP helps for swirl motion, which leads to better air fuel mixture, resulting in complete combustion. The peak cylinder pressure of both 40LFPO10DMC+IJP and 40LFPO10DMC+IJP+20EGR marginally decreased with the use of zeolite adsorbents which may be due to occurrence of back pressure when exhaust gas passes through the tailpipe. Similar reason was reported by Muthiya et al [226].

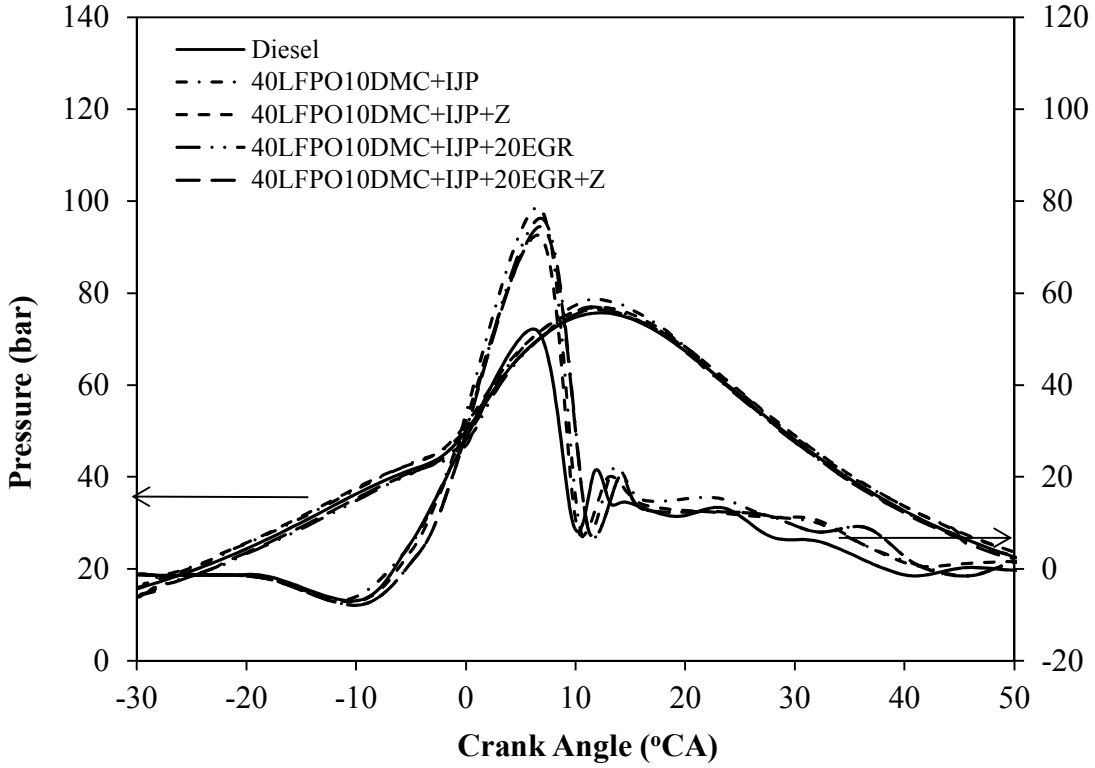

Figure 5.70: Variation of cylinder pressure and HRR with crank angle at full load.

It is apparent from the heat release rate (HRR) curves that the maximum HRR is 78.5 J/°CA and it occurs for the 40LFPO10DMC+IJP operation at full load. The reason is that DMC has higher volatile fuel. The maximum HRRs for diesel, 40LFPO10DMC+IJP, 40LFPO10DMC+IJP+Z, 40LFPO10DMC+IJP+20EGR and 40LFPO10DMC+IJP+20EGR+Z are 52, 78.50, 72.5, 76.2 and 74.41 J/°CA respectively at full load. The HRR also marginally decreases with zeolites adsorbents, because a pressure decrease by back pressure occurs in the tail pipe.

5.8. 3 Emission parameters

5.8.3.1 Hydrocarbon emission

The hydrocarbon (HC) emission of the diesel engine is primarily influenced by the fuel quality and the oxygen availability for complete combustion. Figure 5.69 depicts the variation of HC emission with brake power of diesel, 40LFPO10DMC+IJP,

40LFPO10DMC+IJP+Z, 40LFPO10DMC+IJP+20EGR and 40LFPO10DMC+IJP+20EGR+Z. It can be noticed from the figure that the HC emission of 40LFPO10DMC+IJP and 40LFPO10DMC+IJP20EGR with zeolites adsorption are decreased at all loads. The reason is that zeolites 13X pellets are very attractive adsorbent, which are also used for gas purification. Similar reason was reported by Dirar and Loughlin [227], when they obtained results in CO_2 capture by 5A and 13X zeolites.

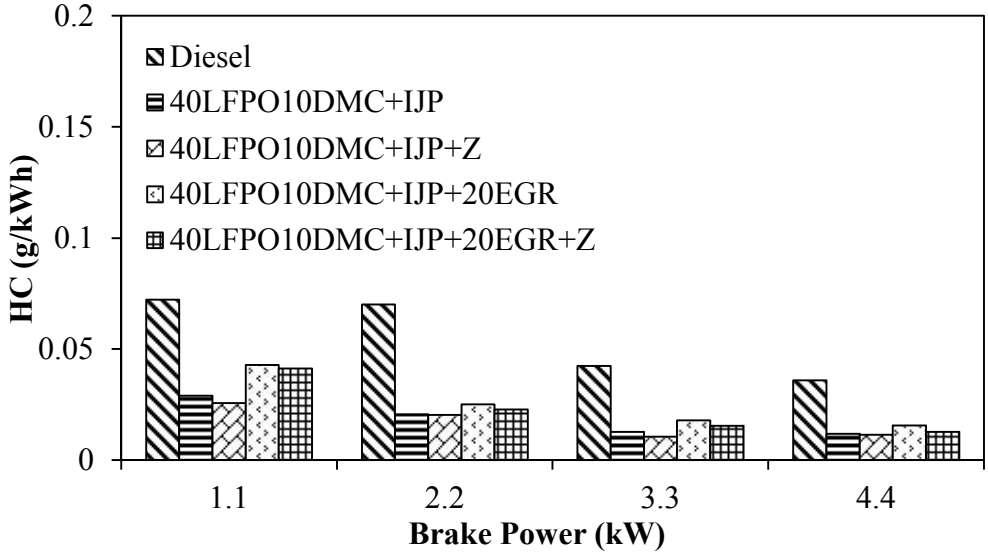

Figure 5.71: Variation of hydrocarbon with brake power

The HC emissions for diesel, 40LFPO10DMC+IJP, 40LFPO10DMC+IJP+Z, 40LFPO10DMC+IJP+20EGR and 40LFPO10DMC+IJP+20EGR+Z are about 0.036, 0.012, 0.011, 0.015 and 0.012 g/kWh at full load respectively.

5.8.3.2 Carbon monoxide emission

Figure 5.70 shows the variation of carbon monoxide (CO) emission with brake power. It can be observed from the figure that the CO emission of 40LFPO10DMC+IJP and 40LFPO10DMC+IJP+20EGR with zeolite adsorption are decreased at entire range of load. The reason may be that small amount of CO emission is absorbed by zeolites. The CO emission for diesel, 40LFPO10DMC+IJP, 40LFPO10DMC+IJP+Z, 40LFPO10DMC+IJP+20EGR and 40LFPO10DMC+IJP+20EGR+Z are about 0.0048, 0.0047, 0.0041, 0.0063, 0.0056 g/kWh at full load respectively. The 40LFPO10DMC with internal jet piston and zeolite in the exhaust exhibited lowest CO emission among all the test environments adopted in this study.

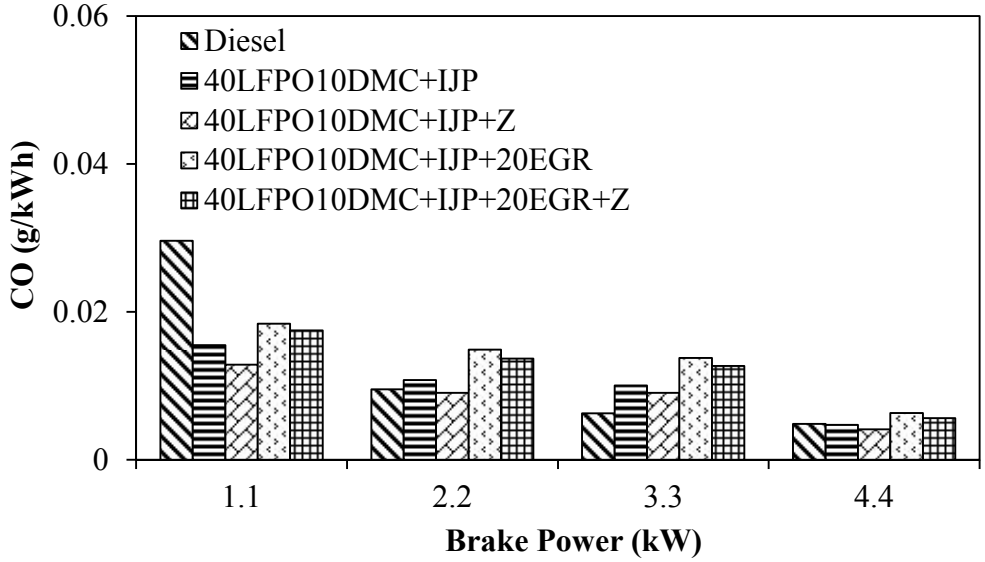

Figure 5.72: Variation of carbon monoxide with the brake power

5.8.3.3 Carbon dioxide emission

Figure 5.71 shows the variation of carbon dioxide (CO_2) with brake power. The CO_2 emission of 40LFPO10DMC+IJP and 40LFPO10DMC+IJP+20EGR with zeolite adsorbents are reduced by about 40 and 48% at full load. The reason may be that zeolite 13X pellets have very good adsorption properties, as each pellet has a cylindrical shape and more surface expose for CO_2 capture. The similar results have been also noticed in the literature [227-229]. The CO_2 emission diesel, 40LFPO10DMC+IJP, 40LFPO10DMC+IJP+Z, 40LFPO10DMC+IJP+20EGR and 40LFPO10DMC+IJP+20EGR+Z are about 1.62, 2.10, 1.25, 1.98 and 1.02 g/kWh at full load respectively.

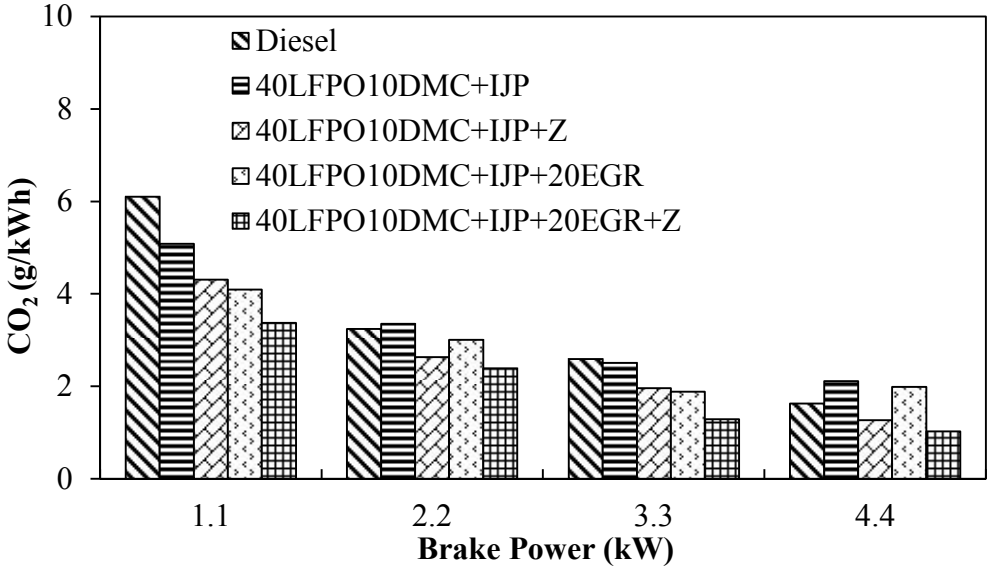

Figure 5.73: Variation of carbon dioxide with brake power

5.8.3.4 Nitric oxide emission

The variation of nitric oxide (NO) emission with load for the fuels tested in this study is illustrated in Figure 5.72. The NO emissions of 40LFPO10DMC+IJP and 40LFPO10DMC+IJP+20EGR with zeolite adsorbents are marginally decreased. This may be due to the marginally low HRR in the combustion chamber.

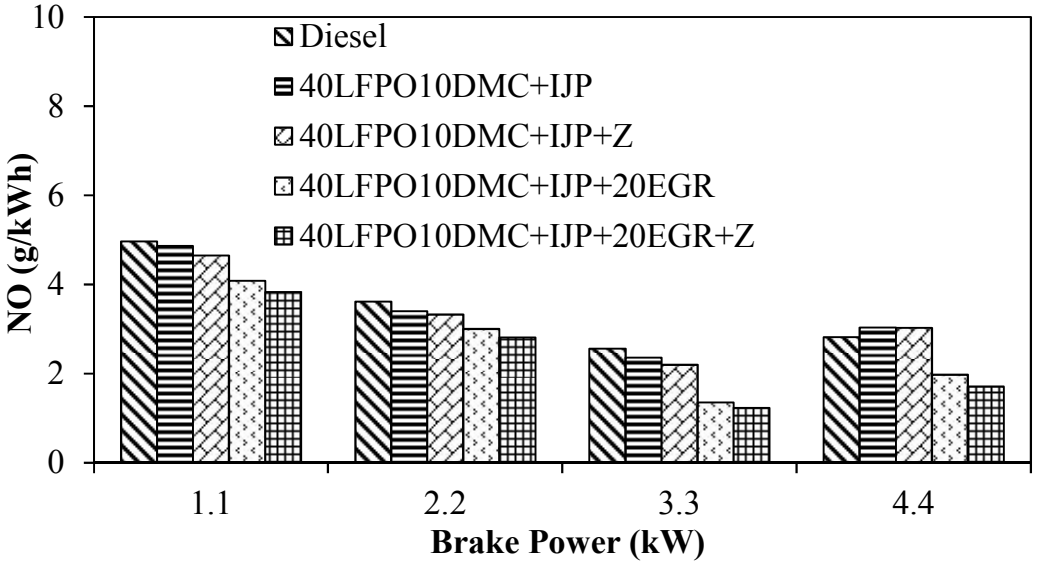

Figure 5.74: Variation of nitric oxide with brake power

The NO emissions for diesel, 40LFPO10DMC+IJP, 40LFPO10DMC+IJP+Z, 40LFPO10DMC+IJP+20EGR and 40LFPO10DMC+IJP+20EGR+Z are about 2.8, 3.03, 3.02, 1.9 and 1.71 g/kWh at full load respectively.

5.8.3.5 Smoke emission

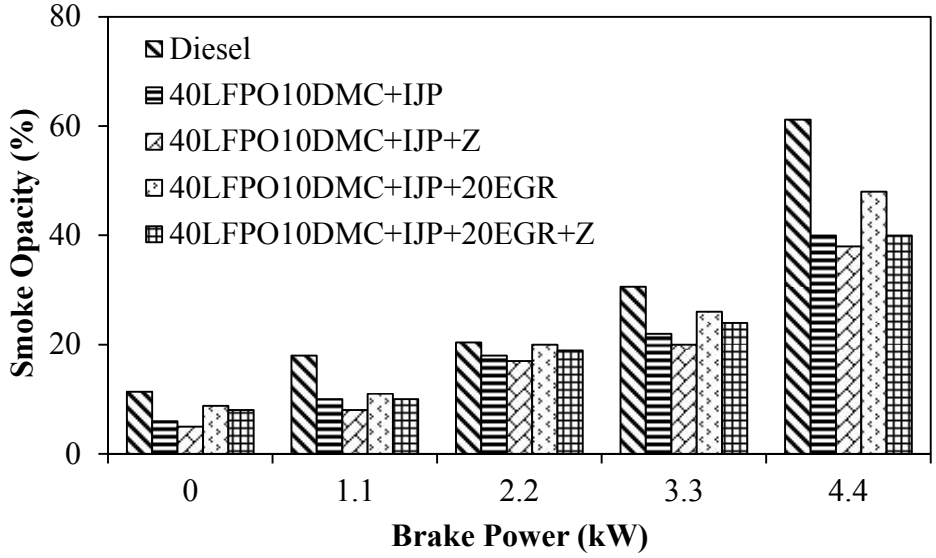

Figure 5.75: Variation of smoke emission with brake power

Figure 5.73 illustrates the variation of smoke emission with brake power for fuels tested in this study. The smoke emissions of 40LFPO10DMC+IJP and 40LFPO10DMC+IJP+20EGR with zeolite adsorbents decreased by about 8 and 10% respectively. The reason may be that zeolite pellets absorb the smoke particles and remove trace or dilute impurities from gas [227, 228]. Similar reason was reported by Dirar and Loughlin [227], when they obtained results on CO_2 capture by 5A and 13X zeolites pellets. The values of smoke emission for diesel, 40LFPO10DMC+IJP, 40LFPO10DMC+IJP+Z, 40LFPO10DMC+IJP+20EGR and 40LFPO10DMC+IJP+20EGR+Z are about 61.2, 40, 38, 48 and 40% respectively at full load.

5.8.4 Conclusions

The combustion performance and emission characteristics of the test diesel engine, run on the 40LFPO10DMC+IJP, 40LFPO10DMC+IJP+20EGR with zeolite adsorbents and diesel were analyzed, and compared to those of diesel operation. The following conclusions are made from the present investigation:

- The CO_2 emission in diesel, 40LFPO10DMC+IJP, 40LFPO10DMC+IJP+Z, 40LFPO10DMC+IJP+20EGR and 40LFPO10DMC+IJP+20EGR+Z are by about 1.62, 2.10, 1.05, 2.38 and 1.26 g/kWh at full load respectively.
- The CO_2 emission of 40LFPO10DMC+IJP and 40LFPO10DMC+IJP+20EGR with zeolite adsorbents are reduced by about 40 and 48% respectively.
- The smoke emission of 40LFPO10DMC+IJP and 40LFPO10DMC+IJP+20EGR with zeolite adsorbents are also decreased by about 8 and 10% respectively.
- With the zeolite adsorbents, the other emissions like NO, CO and HC are also slightly decreased in this investigation.

The important parameters of the engine run on diesel, 40LFPO10DMC+IJP, 40LFPO10DMC+IJP+20EGR without and with zeolites at full load are shown in Table 5.8.

Table 5.8: Values of important parameters of the engine run on diesel, M+Z, M+20EGR and M+20EGR+Z at full load.

Sl No	Parameter	Diesel	40LFPO10 DMC+IJP = M	40LFPO10 DMC+IJP+ Z=M+Z	40LFPO10 DMC+IJP+ 20EGR=M+ 20EGR	40LFPO10DMC +IJP+20EGR+Z =M+20EGR+Z
	Combustion parameters					
1	Maximum cylinder pressure (bar)	75.7	78.8	76.8	77.0	76.42
2	Maximum heat release ($J/^oCA$)	52	78.50	72.5	76.2	74.41
3	Occurrence of maximum pressure (^oCA)	370.4	372.58	372.68	372.80	372.9
	Emission parameters					
4	HC emission (g/kWh)	0.036	0.012	0.011	0.015	0.012
5	CO emission (g/kWh)	0.0048	0.0047	0.0041	0.0063	0.0056
6	CO_2 emission (g/kWh)	1.62	2.10	1.25	1.98	1.02
7	NO emission (g/kWh)	2.8	3.03	3.02	1.98	1.71
8	Smoke opacity (%)	61.2	40	38	48	40

5.9 Durability Test and Lubrication Oil Analysis

5.9.1 General

After conducting a series of experimental studies to assess the engine behavior in terms of combustion, performance, emissions which was run on 40LFPO based operation, it was understood that 40LFPO10DMC+IJP+20EGR gave better performance and lower emission than other 40LFPO based operations and comparable to that of diesel operation. Hence, a short term durability test was carried out. The test procedure was earlier described in Chapter 4. This chapter presents the analysis of the results obtained for the wear characteristics and lubrication oil properties from a single cylinder, four stroke, DI, diesel engine run with 40LFPO10DMC blend as fuel, with 20% EGR and with internal jet piston geometry.

5.9.2 Carbon deposit on engine components

A comparison of the carbon deposits on the cylinder head and piston crown before and after the endurance test is depicted in Figure 5.74. After running the engine with 40LFPO10DMC as fuel 20% EGR and internal jet piston geometry, the cylinder head, the piston crown and the injector tip were observed to have black carbon deposits. A maximum of about 10 mg of carbon deposits were noticed in both cylinder head and combustion chamber. Generally, the carbon deposits are related to soot formation during combustion of fuel and recirculation of combustible gases into the engine in EGR operation causes carbon deposits. Similar reason was reported by Ziejewski et al [230] for the results they obtained from a diesel engine run for durability tests on higholeic sun flower and safflower oils. However, the oxygenated additive dimethyl carbon (DMC) is blended with 40LFPO, which provides oxygen during combustion and reduced the soot formation tendency. Table 5.9 gives the information about the amount of carbon deposit on engine components when the engine was run on diesel and 40LFPO10DMC +IJP+20EGR.

(a) Piston crown (before)

(b) Piston crown (after)

(c) Piston head (before)

(d) Piston head (after)

Figure 5.76: Comparison of carbon deposits before and after the endurance test on piston crown and cylinder head

Table 5.9: Carbon deposit on cylinder head, piston crown and injector nozzle tip.

Sl No.	Component Name	Weight in mg	
		Diesel	40LFPO10DMC +IJP+20EGR
1	Cylinder head	2.8	3.2
2	Piston crown	3	4
3	Injector nozzle tip	0.7	1.5

5.9.2.1 Fuel injector

The fuel injector components were dismantled after running the engine under 40LFPO10DMC+ IJP+20EGR condition. Figure 5.75 shows the photograph of these dismantled components. The photographic views of the fuel injector nozzle tip, before and after the endurance test, are shown in Figure 5.76. The carbon deposits were found in this injector nozzle and in between the holes. The carbon deposits on the injector holes

opposed the fuel spray of the injector to the combustion chamber. Similar reason was reported by Bari et al [231] for the results they obtained from performance deterioration and durability issues while running a diesel engine with crude palm oil. This was due to the carbon deposits on the holes of the injector. The deposited carbon content was measured with the help of the weight balance and found to be approximate 1.5 mg.

Figure 5.77: Photographic views of the dismantled fuel injector components

(a) Injector nozzle tip (before)

(b) Injector nozzle tip (after)

Figure 5.78: Comparison of carbon deposits before and after the endurance test on injector nozzle

5.9.2.2 Fuel injection pump

After finishing the endurance test, the photographic view all the components of the dismantled fuel injection pump were taken and shown in Figure 5.77. The wear analyses of fuel injection pump components were considered. Table 5.9 provides the amount of wear on different components of the fuel injection pump before and after the endurance test. Figure 5.78 shows the photographic view of four major components of the dismantled fuel injection pump, such as plunger, pump barrel, spring and pinion.

Figure 5.79: Photographic view of all components of the dismantled fuel injection pump

(a) Plunger

(b) Pump barrel

(c) Spring

(d) Pinion

Figure 5.80: Photographic view of four major components of dismantled fuel injection pump

Table 5.10: The amount of wear on different components of the fuel injection pump

Sl. No.	Component Name	Component Weight Before Endurance Test (g)	Component Weight After Endurance Test (g)	Decreases in Weight (%)
1	Pump barrel	304	301.2	0.92
2	Spring	210	207.0	1.42
3	Plunger	252	248.0	1.58
4	Pinion	180	176.0	2.22

5.9.3 Lubrication oil analysis

The use of a new alternative fuel in the diesel engine may affect the tribological properties of the lubricating oil. It is very important for assessing the suitability of new fuel for the existing engine. Hence, the various lubricating oil property analyses of the engine run on 40LFPO10DMC+IJP+20EGR was carried out, and the properties of the oil were compared with the diesel operation and presented.

5.9.3.1 Kinematic viscosity

Viscosity can be defined as the measurement of fluid internal resistance to flow at a particular temperature. Viscosity plays a major role in developing and maintaining a film thickness between the two moving surfaces.

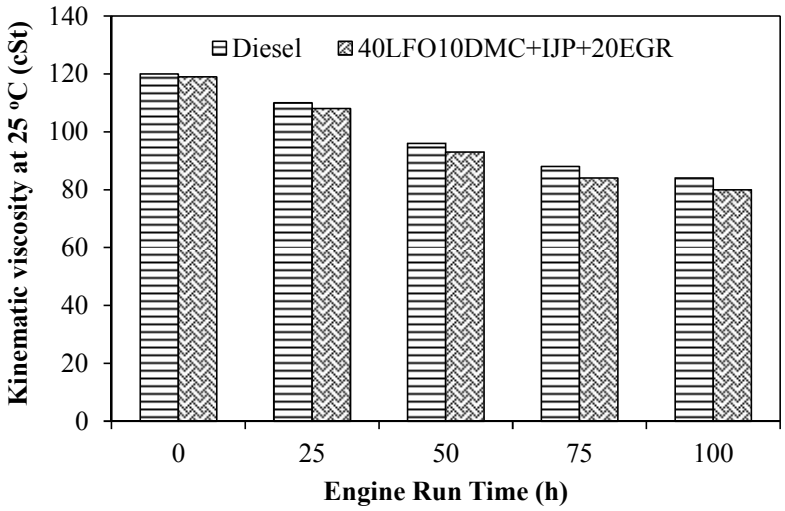

. Figure 5.81: Variation of kinematic viscosity of lubricating oil with engine run time.

Figure 5.79 portrays the variation of kinematic viscosity of lubricating oil with engine run time. It can be observed from the figure that 40LFPO10DMC+IJP+20EGR gives a higher reduction in kinematic viscosity than that of diesel throughout the engine run time. This may be due to the higher density of 40LFO10DMC+IJP+20EGR, which increases the spray time of fuel in the combustion chamber and allows more time for fuel droplets hitting the liner walls. So, there is more chance of mixing fuel with lubricating oil, and thereby it increases fuel dilution.

5.9.3.2 Density

The density of lubricating oil is basically affected by the addition of wear debris, fuel and moisture [231]. Figure 5.80 depicts the variation of the lubricating oil density of diesel

and 40LFPO10DMC+IJP+20EGR during the engine run time. It can be observed from the figure that the density of the lubricating oil increases after the engine run for 25 hours and above. The density of lubricating oil obtained in 40LFPO10DMC+IJP+ 20EGR operation is higher than that of diesel to run the engine. This may be due to the polymerization reaction of the lubricating oil by continuous heating and exposure to moisture, which increases the density. The other reason may be that the lubricating oil density increased by the sludge formation in the oil, which is the mixture of oil, water, dust, dirt from different parts and carbon particles that originate from the incomplete combustion of fuel [231].

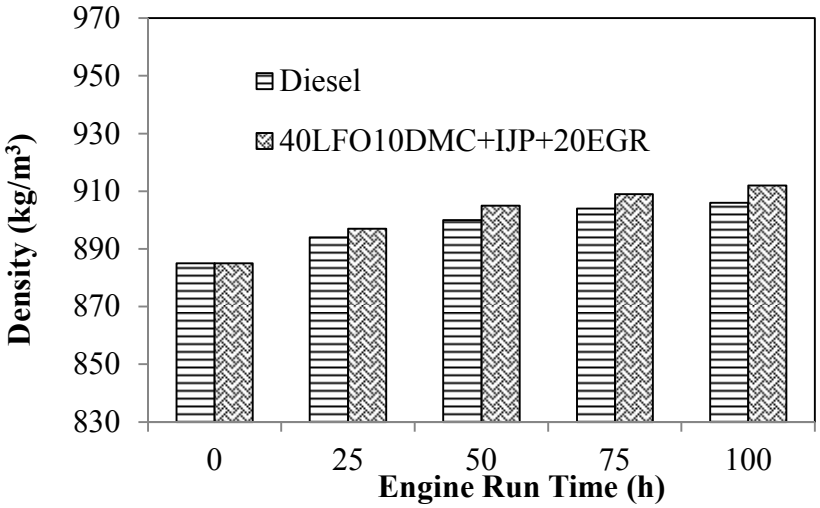

Figure 5.82: Variation of density of lubricating oil with engine run time.

5.9.3.3 Flash point

The flash point is the lowest temperature at which lubricating oil can vaporize, when it is in contact with flame. The variation of flash point temperature of the lubricating oil of diesel and 40LFPO10DMC+IJP+20EGR operation is depicted in Figure 5.81 The flash point of a good lubricating oil should always be higher to reduce the volatility. It can be observed from the figure that the flash point of the lubricating oil decreases with the engine run time. After 100 hours of run, the flash point of diesel was 208^{o}C, which was 3% higher than that of 40LFPO10DMC+IJP+20EGR. The reason for reduction of flash point temperature may be the aromatic content present in the LFPO, which gives a higher percentage of dilution and increases the sump oil temperature.

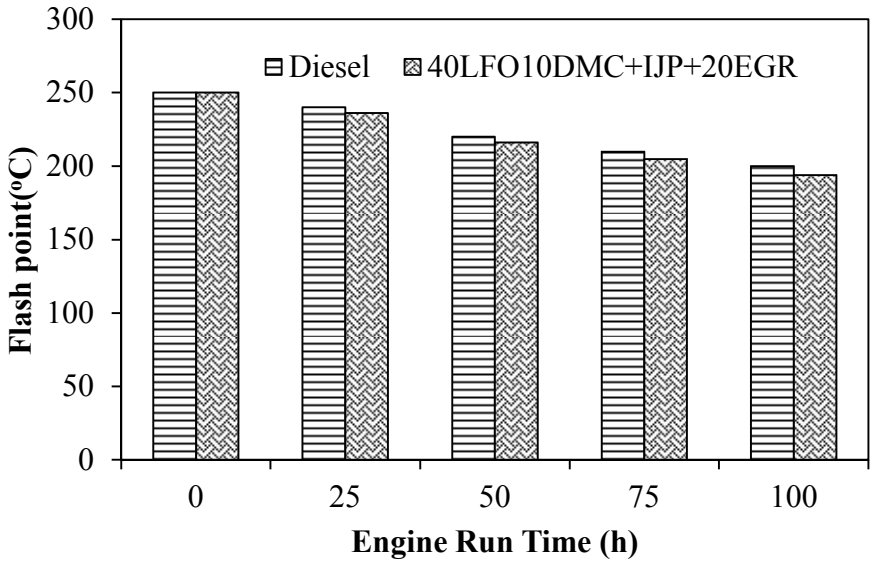

Figure 5.83: Variation of flash point of lubricating oil with engine run time.

5.9.3.4. Moisture content

Moisture content in the lubricating oil is a negative parameter which destroys the strength of the oil film. The moisture content in the oil accelerates the oxidation reaction and causes the corrosion of the metal components. The moisture content in the lubricating oil oxidizes Fe^{2+} ion to Fe^{3+}, which facilitates easy corrosion inside the engine. The very low moisture content also increases the corrosion rate inside the engine. Figure 5.82 portrays the variation of moisture content in the lubricating oil with the variation in engine run time. It can be observed from the figure that the moisture content in the lubricating oil increases in both the fuels with respect to the increase in engine run time. Increase of the moisture content in the lubricating oil is an indication of more fuel dilution and precipitation of additives. The 40LFPO10DMC+IJP+20EGR operation exhibits higher moisture content than that of diesel irrespective of the engine run time. The reason may be that EGR flow rates increase moisture percentage in the lubricating oil. The availability of moisture content may destroy the sealing arrangement between piston rings-liner interfaces and leakage of compression by over-dilution.

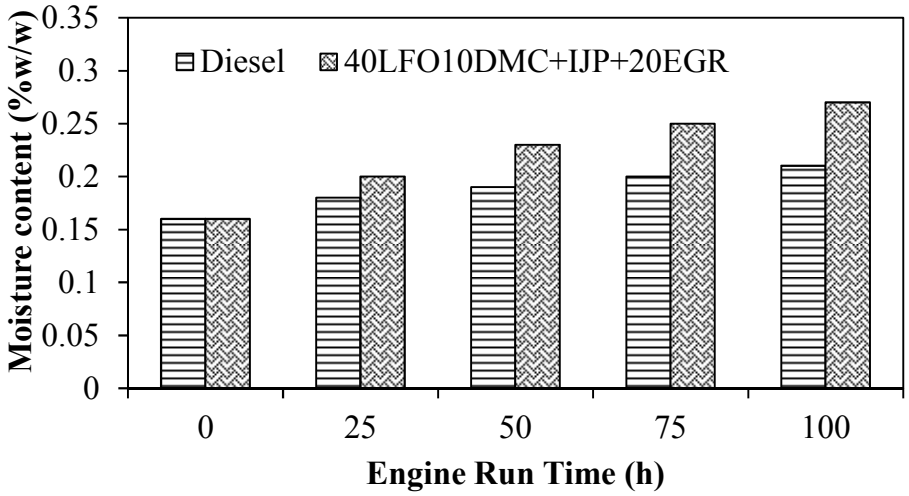

Figure 5.84: Variation of moisture content of lubricating oil with engine run time.

5.9.3.5. Ash content

Figure 5.83 depicts the variation of the ash content of the lubricating oil with engine run time in case of diesel and 40LFPO10DMC+IJP+20EGR.

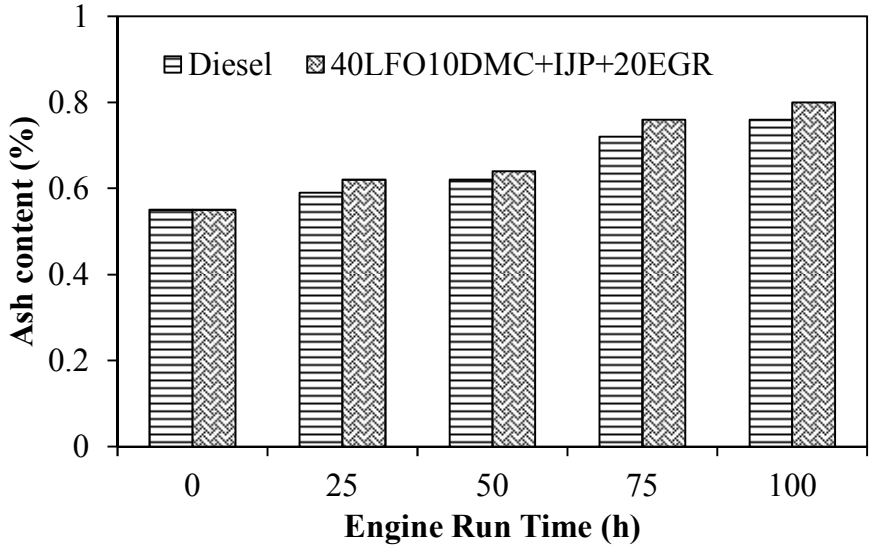

Figure 5.85: Variation of ash content of lubricating oil with engine run time.

The ash content of lubricating oil is the percentage of mass of non-combustible residue that remains after the complete incineration of oil sample. It can be observed from the figure that the ash contents for diesel and 40LFPO10DMC+IJP+20EGR operation increase gradually with increase in engine run hours. The ash content of 40LFPO10DMC+IJP+20EGR is higher than that of diesel after 100 hours run of the engine. This may be due to the higher content of non-combustible polymerized part having higher molecular weight, which remains as carbon residue after combustion.

5.9.3.6. Total base number

Figure 5.84 depicts the variation of Total Base Number (TBN) with the variation in engine run time. TBN is one of the neutralization numbers, which is specially used to measure the alkalinity reserve remaining in the lubricant. It is an indication of lubricant's ability to neutralize corrosive acids that formed during the engine operation. The higher TBN value gives a lower concentration of free acids of lubricating oil. It can be observed from the figure that the TNB value of 40LFPO10DMC+IJP+20EGR operation is lower than that of the diesel operation. This may be due to the high corrosion caused by EGR and LFPO oil in the 40LFPO10DMC+IJP+20EGR. `

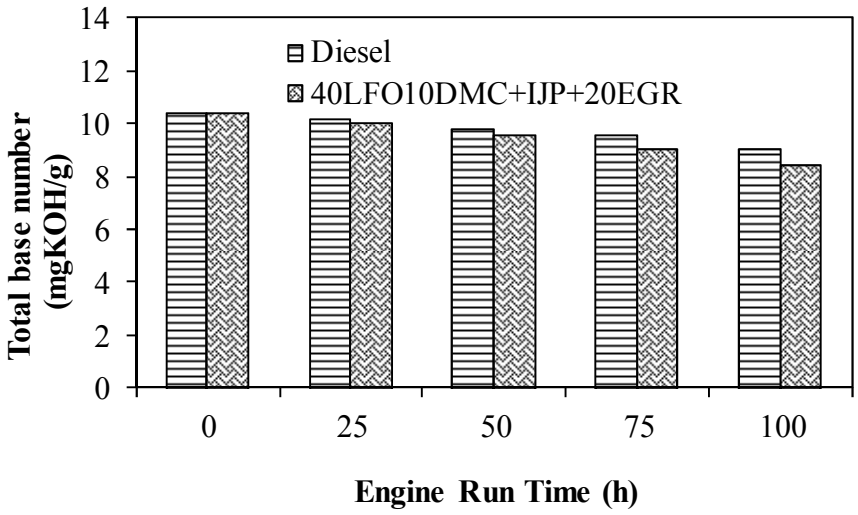

Figure 5.86: Variation of total base number of lubricating oil with engine run time.

5.9.4 Wear trace metal analysis

The determination of various wear metal elements in the lubricating oil sample was measured by atomic absorption spectroscopy (AAS). The spectrometer followed the ASTM D5185/13 test procedure [232]. The possible, wear elements like nickel (Ni), iron (Fe), copper (Cu), lead (Pb), aluminum (Al), chromium (Cr), Zinc (Zn) and magnesium (Mg) were measured in the lubricating oil. The variation of various wear, trace metals in lubricating oil with engine run time are discussed below.

5.9.4.1 Nickel

Figure 5.85 depicts the variation of nickel with engine run time of diesel and 40LFPO10DMC+IJP+20EGR. The nickel concentration in the oil is due to engine wear and the oil itself. The very small quantity of nickel is added as an organometallic additive to the lubricating oil. For increasing the ductility of the material and making high strength

material, nickel based alloy steel is used for making the engine parts like cam, valve stem and valve guide. The wear of the engine components like piston, bearings, valves, crankshaft, liners and gear may give rise to nickel concentration in the lubricating oil. If the nickel concentration value is found to be higher than the expected value, it means there is rapid wear of the bearings and engine components. It can be observed from the figure that 40LFPO10DMC+IJP+20EGR has higher wear than the diesel operation.

5.9.4.2 Iron

The concentration of iron in the lubricating oil with the engine run time of diesel and 40LFPO10DMC+IJP+20EGR is shown in Figure 5.85. The possible sources of iron element in diesel engine are the wear debris from piston, piston rings, valves, cylinder head, camshaft, crankshaft, cylinder block, valve guide, wrist pin and bearings. It can be observed that the concentration of iron is higher for the 40LFPO10DMC+IJP+20EGR than that of diesel operation. This may be due to the LFPO as a fuel, which reduces the lubricity and leads to a higher frictional wear of the components. The iron concentration of 40LFPO10DMC+IJP+20EGR in the lubricating oil after 100 h run is 8.4% higher than that of diesel fuel.

5.9.4.3. Copper

Figure 5.85 depicts the concentration of copper in the lubricating oil with varying engine run time of diesel and 40LFPO10DMC+IJP+20EGR. The concentration of copper content in wear debris originates from the injector shields, thrust washers, valve guides, connecting rod, piston rings, and wear in bushings and bearings [233]. It can be observed from the figure that the copper concentration of 40LFPO10DMC+IJP+20EGR is higher than that of diesel operation. This is because wear in the piston and crankshaft may result in a larger copper concentration. The 40LFPO10DMC+IJP+20EGR as a fuel provides higher cylinder temperature, which reduced the lubricity and hence the wear between the cylinder and piston ring increases. Also, the presence of abrasive and contamination in the oil, causes excessive copper wear in the crankshaft.

5.9.4.4. Lead

The variation of the concentration of lead in the lubricating oil with the variation in engine run time of diesel and 40LFPO10DMC+IJP+20EGR is shown in Figure 5.85. The concentration of lead in the lubricating oil originates from wear of bearings, paints, grease, and fuel blow by thrust bearing, bearing cages, bearing retainers, etc. [233]. It can

be observed from figure that the concentration of lead for 40LFPO10DMC+IJP+20EGR is 35% higher than that of diesel after 100 h of engine run time. The reason may be the reduction of lubricity inside the combustion chamber by the use of LFPO and 20EGR during the endurance test of the engine.

5.9.4.5. Aluminum

The variation of the aluminum concentration in the lubricating oil with run time of diesel and 40LFPO10DMC +IJP +20EGR is shown in Figure 5.86. Aluminum in the lubricating oil originates from wear of piston, bearings, dirt, additives, thrust washers, push rods, oil pump, crankcase oil paint. Similar reason was reported by Anon [233]. The concentration of aluminum in the lubricating oil is higher for 40LFPO10DMC+IJP+20EGR than that of diesel fuel. This may be because 40LFPO10DMC+IJP+20EGR gives higher cylinder temperature, which causes thermal stress on the piston and cylinder head. Also, the higher cylinder pressure of 40LFPO10DMC+IJP+20EGR allows more metal wear from the piston. In a single cylinder CI engine, the wear of aluminum is maximum from the wear of piston and bearings.

5.9.4.6. Chromium

Figure 5.85 portrays the variation of the concentration of aluminum in the lubricating oil with run time of diesel and 40LFPO10DMC+IJP+20EGR. The components built for high pressure and temperature application like IC engines are made up of special grade steel and alloys of aluminum, which contain chromium. Chromium increases tensile and impact strength of the material [233]. The concentration of chromium in the lubricating oil may originate from the wear of cylinder liner, compression rings, gears, crankshaft and bearings. It can be observed from the figure that the 40LFPO10DMC+IJP+20EGR gives higher concentration of chromium in the lubricating oil than the diesel. This may be due to the fact that 40LFPO10DMC+IJP+ 20EGR gives higher cylinder peak pressure and higher cylinder temperature in the combustion chamber, which results higher chromium concentration in the lubricating oil.

5.9.4.7. Zinc

Figure 5.85 depicts the variation of the concentration of zinc in the lubricating oil with a run time of diesel and 40LFPO10DMC+IJP+20EGR. Zinc di-alkyl-di-thio-phosphate (ZDDP) is added to the lubricating oil as a multi-functional additive. It acts as an

antioxidant, anti-wear additive, detergent and extreme pressure additives. The fresh lubricating oil contains a reasonable amount of zinc traces as an organic-metallic complex. It can be observed from the figure that the concentration of zinc in the 40LFPO10DMC+IJP+20EGR is higher than that of the diesel operation. This may be due to additive depletion and wear of bearings due to low lubricity. Zinc in lubricating oil gives certain advantages over the engine components. It is an anti-wear additive, and also prevents the oxidation of the lubricating oil. The zinc based additive is non-biodegradable and aquatically toxic.

5.9.4.8. Magnesium

Figure 5.85 depicts the variation of the concentration of magnesium in the lubricating oil with the engine run time of diesel and 40LFPO10DMC+IJP+20EGR operation. Magnesium is added to the lubricating oil as detergent inhibitor additive. The magnesium in wear debris may originate from additive depletion, wear of the cylinder liner surface, bearings, gear box housing, etc. A small amount of magnesium is generally added to the lubricating oil for the reduction of component corrosion and wear. The 40LFPO10DMC+IJP+20EGR gives a marginally higher concentration of magnesium in the lubricating oil than that of the diesel operation throughout the engine run time. Magnesium in the lubricating oil gives advantages of cleanness and neutralize action of the oil impurities. It is also additive for corrosion and rust inhibitor. The concentration of magnesium in the lubricating oil decreases the oxidation of metal and increases the engine durability.

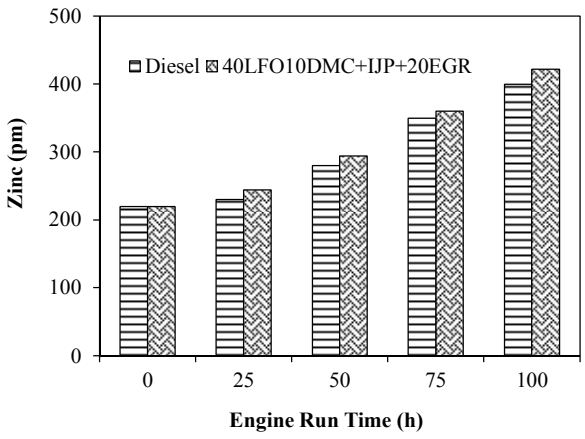

(a) Nickel

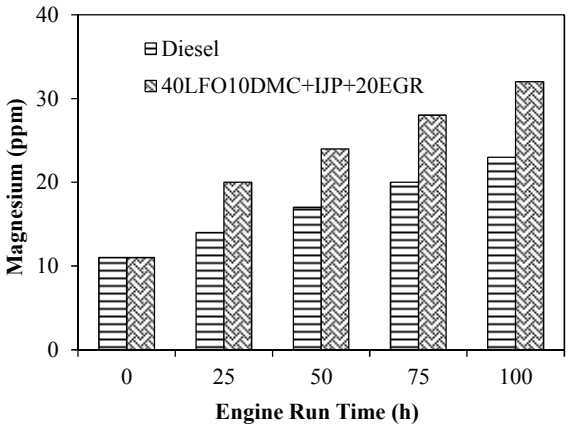

(b) Iron

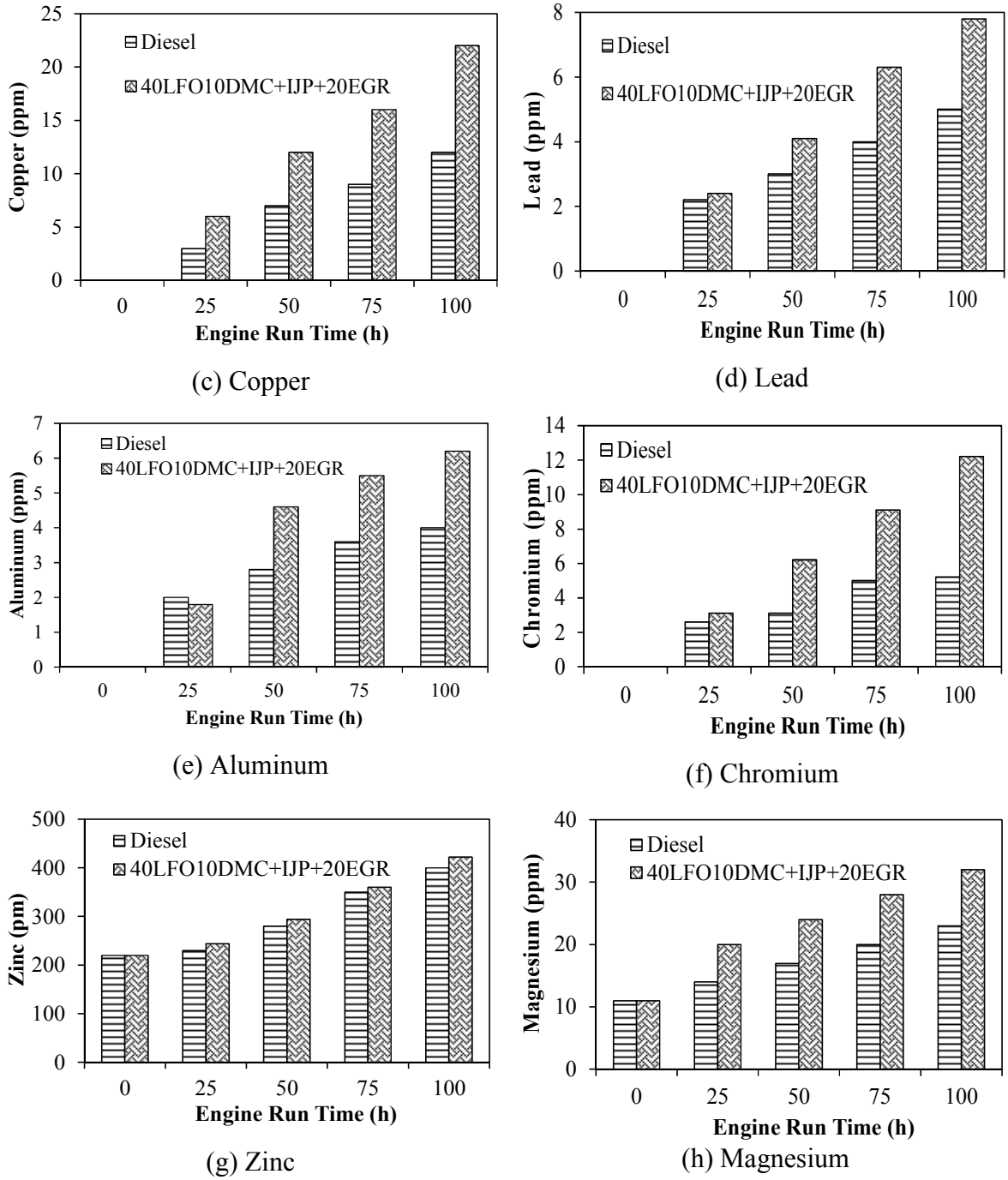

Figure 5.87: Variations of wire trace metals in lubricating oil with engine run time, (a) Nickel, (b) Iron, (c) Copper, (d) Lead, (e) Aluminum, (f) Chromium, (g) Zinc and (h) Magnesium.

5.9.5 Summary

After successfully running the CI engine with 40LFPO10DMC+IJP+20EGR during the endurance test, visual inspection and atomic absorption spectroscopy (AAS) were carried out for the carbon deposits and wear analysis. The results of the visual inspection of

carbon deposits on different engine components showed the traces of carbon deposits in the cylinder head, piston crown and injector nozzle tip of the engine fuelled with 40LFPO10DM+IJP+20EGR blend. The marginal wear of the engine components was also noticed in the case of fuel injection pump. The lubricating oil properties were found to be deteriorated with the 40LFPO10DM+IJP+20EGR operation. This may be the lower lubricity offered by LFPO with the 20EGR operation of the engine.

Chapter 6

CONCLUSIONS

6.1 General

The combustion, performance and emission characteristics of a single cylinder, four stroke, air cooled, direct injection diesel engine capable of producing 4.4 kW at a constant speed of 1500 rpm, fuelled with LFPO based fuels with and without engine modifications were analysed and compared with diesel operation of the engine. Three fuel modifications namely, blending with diesel fuel, blending with an ignition improver and blending with an oxygenate additive, were used. Three engine modification techniques namely, change of injection timing, increasing the turbulence, and exhaust gas recirculation were used. Furthermore, a carbon capture method was carried out for absorbing CO_2 with engine exhaust by using zeolite. A short term durability test was also carried out in the test engine which was run on 40LFPO10DMC+IJP+20EGR. The followings are the important conclusions drawn from the experimental studies:

- A maximum of 80% LFPO can be used in the form of a blend with diesel without any engine modification.
- The 40LFPO blend gives better performance and lower emissions than those of the other blends.
- The performance of the LFPO-diesel blend is lower, and the emissions are higher than those of diesel fuel operation in the same engine at all loads.
- The advanced injection timing of 26^{o}CA improved the performance and reduced the emissions of the diesel engine run on the 40LFPO blend.
- The addition of DEE improves the performance, combustion and reduces the smoke emissions.
- The addition of an oxygenated additive DMC in the range 1-10% to the 40LFPO blend improves the performance and combustion.
- The Y5 blend (i.e., 40% LFPO+10DMC+50% Diesel) gives better results in terms of performance, combustion and emissions compared to all the blends studied.

- The addition of more than 12% DMC to the 40LFPO blend produced a negative impact on the engine behavior.
- The smoke emission for the engine run with the internal jet piston for 40LFPO10DMC is about 13% lower compared to that of the base engine operation. The smoke emission for 40LFPO10DMC+IJP is the lowest among all the tested fuels in this study and 21.2% lower compared to that of diesel fuel at full load operation.
- The M+IJP+20EGR gives better results in terms of performance, combustion and lower emission compared to all the EGR rates studied.
- With increase in EGR rate, the SFC marginally increases and the BTE decreased.
- The CO_2 emission of 40LFPO10DMC+IJP and 40LFPO10DMC+IJP+20EGR with zeolite adsorbents are reduced by about4 0 and 48% respectively.
- The results of the visual inspection of carbon deposits on different engine components showed the traces of carbon deposits in the cylinder head, piston crown and injector nozzle tip of the engine fuelled with 40LFPO10DMC+IJP+ 20EGR blend.
- The marginal wear of the engine components is noticed in the case of fuel injection pump. The lubricating oil properties are found to be deteriorated with the 40LFPO10DMC+IJP+20EGR operation. This may be the lower lubricity offered by LFPO with the 20EGR operation of the engine.
- The weight of the pump barrel, spring plunger and pinion are decreasing by 0.92%, 1.42%, 1.58% and 2.22% after the durability test of the engine fuelled with 40LFPO10DMC+IJP+20EGR operation.
- The durability test after carbon deposits of cylinder head, piston crown and injector nozzle tip are approximately 3.2 and 1.5 mg, when diesel engine is fuelled with 40LFPO10DMC+IJP+20EGR blend respectively.

6.2 Scope for future work

The following areas are identified as the scope for future work related to the present study:

- Mathematical modelling is suggested for supporting the results theoretically.
- 40LFPO10DMC can be used with an internal jet piston operation, with modification of engine such as, different injection timings, nozzle opening pressures, compression ratios.

- CO_2 capture by other adsorbents such as membranes, activated carbons can be used to capture CO_2.
- CFD analysis of the tail pipe can be carried out for better understanding of back pressure.
- The LFPO can be tested in an automotive engine and in gen sets.
- An attempted will be made to reduce acid value of LFPO and then the pretreated LFPO will be tested in both single cylinder and multi cylinder diesel engine.

APPENDICES

Appendix I: Sutiable materials for injector components for wood PL engine operation.

Componets	Required properties	Selected properties / materials
Nozzle body	Corrosion resistance, ability to withstand high temoerature at 260^{o}C, strength 1200 N/mm2, hardness >61HRc	Martensic stainless steel [M390], with a composition of C1.90%, Cr 20%, Mo(%), V(4%) and 0.6% W; which can bethrough hardened to achieve a 62HRc and can withstand upto 500^{o}C.
Injector holders and bodies	--	X35CrMo17-A martesntic steel with a UTS value of 750-900 N/mm^{2} and 49 RHc
Pushrods and needls		X90CrMoV18(AISI 4408) stoff 1.4112 martestic stanless steel, 57 HRc
Springs		Stoff1.4310 austentic stanless stell 600-900 N/mm^{2} UTS.
Sealing		EPDM and tefflon O rings. Viton O rings react with wood PL which causes material expansion. Copper is suitable as washers.

Appendix II: Details of the test engine

Item	**Specification**
Make/model	Kirloskar TAF 1
Brake power (kW)	4.4
Rated speed (rpm)	1500
Bore (mm)	87.5
Stroke (mm)	110
Piston type	Bowl-in-piston
Compression ratio	17.5:1
Nozzle opening pressure (bar)	200
Injection timing	23 BTDC
Nozzle type	Multi holes
Number of holes	3
Cooling system	Air cooling

Appendix III: Specification of the AVL DiGas 444 analyzer

Item	**Measuring range**	**Accuracy**
CO	0-10%	±0.03% vol< 0.6% vol ± 5% of individual value, otherwise
CO_2	0-20%	±0.05% for vol < 10% ≥ 10% vol: ± 5%
HC	0-20000 ppm vol	± 10 for ppm vol < 200 ± 5%, Otherwise
O_2	0-22% vol	< 2% vol: ±0.01% vol ≥ 2% vol: ± 5% of vol
NO	0-5000 ppm vol	< 500 ppm vol: ± 50 ppm vol ≥ 500 ppm vol: ± 10% of initial value
Voltage	11-22 V, DC	
Power consumption	≈25 W	
Warm up time	≈ 7 min	
Operating temperature	5-45^{o}C	
Dimensions (WxDxH)	270 mm x 320 mm x 85 mm	
Weight	4.5 kg net weight without accessories	

Appendix IV: Technical specification of AVL 437C diesel smoke meter

Description	Data
Measuring chamber	0-100% opacity
Accuracy and repeatability	±1% of full scale
Alarming signal temperature	Lights up when temperature of measuring chamber is below 70^{o}C
Linearity check	48.4% - 53.1% or 1.54 m^{-1} - 1.54 m^{-1} of measurement range
Measuring chamber length	430 ± 5 mm
Light source	Halogen lamp, 12V
Sensor	Selenium Photocell
Weight	24 kg

Appendix V: Specification of KISTLER piezo-quartz pressure sensor

Description	Data
Model	KISTLER, Switzerland 601 A, air cooled
Range	0-100 bar
Sensitivity	25 mV/bar
Linearity	0.1 < + % FSO
Acceleration sensitivity	< 0.001 bar / g
Operating temperature range	-196 to 200 ^{o}C
Capacitance	5 PF
Weight	1.7 g
Connector, Teflon insulator	M4 x 0.35

Appendix VI: Specification of the charge amplifier

Description	Data
Make	KISLTER instruments, Switzerland
Measuring ranges	12 stages graded p C 10-50000 1:2:5 and step less 1 to 10
Accuracy of two most sensitive ranges Accuracy of other range stages	<± 3% <± 1%
Linearity of transducer sensitivity	<±0.5%
Calibration capacitor	1000 ± 0.5pF
Operating temperature range	-196 to 200 ^{o}C
Calibration input sensitivity	1±0.5 pC/mV
Input voltage, maximum with pulses	+ 12V
Connector, Teflon insulator	M4 x 0.35

Appendix VII: Range, accuracy and uncertainty of instruments

Instrument	Parameter measured	Range	Accuracy	Uncertainty (%)
Temperature indicator (^{o}C)	Temperature	0-900	±1	±0.15
Load indicator (W)	Engine load	250-6,000	±10	±0.2
Burette (cm^{3})	Fuel volume	1-30	±0.2	±0.5
Speed sensor (rpm)	Engine speed	0-10,000	±10	±1
Pressure transducer (bar)	In-cylinder pressure	0-110	±0.1	±0.15
Crank angle encoder (degree)	Crank position	0-720	±0.6	±0.01
Exhaust gas analyser	CO (%) HC(ppm) NO (ppm)	0-10 0-20,000 0-5,000	0.03 ±1 ±50	±1 ±0.5 ±1
Smoke meter (%)	Smoke opacity	0-100	±1	±1
Data acquisition system (bit)	Converts signal to digital values	64	±0.1	±0.001

References

[1] http://www.epa.gov/region2/superfund/green-remediation/policy.html.

[2] Y. C. Chang, W. J. Lee, L. C. Wang, H. H. Yang, M. T. Cheng, J. H. Lu, Y. I. Tsai and L. H. Young, "Effects of waste cooking oil-based biodiesel on the toxic organic pollutant emissions from a diesel engine", *Applied Energy,* vol. 113, pp. 631-638, 2014.

[3] R. Taylor and A. Allen, "Waste Disposal and Landfill: Information Needs", Chapter 12, pp. 1- 22, 2006.

[4] S. Murugan and S. Gu, "Research and development activities in pyrolysis - Contributions from Indian scientific community: A review", *Renewable and Sustainable Energy Reviews*, vol. 46, pp. 282-295, 2015.

[5] "Urban waste management strategy, international environmental technology centre", *United Nations Environment Program*, pp. 1-14, 2003.

[6] J. I. Reisman, E.H. Pechan and Inc. Associates, "Air emissions from scrap tire combustion", *United States Environmental Protection Agency,* EPA-600/R-97-115 1997.

[7] Y. M. Chang, "On pyrolysis of waste tire: degradation rate and product yields", *Resources, Conservation and Recycling,* vol. 17, no. 2, pp. 125-139, 1996.

[8] A. Zabaniotou, P. Madau, P. D. Oudenne, C. G. Jung, M. P. Delplancke and A. Fontana, "Active carbon production from used tire in two-stage procedure: industrial pyrolysis and bench scale activation with H_2O-CO_2 mixture", *Journal of Analytical and Applied Pyrolysis*, vol. 72, no. 2, pp. 289-297, November 2004.

[9] R. Prakash, R. K. Singh and S. Murugan, "Performance and emission studies in a diesel engine using bio oil-diesel blends", *Second International Conference on Environmental Science and Technology (ICEST 2011)*, Singapore, vol. 6, pp. 428-433, February 26-28, 2011.

[10] G. Lopez, M. Olazar, R. Aguado, G. Elord, M. Amutio, M. Artetxe and J. Bilbao, "Vacuum pyrolysis of waste tyres by continuously feeding into a conical spouted bed reactor", *Industrial and Engineering Chemistry Research*, vol. 49, no. 19, pp. 8990-8997, 2010.

[11] C. Roy, A. Chaala and H. Darmstadt, "The vacuum pyrolysis of used tires: End-uses for oil and carbon black products", *Journal of Analytical and Applied Pyrolysis,* vol. 51, no. 1, pp. 201-221, 1999.

[12] G. Lopez, R. Aguado, M. Olazar, M. Arabiourrutia and J. Bilbao, "Kinetics of scrap tyre pyrolysis under vacuum conditions", *Waste Management*, vol. 29, no. 10, pp. 2649-2655, October 2009.

[13] R. E. Raj, Z. R. Kennedy and B. C. Pillai, "Optimization of process parameters in flash pyrolysis of waste tyres to liquid and gaseous fuel in a fluidized bed reactor", *Energy Conversion and Management,* vol. 67, pp. 145-151, 2013.

[14] T. Araki, K. Niikawa, H. Hosoda, H. Nishizaki, S. Mitsui, K. Endoh and K. Yoshida, "Development of fluidized-bed pyrolysis of waste tyres", *Conservation and Recycling,* vol. 3, no. 2, pp. 155-164, 1979.

[15] W. Kaminsky, M. Predel and A. Sadiki, "Feedstock recycling of polymers by pyrolysis in a fluidised bed", *Polymer Degradation and Stability*, vol. 85, no. 3, pp. 1045-1050, September 2004.

[16] V. A. Kalitko, "Steam thermolysis of tyre shreds: modernization in afterburning of accompanying gas with waste steam", *Journal of Engineering Physics and Thermo Physics,* vol. 83, no. 1, pp. 179-187, March 2010.

[17] N. A. Dung, S. Wongkasemjit and S. Jitkarnka, "Effects of pyrolysis temperature and Pt-loaded catalysts on polar-aromatic content in tyre-derived oil", *Applied Catalysis B: Environmental*, vol. 91, pp. 300-307, 2009.

[18] C. Witpathomwong, R. Longloilert, S. Wongkasemjit and S. Jitkarnka, "Improving light olefins and light oil production using Ru/MCM-48 in catalytic pyrolysis of waste Tyre", *Energy Procedia*, vol. 9, pp. 245-251, 2011.

[19] J. Dodds, W. F. Domenic, D. R. Evans, L. W. Fish, P. L Lassahn and W. J. Toth, "Scrap tyres: a resource and technology evaluation of tyre pyrolysis and other selected alternative technologies", *US Department of Energy*, EGG-2241, November 1983.

[20] A. M. Cunliffe and P. T. Williams, "Composition of oils derived from the batch pyrolysis of tires", *Journal of Analytical and Applied Pyrolysis*, vol. 44, no. 2, pp. 131-52, 1998.

[21] A. V. Bridgwater and G. V. C. Peacocke. "Fast pyrolysis processes for biomass", *Renewable and Sustainable Energy Reviews,* vol. 4, no. 1, pp.1-73, 2000.

[22] J. A. Fairburn, L. A. Behie and W. Y. Svrcek, "Ultrapyrolysis of n-hexadecane in a novel micro-reactor", *Fuel,* vol. 69, no. 12, pp. 1537-1545, 1990.

[23] P. T. Williams and A. J. Brindle, "Catalytic pyrolysis of tyres: influence of catalyst temperature", *Fuel,* vol. 81, no. 18, pp. 2425-2434, 2002.

[24] Y. Kar, "Catalytic pyrolysis of car tire waste using expanded perlite", *Waste Management*, vol. 31, no. 8, pp. 1772-1782, 2011.

[25] X. Zhang, T. Wang, L. Ma, and J. Chang, "Vacuum pyrolysis of waste tires with basic additives", *Waste Management*, vol. 28, no. 11, pp. 2301-2310, 2008.

[26] N. A. Dung, R. Klaewkla, S. Wongkasemjit and S. Jitkarnka, "Light olefins and light oil production from catalytic pyrolysis of waste tire", *Journal of Analytical and Applied Pyrolysis*, vol. 86, no. 2, pp. 281-286, November 2009.

[27] I. F. Elbaba, C. Wu, and P. T. Williams, "Catalytic pyrolysis-gasification of waste tire and tire elastomers for hydrogen production", *Energy and Fuels*, vol. 24, pp. 3928-3935, 2010.

[28] R. Prakash, R. K. Singh and S. Murugan, "Experimental investigation on diesel engine fueled with bio-oil derived from waste wood-biodiesel emulsions", *Energy,* vol. 55, pp. 610-618, 2013.

[29] R. Prakash, R. K. Singh and S. Murugan, "Experimental investigation on diesel engine fueled by biodiesel and its emulsions with wood pyrolysis oil", *International Journal of Green Energy*, vol. 9, pp. 749-765, 2012.

[30] A. V. Bridgwater, A. J. Toft and J. G. Brammer, "Techno-economic comparison of power production by biomass fast pyrolysis with gasification and combustion", *Renewable and Sustainable Energy Reviews*, vol. 6, no. 3, pp. 181-246, 2002.

[31] M. K. Jamil and F.Nasir, "Pyrolysis Rubber Oil as an Alternative Renewable Fuel in Diesel Engines", *Proceedings of Fifth Asia Pacific International Symposium on Combustion and Energy*, China, Shanghai, October 24-29, 1999, pp. 38-43, 1999.

[32] A. Sarkar and R. Chowdhury, "Studies on catalytic pyrolysis of mustard seed press cake with NaCl", *International Journal of Engineering Sciences and Research Technology*, vol. 3, no. 6, pp. 90-96, 2014.

[33] M. R. Islam, H. Haniu and M. R. A. Beg, "Liquid fuels and chemicals from pyrolysis of motorcycle tire waste: product yields, compositions and related properties", *Fuel*, vol. 87, no. 13, pp. 3112-3122, 2008.

[34] A. Chaala and C. Roy, "Production of coke from scrap tyre vacuum pyrolysis oil", *Fuel Processing Technology*, vol. 46, no. 3, pp. 227-239, 1996.

[35] I. de M. Rodriguez, M.F. Laresgoiti, M.A. Cabrero, A. Torres, M. J. Chomon and B. Caballero, "Pyrolysis of Scrap Tyres", *Fuel Processing Technology*, vol. 72, no. 1, pp. 9-22, 2001.

[36] A. A. Zabaniotou and G. Stavropoulos, "Pyrolysis of Used Automobile Tyres and Residual Char Utilization", *Journal of Analytical and Applied Pyrolysis*, vol.70, no. 2, pp. 711-722, 2003.

[37] S. Ucara, S. Karagoza, A. R. Ozkanb and J. Yanikc, "Evaluation of two different scrap tyres as hydrocarbon source by pyrolysis", *Fuel*, vol. 84, pp. 1884-1892, 2005.

[38] A. Ayanoglua and R. Yumrutas, "Rotary kiln and batch pyrolysis of waste tire to produce gasoline and diesel like fuels", *Energy Conversion and Management*, vol. 111, pp. 261-270, 2016.

[39] E. E. Kwona, J.I. Ohb and K. H. Kimc, "Polycyclic aromatic hydrocarbons (PAHs) and volatile organic compounds (VOCs) mitigation in the pyrolysis process of waste tires using CO_2 as a reaction medium", *Journal of Environmental Management*, vol. 160, pp. 306-311, 2015.

[40] I. Hita, A. Gutiérrez, M. Olazar, J. Bilbao, J. M. Arandes and P. Castaño, "Upgrading model compounds and scrap tires pyrolysis oil (STPO) on hydrotreating NiMo catalysts with tailored supports", *Fuel*, vol. 145, pp. 158-169, 2015.

[41] I. Hita, T. Cordero-Lanzac, A. Gallardo, J. M. Arandes, J. Rodríguez-Mirasol, J. Bilbao, T. Cordero and P. Castaño, "Phosphorus-containing activated carbon as acid support in a bifunctional Pt-Pd catalyst for tire oil hydrocracking", *Catalysis Communications*, vol. 78, pp. 48-51, 2016.

[42] N. Jantaraksa, P. Prasassarakich, P. Reubroycharoen and N. Hinchiranan, "Cleaner alternative liquid fuels derived from the hydrodesulfurization of waste tire pyrolysis oil", *Energy Conversion and Management,* vol. 95, pp. 424-434, 2015.

[43] A. K. Panda, "Studies on process optimization for production of liquid fuels from waste plastics", *PhD dissertation*, 2011, (ethesis.nitrkl.ac.in/3850/1/PhD-Thesis-A-K-Panda.pdf).

[44] R. Babu, "Recovery of liquid hydrocarbon fuels from waste plastics", *M.Tech dissertation*, *NIT Rourkela*, 2007.

[45] A. K. Panda, D. K. Mishra and R. K. Singh, "Catalytic performances of kaolin and silica alumina in the thermal degradation of polypropylene", *Journal of Fuel Chemistry and Technology*, vol. 39, pp. 198-202, 2011.

[46] A. K. Panda and R. K. Singh, "Experimental optimization of process for the thermo-catalytic degradation of waste polypropylene to liquid fuel", *Advances in Energy Engineering (AEE)*, vol. 1, no. 3, pp. 74- 84, 2013.

[47] A. K. Panda, D. K. Mishra, B. G. Mishra and R. K. Singh, "Effect of Sulphuric acid treatment on the physicochemical characteristics of kaolin clay, colloids and surfaces", *A: Physicochemical and Engineering Aspects*, vol. 363, no. 20, pp. 98-104, June 2010.

[48] A. Raja and A. Murali, "Conversion of plastic wastes into fuels", *Journal of Materials Science and Engineering*, ISSN 1934-8959, 2011.

[49] S. Kumar and R. K. Singh, "Recovery of hydrocarbon liquid from waste high density polyethylene by thermal pyrolysis", *Brazilian Journal of Chemical Engineering*, vol. 28, no. 4, pp. 659 – 667, October-December 2011.

[50] S. Kumar and R. K. Singh, "Thermolysis high density polyethelyene to petroleum products", *Journal of Petroleum Engineering*, pp. 7, 2013, Article ID 987568.

[51] S. Kumar and R. K. Singh, "Thermolysis of high-density polyethylene to petroleum products", *Journal of Petroleum Engineering*, pp. 1-7, 2013, Article ID 987568.

[52] S. Kumar and R. K. Singh, "Pyrolysis kinetics of waste high-density Polyethylene using thermo gravimetric analysis", *International Journal of Chemical Technology Research*, vol. 6, no. 1, pp. 131-137, 2014.

[53] S. Kumar, R. Prakash, S. Murugan and R. K. Singh, "Performance and emission analysis of blends of waste plastic oil obtained by catalytic pyrolysis of waste HDPE with diesel in a CI engine", *Energy Conversion and Management*, vol. 74, pp. 323-331, 2013.

[54] C. Cleetus, S. Thomas and S. Varghese, "Synthesis of petroleum based fuel from waste plastics and performance analysis in a CI engine", *Journal of Energy*, Article ID 608797, http://dx.doi.org/10.1155/2013/608797, 2013.

[55] R. Guntur, M. L. S. Deva Kumar and K. Vijaya Kumar Reddy, "Experimental evaluation of a diesel engine with blends of diesel-plastic pyrolysis oil", *International Journal of Engineering Science and Technology* (IJEST), vol. 3, no. 6, pp. 5033-5040, 2011.

[56] B. Parasuram, S. Karthikeyan and S. Sundram, "Catalytic pyrolysis of polystyrene waste using bentonite as a catalyst", *Journal of Environment Nano Technology*, vol. 2, pp. 97-100, 2013.

[57] Y. Liu, J. Qian and J. Wang, "Pyrolysis of polystyrene waste in a fluidized-bed reactor to obtain styrene monomer and gasoline fraction", *Fuel Processing Technology*, vol. 63, no. 1, pp. 45-55, 2000.

[58] C. G. Lee, Y. J. Cho, P. S. Song, Y. Kang, J. S. Kim and M. J. Choi, "Effects of temperature distribution on the catalytic pyrolysis of polystyrene waste in a swirling fluidized-bed reactor", *Catalysis Today*, vol. 79-80, pp. 453-464, 2003.

[59] J. D. Martínez, A. Veses, A. M. Mastral, R. Murillo, M. V. Navarro, N Puy, A. Artigues, J. Bartrolí and T. García, "Co-pyrolysis of biomass with waste tyres: Upgrading of liquid bio-fuel", *Fuel Processing Technology*, vol. 119, pp. 263-271, 2014.

[60] P. Duan, B. Jin, Y. Xu and F. Wang, "Co-pyrolysis of microalgae and waste rubber tire in supercritical ethanol", *Chemical Engineering Journal*, vol. 269, pp. 262-271, 2015.

[61] K. Z. Rober and K. Prakash, "Characterization pyrolysis oils from conventional fixed bed reactor", *Journal of Energy and Fuel Users*, pp. 1-10, September 2006.

[62] R. C. Prabhakar, "Studies on droplet size measurement and engine performance using non edible oils as alternate fuels", *Proceedings of the IC Engines and Combustion Conference*, pp. 197-204, 1999.

[63] A. R. Arankalle, V. G. Kenjale, M. K. Chaudhari and B. Bhanot, "Significance of flash point in diesel fuel specification", *SAE Paper*, pp. 508-514, 2004. 10.4271/2004-28-0078.

[64] V. Ganesan, *Internal Combustion Engines.* Second Edition, Tata Mc Graw Hill Publications, New Delhi, 2003.

[65] Y. Akasaka and Y. Sakurai, "Effects of fuel properties on exhaust emission from DI diesel engine", *JSME International Journal Series B*, vol. 41, no.1, pp. 13-18, 1998.

[66] S. Murugan, M. C. Ramaswamy and G. Nagarajan, "A comparative study on the performance, emission and combustion studies of a DI diesel engine using distilled tyre pyrolysis oil-diesel blends", *Fuel*, vol. 87, no. 10, pp. 2111-2121, 2008.

[67] D. Pradhan and R. K. Singh, "Bio-oil from biomass: thermal pyrolysis of mahua seed", *Energy Efficient Technologies for Sustainability (ICEETS), 2013 International Conference*, pp. 487-490, 2013.

[68] R. E. Raj, Z. R. Kennedy and B. C. Pillai, "Optimization of process parameters in flash pyrolysis of waste tyres to liquid and gaseous fuel in a fluidized bed reactor", *Energy Conversion and Management,* vol. 67, pp. 145-151, 2013.

[69] A. Sharma and S. Murugan, "Investigation on the behaviour of a DI diesel engine fueled with Jatropha methyl ester (JME) and tyre pyrolysis oil (TPO)", *Fuel*, vol. 108, pp. 699-708, 2013.

[70] P. M. Bhatt and P. D. Patel, "Suitability of tyre pyrolysis oil (TPO) as an alternative fuel for internal combustion engine", *International Journal of Advanced Engineering Research and Studies,* vol. 4, pp. 61-65, 2012.

[71] B. Challen and R. Baranescu, "Diesel engine reference book", *Society Of Automotive Engineers*, England, 1999.

[72] N. A. Chigier, *Energy and Combustion Science*, University of Sheffield, England, 1975.

[73] L. Terry, B. Kent and L. M. Robert, "Effects of cetane number and cetane improver on emissions from 1991 heavy duty-diesel engine emissions with exhaust catalyst", *SAE paper*, No. 902171, 1990.

[74] B. Kent, L. Terry, L. Ullman and L. M. Robert, "Effects of cetane number, cetane improver, aromatics and oxygenates on 1994 heavy duty-diesel engine emission with exhaust catalyst", *SAE paper,* No.95020, 1995.

[75] B. Kent, L. Terry, L. Ullman and L. M. Robert, "Effects of cetane number, cetane improver, aromatics and oxygenates on 1994 heavy duty-diesel engine emissions", *SAE paper*, No.941020, 1994.

[76] N. Govindan, S. Renganarayanan and A. N. Rao, "Emission and performance characteristics of neat ethanol fueled di diesel engine", *International Journal of Ambient Energy*, vol. 23, no. 3, pp. 149-158, 2002.

[77] Z. Huang, H. B. Lu, D. M. Jiang, K. Zeng, B. Liu, J. Q. Zhang and X. B. Wang, "Combustion characteristics and heat release analysis of a compression ignition engine operating on a diesel/methanol blend", *Proceedings of the Institution of Mechanical Engineers Part D Journal of Automobile Engineering*, vol 218, no.9, pp. 1011-1024, 2004.

[78] Y. Luo, I. Ahmed, A.Kubátová, J. Šťávová, T. Aulich, S. M. Sadrameli and W.S. Seames, "The thermal cracking of soybean/canola oils and their methyl esters", *Fuel Processing Technology*, vol. 91, pp. 613-617, 2010.

[79] P. Pradhan, H. Raheman and D. Padhee, "Combustion and performance of a diesel engine with preheated Jatropha curcas oil using waste heat from exhaust gas", *Fuel*, vol. 115, pp. 527-533, 2014.

[80] R. Parvizsedghy, S. M. Sadrameli and J. T. Darian, "Upgraded biofuel diesel production by thermal cracking of castor biodiesel", *Energy Fuels,* vol. 30, 326-333, 2016.

[81] L. Broering and L. Holtman, "Effect of diesel fuel properties on emissions and performance", *SAE Technical Paper 740692*, 1974, doi:10.4271/740692.

[82] C. F. Taylor, *Internal Combustion Engines*. Second Edition, Seranton, Pennsylvania: International Text Book Company, 1989.

[83] N. Ladommatos, M. Parsi and A. Knowles, "The Effect of fuel cetane improver on diesel pollutant emissions", *Fuel*, vol. 75, no. 1, pp. 8-14, 1996.

[84] M. Mbarawa, B. E. Milton, R. T. Casey and H. Miao, "Fuel injection characteristics of diesel stimulated natural gas combustion", *International Journal of Energy Research*, vol. 23, no. 15, pp. 1359-71, 1999.

[85] H. Watanabe, T. Tahara, M. Tamanouchi and J. Iida, "Study on the effects on exhaust emissions in direct injection diesel engines: Effect of fuel injection system, distillation properties and cetane number", *JSAE Review*, vol. 19, no. 1, pp. 21-26, 1998.

[86] Y. Solantausta, N. O. Nylund, M. Westerholm, T. Koljonen and A. Oasmaa, "Wood-pyrolysis oil as fuel in a diesel-power plant", *Bioresource Technology*, vol. 46, no. 1-2, pp. 177-188, 1993.

[87] S. Frigo, R. Gentil, L. Tognotti, S. Zanforlin and G. Benelli "Feasibility of using flash wood pyrolysis oil in diesel engines", *SAE Technical Paper* 982529, 1998, doi:10.4271/982529.

[88] C. Bertoli, J. D'Alessio, N. Del Giacomo, M. Lazzaro, P. Massoli and V. Moccia, "Running light duty di diesel engines with wood pyrolysis oil", *SAE Technical Paper 2000-01-2975*, 2000*,* doi:10.4271/2000-01-2975.

[89] R. Prakash, "Experimental studies on a di diesel engine fueled with jatropha methyl ester-wood pyrolysis oil emulsions", Ph.D Thesis, NIT Rourkela, 2013.

[90] M. Mani, G. Nagarajan and S. Sampath, "Characterisation and effect of using waste plastic oil and diesel fuel blends in compression ignition engine", Energy, vol. 36 pp. 212-219, 2011.

[91] M. Mani, S. Subash and G. Nagarajan, "Performance, emission and combustion characteristics of a DI diesel engine using waste plastic oil", *Applied Thermal Engineering*, vol. 29, pp. 2738-2744, 2009.

[92] M. Mani and G. Nagarajan, "Influence of injection timing on performance, emission and combustion characteristics of a DI diesel engine running on waste plastic oil", *Energy*, vol. 34, pp. 1617-1623, 2009.

[93] M. Mani, G. Nagarajan and S. Sampath, "An experimental investigation on a DI diesel engine using waste plastic oil with exhaust gas recirculation", *Fuel*, vol. 89, pp. 1826-1832, 2010.

[94] S. Murugan, M. R. C. Ramaswamy, Nagarajan and G. Natarajan, "Influence of distillation on performance, emission, and combustion of a di diesel engine, using tyre pyrolysis oil diesel blends", *Thermal Science*, vol. 12, no. 1, pp. 157-167, 2008.

[95] S. Murugan, M. C. Ramaswamy and G. Nagarajan, "Assessment of pyrolysis oil as an energy source for diesel engines", *Fuel Processing Technology*, vol. 90, no. 1, pp. 67-74, 2009.

[96] S. Hariharan, S. Murugan and G. Nagarajan, "Effect of diethyl ether on tyre pyrolysis oil fueled diesel engine", *Fuel*, vol. 104, pp. 109-115, 2013.

[97] O. Dogan, M. B. Çelik and B. Özdalyana, "The effect of tire derived fuel/diesel fuel blends utilization on diesel engine performance and emissions", *Fuel*, vol. 95, pp. 340-346, 2012.

[98] A. B. Koc and M. Abdullah, "Performance of a 4-cylinder diesel engine running on tire oil-biodiesel-diesel blend", *Fuel Processing Technology*, vol. 118, pp. 264-269, 2014.

[99] S. Frigo, M. Seggiani, M. Puccini and S. Vitolo, "Liquid fuel production from waste tyre pyrolysis and its utilization in a Diesel engine", *Fuel*, vol. 116, pp. 399-408, 2014.

[100] J. D. Martínez, J. Rodríguez-Fernández, J. Sánchez-Valdepeñas, R. Murillo and T. García, "Performance and emissions of an automotive diesel engine using a tire pyrolysis liquid blend", *Fuel*, vol. 115, pp. 490-499, 2014.

[101] J. D. Martínez, Á. Ramos, O. Armas, R. Murillo and T. García, "Potential for using a tire pyrolysis liquid-diesel fuel blend in a light duty engine under transient operation", *Applied Energy*, vol. 130, pp. 437-446, 2014.

[102] W. C. Wang, C. J. Bai, C. T. Lin and S. Prakash, "Alternative fuel produced from thermal pyrolysis of waste tires and its use in a DI diesel engine", *Applied Thermal Engineering*, vol. 93, pp. 330-338, 2016.

[103] A. Sarkar, M. Langanaki and R. Chouwdhry, "Studies on pyrolysis of spent engine oil in a quartz load cell", *International Journal of Research in Engineering and Technology*, vol. 3, no. 6, pp. 221-226, 2014.

[104] L.U. Qiang, Z.Jian and Z.Xifeng, "Corrosion properties of bio-oil and its emulsions with diesel", *Chinese Science Bulletin,*vol.53,pp.3726-3734, 2008.

[105] D.C. Jay, K.H. Sipla, O.A. Rantanen and N. Nylun, "Wood pyrolysis oil for diesel engine", *In:Proceedings of the 17th annual fall technical conference of the ASME IC engine division*, Milwaukee, Wisconsin; September 24-27, 1995.

[106] A.K. Hossain, P.A. Davies, "Pyrolysis liquid and gases as alternative fuels in internal combustion engines- A review", *Renewable and sustainable energy reviews*,vol. 21,pp. 165-189, 2013.

[107] N. Nhlanhla and M. Edison, "A Review and disscussion of waste tyres pyrolysis and derived products", *Proceedings of the World Congress on Engineering*, London, U.K., vol. 2, WCE 2014, July 2- 4, 2014.

[108] New Maxico state University, College of Arts and Sciences, Department of Chemistry and Biochemistry, http://web.nmsu.edu/~kburke/Instrumentation/FTIR-RX1.html.

[109] F. Douglas, "GC/MS Analysis", Scientific Testimony an online journal, 2004.

[110] K. Owen, T. Coley, C. S. Weaver and K.Owen, "Automotive fuels reference book", *PA, Society of Automotive Engineers*, 1995.

[111] Tat, E. Mustafa, H. Jon and V. Gerpen. "The kinematic viscosity of biodiesel and its blends with diesel fuel," *Journal of the American Oil Chemists' Society 76.12,* pp. 1511-1513, 1999.

[112] D. Craecker and Roger, "Method and apparatus for measuring cetane number of diesel fuel." *U.S. Patent no. 6,609,413*, 26 August, 2003.

[113] V. R. Mamilla, M. V. Mallikarjun and G. L. N. Rao, "Prediction of Cetane Number for Biodiesel Fuels: Karanja, Jatropha, Sunflower, Palm and Waste Cooking Oil Methyl Esters", *CiiT International Journal of Artificial Intelligent Systems and Machine Learning*, February 2013.

[114] S. Murugan, M. C. Ramaswamy and G. Nagarajan, "The use of tyre pyrolysis oil in diesel engines", Waste Management, vol. 28, pp. 2743-2749, 2008.

[115] B. P. Pundir, "IC Engines Combustion and Emissions", *Narosa Publishing House, New Delhi*, 2013.

[116] J. P. Holman, "Experimental methods for engineers", *Mc Graw-Hill, Americas, New York*, 2012.

[117] T. A. D. E. U. S. Z. Malinski and L. E. S. Z. E. K. Czuchajowski, "Nitric oxide measurements by electrochemical methods", Methods of Nitric Oxide Research. New York, NY: John Wiley and Sons, pp. 319-339, 1996.

[118] R. K. Rajput, "A Text Book of Automobile Engineering", *Laxmi Publications, New Delhi*, 2005.

[119] R. B. Krieger and G. L. Borman, "The computation of apparent heat release in I. C. engines", *ASME*, Paper 66 WA/DGP4, 1966.

[120] S. Swami Nathan, J.M. Mallikarjuna and A. Ramesh, "An experimental study of the biogas–diesel HCCI mode of engine operation", *Energy Conversion and Management,* vol. 51, pp.1347-1355, 2010.

[121] J. B. Heywood, "Internal combustion engines fundamentals", *Mc Graw Hill, London*, 1989.

[122] H. W. Coleman and W. G. Steele Jr, "Experimentation and Uncertainty Analysis for Engineers", *John Wiley and Sons, New York*, 1989.

[123] D. C. Rakopoulos, C. D. Rakopoulos, E. G. Giakoumis, R. G. Papagiannakis and D. C. Kyritsis, "Influence of properties of various common bio-fuels on the combustion and emission characteristics of high-speed DI (direct injection) diesel engine: Vegetable oil, bio-diesel, ethanol, n-butanol, diethyl ether", *Energy*, vol. 73, pp. 354-366, 2014.

[124] L. Ruina, W. Zhong, N. Peiyong, Z. Yang, L. Mingdi and L. Lilin, "Effects of cetane number improvers on the performance of diesel engine fuelled with methanol/biodiesel blend", *Fuel*, vol. 128, pp. 180-187, 2014.

[125] D. Hansdah and S. Murugan, "Bioethanol fumigation in a DI diesel engine", *Fuel*, vol. 130, pp. 324-333. 2014.

[126] M. Karabektas, G. Ergen and M. Hosoz, "The effects of using diethyl ether as additive on the performance and emissions of a diesel engine fuelled with CNG", *Fuel*, vol. 115, pp. 855-860, 2014.

[127] S. S. Sayi Likhitha, B. Durga Prasad and Ch. R. Vikram Kumar, "Investigation on the effect of diethyl ether additive on the performance of variable compression ratio diesel engine", *International Journal of Engineering Research*, vol. 3, pp. 11-15, 2014.

[128] T. Lei, Z. Wang, X. Chang, L. Lin, X. Yan, Y. Sun, X. Shi, X. He and J. Zhu, "Performance and emission characteristics of a diesel engine running on optimized ethyl levulinate–biodiesel–diesel blends", *Energy*, vol. 95, pp. 29-40, 2016.

[129] A. K. Wamankar and S. Murugan, "Effect of injection timing on a DI diesel engine fuelled with a synthetic fuel blend", *Journal of the Energy Institute*, vol. 88, no. 4, pp. 406-413, 2015.

[130] L. Xing-cai, Y. Jian-Guang, Z. Wu-Gao and H. Zhen, "Effect of cetane number improver on heat release rate and emissions of high speed diesel engine fueled with ethanol–diesel blend fuel", *Fuel,* vol. 83, no. 14, pp. 2013-2020, 2004.

[131] Y. Ren, Z. Huang, H. Miao, Y. Di, D. Jiang, K. Zeng, B. Liu and X. Wang, "Combustion and emissions of a DI diesel engine fuelled with diesel-oxygenate blends", *Fuel*, vol. 87, no. 12, pp. 2691-2697, 2008.

[132] D. Hansdah, B. Suna, and M. Sivalingam, "Experimental analysis of diesel engine fueled with e-diesel produced from madhuca indica flowers with the addition of an ignition improver", *SAE Technical Paper*, No. 2013-01-1700, 2013. doi:10.4271/2013-01-1700.

[133] R. Munsin, Y. Laoonual, S. Jugjai, M. Matsuki and H. Kosaka, "Effect of glycerol ethoxylate as an ignition improver on injection and combustion characteristics of

hydrous ethanol under CI engine condition", *Energy Conversion and Management*, vol. 98, pp. 282-289, 2015.

[134] I. Sezer, "Thermodynamic, perfomance and emission investigation of a diesel engine running on dimethyl ether and diethyl ether", *International Journal of Thermal Science,* vol. 50, no.8, pp. 1594-1603, 2011.

[135] B. Bailey, J. Eberhardt, S. Goguen and J. Erwin, "Diethyl ether (DEE) as a renewable diesel fuel", *SAE Technical Paper 972978*, 1997, doi:10.4271/972978.

[136] W. Tutak, A. Jamrozik, M. Pyrc and M. Sobiepański, "Investigation on combustion process and emissions characteristic indirect injection diesel engine powered by wet ethanol using blend mode", *Fuel Processing Technology,*vol. 149, 86-95, 2016.

[137] K. R. Patil and S. S. Thipse, "Experimental investigation of CI engine combustion, Performance and emissions in DEE-kerosene-diesel blends of high DEE concentration", *Energy Conversion and Management*, vol. 89, pp. 396-408, 2015.

[138] K. Purushothaman and G. Nagarajan "Performance, emission and combustion characteristics of a compression ignition engine operating on neat orange oil", *Renewable Energy,*vol. 34, pp. 242-245, 2009.

[139] A. K. Wamankar and S. Murugan, "Experimental investigation of carbon black-water-diesel emulsion in a stationary DI diesel engine", *Fuel Processing Technology*, vol. 125, pp. 258-266, 2014.

[140] S. Imtenan, H. H. Masjuki, M. Varman, M. A. Kalam, M. I. Arbab, H. Sajjad and S. M. Ashrafur Rahman, "Impact of oxygenated additives to palm and jatropha biodiesel blends in the context of performance and emissions characteristics of a light-duty diesel engine", *Energy Conversion and Management*, vol. 83, pp. 149-158, 2014.

[141] A. Haiter lenin, N. Azhagesan, C. R. Berlin Selva Rex and K. Thyagarajan, "Performance of diesel engine operating with pongamia methyl ester as a biodiesel", *Asian Journal of Scientific Research*, vol. 5, pp. 153-161, 2012.

[142] M. V. Mallikarjun, V. R. Mamilla and G. Lakshmi Narayana Rao, "NOx emission control techniques when ci engine is fuelled with blends of mahua methyle esters and diesel", *International Journal of Engineering Sciences & Emerging Technologies*, vol. 4, no. 2, pp. 96-104, 2013.

[143] O. M. Ali, R. Mamat and C. K. M. Faizal, "Effects of diethyl ether additives on Palm biodiesel fuel characteristics and low temperature flow properties", *International Journal of Science and Technology*, vol. 52, pp. 111-120, 2013.

[144] D.C. Rakopoulos, "Combution and emission of cotton seed oil and its bio-diesel in blends with either n-butanol and diethyl ether in HSDI diesel engine", *Fuel*, vol. 105, pp. 603-613, 2013.

[145] S. Sivalaksmi and T. Balusamy, "Effect of biodiesel and its blends with oxygenated additives on performance and emission from a diesel engine", *Journal of Science and Industrial Research,* vol. 70, pp. 879-883, 2011.

[146] D. H. Qi, H. Chen, L. M. Geng and Y. Z. Bian, "Effect of diethyl ether and ethanol additives on the combustion and emission characteristics of biodiesel-diesel blended fuel engine", *Renewable Energy*, vol. 36, pp. 1252-1258, 2011.

[147] C. Cinar, O. Can, F. Sahin and H. S. Yucesu, "Effects of premixed diethyl ether on combustion and exhaust emissions in a HCCI-DI diesel engine", *Applied Thermal Engineering*, vol. 30, no. 4, pp. 360-365, 2010.

[148] S. Sudhakar and S. Sivaprakasam, "Effect of diethyl ether fumigation in di diesel engine using bio ethanol blended diesel", *International Journal of Innovation and Scientific Research*, vol. 11, pp. 65-71, 2014.

[149] K. Purushothaman and G. Nagarajan, "Experimental investigation on a C.I. engine using orange oil and orange oil with DEE", *Fuel*, vol. 88, no.9, pp. 1732-1740, 2009.
[150] Wikipedia, the free encyclopedia (diethyl ether). [Online]. Available: https://en.wikipedia.org/wiki/Diethyl-ether.
[151] J. Devaraj, Y. Robinson and P. Ganapathi, "Experimental investigation of performance, emission and combustion characteristics of waste plastic pyrolysis oil blended with diethyl ether used as fuel for diesel engine", *Energy*, vol. 85, pp. 304-309, 2015.
[152] Y. Zhao, Y. Wang, D. Li, X. Lei and S. Liu, "Combustion and emission characteristics of a DME (dimethyl ether)-diesel dual fuel premixed charge compression ignition engine with EGR (exhaust gas recirculation)", *Energy*, vol. 72, pp. 608-617, 2014.
[153] J. Hou, Z. Wen, Z. Jiang and X. Qiao, "Study on combustion and emissions of a turbocharged compression ignition engine fueled with dimethyl ether and biodiesel blends", *Journal of the Energy Institute*, vol. 87, no. 2, pp. 102-113, 2014.
[154] Y. Liang, G. Shu, H. Wei and W. Zhang, "Effect of oxygen enriched combustion and water-diesel emulsion on the performance and emissions of turbocharged diesel engine", *Energy Conversion and Management*, vol. 73, pp. 69-77, 2013.
[155] E. Hu, Y. Chen, Z. Zhang, L. Pan, Q. Li, Y. Cheng and Z. Huang, "Experimental and kinetic study on ignition delay times of dimethyl carbonate at high temperature", *Fuel*, vol. 140, pp. 626-632, 2015.
[156] D. Gopinath and E.G. Sundaram, "Experimental investigation on the effect of adding di methyl carbonate to gasoline in a si engine performance", *International Journal of Scientific & Engineering Research*, vol. 3, no. 6, pp.1-5, June-2012.
[157] A. R. Patil and S. G. Taji, "Effect of oxygenated fuel additive on diesel engine performance and emission: A Review", *IOSR Journal of Mechanical and Civil Engineering (IOSR-JMCE)*, ISSN(e) : 2278-1684, ISSN(p) : 2320–334X, pp. 30-35, 2013.
[158] L. Wen, C. Y. Xin and S. C. Yang, "The effects of adding dimethyl carbonate (DMC) and ethanol to unleaded gasoline on exhaust emission", *Applied Energy*, vol. 87, no.1, pp. 115-121, 2010.
[159] S. B. Prajapati, P. Rathod and N. K. Patel, "Effect of oxygenated fuel additives on performance and emission characteristics of CI engines - A review study", *Journal of Engineering Research and Studies*, E-ISSN0976-7916, pp. 108-110, 2012.
[160] R. Zhu, X. Wang, H. Miao, X. Yang and Z. Huang, "Effect of dimethoxy-methane and exhaust gas recirculation on combustion and emission characteristics of a direct injection diesel engine", *Fuel*, vol. 90, no.5, pp. 1731-1737, 2011.
[161] S. H. Park and C. S. Lee, "Applicability of dimethyl ether (DME) in a compression ignition engine as an alternative fuel", *Energy Conversion and Management*, vol. 86, pp. 848-863, 2014.
[162] L. Xiaolu, C. Hongyan, Z. Zhiyonga and H. Zhen, "Study of combustion and emission characteristics of a diesel engine operated with dimethyl carbonate", *Energy Conversion and Management*, vol. 47, no. 11-12, pp. 1438-1448, 2006.
[163] L. Wei, C. S. Cheung and Z. Huang, "Effect of n-pentanol addition on the combustion, performance and emission characteristics of a direct-injection diesel engine", *Energy*, vol. 70, pp. 172-180, 2014.
[164] H. Liu, Z. Wang, J. Wang, X. He, Y. Zheng, Q. Tang and J. Wang, "Performance, combustion and emission characteristics of a diesel engine fueled with

polyoxymethylene dimethyl ethers (PODE 3-4)/diesel blends", *Energy*, vol. 88, pp. 793-800, 2015.

[165] C. S. Cheung, S. C. Lee, A. Kwok and C. W. Tung, "Effect of dimethyl carbonate blended diesel on emissions of a 4-cylinder diesel engine", *Taylor and Francis*, vol. 12, no. 3, pp. 15-20, 2005.

[166] P. Tundo, "New developments in dimethyl carbonate chemistry", *Pure and Applied Chemistry*, vol. 73, no. 7, pp. 1117-1124, 2001.

[167] T. B. Shinde, "Experimental investigation on effect of combustion chamber geometry and port fuel injection system for CNG engine", *IOSR Journal of Engineering* (*IOSRJEN) ISSN*: 2250-3021, vol. 2, no. 7, pp. 49-54, July 2012.

[168] S. Jafarmadar and M. Khanbabazadeh, "A computational study of the effects of combustion chamber geometries on combustion process and emission in a DI diesel Engine", *Journal of Fuel and Combustion*, vol. 1, no. 1, pp. 1-16, 2008.

[169] A. M. Indrodia, N. J. Chotai and B. M. Ramani, "Investigation of different combustion chamber geometry of diesel engine using CFD modelling of in cylinder flow for improving the performance of engine", *5th International & 26th All India Manufacturing Technology, Design and Research Conference* (AIMTDR 2014), December 12th–14th, 2014, IIT Guwahati, Assam, India.

[170] M. N. channappagoudra, s. thaned, k. ramesh and g. manavendra, "Optimization of combustion chamber geometry for a direct injection diesel engine:A review", *International Journal of Engineering Research & Technology*, vol. 2, ISSN: 2278-0181, 2013.

[171] L. Ranganatha Swamy, T. K. Chandrashekar, N. R. Banapurmath and P. Nashipudi, "Effect of injection timing, combustion chamber shapes and nozzle geometry on the diesel engine performance", *Universal Journal of Petroleum Sciences*, vol. 2, pp. 74-95, 2014.

[172] D. B. Mercer, P. R. Amyotte, D. J. Dupuis, M. J. Pegg, A. Dahoe, W. B. C. Heij, J. F. Zevenbergen and B. Scarlett, "The influence of injector design on the decay of pre-ignition turbulence in a spherical explosion chamber", *Journal of Loss Prevention in the Process Industries*, vol. 14, no.4. pp. 269-282, 2001.

[173] C. R. Rajashekhar, T. K. Chandrashekar, C. Umashankar and R. H. Kumar, "Studies on effects of combustion chamber geometry and injection pressure on biodiesel combustion", *Transactions of the Canadian Society for Mechanical Engineering*, vol. 36, no. 4, pp. 429-438, 2012.

[174] C. Kirner, J. Halbhuber, B. Uhlig, A. Oliva, S. Graf and G. Wachtmeister, "Experimental and simulative research advances in the piston assembly of an internal combustion engine", *Tribology International*, vol. 99, pp.159-168, 2016.

[175] I. Saad and S. Bari, "Guide vane swirl and tumble device to improve in-cylinder air flow of CI engine using vegetable oil", *Procedia Engineering*, vol. 90, pp. 425-430, 2014.

[176] K. Rajan and K. R. Senthil kumar, "Reduction of NOx and smoke emissions on a diesel engine with internal jet piston using bio-diesel with exhaust gas recirculation (EGR) Technique", *International Journal on Design and Manufacturing Technology*, vol. 6, pp. 41-47, 2012.

[177] K. Rajan and K. R. Senthil Kumar, "Performance and emissions characteristics of a diesel engine with internal jet piston using biodiesel", *International Journal of Environmental Studies*, vol. 67, no. 4, pp. 557-566, 2010.

[178] B. R. kumar and S. Saravanan, "Effect of exhaust gas recirculation (EGR) on performance and emissions of a constant speed DI diesel engine fueled with pentanol/diesel blends", *Fuel*, vol. 160, pp. 217-226, 2015.

[179] L. Niranjan, S. Thomas and V. Sajith, "Experimental investigation on the effects of cold and hot EGR using diesel and bio-diesel as fuel", *Energy and Environment*, pp. 1-8, 2006.

[180] P. Saichaitanya, K. Simhadri and G. Vamsidurgamohan, "Impact of cold and hot exhaust gas recirculation on diesel engine", *International Journal of Engineering Research and Applications www.ijera.com*, vol. 3, no. 5, pp. 430-434, 2013.

[181] M. K. Mondal, H. K. Balsora and P. Varshney, "Progress and trends in CO_2 capture/separation technologies: A review", *Energy,* vol. 46, pp. 43-441, 2012.

[182] S. H. Yoon and C. S. Lee, "Experimental investigation on the combustion and exhaust emission characteristics of biogas biodiesel dual-fuel combustion in a CI engine", *Fuel Processing Technology*, vol. 92, pp. 992-1000, 2011.

[183] A. K. Agrawal, "Biofuels (alcohols and biodiesel) applications as fuels for internal combustion engines", *Progress in Energy and Combustion Science*, vol. 33, no. 3, pp. 233-271, 2007.

[184] D. Barik and S. Murugan, "Experimental investigation on the behavior of a DI diesel engine fueled with raw biogas -diesel dual fuel at different injection timing", *Journal of the Energy Institute*, doi:10.1016/j.joei.2015.03.002, 2015.

[185] D. Barik and S. Murugan, "Simultaneous reduction of NOx and smoke in a dual fuel DI diesel engine", *Energy Conversion and Management*, vol. 84, pp. 217-226, 2014.

[186] H. Raheman and S. V. Ghadge, "Performance of diesel engine with biodiesel at varying compression ratio and ignition timing", *Fuel*, vol. 87, no. 12, pp. 2659–2666, 2008.

[187] A. K. Wamankar and S. Murugan, "Effect of injection timing on a DI diesel engine fuelled with a synthetic fuel blend", *Journal of the Energy Institute*, vol.88, no. 4 pp. 406-413, 2015.

[188] S. A. Khabbaz and R. Mobasheri, "Experimental investigation of the effects of tri-aromatic utilization on combustion process, emission characteristics and engine performance of a DI diesel engine", *Fuel*, vol. 123, pp. 26-32, 2014.

[189] J. Pilusa and E. Muzenda, "Pyrolytic tyre derived fuel: potential diesel additive", *International Conference on Emerging Trends in Engineering and Technology (ICETET'2013),* Dec. 7-8, Patong Beach, Phuket (Thailand), pp. 143-147, 2013.

[190] A. K. Agarwal, D. K. Srivastava, A. Dhar, R. K. Maurya, P. C. Shukla and A. P. Singh, "Effect of fuel injection timing and pressure on combustion, emissions and performance characteristics of a single cylinder diesel engine", *Fuel*, vol. 111, pp. 374-383, 2013.

[191] A. Sharma and S. Murugan, "Combustion, performance and emission characteristics of a DI diesel engine fuelled with non-petroleum fuel: A study on the role of fuel injection timing", *Journal of the Energy Institute*, vol. 88, no. 4, pp. 364-375, 2015.

[192] G. Zhang, X. Qiao, X. Miao, J. Hong and J. Zheng, "Effects of highly dispersed spray nozzle on fuel injection characteristics and emissions of heavy-duty diesel engine", *Fuel*, vol. 102, pp. 666-673, 2012.

[193] L. Wei, C. Yao, G. Han and W. Pan, "Effects of methanol to diesel ratio and diesel injection timing on combustion, performance and emissions of a methanol port premixed diesel engine", *Energy*, vol.95, pp. 223-232, 2016.

[194] C. Sayin, M. Ilhan, M. Canakci and M. Gumus, "Effect of injection timing on the exhaust emissions of a diesel engine using diesel, methanol blends", *Renewable Energy*, vol. 34, pp. 1261-1269, 2009.

[195] Y. Kidoguchi, C. Yang, R. Kato and K. Miwa, "Effects of fuel cetane number and aromatics on combustion process and emissions of a direct injection diesel engine", *JSAE Review*, vol. 21, no. 4, pp. 469-475, 2000.

[196] P. Chaisermtawan, S. Jarungthammachote, S. Chuepeng and T. Kiatiwat, "Gaseous emissions and combustion efficiency analysis of hydrogen-diesel dual fuel engine under fuel-lean condition", *America Journal of Applied Science*, vol. 9, pp. 1813-1817, 2012.

[197] A. K. Wamankar and S. Murugan, "Combustion, performance and emission of a diesel engine fuelled with diesel doped with carbon black", *Energy*, vol. 86, pp. 467-475, 2015.

[198] O. M. Ali, R. Mamat, H.H. Masjuki and A. A. Abdullah, "Analysis of blended fuel properties and cycle-to-cycle variation in a diesel engine with a diethyl ether additive", *Energy Conversion and Management*,vol.108, pp. 511-519, 2016.

[199] V. K. Kaimal and P. Vijayabalan, "An investigation on the effects of using DEE additive in a DI diesel engine fuelled with waste plastic oil", *Fuel*, vol. 180, pp. 90-96, 2016.

[200] D. Barik and S. Murugan, "Effects of diethyl ether (DEE) injection on combustion performance and emission characteristics of Karanja methyl ester (KME)-biogas fuelled dual fuel diesel engine", *Fuel*, vol. 164, pp. 286-296, 2016.

[201] V. Edwin Geo, G. Nagarajan and B. Nagalingam, "Studies on improving the performance of rubber seed oil fuel for diesel engine with DEE port injection", *Fuel*, vol. 89, pp. 3559-3567, 2010.

[202] Y. Robinson, P. Ganapathi and J. Devaraj, "Experimental investigation of performance, emission and combustion characteristics of waste plastic pyrolysis oil blended with diethyl ether used as fuel for diesel engine", *Energy*, vol. 85, pp. 304-309, 2015.

[203] X. C. Lu, J. G. Yang, W. G. Zhang and Z. Huang, "Improving the combustion and emissions of direct injection compression ignition engines using oxygenated fuel additives combined with a cetane number improver", *Energy and Fuels*, vol. 19, pp. 1879-1888, 2005.

[204] J. Ghosel and D. Honnery, "Heat release model for the combustion of diesel oil emulsions in DI diesel engines", *Applied Thermal Engineering*, vol. 25, pp. 2072-2085, 2005.

[205] E. Hu, Y. Chen, Z. Zhang, L. Pan, Q. Li, Y. Cheng and Z. Huang, "Experimental and kinetic study on ignition delay times of dimethyl carbonate at high temperature", *Fuel*, vol. 140, pp. 625-632, 2015.

[206] R. Cataluna and R. Silva, "Effect of cetane number on specific fuel consumption and particulate matter and unburned hydrocarbon emissions from diesel engines", *Journal of Combustion Combust*, pp.1-6, http://dx.doi.org/10.1155/2012/738940 2012.

[207] J. Wang, F. Wu, J. Xiao and S. Shuai, "Oxygenated blend design and its effects on reducing diesel particulate emissions", *Fuel*, vol. 88, pp. 2037-2045, 2009.

[208] Z. H. Zhang and R. Balasubramanian, "Effects of oxygenated fuel blends on carbonaceous particulate composition and particle size distributions from a stationary diesel engine", *Fuel*, vol. 141, pp. 1-8, 2015.

[209] Diesel Technology Forum. http://www.dieselforum.org/index.cfm

[210] M. Happonen, J. Heikkilä, P. Aakko-Saksa, T.Murtonen, K. Lehto, A. Rostedt, T. Sarjovaara, M. Larmi, J. Keskinen and A. Virtanen, "Diesel exhaust emissions and particle hygroscopicity with HVO fuel-oxygenate blend", *Fuel*, vol. 103, pp.380-386, 2013.

[211] H. An, W. M. Yang, J. Li and D. Z. Zhou, "Modeling of oxygenated fuels on diesel combustion: Effect of oxygen concentration, cetane number and C/H ratio", *Energy Convers Manage*, vol. 90, pp. 261-271, 2015.

[212] A. K. Wamankar and S. Murugan, "Combustion, performance and emission characteristics of a diesel engine with internal jet piston using carbon black- water-diesel emulsion", *Energy*, vol. 91, pp. 1030-1037, 2015.

[213] J. I. J. R. Lalvani, M. Parthasarathy, B. Dhinesh and K. Annamalai, "Pooled effect of injection pressure and turbulence inducer piston on performance, combustion, and emission characteristics of a DI diesel engine powered with biodiesel blend", *Ecotoxicology and Environmental Safety*, doi:10.1016/j.ecoenv.2015.08.020, 2015.

[214] K. R. Kumar Senthil and P. S. Mehta, "Investigation on the improvement of diesel engine combustion through the use of fuel additives and in-cylinder turbulence inducements techniques", *PhD dissertation, IIT Madras*, 2004.

[215] B. R. Kumar, S. Saravanan, D. Rana, V. Anish and A. Nagendran, "Effect of a sustainable biofuel-n-octanol on the combustion, performance and emissions of a DI diesel engine under naturally aspirated and exhaust gas recirculation (EGR) modes", *Energy Conversion and Management*, vol. 118, pp. 275-286, 2016.

[216] A. Maiboom, X. Tauzia and J. F. Hetet, "Experimental study of various effects of exhaust gas recirculation (EGR) on combustion and emissions of an automotive direct injection diesel engine", *Energy*, vol. 33, no. 1, pp. 22-34, 2008.

[217] Ö. Can, E. Öztürk, H. Solmaz, F. Aksoy, C. Çinar and H. S. Yücesu, "Combined effects of soybean biodiesel fuel addition and EGR application on the combustion and exhaust emissions in a diesel engine", *Applied Thermal Engineering*, vol. 95, pp. 115-124, 2016.

[218] M. M. Abdelaal and A. H. Hegab, "Combustion and emission characteristics of a natural gas-fueled diesel engine with EGR", *Energy Conversion and Management*, vol. 64, pp. 301–312, 2012.

[219] Y. Zhao, Y. Wang, D. Li, X. Lei and S. Liu, "Combustion and emission characteristics of a DME (dimethyl ether)-diesel dual fuel premixed charge compression ignition engine with EGR (exhaust gas recirculation)", *Energy*, vol. 72, pp. 608-617, 2014.

[220] T. Lattimore, C. Wang, H. Xu, M. L. Wyszynski and S. Shuai, "Investigation of EGR effect on combustion and PM emissions in a DISI engine", *Applied Energy*, vol. 161, pp. 256–267, 2016.

[221] Z. Chen, Z. Wua, J. Liu and C. Lee, "Combustion and emissions characteristics of high n-butanol/diesel ratio blend in a heavy-duty diesel engine and EGR impact", *Energy Conversion and Management*, vol. 78, pp. 787–795, 2014.

[222] M. Zheng, G. T. Reader and J. G. Hawley, "Diesel engine exhaust gas recirculation-a review on advanced and novel concepts", *Energy Conversion and Management*, vol. 45, pp. 883-900, 2004.

[223] G. Zamboni, S. Moggia and M. Capobianco, "Hybrid EGR and turbocharging systems control for low NO_X and fuel consumption in an automotive diesel engine", *Applied Energy*, vol. 165, pp. 839-848, 2016.

[224] R. Verschaeren,W. Schaepdryver, T. Serruys, M. Bastiaen, L. Vervaeke and S. Verhelst, "Experimental study of NOx reduction on a medium speed heavy duty diesel engine by the application of EGR (exhaust gas recirculation) and Miller timing", *Energy*, vol.76, pp. 614-621, 2014.

[225] P. S. Divekar, X. Chen, J. Tjong and M. Zheng, "Energy efficiency impact of EGR on organizing clean combustion in diesel engines," *Energy Conversion and Management*, vol. 112, pp. 369–381, 2016.

[226] S. J. Muthiya, V. Amarnath, P. Senthil Kumar and S. Mohan Kumar, "Carbon capture and storage from automobile exhaust to reduce CO_2 emission", *International Journal of Innovative Research in Science, Engineering and Technology*, vol. 3, no. 2, April 2014.

[227] Q. H. Dirar and K. F. Loughlin, "Intrinsic adsorption properties of CO_2 on 5A and 13X zeolites", *Springer*, vol. 19, pp. 1149-1163, 2013.

[228] A. S. Bhown and B. C. Freeman, "Analysis and status of post-combustion carbon dioxide capture technology", *Environmental Science and Technology*, 2011, doi:10.102/es104291d.

[229] P. S. Prasad and K. V. Raghavan, "Techno-economic aspects of the post-combustion CO_2 capture processes", *Indian Journal of Chemistry*, vol. 51, pp. 1201-1213, 2012.

[230] M. Ziejewski, H. J. Goettler, H. Hainees and C. Huang, "EMA durability tests on higholeic sun flower and safflower oils in diesel engines", *SAE paper*, No. 961856, 1996.

[231] S. Bari, C. W. Yu and T. H. Lim, "Performance deterioration and durability issues while running a diesel engine with crude palm oil", *Proceedings of the Institution of Mechanical Engineers, Part D: Journal of Automobile Engineering*, vol. 216, no. 9, pp. 785-792, 2002.

[232] M. Beauvir, "Lubricating oil analysis according to ASTM D5185 using the Thermo Scientific iCAP 7400 ICP-OES, Application Specialist", Thermo Fisher Scientific, Cambridge, UK.

[233] Anon, Lube Analyst User's Manual, Gas Tops Ltd, 1011 Polytek Street, Ottawa, Ontario K1J9J3, Canada, pp 5.2-5.4, 1995.

Dissemination

List of Publications

A. International Journals

1. K. Tudu, S. Murugan and S.K. Patel, "Experimental analysis of a DI diesel engine fuelled with light fraction of pyrolysis oil," *International Journal of Oil, Gas and Coal Technology*, vol. 11, no. 3, 2016.
2. K. Tudu, S. Murugan and S.K. Patel, "Effect of diethyl ether in a DI diesel engine run on a tyre derived fuel-diesel blend," *Journal of Energy Institute* 2015; vol. 89, no. 4, pp. 525-535, 2016.
3. K. Tudu, S. Murugan and S.K. Patel, "Experimental study of diethyl ether addition on the performance and emissions of a diesel engine," *International Journal of Ambient Energy*, 2015. doi.org/10.1080/01430750.2015.1100679
4. K. Tudu, S. Murugan and S.K. Patel, "Effect of tyre derived oil-diesel blend on the combustion and emissions characteristics in a compression ignition engine with internal jet piston geometry," vol. 184, pp. 89-99, 2016.

B. Conference proceedings (International and National)

1. K. Tudu, S. Murugan and S.K. Patel, "Production, characterisation and utilisation of bio-gas; A Review, International Conference on Alternative fuels for IC Engine (ICAFICE-2013), 6-8 February, 2013, MNIT Jaipur.
2. K. Tudu, S. Murugan and S.K. Patel, 'Light oil fractions from a pyrolysis plant-an option for energy use," 4th International Conference on Advances in Energy Research (ICAER 2013), 10 -12, December 2013, IIT Bombay.
3. K. Tudu, Shubharanshu Shehkar Mahapatra, S. Murugan and S.K. Patel, "Experimental analysis on the combustion parameters of a DI diesel engine fueled with diesel and LFPO blends tyres," 23rd National Conference on I.C. Engines and Combustion Theme: Green Combustion SNIT, Surat, 13-16 December 2013.
4. K. Tudu, S. Murugan and S.K. Patel, "Light oil fractions from a pyrolysis plant-an option for energy use," *Energy Procedia*; vol. 54, pp. 615-626, 2014.

Vitae

Mrs. Kapura Tudu was born in July'1982 in Kumbhirda, Odisha. She has completed her class XII from S. B. Women's College (Cuttack), in 2001 and Bachelor of Engineering in Mechanical Engineering from College of Engineering and Technology, Bhubaneswar (BPUT University) in 2005. She got her Master of Technology in Mechanical Engineering (Specialization Thermal Engineering) from National Institute of Technology (Rourkela) in 2009. After completion of her Post-Graduation, she joined the Ph.D. program at Department of Mechanical Engineering, National Institute of Technology, Rourkela in January 2012 and submitted her Ph.D. thesis in June 2016. Her research interest includes IC engine and alternative fuels.